FINAL

SEDFLUME ANALYSIS DATA REPORT
NEWARK BAY, NEW JERSEY

June 2013

Prepared for:

U.S Environmental Protection Agency

Prepared by:
Sea Engineering, Inc.
200 Washington Street, Suite 210
Santa Cruz, CA 95060
Tel: (831) 421-0871
Fax: (831) 421-0875

EXECUTIVE SUMMARY

Sea Engineering, Inc. conducted a SEDFlume analysis on twenty-nine (29) intact field cores collected from the Newark Bay Study Area in New Jersey. These cores were collected and processed between October 16, 2012 and November 4, 2012. In addition, surface sediment grab samples were collected from five (5) locations within the study area and shipped to the Sea Engineering Santa Cruz, CA, laboratory for processing. The surface sediment was slurried to a target initial sediment-water concentration, poured into empty SEDFlume core barrels, and allowed to consolidate for a pre-determined amount of time (1-day, 4-days, 7-days, 14-days and 28-days). The laboratory cores were prepared and processed between November 11, 2012 and March 15, 2013. In total, thirty-five (35) laboratory consolidation cores were analyzed with the SEDFlume.

The SEDFlume analysis consisted of erosion of sediment at specific flow rates to estimate erosion rates as a function of shear stress and core depth. Each core was sub-sampled periodically during the analysis to determine loss on ignition, wet bulk density (from moisture content and loss on ignition data), and particle size distributions of the material at depth. Critical shear stresses for erosion were also estimated within each depth interval of each core based on the measured erosion rates.

Since the prediction of cohesive sediment erosion is dependent upon many factors, two methods were employed to estimate the critical shear stresses of sediments within a particular depth interval of a core. The first technique involved a linear interpolation, through which the critical shear stress of a depth interval was estimated by interpolating between the measured erosion rates directly. The second involved fitting the measured erosion rates and applied shear stresses to a power law equation (via a least squares regression) that included two non-dimensional coefficients. When solved, this equation yielded the critical shear stress estimation for a particular depth interval. The latter technique provided an analytic means of estimating erosion rates based on predicted shear stresses (e.g. from a hydrodynamic model).

The linear interpolation and power law regression techniques are described within this report. Further, the critical shear stress bounds are reported, for comparison, to the analytic solutions. These bounds are defined as the largest shear stress that *did not* cause erosion and the lowest shear stress that *did* cause erosion. Intuition dictates that the critical shear stress of the depth interval lies between these values.

As a part of the overall project, the following data were measured, collected, computed and/or recorded:

- SEDFlume processing of 29 intact field cores
  - Down-core erosion rate measurements
  - Moisture content measurements (up to five samples/core)
  - Loss on ignition measurements (up to five samples/core)
  - Particle grain size distribution measurements (up to five samples/core)
- Atterberg Limit samples from the field
  - 14 surface sediment samples from each of the 14 SEDFlume coring locations

- 29 at-depth sediment samples from the bottom of each of the processed field cores
- Loss on ignition measurements from each Atterberg Limit sample
- Particle grain size distribution measurements from each Atterberg Limit sample

- SEDFlume processing of 35 consolidation laboratory cores
  - Down-core erosion rate measurements
  - Moisture content measurements (up to six samples/core)
  - Loss on ignition measurements (up to six samples/core)
  - Particle grain size distribution measurements (up to six samples/core)
- Sediment settling column measurements from the laboratory consolidation cores
- Water quality CTD profiles at the time that water samples were collected in field
- Raw (handwritten) and scanned notes from all field and laboratory activities
- Raw (handwritten) and scanned SEDFlume datasheets generated during the analysis
- Formatted SEDFlume datasheets in electronic form (spreadsheets)
- Photographs and videos from all field and laboratory activities, including during processing of field and laboratory cores.

The report outlines the procedures followed during the field and laboratory efforts, describes the SEDFlume analysis, presents the measured data, and provides a basic description and analysis of the results. It comprises mostly a data report; a detailed data analysis was not a part of the present scope of work. However, basic analysis within the techniques employed, criteria specified, equations utilized, and assumptions made are described in detail.

CONTENTS

FIGURES

TABLES

SECTION 1 – SEDFLUME AND PROCEDURES

1.1 INTRODUCTION

Sea Engineering, Inc. (SEI) recently completed a Sediment Erosion at Depth Flume (SEDFlume)[1] analysis on intact and reconstructed sediment cores from Newark Bay in New Jersey. The work was completed to support the ongoing Remedial Investigation/Feasibility Study in the Newark Bay Study Area (NBSA) for the U.S. Environmental Protection Agency. The primary goal of this work was to characterize the erosion rates and physical properties of sediments in the NBSA with respect to depth.

The project was accomplished in two phases: a field effort and a laboratory effort. During the Phase I Field Effort, twenty-nine (29) intact sediment cores were collected from fourteen (14) locations within the NBSA. In addition, surface sediment grabs from five (5) locations were placed in 5-gallon buckets, sealed and shipped to the SEI laboratory in Santa Cruz, CA for Phase II sediment consolidation SEDFlume testing.

After initial recovery, field cores were transported via vessel to a processing facility in Newark, NJ. The cores were transferred and subsequently processed on-site, avoiding possible sediment structure disturbance due to over-land, long-distance transport. The SEDFlume analysis consisted of erosion of sediment at specific flow rates to estimate erosion rates as a function of shear stress and core depth. Each core was sub-sampled periodically during the analysis to determine loss on ignition (LOI), wet bulk density (from moisture content and LOI data), and particle grain size distributions (PSD) of the material at depth.

During the Phase II Laboratory Effort, the surface sediment grab samples from each sampling location were mixed into separate slurries, poured into empty SEDFlume core barrels and allowed to settle and consolidate for specific durations. From each of the five locations at which sediment was collected, a set of consolidation cores[2] was prepared with a target initial dry sediment-water concentration of 350 g/L. Two additional sets of consolidation cores from one location were prepared with a target initial concentration of 100 g/L and 125 g/L. The purpose of the additional dilution sets was to ascertain the effects of slurry concentration on consolidation and erosion rates. A total of thirty-five (35) laboratory consolidation cores were prepared and processed.

Like the field cores, each consolidation core was eroded during the SEDFlume analysis to determine erosion rates as a function of shear stress and core depth. Each core was also sub-sampled during the analysis to determine sediment wet bulk density, PSD, and LOI at depth.

For both phases efforts critical shear stresses were estimated for each core at the respective sub-sampling depths using two methods. The following report outlines the procedures used

[1] McNeil et al., 1996

[2] There were five cores in each set of consolidation cores, corresponding to a 1-, 4-, 7-, 14- and 28-day duration of consolidation.

in the SEDFlume analysis, presents the measured data, and provides a basic description and analysis of the results.

1.2 EXPERIMENTAL PROCEDURES

A detailed description of SEDFlume and its application are given in McNeil et al. (1996) and Roberts et al. (1998) and will not be reiterated here. The following sections supplement those reports with a general description of the SEDFlume analysis procedures conducted in the NBSA Phase I and Phase II efforts.

1.2.1 DESCRIPTION OF SEDFLUME

A SEDFlume is essentially a straight flume with an open bottom section through which a rectangular cross-section core barrel containing sediment can be inserted (schematic shown in Figure 1). The main components of the flume are the water tank, pump, inlet flow converter (which establishes uniform, fully-developed, turbulent flow), the main duct, test section, hydraulic jack and the SEDFlume core barrel containing sediment (Figure 2). The core barrel, test section, flow inlet section, and flow exit section are of transparent acrylic so the sediment-water interactions can be observed visually. The core barrel has a rectangular cross-section, 10 cm by 15 cm, and can be up to 1 m in length. For the NBSA project, the core barrel lengths were 60 cm.

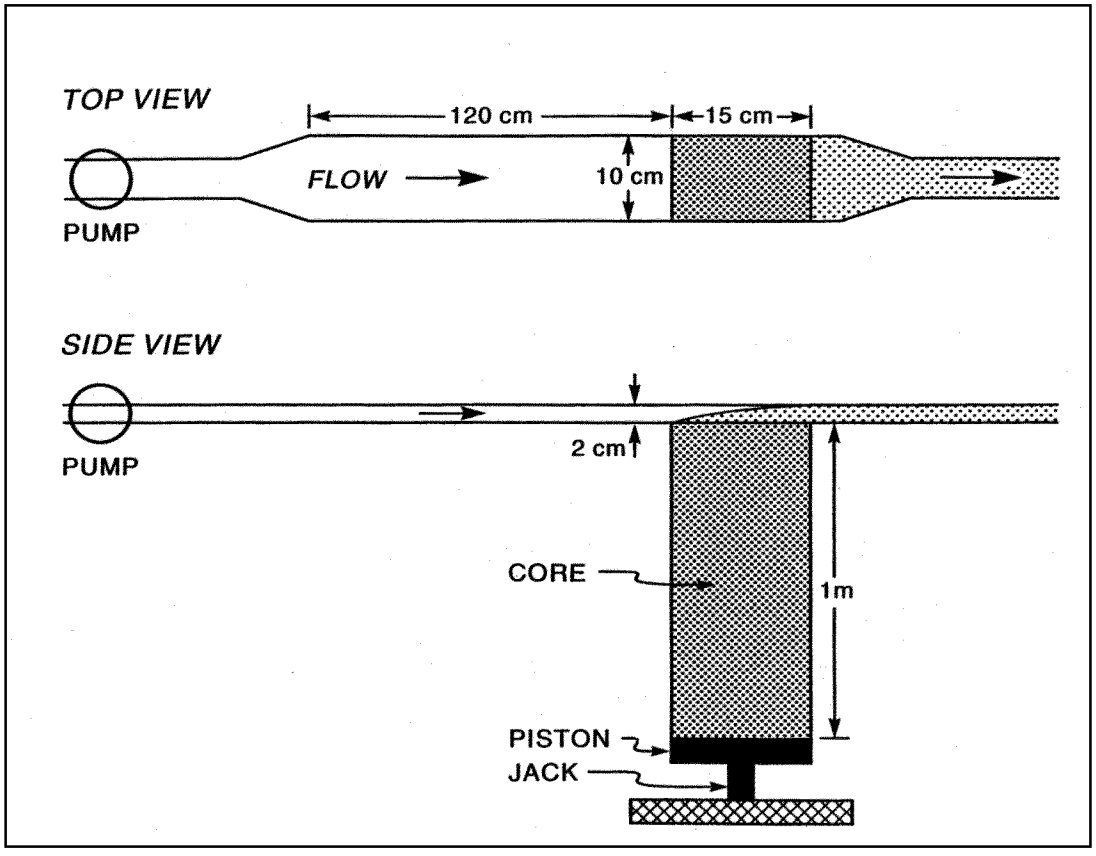

Figure 1. Schematic of the SEDFlume setup showing top and side views.

Water is re-circulated through the system from a 300-gallon storage tank, through a 5 cm diameter pipe, and then through the flow converter into the duct. The main duct is rectangular, 2 cm in height, 10 cm in width, and 120 cm in length; it connects to the test section, which has the same cross-sectional area (2 cm by 10 cm) and is 15 cm long. The flow converter changes the incoming shape of the cross-section from circular to rectangular while maintaining a constant cross-sectional area. An operator regulates the amount of water entering the flume with an in-line ball valve so that flow rates can be carefully controlled. The flume also has a small valve immediately downstream from the test section that is opened to atmospheric pressure to prevent a pressure vacuum from forming over the test section and enhancing sediment erosion.

At the start of each test, a core barrel and the sediments it contains are inserted from beneath the test section. The sediment surface is aligned vertically with the bottom of the SEDFlume channel. When fully enclosed, water is forced through the duct and test section over the surface of the sediments. The shear stress produced by the flow, and imparted on the particles, causes the sediments to erode. As the sediments on the surface of the core erode, the remaining sediments in the core barrel are slowly moved upward so that the sediment-water interface remains level with the bottom of the flume.

An operator controls the upward sediment movement using a hydraulic jack with a 1 m drive stroke attached to a piston at the base of the sediment core. The jack is driven by the release of pressure that is regulated with a switch and valve system. In this manner, the sediments can be raised and the surface made level with the bottom of the test section. The movement of the hydraulic jack can be controlled for measurable increments as small as 0.5 mm.

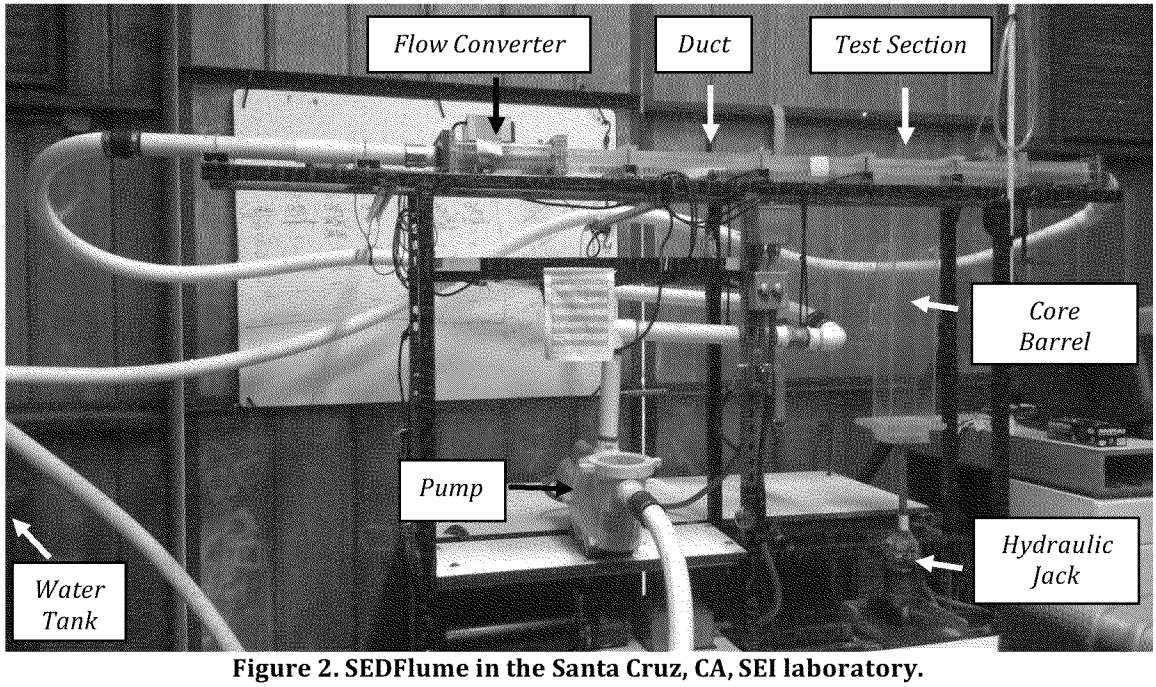

Figure 2. SEDFlume in the Santa Cruz, CA, SEI laboratory.

1.2.2 MEASUREMENTS OF SEDIMENT EROSION RATE

At the start of analysis of each core an initial reference measurement was made of the starting core length. The flume was then operated at a specific flow rate corresponding to a particular shear stress (following McNeil et al., 1996).

Erosion rates were determined by measuring the amount that the sediment was raised between measurement time periods and dividing by the time interval between measurements as shown in Equation 1:

$$E = \frac{\Delta z}{T} \qquad [1]$$

E = Erosion rate
Δz = Amount that the sediment was raised during a particular measurement period
T = Time between measurement periods

The SEDFlume analysis is a destructive test: material is eroded and the core structure is broken down; therefore, repetitive measurements in a controlled manner are not possible. To best determine the erosion rate at several different shear stresses and depths using only one core, the following procedures were performed for each core (from NBSA QAPP Version 2012/10/12):

1) The core was inserted into the bottom of the SEDFlume test section.
2) The shear stresses to be applied to the sediment core were determined prior to test initiation[3].
3) The total length of the sediment in the core barrel was measured and recorded.
4) Two (2) 5-gram (approximately) subsamples of sediment from the surface of the sediment core were collected using a clean spoon, the collection of sediment to the "downstream" (relative to the SEDFlume flow direction) end of the core barrel's surface cross-section.
5) The shear stresses were applied in the flume (lowest shear stresses were tested first in a given cycle). As the sediment in the core barrel eroded, the jack and piston were used to raise the sediment column upwards into the test section so it remained level with the bottom of the flume.
6) During each shear stress cycle, the shear stress was applied for a minimum of 20 seconds and a maximum of 10 minutes; and, to the extent possible, no more than 2 cm of sediment was allowed to erode at a single shear stress[4].
7) At least 0.5 mm of core length was eroded to be considered "measurable" erosion; however, this was not always achievable within 10-minute duration.
8) The duration of the shear stress application was recorded (using a stop watch) and the distance the sediment column was moved during that period of time was noted.
9) The next higher shear stress in the cycle was then applied, following the procedure in Steps 5 through 8.

[3] Standard SEI SEDFlume applied shear stresses range between 0.1 Pa and 12.8 Pa, with each shear stress twice that of the previous.
[4] During the final depth interval (deepest part of the core), more than 2 cm of sediment was, at times, allowed to erode so that measurements further down-core were collected.

10) After attempting to measure erosion over three to four different shear stresses[5], the SEDFlume device was shut-off, the test section drained, the top lid opened and a subsample of sediment was collected for analysis according to Step 4.
11) If a particular shear stress did not cause any observable erosion over a 10 minute period for 2 consecutive depth intervals (e.g. less than 0.5 mm eroded in 10 minutes), that shear stress was removed from subsequent testing cycles; higher shear stresses were added, as appropriate, to attempt to measure at least 3 erosion rates[6].
12) Steps 5 through 10 were repeated until the sediment in the core was eroded or until the erosion rates in 5 depth intervals had been sampled using appropriately selected shear stress cycles based on test operator judgment and the direction provided in Step 11.

If the composition of the material changed at a sediment interface, resulting in an observable change of erosion properties, the cycle was stopped, sediment sub-samples were collected, and a new cycle re-started at the lowest appropriate flow rate. Moreover, if large debris blocked flow in the test section or a large mass of sediment became an obstacle to the flow, cycles were stopped and the flume was cleaned before re-starting the analysis.

1.2.3 ESTIMATION OF CRITICAL SHEAR STRESS

The critical shear stress of a sediment bed, τ_{cr}, is defined as the applied stress at which sediment motion is initiated. In this study, however, it was defined as the shear stress at which a very small, but accurately measurable, rate of erosion occurred; this rate of erosion was operationally defined as 10^{-4} cm/s[7]. This represented 1 mm of erosion in approximately 15 minutes.

Since it is difficult to measure exactly at the 10^{-4} cm/s threshold, erosion was instead measured over a range of shear stresses designed to bracket the initiation of erosion threshold. The highest applied shear stress where erosion *did not occur* is defined by τ_0; and τ_1 is defined as the lowest applied shear stress where erosion *did occur*. These values imply that the critical shear stress (as defined here) existed between these two 'bounds' and provided a means for bracketing the expected critical shear stress value.

The critical shear stress at each depth interval was then estimated via two methods: a linear interpolation and a power law least squares regression analysis. The linear interpolation technique solved for the critical shear stress estimate (τ_{linear}) between τ_0 and τ_1 which corresponded to an erosion rate of 10^{-4} cm/s.

The power law regression technique utilized the measured erosion rate data and corresponding shear stresses in each depth interval to fit a power law equation (defined below). The solution was the critical shear stress estimate (τ_{power}) required to cause 10^{-4} cm/s of erosion.

[5] It was not always possible to measure erosion over a minimum of 3 shear stress applications.
[6] At least 3 erosion rate measurements were attempted in order to best fit a regression line to the data.
[7] Though other definitions of critical shear stress erosion rate thresholds can be argued (and considered valid), the value of 10^{-4} cm/s threshold is used here for consistency with previous SEDFlume efforts and in order to keep testing times to a practical duration.

Because of the uncertainty in analytically determining a critical shear stress, all of these variables (τ_1, τ_1, τ_{linear} and τ_{power}) are included in the report below. It is anticipated that the end-user will use proper judgment in determining how to characterize the NBSA seafloor when specifying critical shear stresses.

Power Law Least Squares Regression

Following the methods of Roberts et al. (1998), the erosion rate for sediments can be approximated by the power law regression:

$$E = A\tau^{n}\rho^{m} \quad [2]$$

E = erosion rate (cm/s)
τ = bed shear stress (Pa)
ρ = sediment wet bulk density (g/cm^3)
A, n and m = constants that depend on the sediment characteristics

The equation used in the present NBSA SEDFlume analysis is a variation of Equation 2:

$$E = A\tau^{n} \quad [3]$$

where the constant, A, is a function of the sediment wet bulk density and other, non measurable properties. The variation of erosion rate with density typically cannot be determined for field sediments due to natural variation in other sediment properties (e.g. mineralogy, particle size and electrostatic forces). Therefore, the density term from the equation above, for a particular interval of approximately constant density, is incorporated into the constant A.

The measured erosion rates (E) and applied shear stresses (τ) within each depth interval were used to determine the A and n constants that provided a best fit power law curve to the data for that depth interval. A coefficient of determination, r^2, of 0.70 was used as a criteria threshold for acceptance [8]. Using the accepted regression fit constants, the critical shear stress for the corresponding depth intervals was estimated by solving Equation 3 for the shear stress required to cause 10^{-4} cm/s of erosion.

1.2.4 Measurement of Sediment Bulk Properties

In addition to measuring erosion rates during the SEDFlume analysis, samples were periodically collected at depth to determine the loss on ignition (LOI), the combustible materials, the water content (for wet bulk density when combined with LOI), and the particle size distributions of the sediments in each core. Sub-samples were collected from the undisturbed core surface (prior to analysis) as well as the sediment surface at the beginning of each subsequent depth interval.

[8] The coefficient of determination, r^2, is a function of the *Pearson's r*, which is a measure of the linear dependence (correlation) between two variables. *Pearson's r* can be positive or negative, and is a value between -1 and +1. The more common usage of the correlation coefficient is to square the *Pearson's r*, r^2, and report that value, the coefficient of determination.

Wet bulk density was determined using methods outlined in Hakan son and Jansson (2002). Samples were first weighed in their wet state and then dried in the SEI Laboratory oven to remove moisture. Then the water content (W) was determined following ASTM D2216-05 recommendations:

$$W = \frac{M_w - M_d}{M_w} \quad [4]$$

W = water content
M_w = wet weight of sample
M_d = dry weight of sample

Loss on ignition was determined following ASTM D2974 Version C. Samples were first dried in the SEI Laboratory oven to remove moisture (as described above). Then, the samples were placed in a furnace and ignited at 440°C until the mass remained constant (typically less than 24 hours). The change in combustible mass is the loss on ignition:

$$LOI = \frac{M_d - M_{d,combustion}}{M_d} \quad [5]$$

M_d = dry weight of sample
$M_{d, combustion}$ = dry weight of sample after combustion.

Once the water content and LOI was determined, the wet bulk density, ρ_b, was determined from Equations 6 and 7:

$$\rho_b = \frac{\rho_w \rho_t}{\rho_w + (\rho_t - \rho_w) W} \quad [6]$$

where

$$\rho_t = \chi_s \rho_s + \chi_o \rho_o \quad [7]$$

and
ρ_w = density of water (assumed 1 g/cm^3)
ρ_t = total solids density (sum of organic and inorganic fractions)
ρ_s = density of inorganic material (assumed 2.60 g/cm^3)
ρ_o = density of organic material (assumed 1.25 g/cm^3)
χ_o = organic fraction of oven dry material (computed as fraction lost on ignition)
χ_s = inorganic fraction of dry material (1-χ_o)

Finally, particle size distributions were determined using laser diffraction analysis in the SEI laboratory in Santa Cruz. Sediment samples were dispersed in water and inserted into a Beckman Coulter LS 13 320 laser diffraction particle size analyzer. Each sample was analyzed in three 1-minute intervals and the results of the three analyses were averaged.

The relationships used to determine sediment bulk properties are summarized in Table 1.

Table 1. Parameters measured and computed during the SEDFlume analysis.

Measurement	Definition	Units	Detection Limit	Internal Consistency
Water Content	$W = \frac{M_w - M_d}{M_w}$	unit-less	0.001 g in sample weight ranging from 1 to 50 g	0 < W < 1
Wet Bulk Density	$\rho_b = \frac{\rho_w - \rho_t}{\rho_w - (\rho_t - \rho_w)W}$	g/cm^3	Same as water content	$\rho_w < \rho_b < 2.6\rho_w$
Total Sediment Particle Density	$\rho_t = \rho_s \rho_s + \rho_o \rho_o$	g/cm^3	Same as water content	$\rho_t <= 2.6$
Particle Size Distribution Below 2000 µm	Distribution of particle sizes by volume percentage using laser diffraction	µm	Method Specific	1µm<Grain Size<2000µm
Weight Fraction of Particles Above 2000 µm	$f_{2000} = \frac{W_{d2000}}{W_d}$	unit-less	0.001 g in sample weight ranging from 1.5 to 105 g	Grain Size>2000µm
Loss on Ignition	$LOI = \frac{M_d - M_{d,combustion}}{M_d}$	unit-less	Same as water content	Wet and dry mass of sample

W_{2000} = Weight of sample above 2000 µm grain size
W_d = Total weight of sample

1.2.5 Intra-core and Inter-core Comparisons

A potentially useful method of comparing spatial sediment erosion characteristics at a specific site (e.g. throughout the NBSA site) was employed to compute *intra*-core and *inter*-core erosion rates. This method provided a means to quantify (and visualize) the erosion rate susceptibility within each core (intra-core) as well as the general erosion rate susceptibility of the cores throughout the site (inter-core).

Intra-core Erosion Rate Ratios

Once the *A* and *n* coefficients for each depth interval within an individual core had been determined, the *interval-average* erosion rate was computed for each interval using the corresponding *A* and *n* values, and the logarithmic average of the range of shear stre

expected to exist in the NBSA (Equation 3)[9]. C*ore-average* erosion rates were then computed by:

1) Log-averaging the *A* coefficient values from each depth interval within a core to arrive at an average *A* coefficient for the entire core.
2) Arithmetically averaging the *n* coefficient values from each depth interval within a core to arrive at an average *n* coefficient for the entire core.
3) Solving for the *core-average* erosion rate using Equation 3 and the log-average of the range of shear stresses applied to the depth interval (1.13 Pa).

When each *interval-average* erosion rate was divided by the corresponding *core-average* erosion rate, the result was an intra-core erosion rate *ratio,* which provided an estimation of the erosion susceptibility of each depth interval in the core relative to the *core-average*. This method highlighted the core intervals that are more or less susceptible to erosion within a particular core and may indicate where layering existed within a core. Intervals for which r^2 was less than 0.70 were omitted from the comparison and the corresponding bar plots and tables below.

Inter-core Erosion Rate Ratios

Two additional ratios were computed to evaluate large-scale spatial erosion susceptibility. Both were inter-core erosion rate ratios, the first computed by dividing the individual *core-average* erosion rate by the *site-wide average* erosion rate. The *site-wide average* erosion rate was computed by:

1) Log-averaging the *core-average A* coefficient values from each core to arrive at an average *A* coefficient for the entire site.
2) Arithmetically averaging the *core-average n* coefficient values in each core to arrive at an average *n* coefficient for the entire site.
3) Solving for the *site-wide average* erosion rate using Equation 3 and the log-average of the range of shear stresses (1.13 Pa).

The *inter-core* erosion rate ratio computed in this manner provided a qualitative estimate of the erosion susceptibility of each core (as a whole) relative to other cores in the site, potentially indicating spatial locations that are more or less susceptible to erosion than other locations.

In a variation, the erosion rate for each depth *interval* within each core was compared to the *site-wide average* erosion rate yielding another means for comparing the spatial and depth-dependent erosion rate susceptibility of core sediments. Solving for *inter-core* erosion rate ratios in this manner indicated the depth intervals (and spatial locations) which were most susceptible to erosion (relative to the other core locations and depths). A spatial assessment of erosion probability can be generated from this information but was outside the scope of this document.

[9] The shear stress values averaged were the range applied to the NBSA field cores: 0.1, 0.2, 0.4, 0.8, 1.6, 3.2, 6.4 and 12.8 Pa. The logarithmic average of these, used to compute erosion rate ratios in Equation 3, was 1.13 Pa.

SECTION 2 – PHASE I FIELD EFFORT

2. 1 FIELD ACTIVITIES

The field effort phase of this project occurred in October and November 2012. Twenty-nine intact sediment cores were recovered from October 16, 2012 through October 19, 2012: Two cores were extracted from each of 14 locations within the NBSA and a triplicate core was collected from location SF-6 for a total of 29 field cores. The approximate locations at which cores were collected are shown in Figure 3. Surface sediment grab samples were also collected from five locations and surface water samples were collected from one location within the NBSA (locations shown in Figure 4).

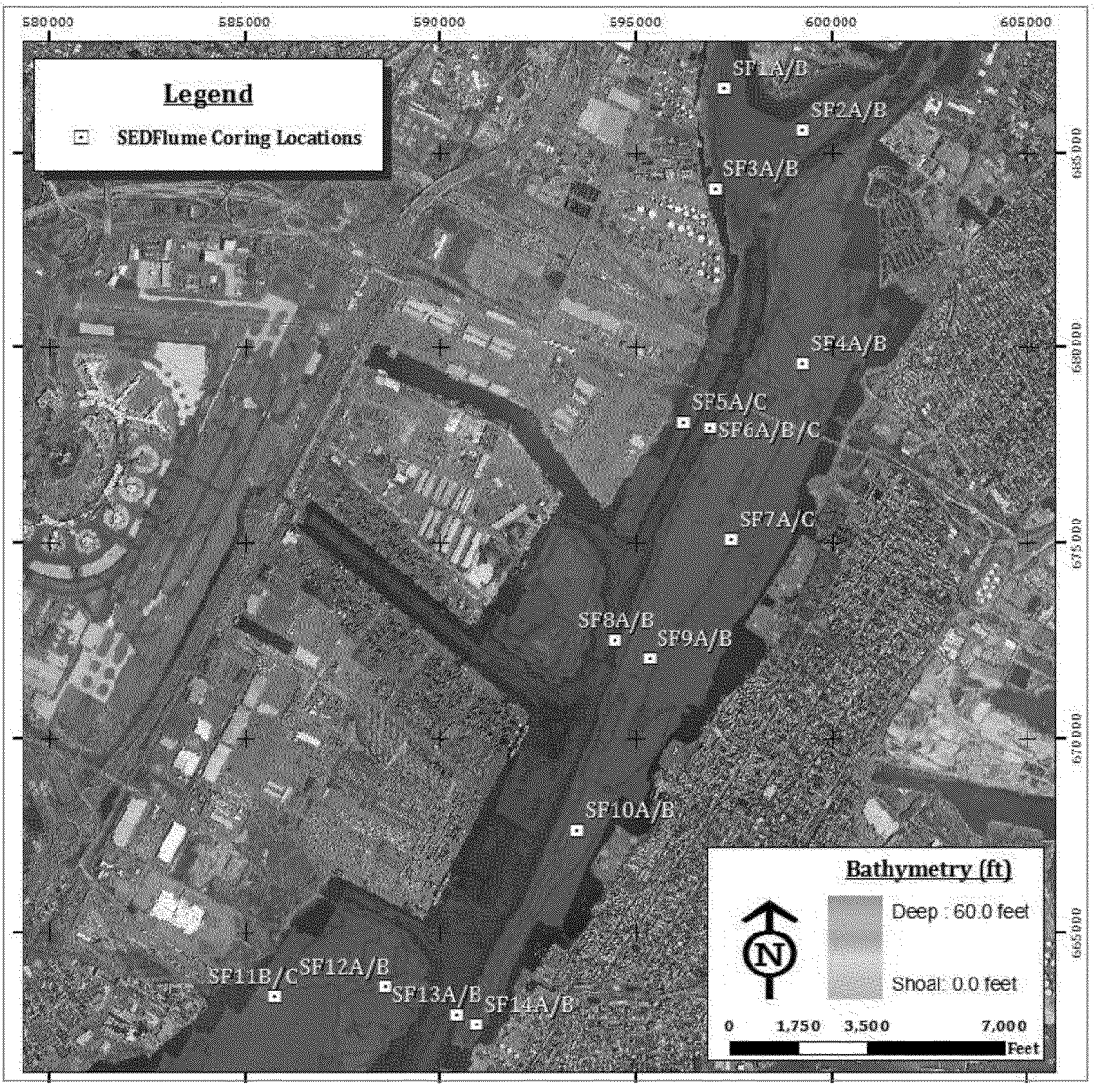

Figure 3. SEDFlume coring locations within the NBSA[10].

[10] The locations are approximated in this figure for ease of viewing on the large-scale map. Duplicate cores were collected very near each other at this scale.

The sediment surface grabs were collected with a Van Veen grab sampler, penetrating approximately to a depth of 0.5-1.0 ft below the sediment surface. At each of the sediment grab sample locations, three 5-gallon buckets were filled with sediment and slurry. At location SF8-C, twice as much material (six 5-gallon buckets) was collected to facilitate additional analyses with different sediment to water dilutions. A total of eighteen 5-gallon buckets were filled with sediment and sealed with lids.

The water samples were collected immediately beneath the water surface directly into 5-gallon buckets. Ten buckets of NBSA seawater were collected and sealed with lids. All buckets were shipped to SEI's laboratory in Santa Cruz for the Phase II Laboratory Effort.

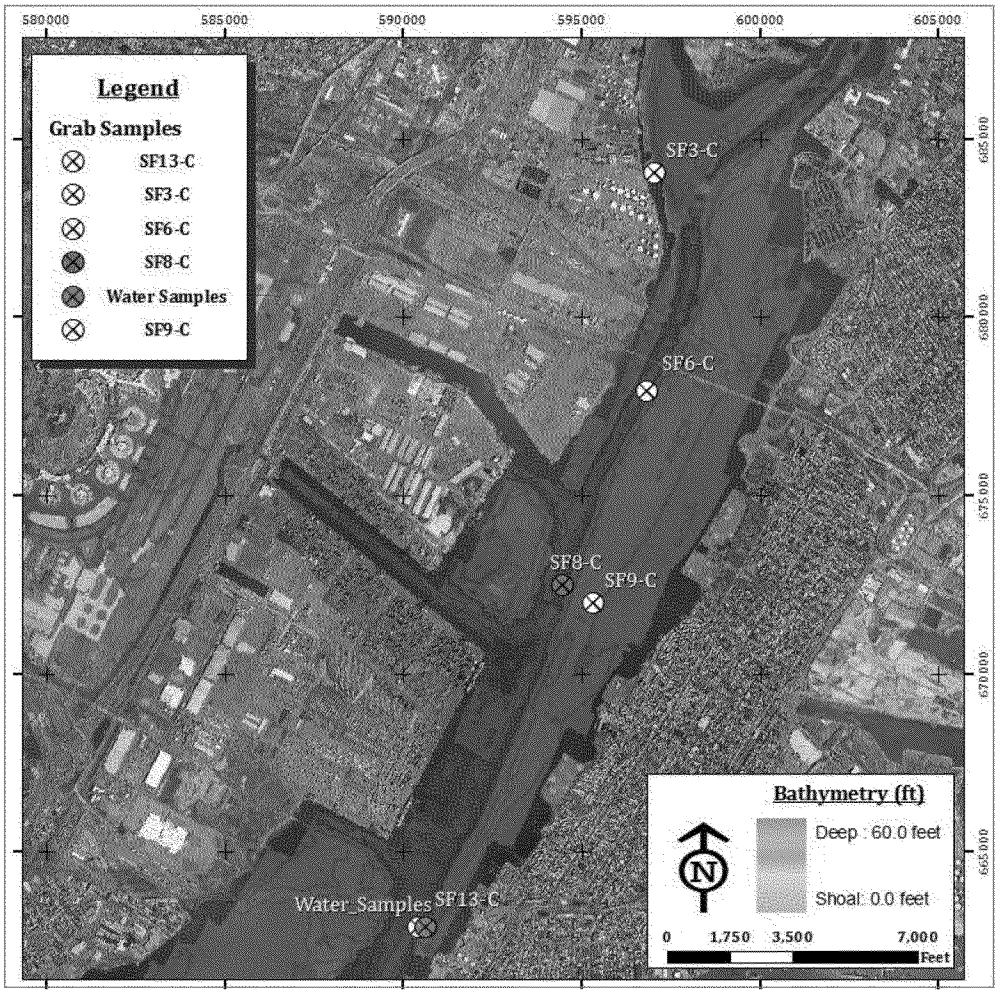

Figure 4. Sediment grab and water sample locations within the NBSA. Location SF8-C, where twice as much material was collected, is shown in green.

The sampling stations, coordinates and approximate water depths from where each core and grab sample was extracted are listed in Table 2. Intact field cores are noted throughout this report in the format "SF#L" where SF designates "SEDFlume", "#" is the sampling station location number (1-14), and L is a letter designation (A, B or C). Primary and duplicate cores are typically named with an 'A' and 'B' designation (e.g. SF1A and SF1B). Cores that include

a 'C' designation indicate that more than 2 cores were initiall y extracted from that location, and the two best recoveries were retained for the analysis (e.g . SF5A and SF5C). Triplicate cores were collected, retained and processed at station 6 (e.g. SF6A, SF6B and SF6C).

Laboratory consolidation cores are noted as "SF#-C" where SF refers to "SEDFlume", the # is the sampling station location number from which the grab sample s were collected (1-14), and the "-C" indicates a consolidation core. Table 3 lists the ve descriptions of each of the core and surface sediment grab sample collection locations.

Table 2. Core, sediment grabs and water sample location coordinates.

Sample ID[11]	Water Depth (ft)[12]	New Jersey State Plane Coordinate System (NAD-83)		Geographic Coordinates (NAD-83)	
		Easting (ft)	Northing (ft)	Longitude (°W)	Latitude (°N)
SF1A	8.5	597276.1	686669.6	74.120639	40.717944
SF1B	9.3	597268.4	686669.6	74.120667	40.717944
SF2A	11.1	599290.4	685595.6	74.113389	40.714972
SF2B	11.9	599290.4	685595.6	74.113389	40.714972
SF3-C	***17.0***	***597038.3***	***684073.3***	***74.121537***	***40.710821***
SF3A	24.9	597047.4	684059.7	74.121505	40.710783
SF3B	16.6	597046.3	684077.1	74.121508	40.710831
SF4A	n/a	599285.1	679581.5	74.113504	40.698464
SF4B	5.0	599298.3	679588.8	74.113456	40.698484
SF5A	6.0	596222.8	678106.7	74.124571	40.694452
SF5C	4.0	596213.4	678111.3	74.124605	40.694465
SF6-C	***45.0***	***596843.7***	***677947.3***	***74.122334***	***40.694007***
SF6A	44.0	596890.3	677933.7	74.122166	40.693969
SF6B	45.0	596870.7	677948.4	74.122237	40.694010
SF6C	45.0	596865.6	677938.5	74.122255	40.693983
SF7A	6.0	597446.9	675079.0	74.120203	40.686127
SF7C	6.0	597441.1	675064.8	74.120225	40.686088
SF8-C	***39.0***	***594458.4***	***672489.3***	***74.131019***	***40.679053***
SF8A	39.0	594458.4	672489.3	74.131019	40.679053
SF8B	39.0	594458.4	672489.3	74.131019	40.679053
SF9-C	***7.5***	***595330.7***	***671989.2***	***74.127882***	***40.677670***
SF9A	8.4	595367.1	672018.5	74.127750	40.677750
SF9B	8.0	595367.1	672018.5	74.127750	40.677750
SF10A	13.5	593493.3	667618.9	74.134572	40.665695
SF10B	13.5	593493.3	667618.9	74.134572	40.665695
SF11B	12.0	585746.4	663354.1	74.162558	40.654073
SF11C	12.0	585746.4	663354.1	74.162558	40.654073
SF12A	13.0	588588.5	663625.3	74.152310	40.654787
SF12B	13.0	588588.5	663625.3	74.152310	40.654787
SF13-C	***57.0***	***590432.5***	***662895.7***	***74.145674***	***40.652764***
SF13A	57.0	590432.5	662895.7	74.145674	40.652764
SF13B	57.0	590432.5	662895.7	74.145674	40.652764
SF14A	10.0	590929.0	662629.6	74.143889	40.652028
SF14B	8.7	590921.3	662619.4	74.143917	40.652000
Water Samples	32.0	590653.8	662894.3	74.144876	40.652757

[11] Surface sediment grab samples are denoted by gray shading, bold font and a dash ("-") in the Sample ID.
[12] Water depths are those at the time of coring/sediment collection and are not corrected to any datum.

Table 3. Core, sediment grabs and water sample qualitative descriptions of locations.

Sample ID	General Description and Location	Sample ID	General Description and Location
SF1A	Core SF1A - East side of Mouth of the Passaic River	***SF8-C***	Six (6) 5-gallon buckets sediment grab samples for Consolidation Cores SF8-C (Navigation Channel, east of CDF[13])
SF1B	Core SF1B - East side of Mouth of Passaic River (Duplicate)	**SF8A**	Core SF8A - Navigation Channel east of CDF
SF2A	Core SF2A - West side of Mouth of Hackensack River	**SF8B**	Core SF8B - Navigation Channel east of CDF (Duplicate)
SF2B	Core SF2B - West side of Mouth of Hackensack River (Duplicate)	***SF9-C***	Three (3) 5-gallon buckets sediment grab samples for Consolidation Cores SF9-C (eastern mudflats, across from CDF)
SF3-C	Three (3) 5-gallon buckets sediment grab samples for Consolidation Cores SF3-C (Navigation Channel, Mouth of Passaic River)	**SF9A**	Core SF9A - Eastern mudflats east of CDF and SF8 location
SF3A	Core SF3A - Navigation Channel of Mouth of Passaic River	**SF9B**	Core SF9B - Eastern mudflats east of CDF and SF8 location (Duplicate)
SF3B	Core SF3B - Navigation Channel of Mouth of Passaic River (Duplicate)	**SF10A**	Core SF10A - Eastern mudflats east of Port of Elizabeth
SF4A	Core SF4A - Eastern mudflats, NE Newark Bay, North of I-78 Newark Bay Bridge	**SF10B**	Core SF10B - Eastern mudflats east of Port of Elizabeth (Duplicate)
SF4B	Core SF4B - Eastern mudflats, NE Newark Bay, North of I-78 Newark Bay Bridge (Duplicate)	**SF11B**	Core SF11B - Southwestern mudflats, western portion of the mudflats
SF5A	Core SF5A - Western mudflats, NW Newark Bay, South of I-78 Newark Bay Bridge	**SF11C**	Core SF11C - Southwestern mudflats, western portion of the mudflats (Duplicate)
SF5C	Core SF5C - Western mudflats, NW Newark Bay, South of I-78 Newark Bay Bridge (Duplicate)	**SF12A**	Core SF12A - Southwestern mudflats, eastern portion of the mudflats
SF6-C	Three (3) 5-gallon buckets sediment grab samples for Consolidation Cores SF6-C (Navigation Channel, Port Newark)	**SF12B**	Core SF12B - Southwestern mudflats, eastern portion of the mudflats (Duplicate)
SF6A	Core SF6A - Navigation Channel, east of Port of Newark	***SF13-C***	Three (3) 5-gallon buckets sediment grab samples for Consolidation Cores SF13-C (Navigation Channel, South end Newark Bay
SF6B	Core SF6B - Navigation Channel east of Port of Newark (Duplicate)	**SF13A**	Core SF13A - Navigation Channel, South End of Newark Bay
SF6C	Core SF6C - Navigation Channel east of Port of Newark (Triplicate)	**SF13B**	Core SF13B - Navigation Channel, South End of Newark Bay (Duplicate)
SF7A	Core SF7A - Eastern mudflats, east of Port of Newark	**SF14A**	Core SF14A - Eastern mudflats, Southeast end of Newark Bay
SF7C	Core SF7C - Eastern mudflats, east of Port of Newark (Duplicate)	**SF14B**	Core SF14B - Eastern mudflats, Southeast end of Newark Bay (Duplicate)
Water Samples	Ten (10) 10-gallon buckets of water samples collected from near-surface of Newark Bay		

[13] Confined Disposal Facility

2.2 FIELD EFFORT SUMMARY

The following list provides a breakdown of the daily field activities during the Phase I Field Effort:

- **October 16, 2012**
  - The SEI team mobilized the vessel and began coring at location SF3.
  - The mobile SEDFlume laboratory was prepared at 80 Lister Ave. (Newark, NJ).
- **October 17, 2012**
  - The SEI team continued coring at locations SF4, SF5, SF6 and SF7.
  - SEI began processing core SF3A at the mobile laboratory.
- **October 18, 2012**
  - The SEI team continued coring at locations SF1, SF2, SF8, SF13 and SF9, SF14.
  - No SEDFlume cores were processed on this day.
- **October 19, 2012**
  - The SEI team completed the coring effort at locations SF10, SF11 and SF12.
  - SEI continued core processing at the mobile laboratory (SF3B and SF6C).
- **October 20-November 4, 2012**
  - The SEI core collection crew demobilized on October 20, 2012.
  - SEDFlume core processing continued until November 4, 2012[14].
  - SEI completed final demobilization from the field site on November 4, 2012.

2.3 FIELD EFFORT METHODS

In order to collect sediment core samples that contain undisturbed surficial and preserved internal core structure, it was necessary to push-core. Other methods of coring (e.g. vibra-coring, gravity coring) potentially lead to surface sediment structure damage or down-core sediment structure alteration, neither of which are desirable when ascertaining the critical shear stresses of in-situ sediments.

2.3.1 SHALLOW WATER CORING

The shallow-water coring system was used when coring in water depths less than 25 feet. It consisted of a set of aluminum poles and a cage that was bolted together in different lengths depending upon the water depth (Figure 5). A one-way valve was secured to the top of an empty SEDFlume core barrel. The barrel was inserted into the cage and affixed by means of a hose clamp. The cage was then attached to the proper number of aluminum poles for the specific water depth.

The equipment was lowered into the water, and, when at the seafloor, the operator pushed the core barrel into the seafloor until sufficient resistance was encountered or sufficient core length recovered. The target length of a recovered core was 30 cm, and no more than 60 cm[15]. If insufficient penetration occurred, the operator resorted to light tapping with a post-hammer to assist in driving the core further into the bed[16]. As the core penetrated the

[14] A two-day postponement of core processing occurred on October 29, 2012 and October 30, 2012 due to the passing of Hurricane Sandy.
[15] At times, less than 30 cm of material was recoverable from the NBSA.
[16] This situation often arises when coring in coarse (e.g. sand) and high density material (e.g. dense clays).

sediment bed, water was allowed to pass freely through the one- way valve at the top of the core barrel.

The operator, with the assistance of a technician, then manually extracted the core from the bed. The one-way valve closed and created a vacuum which held the sediment as the setup was recovered. Upon retrieval, sediment cores were immediately inspected for quality and disturbance of the sediment surface. Cores that did not meet the quality criteria were discarded and the process was repeated.

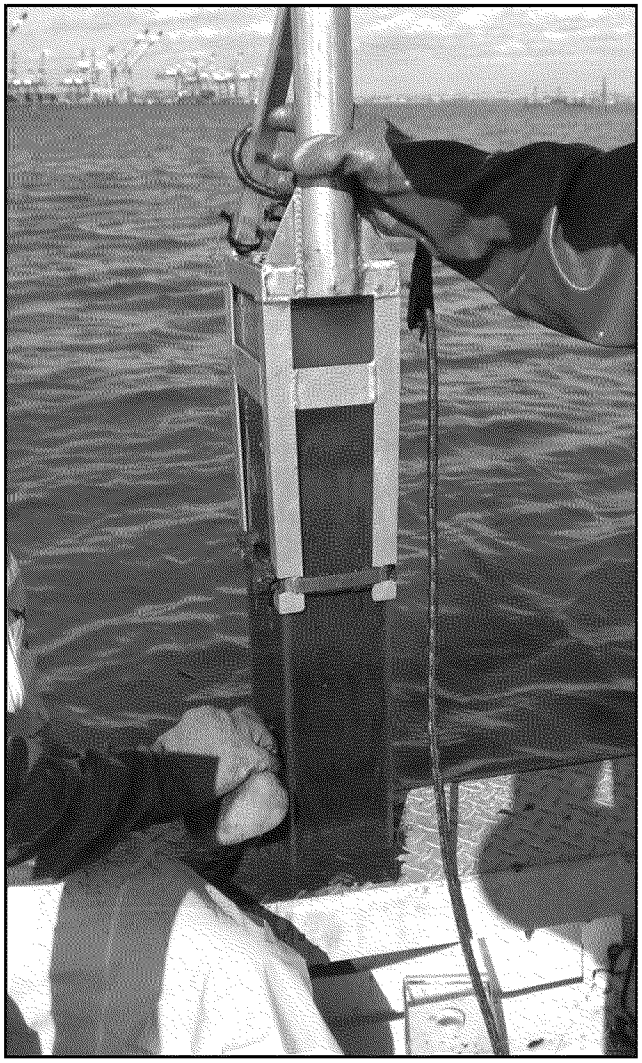

Figure 5. Shallow-water coring system with cage attached to a recently extracted core.

2.3.2 DEEP WATER CORING

The deep-water coring system used during field sampling efforts was used in water depths deeper than 25 feet. It comprised a pneumatic piston mounted in a weighted aluminum frame (Figure 6). A standard SEDFlume core barrel was inserted into the frame and attached to the piston. The frame was lowered to the seafloor by means of an A-Frame off of the bow of the coring vessel.

Once in position, the piston pushed the core barrel into the sediment. Approximately 400 lbs of weight in the aluminum frame offset the sediment resistance and provided leverage to push the core into the sediment bed. As the core was pushed into the bed, water was allowed to escape through a one-way valve near the top of the barrel. The core was extruded from the seafloor (one-way valve closed and provided a vacuum). Upon full extraction from the seafloor a spring-loaded door closed beneath the core to prevent sediment from falling out of the core barrel during the transit to the water surface.

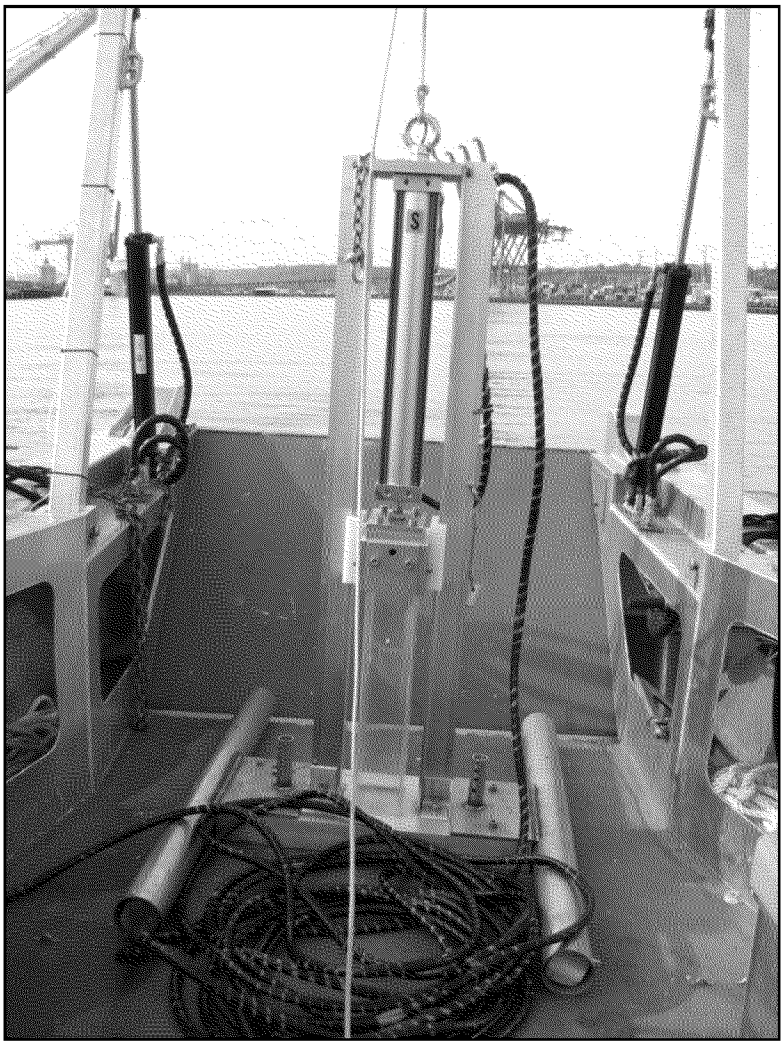

Figure 6. Deep-water coring system with SEDFlume core inserted.

SEI personnel typically push-core in water depths up to 20-25 feet. At greater depths, the coring equipment becomes unwieldy and the quality of the extracted core deteriorates. In deeper waters, SEI partners with Gravity Environmental (Seattle, WA) to utilize their deep-water push-coring system. Gravity Environmental assisted SEI on this project in the same manner.

2.4 FIELD CORE ANALYSIS

2.4.1 CORES SF1A AND SF1B

Cores SF1A and SF1B were collected from the eastern mudflats at the mouth of the Passaic River. Core SF1A comprised 2-3 cm of tan-colored, silt with visible benthic activity (worms, tubes) and fine organic material (leaves and sticks) on the surface. Sand lenses were observed at deeper depths, surrounded by clay and silt material. The surface of core SF1B consisted of 2-3 cm of tan-colored, low-density silt and fine sand. A 5 cm long stick was removed from the surface prior to processing. The surface also contained fine organic material and evidence of small benthic activity (worms, tubes). Sand lenses were again visible down core. Stiffer, clayey-silt and fine sand were observed at the deeper depth intervals in both cores.

A photograph of the cores aligned with each other is presented in Figure 7. Their respective erosion rate data are plotted in Figure 8. Because the logarithm of 0 is invalid, erosion rates of zero are shown at a value of 1.0 cm/s for plotting purposes (this holds for all erosion rate plots presented herein). The sediment surface is plotted at the top of the graph (where the depth = 0) with depth into the sediments increasing down the y-axis. Shear stresses ranging between 0.1 and 6.4 Pa were applied to these cores. In general, the erosion rates decreased with depth into the cores.

The intra-core erosion rate ratios of the depth intervals evaluated in each core are shown in Figure 9. The numbers plotted on the y-axis represent the starting depth (i.e. top) of each interval. The vertical dashed line denotes an erosion rate ratio of 1.0 (i.e. equivalent to the *core-average* erosion rate for each respective core). Ratios to the right of the line indicate depth intervals that were more susceptible to erosion; ratios to the left of the line indicate less susceptibility to erosion. In general, the near surface sediments appeared to be more susceptible to erosion than those at depth, which is expected behavior in typically consolidated sediments.

The power law regression fit within each depth interval of the cores is illustrated in Figure 10. Coefficients derived from the power law least squares regression (i.e., A and n) for which the r^2 value was less than 0.70 are shown in the regression plots for reference but are omitted from the corresponding tables. Coefficients and regression statistics from the power law fit analysis are presented in Table 4 and Table 5 for the cores, respectively. The measured median grain sizes, the computed wet bulk density and critical shear stress estimates for each depth interval are provided in Table 6 and Table 7.

The vertical profiles of median grain size, d_{50}, and wet bulk density from each core are presented in Figure 11. The median grain size in SF1A varied between a maximum of 69.33 µm (very fine sand) at the surface and a minimum of 15.45 µm (fine silt) at a depth of 9.40 cm. In SF1B, the median grain size was a maximum of 69.37 µm (very fine sand) at the surface and a minimum of 8.45 µm (fine silt) at a depth of 7.80 cm. The core-averaged d_{50} in SF1A and SF1B was 34.10 µm (coarse silt) and 24.73 µm (medium silt), respectively[17].

[17] All sediment grain size qualitative size descriptions are from the Wentworth Grain Size Chart.

The wet bulk density in SF1 A varied between a maximum of 1.69 g/cm^3 at the surface to a minimum of 1.39 g/cm^3 at a depth of 4.90 cm. The wet bulk density in SF1B was a maximum of 1.49 g/cm^3 at the surface and a minimum of 1.35 g/cm^3 at a depth of 6.70 cm. The core-averaged wet bulk density in the cores was 1.48 g/cm^3 and 1.42 g/cm^3, respectively.

The critical shear stress estimates, τ_{linear} and τ_{power}, followed similar down-core trends within each core, though the magnitudes in SF1B were slightly higher than SF1A at corresponding depths. The core-averaged linearly interpolated critical shear stress estimates were 0.93 Pa and 1.17 Pa for SF1A and SF1B, respectively; the power law core-averaged estimates were 0.86 Pa and 1.15 Pa for the cores, respectively.

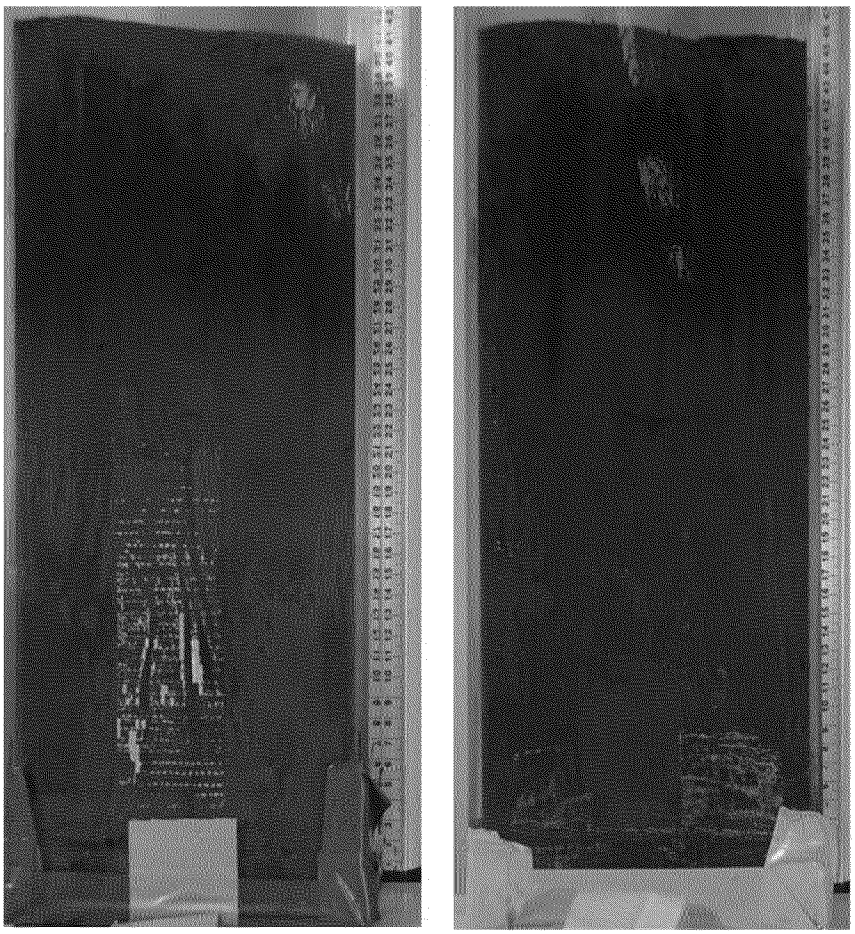

Figure 7. Pre-processing photo of cores SF1A (left) and SF1B (right).

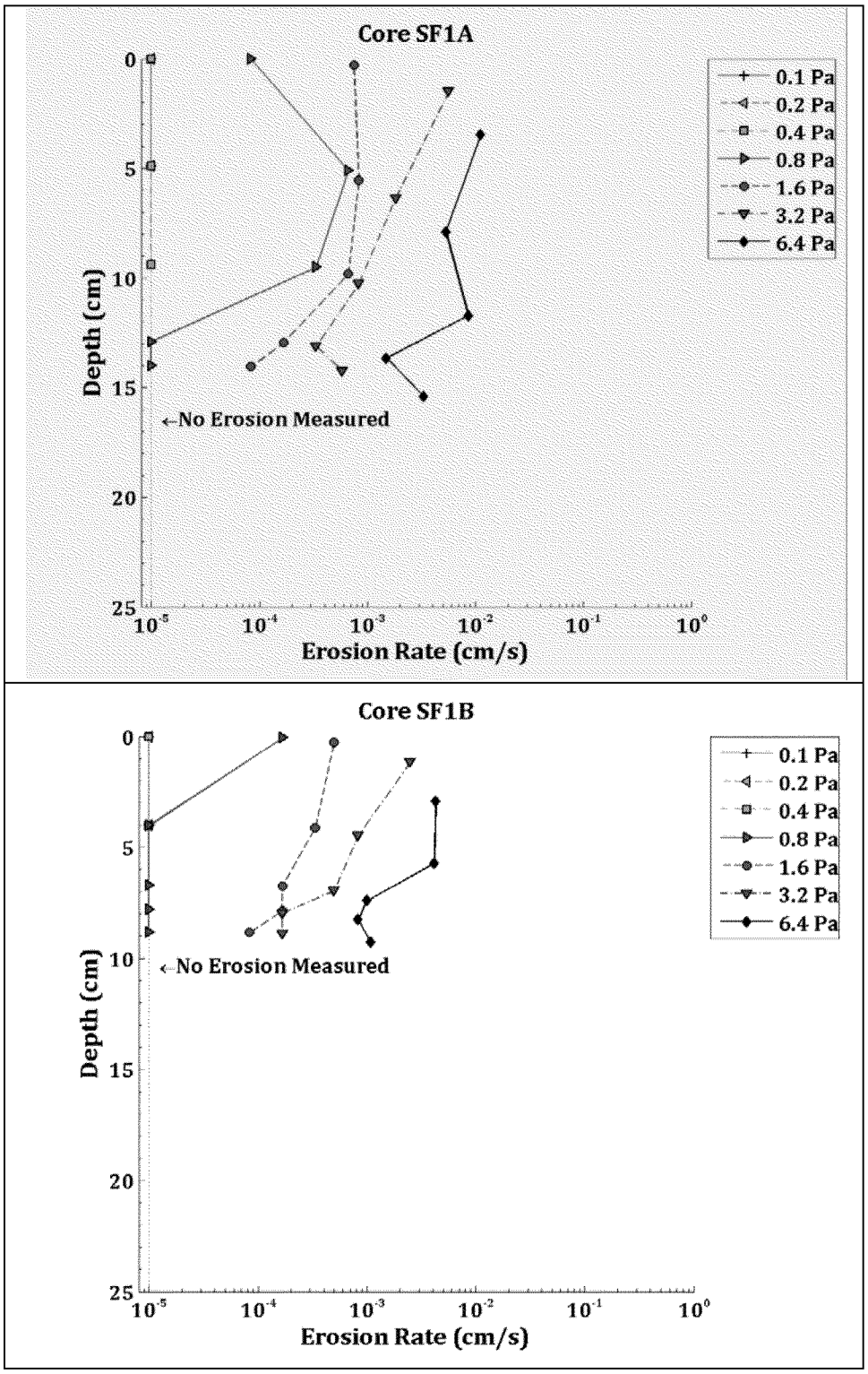

Figure 8. Down-core erosion rates for SF1A (top) and SF1B (bottom).

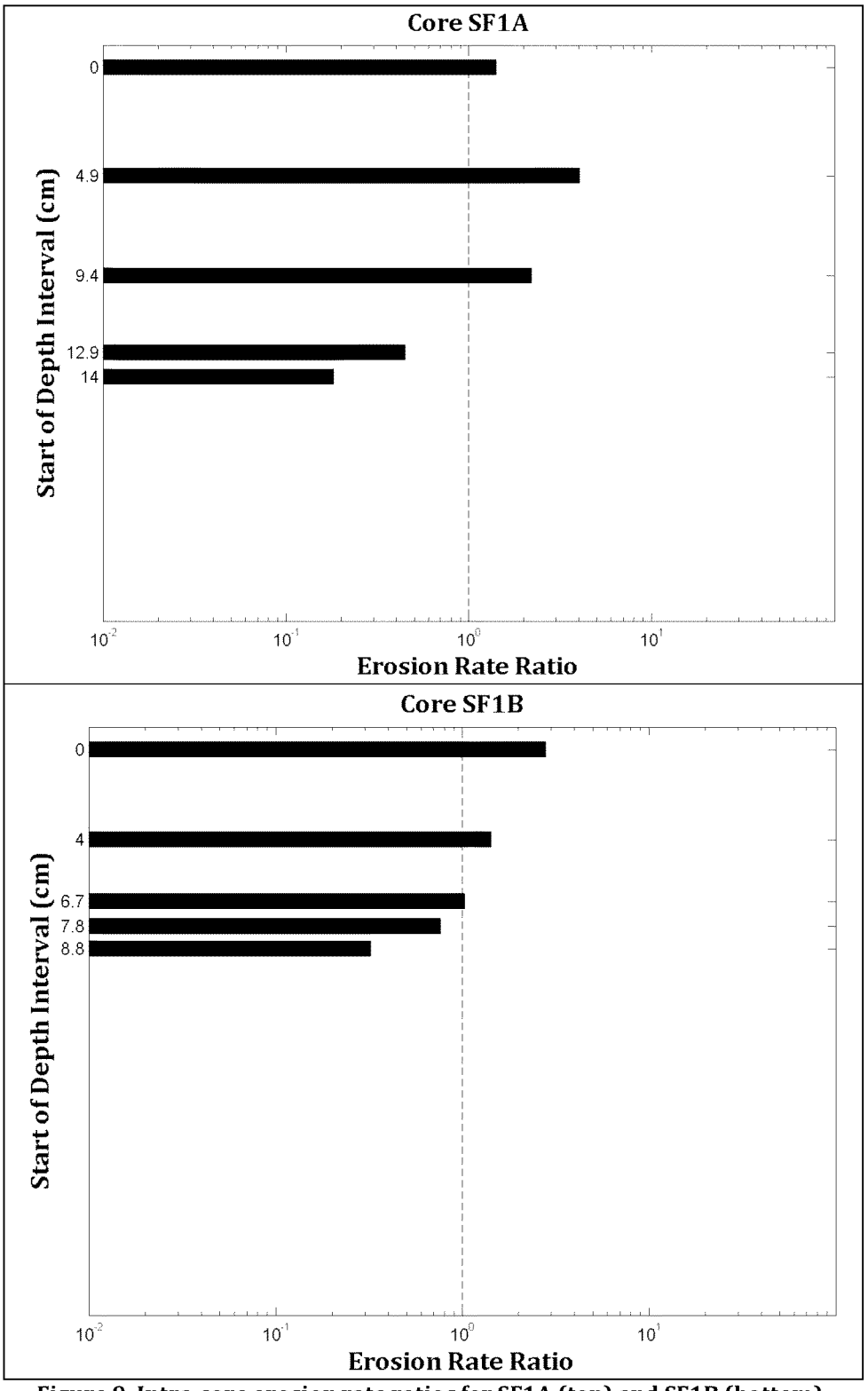

Figure 9. Intra-core erosion rate ratios for SF1A (top) and SF1B (bottom).

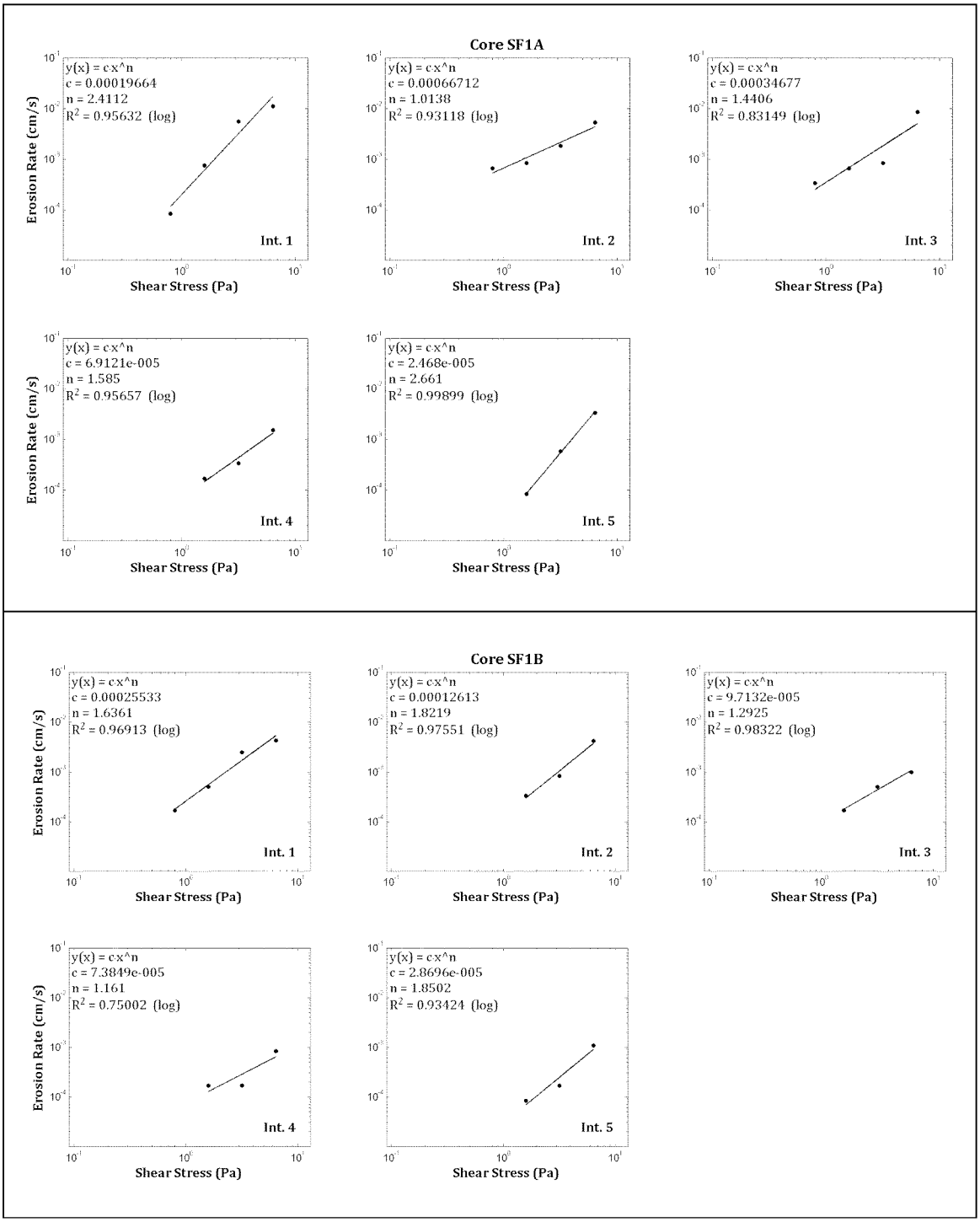

Figure 10. Power law best-fit regression solutions for SF1A (top) and SF1B (bottom).

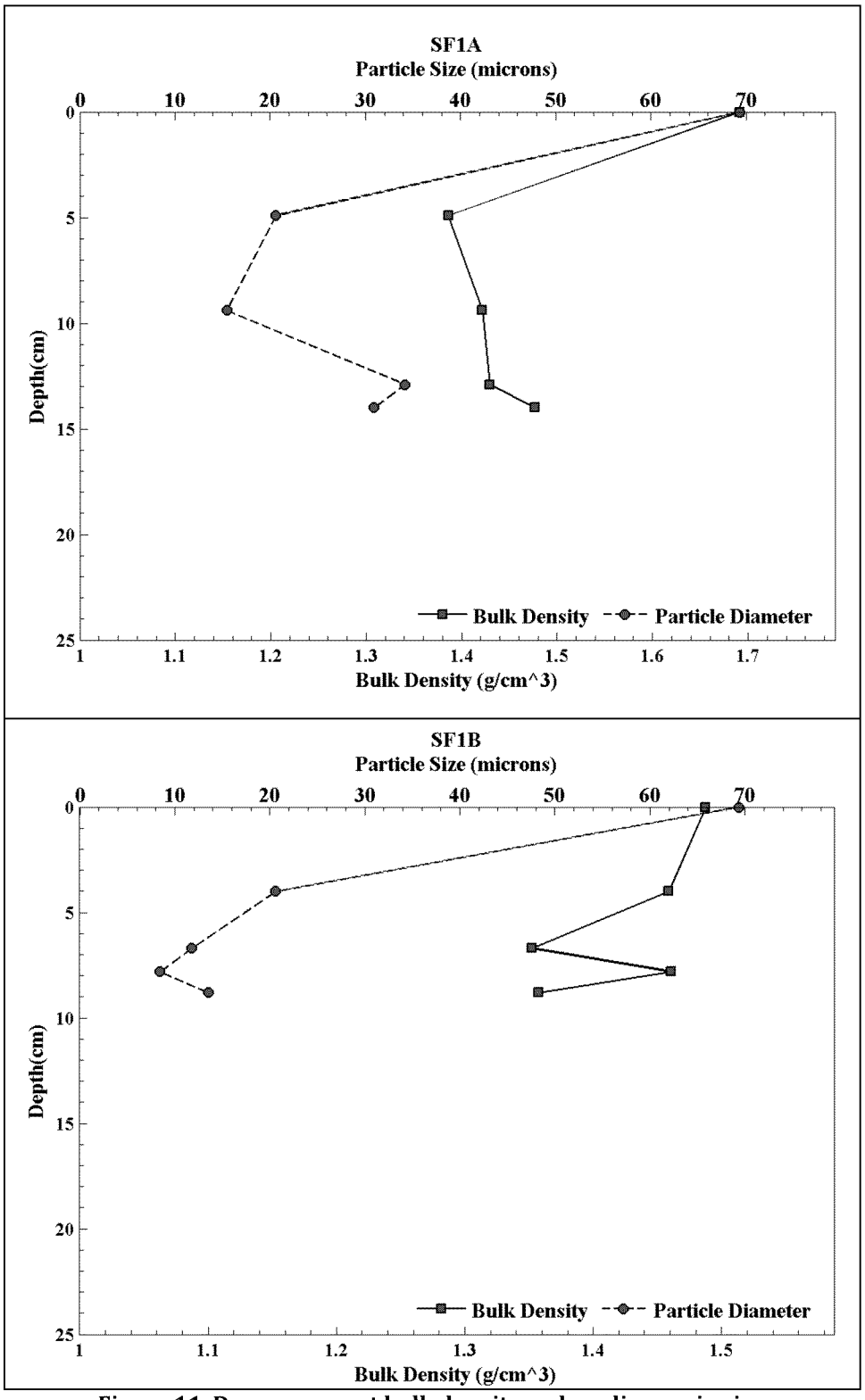

Figure 11. Down-core wet bulk density and median grain size for SF1A (top) and SF1B (bottom).

Table 4. Power law best-fit variables for the measured depth intervals in SF1A.

Depth Interval	Interval Start Depth (cm)	Interval End Depth (cm)	A	n	r^2
1	0.00	4.40	0.000197	2.41	0.96
2	4.90	8.90	0.000667	1.01	0.93
3	9.40	12.90	0.000347	1.44	0.83
4	12.90	14.10	0.000069	1.58	0.96
5	14.10	16.50	0.000025	2.66	1.00

Table 5. Power law best-fit variables for the measured depth intervals in SF1B.

Depth Interval	Interval Start Depth (cm)	Interval End Depth (cm)	A	n	r^2
1	0.00	3.95	0.000255	1.64	0.97
2	4.00	6.70	0.000126	1.82	0.98
3	6.70	7.70	0.000097	1.29	0.98
4	7.80	8.50	0.000074	1.16	0.75
5	8.80	9.60	0.000029	1.85	0.93

Table 6. Median grain size, wet bulk density, fraction LOI and critical shear stress estimates for SF1A.

Sample Depth (cm)	Grain Size (µm)	Wet Bulk Density (g/cm^3)	Fraction LOI	τ_0 (Pa)	τ_1 (Pa)	τ_{linear} (Pa)	τ_{power} (Pa)
0.00	69.33	1.69	0.08	0.40	0.80	0.80	0.76
4.90	20.60	1.39	0.08	0.40	0.80	0.46	0.15
9.40	15.45	1.42	0.07	0.40	0.80	0.52	0.42
12.90	34.20	1.43	0.10	0.80	1.60	1.28	1.26
14.10	30.93	1.48	0.09	0.80	1.60	1.60	1.69
Mean	**34.10**	**1.48**	**0.08**	**0.56**	**1.12**	**0.93**	**0.86**

Table 7. Median grain size, wet bulk density, fraction LOI and critical shear stress estimates for SF1B.

Sample Depth (cm)	Grain Size (µm)	Wet Bulk Density (g/cm^3)	Fraction LOI	τ_0 (Pa)	τ_1 (Pa)	τ_{linear} (Pa)	τ_{power} (Pa)
0.00	69.37	1.49	0.05	0.40	0.80	0.64	0.56
4.00	20.61	1.46	0.07	0.80	1.60	1.04	0.88
6.70	11.73	1.35	0.08	0.80	1.60	1.28	1.02
7.80	8.45	1.46	0.07	0.80	1.60	1.28	1.30
8.80	13.50	1.36	0.10	0.80	1.60	1.60	1.96
Mean	**24.73**	**1.42**	**0.07**	**0.72**	**1.44**	**1.17**	**1.15**

2.4.2 CORES SF2A AND SF2B

Cores SF2A and SF2B were collected from the mudflat west of the extreme western extent of the mouth of the Hackensack River. Core SF2A comprised of 2-4 cm of tan-colored, low-density silt and fine sand on the surface, with some fine organic material visible. One 1 cm long snail was observed at the downstream end of the core (when loaded into SEDFlume). Darker-colored silt and fine sand was visible below, with lenses of sand visible further down-core. Core SF2B also consisted of 2-4 cm of tan-colored, low-density silt and fine sand on the surface. Darker-colored silt and fine sand existed at the next layer down, and a layer of coarse sand was visible beginning at a depth of 30 cm. Small worms and fine organics were visible within the surface fluff layer. Both cores comprised primarily of silt and fine sand at deeper depths.

A photograph of the cores aligned with each other is presented in Figure 12. Their respective erosion rate data are plotted in Figure 13. Shear stresses ranging between 0.1 and 6.4 Pa were applied to these cores. The intra-core variation of the depth intervals evaluated in each core are shown in Figure 14. The erosion rates in SF2A generally decreased with depth. The erosion rate *ratios* in both cores generally decreased with depth.

The power law regression fit within each depth interval of the cores is illustrated in Figure 15. Coefficients and regression statistics from the power law analysis are presented in Table 8 and Table 9 for the cores, respectively. The measured median grain sizes, and the computed wet bulk densities and critical shear stresses for each depth interval are provided in Table 10 and Table 11.

The vertical profiles of d_{50} and ρ_b from each core are shown in Figure 16. For both cores, the median grain size was largest at the surface and decreased with depth. The surface median grain size in each core was 38.04 µm and 44.95 µm for SF2A and SF2B, respectively (coarse silt for both). The core-averaged d_{50} in cores SF2A and SF2B was 24.10 µm and 23.18 µm, respectively (medium silt for both).

The wet bulk density in SF2A was lowest at the surface and generally increased with depth into the core. In SF2B, the wet bulk density increased immediately below the surface, and then decreased slightly with depth. The core-averaged wet bulk density in the cores was 1.49 g/cm^3 and 1.46 g/cm^3 for SF2A and SF2B, respectively.

The critical shear stress estimates in each core generally increased with depth, though the down-core magnitudes calculated at deeper depths in SF2A were larger than those in SF2B. The core-averaged linearly interpolated critical shear stress estimates were 0.68 Pa and 0.57 Pa for SF2A and SF2B, respectively; the core-averaged power law estimates were 0.86 Pa and 0.62 Pa for the cores, respectively.

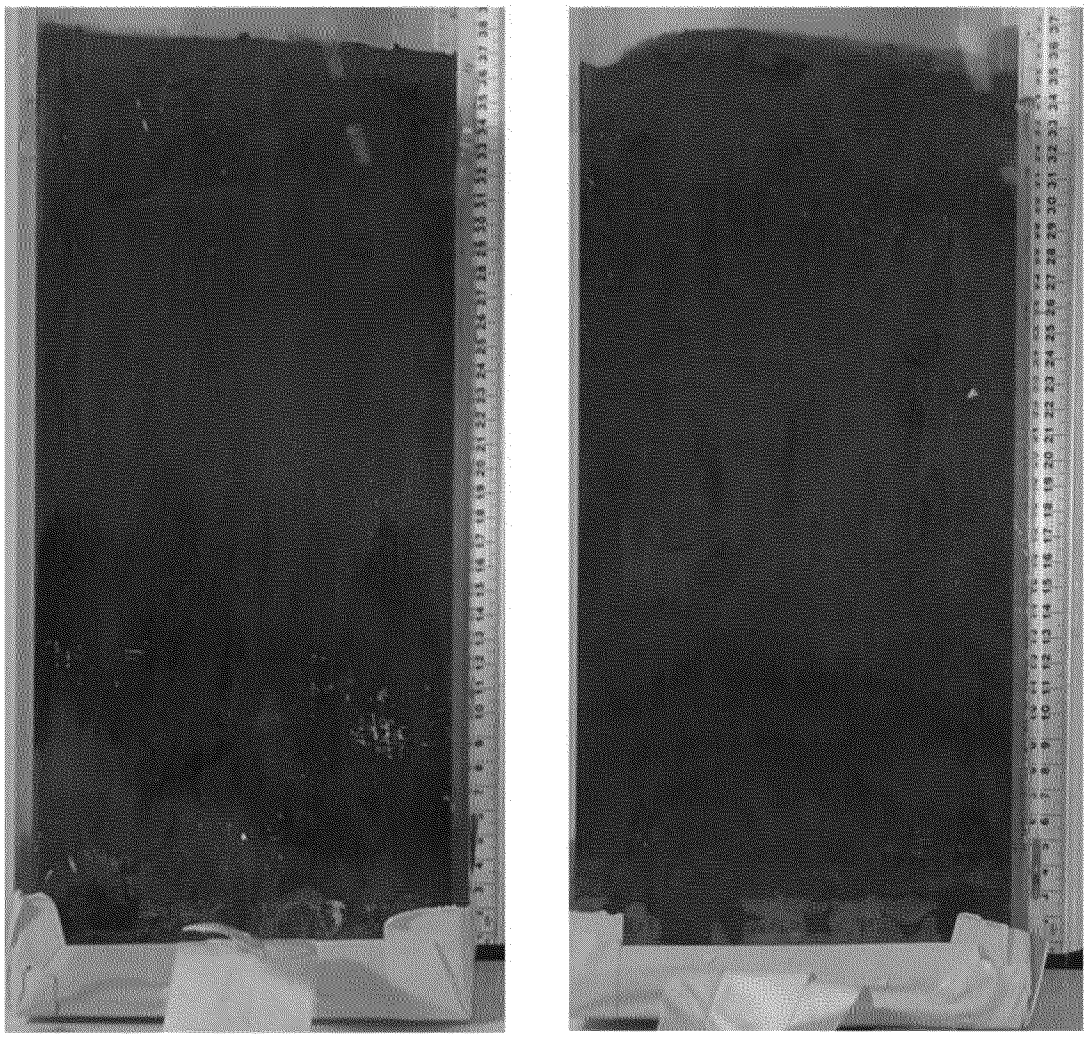

Figure 12. Pre-processing photo of cores SF2A (left) and SF2B (right).

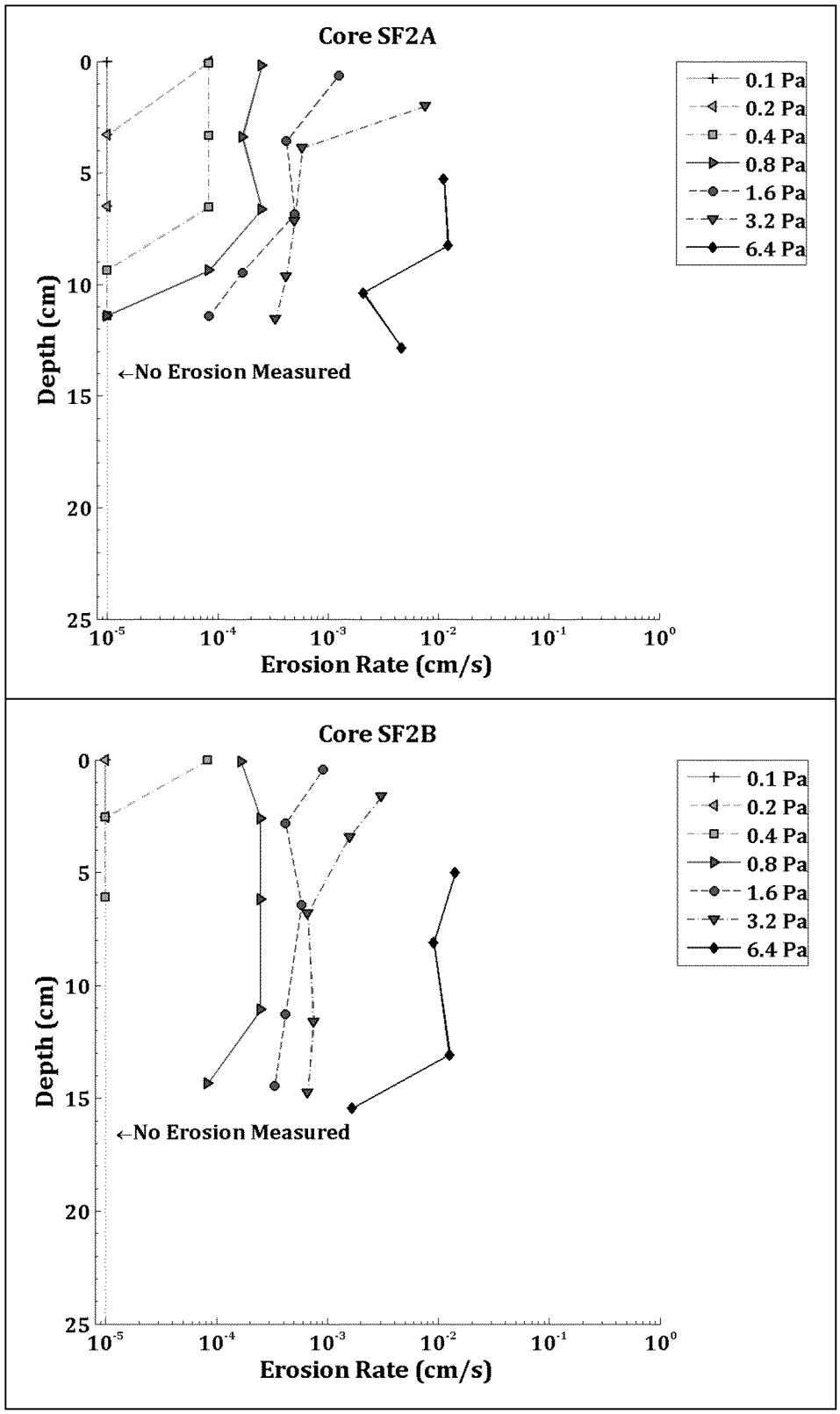

Figure 13. Down-core erosion rates for SF2A (top) and SF2B (bottom).

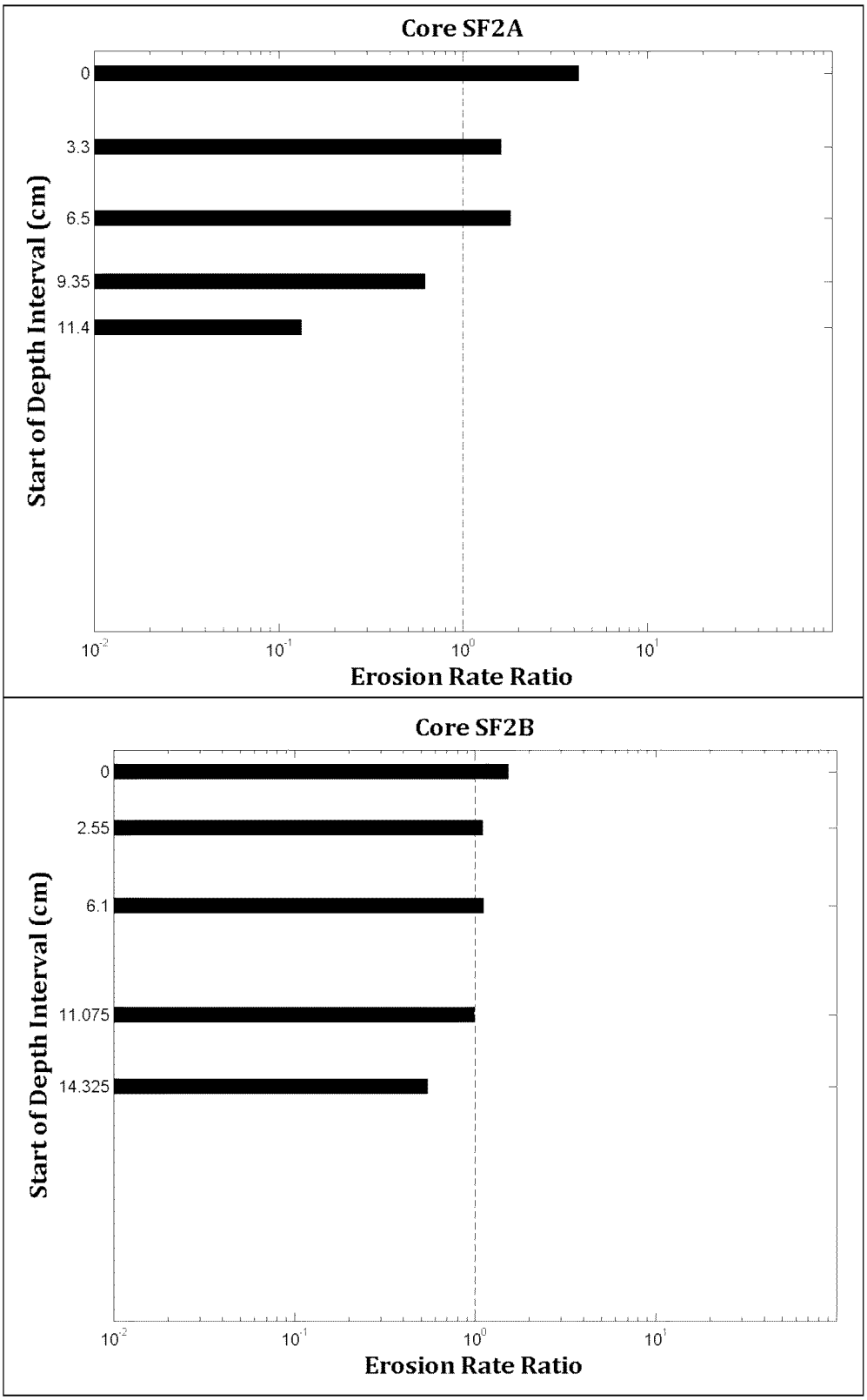

Figure 14. Intra-core erosion rate ratios for SF2A (top) and SF2B (bottom).

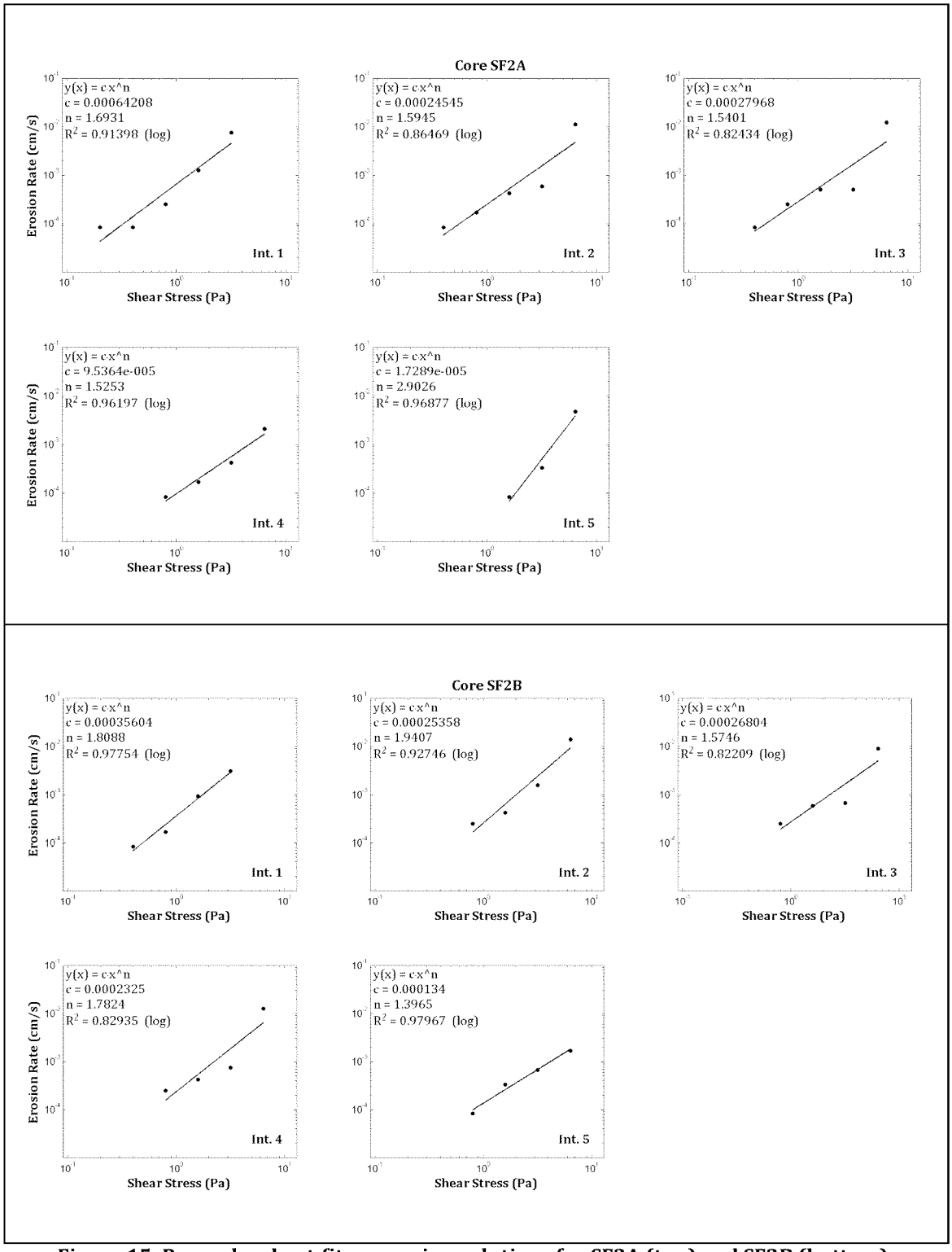

Figure 15. Power law best-fit regression solutions for SF2A (top) and SF2B (bottom).

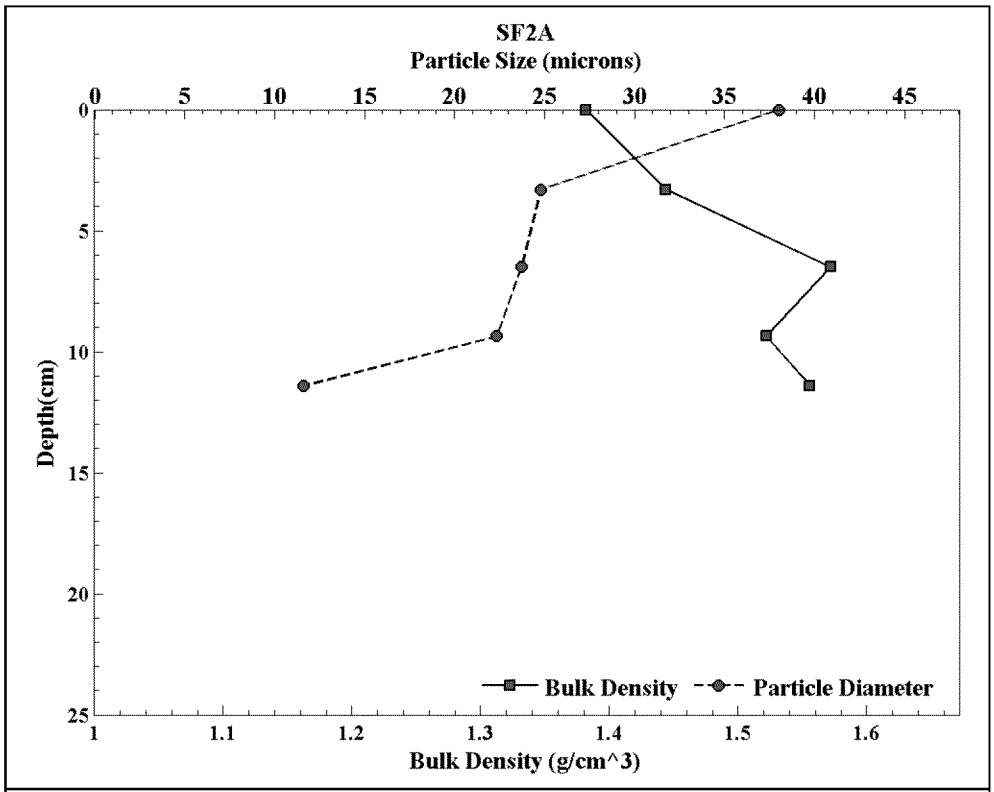

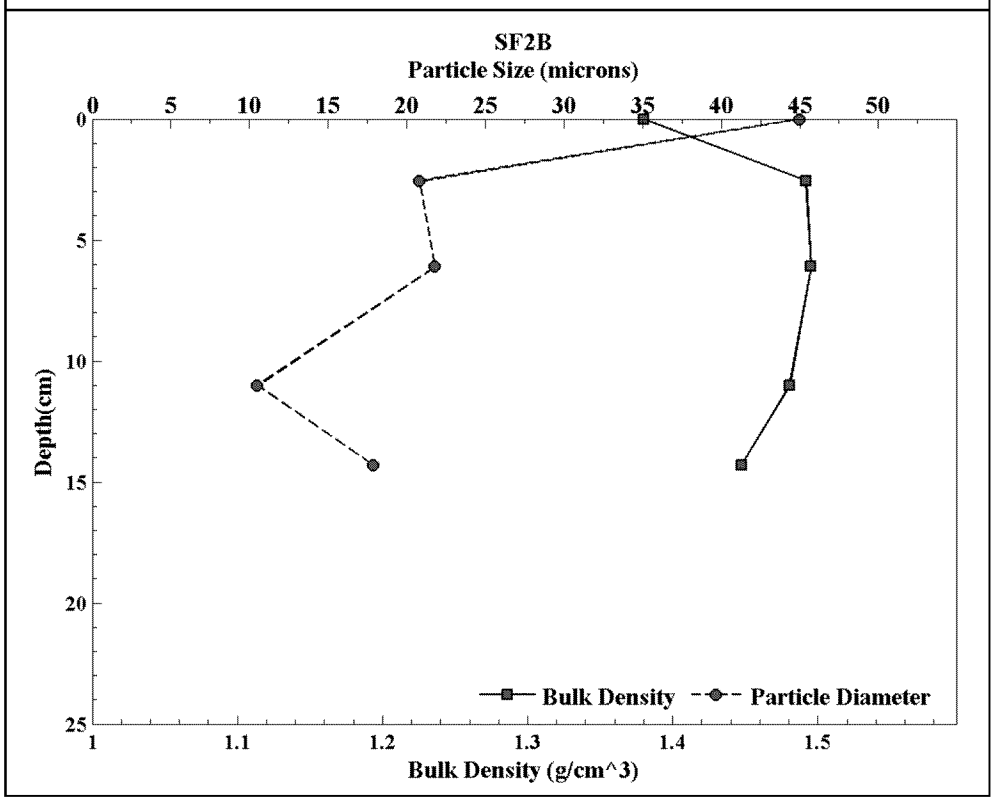

Figure 16. Down-core wet bulk density and median grain size for SF2A (top) and SF2B (bottom).

Table 8. Power law best-fit variables for the measured depth intervals in SF2A.

Depth Interval	Interval Start Depth (cm)	Interval End Depth (cm)	A	n	r^2
1	0.00	3.00	0.000642	1.69	0.91
2	3.30	6.50	0.000245	1.59	0.86
3	6.50	9.20	0.000280	1.54	0.82
4	9.35	11.00	0.000095	1.53	0.96
5	11.40	14.05	0.000017	2.90	0.97

Table 9. Power law best-fit variables for the measured depth intervals in SF2B.

Depth Interval	Interval Start Depth (cm)	Interval End Depth (cm)	A	n	r^2
1	0.00	2.55	0.000356	1.81	0.98
2	2.55	6.10	0.000254	1.94	0.93
3	6.10	9.20	0.000268	1.57	0.82
4	11.00	14.30	0.000233	1.78	0.83
5	14.30	15.95	0.000134	1.40	0.98

Table 10. Median particle size, wet bulk density, fraction LOI and critical shear stress estimates for SF2A.

Sample Depth (cm)	Grain Size (μm)	Wet Bulk Density (g/cm³)	Fraction LOI	τ_0 (Pa)	τ_1 (Pa)	τ_{linear} (Pa)	τ_{power} (Pa)
0.00	38.04	1.38	0.06	0.10	0.20	0.20	0.33
3.30	24.78	1.44	0.06	0.20	0.40	0.40	0.57
6.50	23.71	1.57	0.05	0.20	0.40	0.40	0.51
9.35	22.34	1.52	0.05	0.40	0.80	0.80	1.03
11.40	11.63	1.56	0.05	0.80	1.60	1.60	1.83
Mean	**24.10**	**1.49**	**0.05**	**0.34**	**0.68**	**0.68**	**0.86**

Table 11. Median particle size, wet bulk density, fraction LOI and critical shear stress estimates for SF2B.

Sample Depth (cm)	Grain Size (μm)	Wet Bulk Density (g/cm³)	Fraction LOI	τ_0 (Pa)	τ_1 (Pa)	τ_{linear} (Pa)	τ_{power} (Pa)
0.00	44.95	1.38	0.05	0.20	0.40	0.40	0.50
2.55	20.81	1.49	0.05	0.40	0.80	0.56	0.62
6.10	21.79	1.50	0.06	0.40	0.80	0.56	0.53
11.10	10.50	1.48	0.05	0.40	0.80	0.54	0.62
14.30	17.85	1.45	0.07	0.40	0.80	0.80	0.81
Mean	**23.18**	**1.46**	**0.06**	**0.36**	**0.72**	**0.57**	**0.62**

2.4.3 CORES SF3A AND SF3B

Cores SF3A and SF3B were collected from within the navigation channel limits of the mouth of the Passaic River. It was very difficult to obtain undisturbed cores at this location. The core material in both cores consisted of a large amount of organic material (leaves and twigs). The organic material likely caused the core structure to be very porous. As the cores were extracted and brought out of the water, a large amount of trapped air expanded and percolated up through the core, causing disturbances to the core structure and surface. Because the one-way valve at the top of the core barrel provided a vacuum to retain the material in the core during extraction, once the coring system broke the water surface, the porous core material allowed air to be pulled through the sediment due to the overlying vacuum. As a result, many of the initial core recoveries failed, requiring a large number of attempts to retrieve acceptable cores for analysis. The cores that were successfully collected are described here.

The surface of core SF3A comprised a light-colored 1 cm sediment layer over a tan-colored 5 cm silty layer of material. At deeper depths, the sediment was darker-colored and some air pockets (gas pockets) were visible. Throughout the core, the core was observed to contain a large amount of organic material (leaves and sticks) mixed with silty and sandy sediment. A strong petroleum odor was sensed at the deepest analyzed depth interval. The surface of core SF3B consisted of 2-3 cm of a tan-colored, low-density silt layer. The top 6-7 cm of SF3B, including the surface, comprised loosely and loose-clumped material entrained with organic material. This core also contained a large amount of organic material down-core, mixed with silts and sands. In both cores, the material became stiffer and more difficult to erode with depth.

A photograph of the cores aligned with each other is presented in Figure 17. Their respective erosion rate data are plotted in Figure 18. Shear stresses ranging between 0.1 and 6.4 Pa were applied to these cores (the maximum shear stress applied to SF3B was 3.2 Pa). The intra-core erosion rate ratios of the depth intervals in each core are shown in Figure 19. The erosion rates and ratios varied little with depth. The exception was one depth interval in each that was significantly more susceptible to erosion (at a depth of 12.5 cm in SF3A and at the surface in SF3B).

The power law regression fit within each depth interval of the cores is illustrated in Figure 20. Coefficients and regression statistics from the power law analysis are presented in Table 12 and Table 13 for the cores, respectively. The measured median grain sizes, and the computed wet bulk densities and critical shear stresses for each depth interval are provided in Table 14 and Table 15.

The vertical profiles of d_{50} and ρ_b from each core are presented in Figure 21. For both cores, the median grain size was largest at the surface with depth. The core-averaged d_{50} in SF3A and SF3B was 32.75 µm (coarse silt) and 29.7 µm (medium silt), respectively.

The wet bulk density in SF3A varied from a maximum of 1.38 g/cm^3 at a depth of 5.20 cm to a minimum of 1.24 g/cm^3 at a depth of 12.90 cm. The wet bulk density in SF3B varied

between a maximum of 1.38 g/cm^3 at the surface and a minimum of 1.23 g/cm^3 at a depth of 10.20 cm. The core-averaged wet bulk density in the cores was 1.33 g/cm^3 and 1.28 g/cm^3 for SF3A and SF3B, respectively.

The critical shear stress estimates in each core indicated little variation with depth. The overall core-averages were similar between SF3A and SF3B: The linearly interpolated critical shear stress estimates were 0.38 Pa and 0.40 Pa for cores SF3A and SF3B, respectively; the power law estimates were 0.30 Pa and 0.35 Pa, respectively.

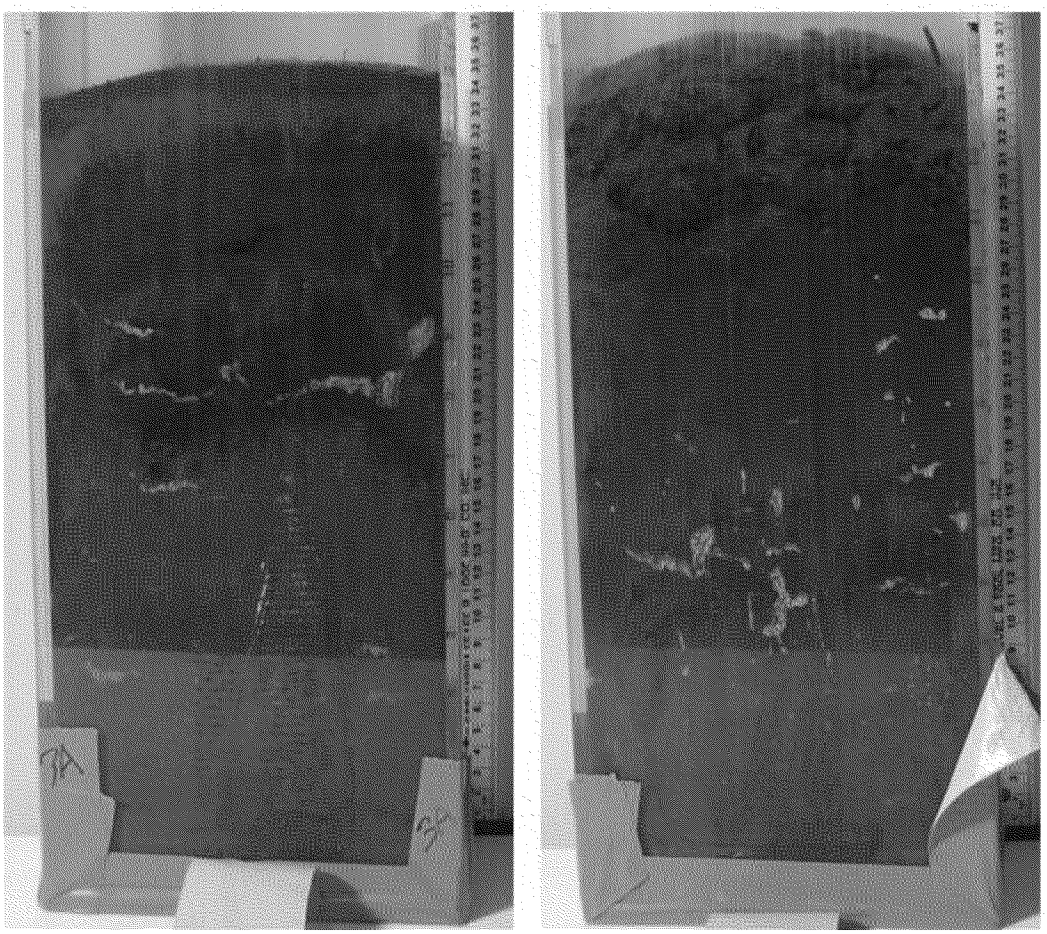

Figure 17. Pre-processing photo of cores SF3A (left) and SF3B (right).

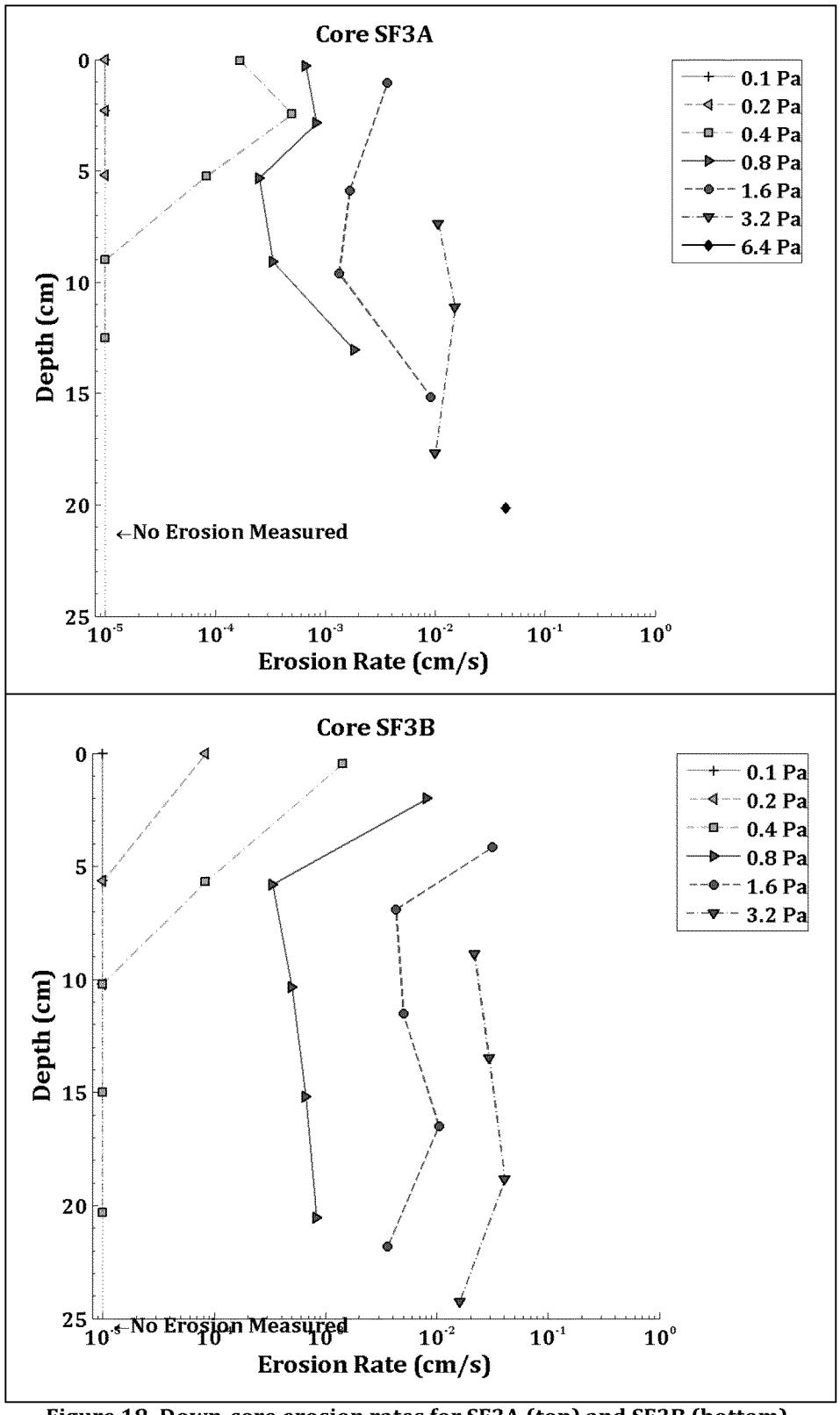

Figure 18. Down-core erosion rates for SF3A (top) and SF3B (bottom).

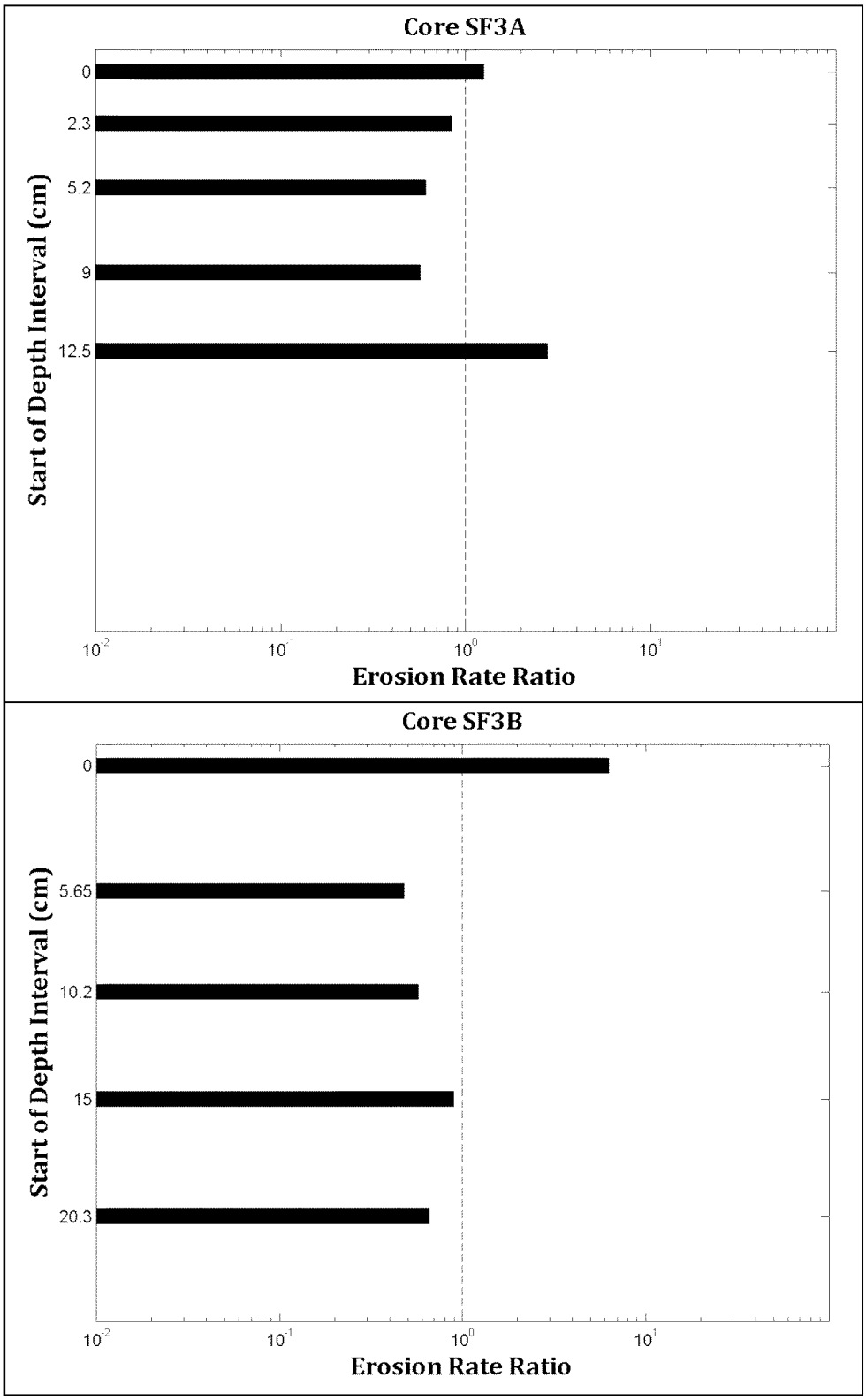

Figure 19. Intra-core erosion rate ratios for SF3A (top) and SF3B (bottom).

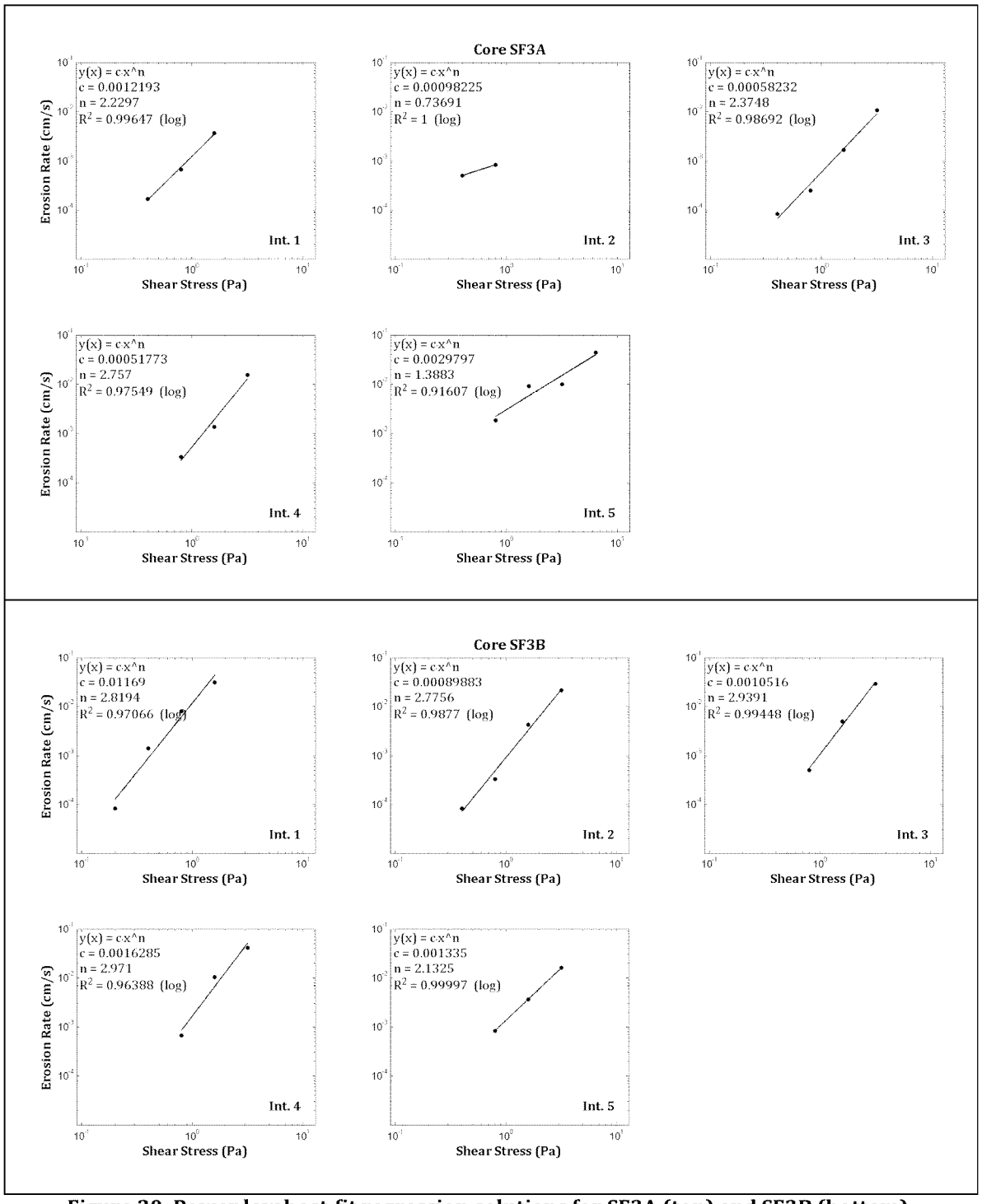

Figure 20. Power law best-fit regression solutions for SF3A (top) and SF3B (bottom).

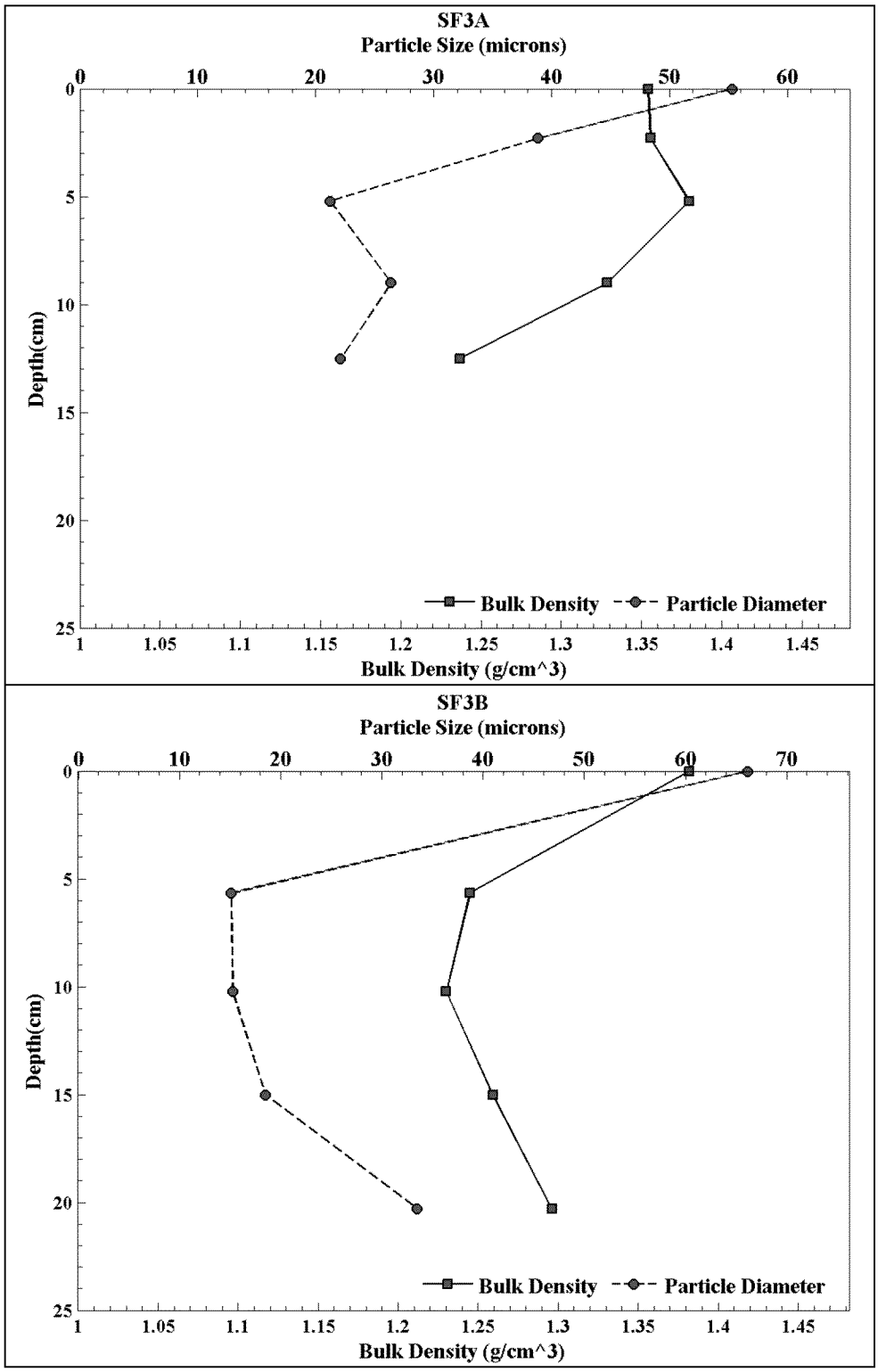

Figure 21. Down-core wet bulk density and median grain size for SF3A (top) and SF3B (bottom).

Table 12. Power law best-fit variables for specified depth intervals in core SF3A.

Depth Interval	Interval Start Depth (cm)	Interval End Depth (cm)	A	n	r^2
1	0.00	1.60	0.001219	2.23	1.00
2	2.30	3.10	0.000982	0.74	1.00
3	5.20	8.40	0.000582	2.37	0.99
4	9.00	12.30	0.000518	2.76	0.98
5	12.50	21.60	0.002980	1.39	0.92

Table 13. Power law best-fit variables for specified depth intervals in core SF3B.

Depth Interval	Interval Start Depth (cm)	Interval End Depth (cm)	A	n	r^2
1	0.00	5.20	0.011690	2.82	0.97
2	5.65	9.90	0.000899	2.78	0.99
3	10.20	14.50	0.001052	2.94	0.99
4	15.00	20.10	0.001629	2.97	0.96
5	20.30	25.70	0.001335	2.13	1.00

Table 14. Median particle size, wet bulk density, fraction LOI and critical shear stress estimates for SF3A.

Sample Depth (cm)	Grain Size (μm)	Wet Bulk Density (g/cm^3)	Fraction LOI	τ_0 (Pa)	τ_1 (Pa)	τ_{linear} (Pa)	τ_{power} (Pa)
0.00	55.28	1.35	0.07	0.20	0.40	0.32	0.33
2.30	38.81	1.36	0.06	0.20	0.40	0.24	0.05
5.20	21.21	1.38	0.09	0.20	0.40	0.40	0.48
9.00	26.37	1.33	0.09	0.40	0.80	0.52	0.55
12.50	22.09	1.24	0.14	0.40	0.80	0.43	0.09
Mean	**32.75**	**1.33**	**0.09**	**0.28**	**0.56**	**0.38**	**0.30**

Table 15. Median particle size, wet bulk density, fraction LOI and critical shear stress estimates for SF3B.

Sample Depth (cm)	Grain Size (μm)	Wet Bulk Density (g/cm^3)	Fraction LOI	τ_0 (Pa)	τ_1 (Pa)	τ_{linear} (Pa)	τ_{power} (Pa)
0.00	66.16	1.38	0.11	0.10	0.20	0.20	0.18
5.65	15.12	1.24	0.17	0.20	0.40	0.40	0.45
10.20	15.24	1.23	0.15	0.40	0.80	0.48	0.45
15.00	18.53	1.26	0.13	0.40	0.80	0.46	0.39
20.30	33.50	1.30	0.13	0.40	0.80	0.45	0.30
Mean	**29.71**	**1.28**	**0.14**	**0.30**	**0.60**	**0.40**	**0.35**

2.4.4 CORES SF4A AND SF4B

Cores SF4A and SF4B were collected from the eastern mudflats along the northeast side of Newark Bay and north of the I-78/Newark Bay Bridge. Core SF4A comprised 2-3 cm of tan-colored, low-density silt on the surface, with many small benthic organisms (worms and tubes) visible. Below the surface, the material was darker-colored and became stiffer with depth, consisting of clayey-silt and sand. Sand was visible at the bottom 6 cm of the core, approximately; and an additional sediment sub-sample was collected from this material for characterization. The surface of Core SF4B consisted of a 2-3 cm low-density, tan-colored layer of silt with a large amount of fine organic material and small worms or other benthic organisms. At deeper depths, the material became stiffer and more difficult to erode, comprised of clayey-silt and fine sand.

A photograph of the cores aligned with each other is presented in Figure 22. Their respective erosion rate data are plotted in Figure 23. Shear stresses ranging between 0.1 and 12.8 Pa were applied to these cores. The intra-core erosion rate ratios of the depth intervals evaluated in each core are shown in Figure 24. In both cores, the erosion rates decreased slightly with depth, which is expected of consolidated sediments. In both, erosion susceptibility trends varied slightly with depth, but decreased at the deepest depths.

The power law regression fit within each depth interval of the cores is illustrated in Figure 25. Coefficients and regression statistics from the power law analysis are presented in Table 16 and Table 17 for the cores, respectively. The measured median grain sizes, and the computed wet bulk densities and critical shear stresses for each depth interval are provided in Table 18 and Table 19.

The vertical profiles of d_{50} and ρ_b from each core are presented in Figure 26. The median grain size in core SF4A varied very little down-core: between a minimum of 11.71 µm (fine silt) at a depth of 4.90 cm to a maximum of 16.40 µm (medium silt) at a depth of 18.40 cm. The median grain size in core SF4B also varied little down-core: between 21.94 µm (medium silt) at the surface to 24.68 µm at a depth of 13.50 cm. One exception to this generalization was in SF4B where a d_{50} of 10.87 µm (fine silt) was measured at a depth of 9.40 cm. The core-averaged d_{50} in the cores was 18.46 µm and 20.85 µm (medium silt for both), respectively.

The wet bulk density in SF4A varied between 1.25 g/cm^3 at the surface to a maximum of 1.78 g/cm^3 at a depth of 32.00 cm. The wet bulk density in SF4B was 1.26 g/cm^3 at the surface and a maximum of 1.51 g/cm^3 at a depth of 17.20 cm. The core-averaged wet bulk density in the cores was 1.47 g/cm^3 and 1.42 g/cm^3, respectively.

The critical shear stress estimates in each core fluctuated slightly with depth, but, in general, became larger down-core. The overall core-averages were similar between SF4A and SF4B: The linearly interpolated critical shear stress estimate core-averages were 0.95 Pa and 0.89 Pa, respectively; the power law estimates were 0.80 Pa and 0.74 Pa, respectively.

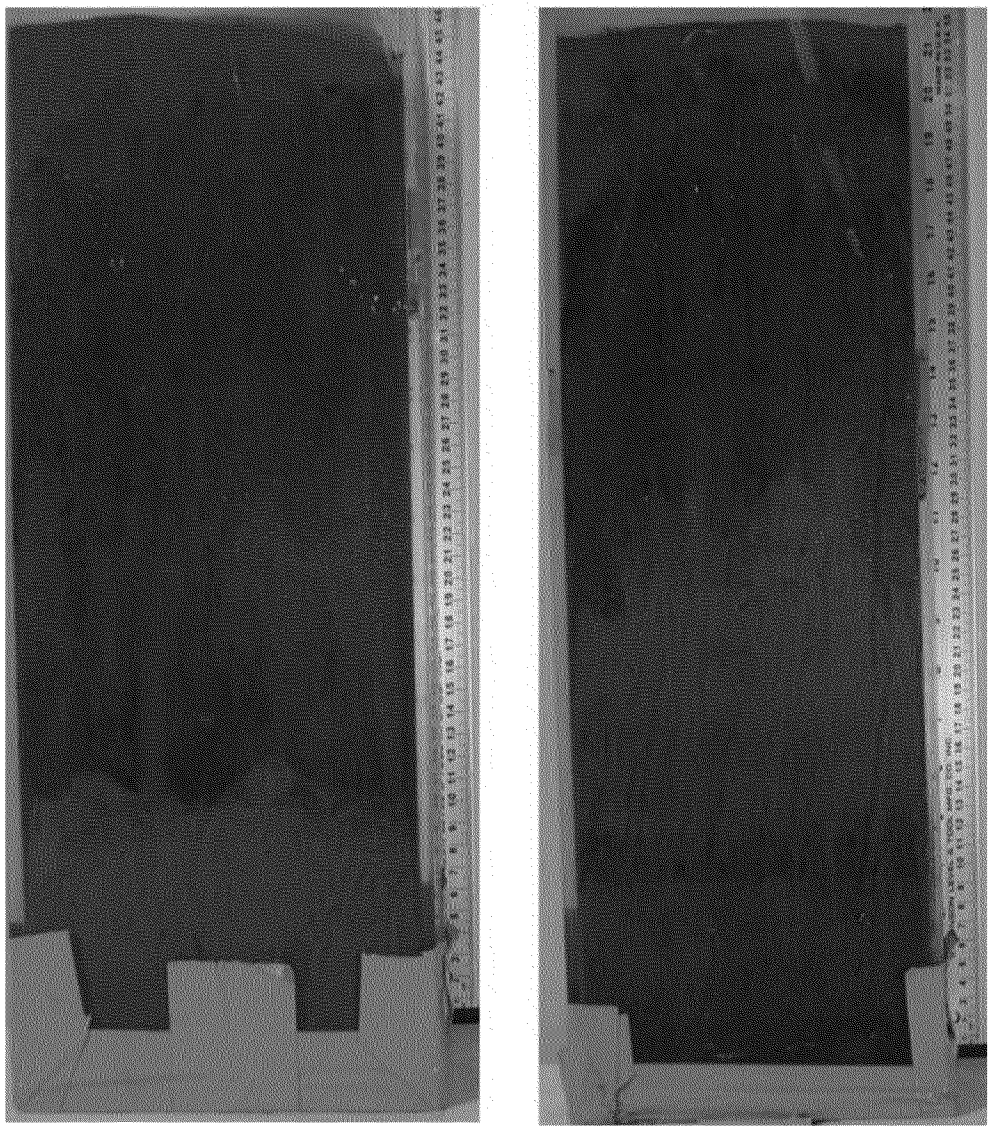

Figure 22. Pre-processing photo of cores SF4A (left) and SF4B (right).

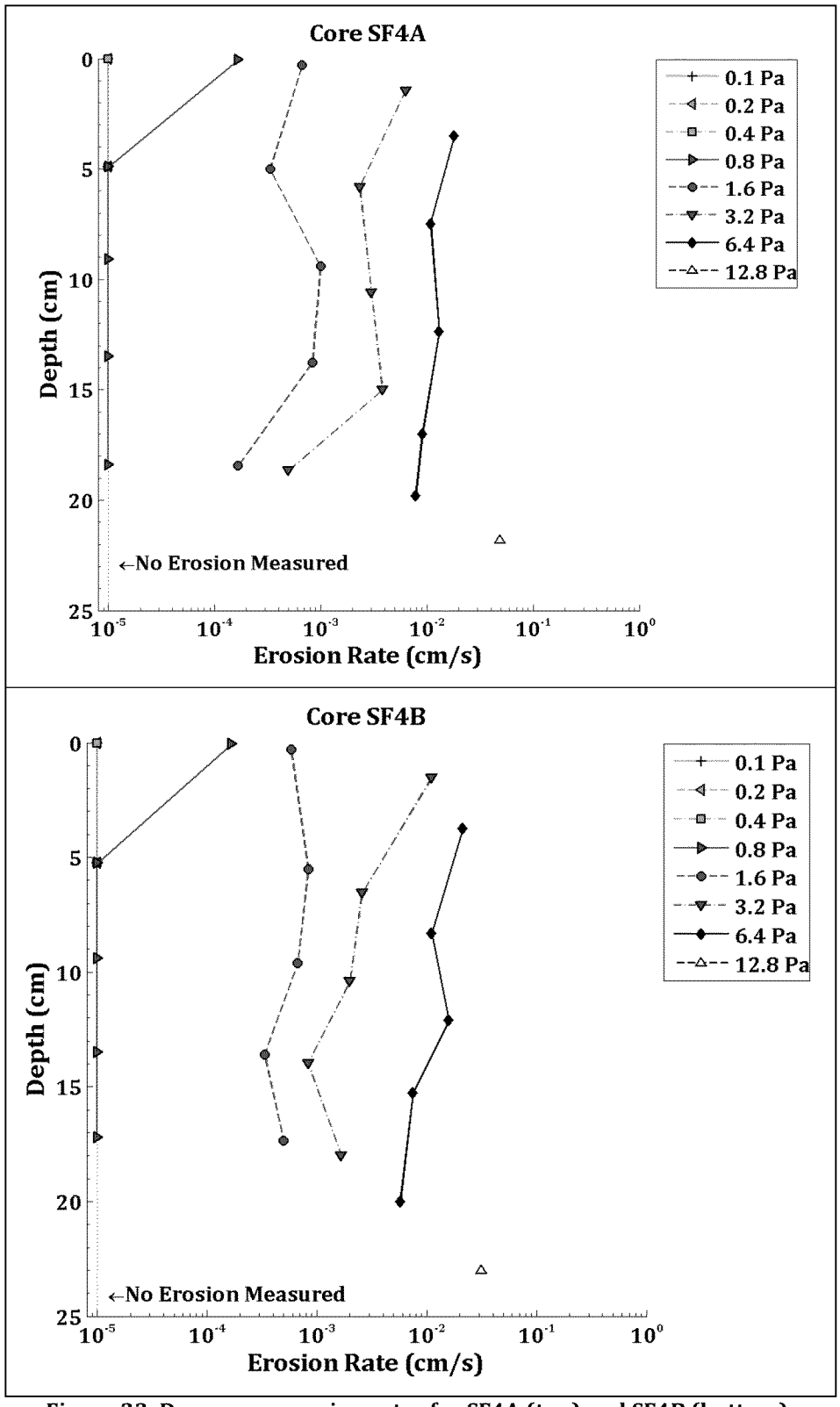

Figure 23. Down-core erosion rates for SF4A (top) and SF4B (bottom).

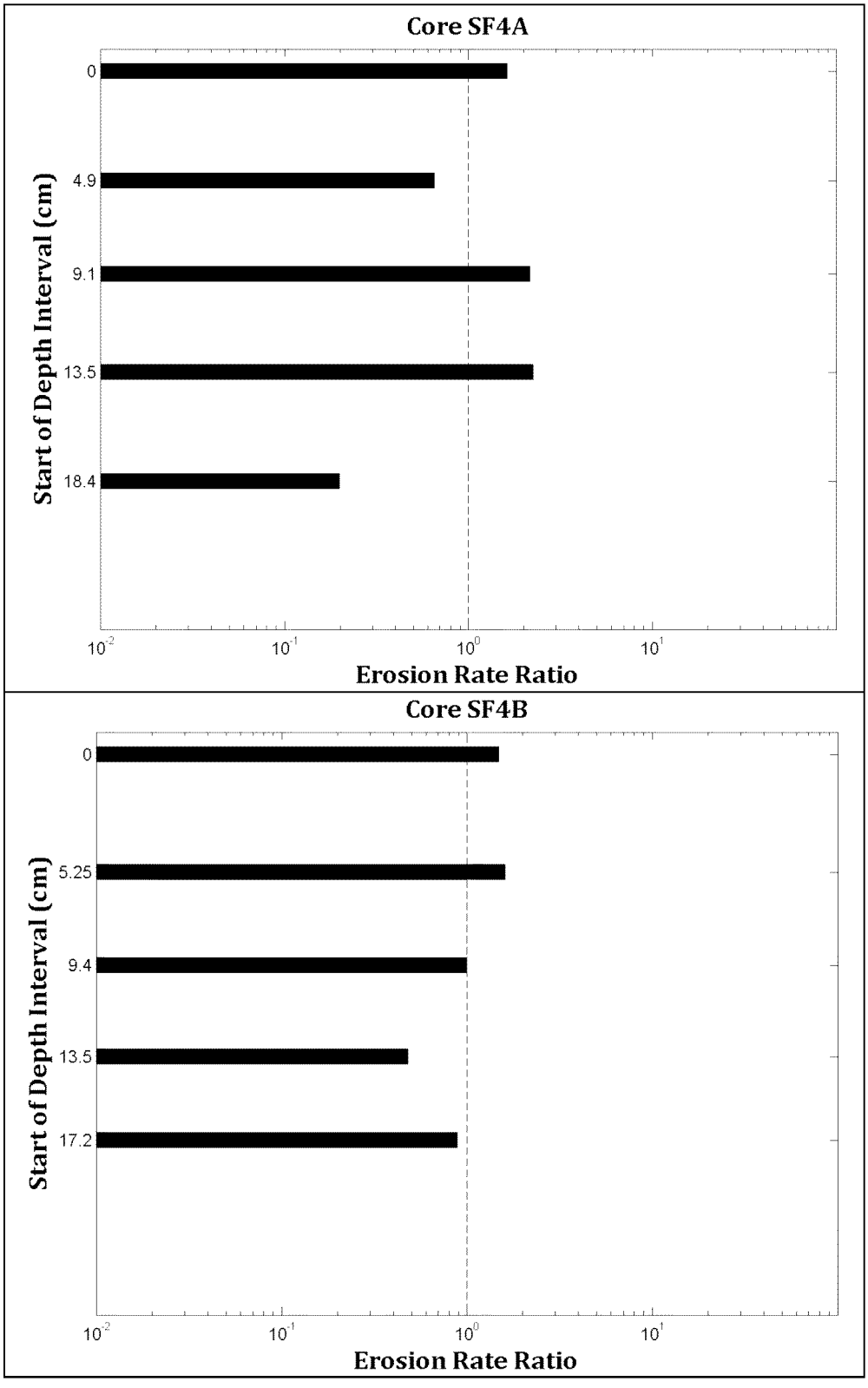

Figure 24. Intra-core erosion rate ratios for SF4A (top) and SF4B (bottom).

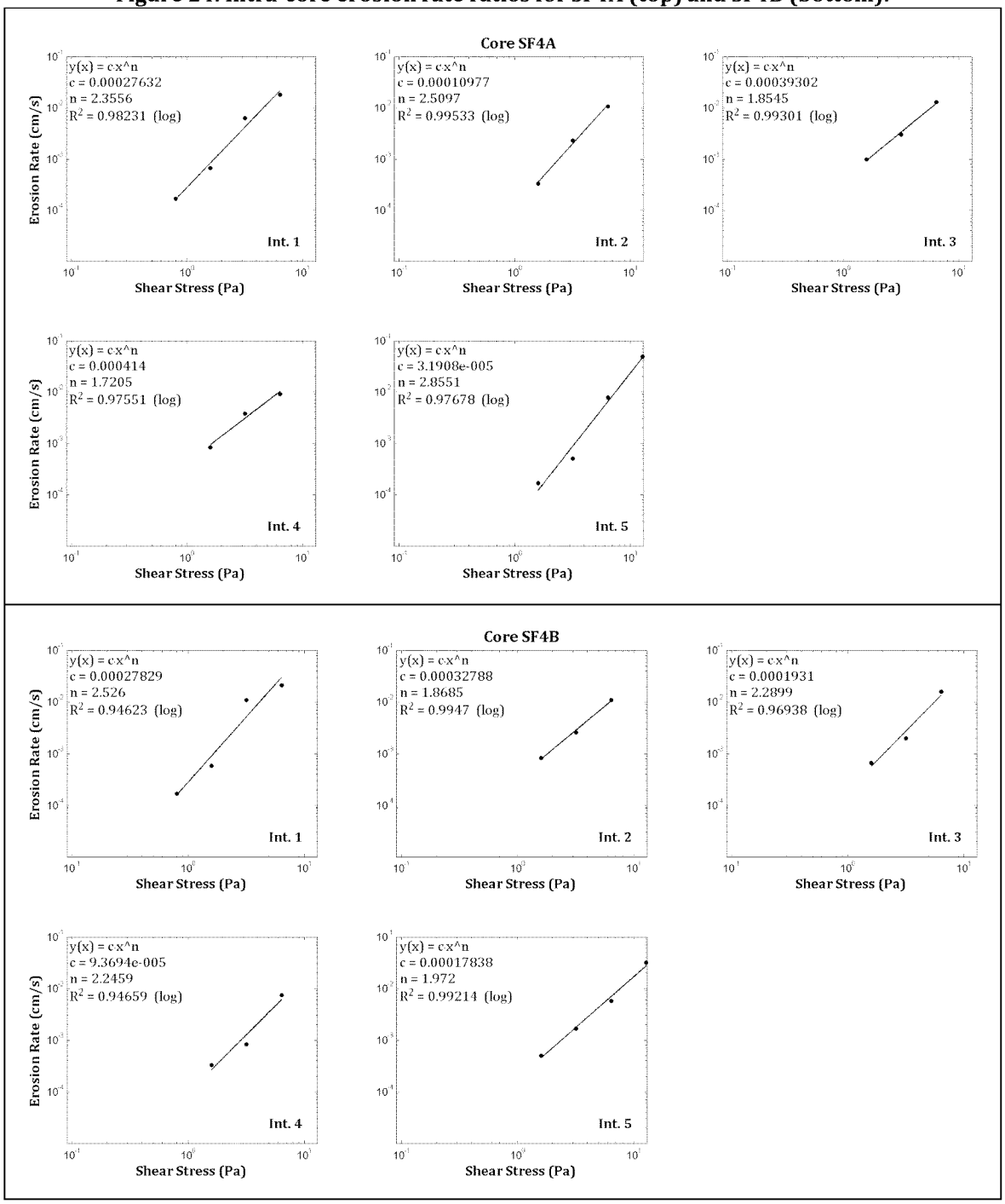

Figure 25. Power law best-fit regression solutions for SF4A (top) and SF4B (bottom).

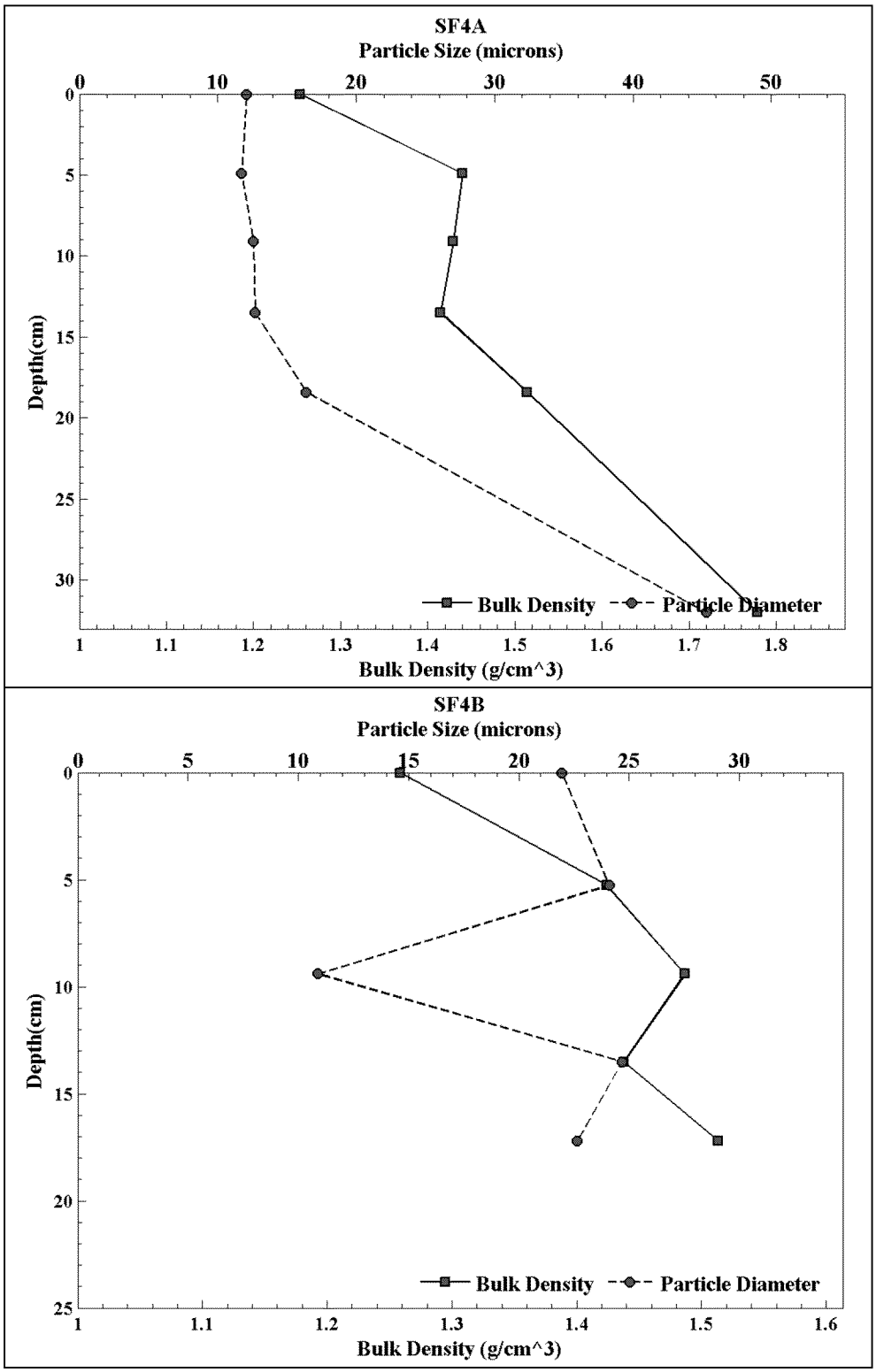

Figure 26. Down-core wet bulk density and median grain size for SF4A (top) and SF4B (bottom).

Table 16. Power law best-fit variables for the measured depth intervals in SF4A.

Depth Interval	Interval Start Depth (cm)	Interval End Depth (cm)	A	n	r^2
1	0.00	4.60	0.000276	2.36	0.98
2	4.90	8.50	0.000110	2.51	1.00
3	9.10	13.20	0.000393	1.85	0.99
4	13.50	18.00	0.000414	1.72	0.98
5	18.40	22.80	0.000032	2.86	0.98

Table 17. Power law best-fit variables for the measured depth intervals in SF4B.

Depth Interval	Interval Start Depth (cm)	Interval End Depth (cm)	A	n	r^2
1	0.00	4.85	0.000278	2.53	0.95
2	5.25	9.30	0.000328	1.87	0.99
3	9.40	13.20	0.000193	2.29	0.97
4	13.50	16.30	0.000094	2.25	0.95
5	17.20	24.50	0.000178	1.97	0.99

Table 18. Median grain size, wet bulk density, fraction LOI and critical shear stress estimates for SF4A.

Sample Depth (cm)	Grain Size (μm)	Wet Bulk Density (g/cm^3)	Fraction LOI	τ_0 (Pa)	τ_1 (Pa)	τ_{linear} (Pa)	τ_{power} (Pa)
0.00	12.08	1.25	0.08	0.40	0.80	0.64	0.65
4.90	11.71	1.44	0.07	0.80	1.60	1.04	0.96
9.10	12.57	1.43	0.07	0.80	1.60	0.89	0.48
13.50	12.70	1.41	0.07	0.80	1.60	0.90	0.44
18.40	16.40	1.51	0.06	0.80	1.60	1.28	1.49
32.00	45.29	1.78	0.12	*n/a*	*n/a*	*n/a*	*n/a*
Mean	**18.46**	**1.47**	**0.08**	**0.72**	**1.44**	**0.95**	**0.80**

Table 19. Median grain size, wet bulk density, fraction LOI and critical shear stress estimates for SF4B.

Sample Depth (cm)	Grain Size (μm)	Wet Bulk Density (g/cm^3)	Fraction LOI	τ_0 (Pa)	τ_1 (Pa)	τ_{linear} (Pa)	τ_{power} (Pa)
0.00	21.94	1.26	0.08	0.40	0.80	0.64	0.67
5.25	24.10	1.42	0.07	0.80	1.60	0.90	0.53
9.40	10.87	1.49	0.07	0.80	1.60	0.92	0.75
13.50	24.68	1.44	0.06	0.80	1.60	1.04	1.03
17.20	22.64	1.51	0.06	0.80	1.60	0.96	0.75
Mean	**20.85**	**1.42**	**0.07**	**0.72**	**1.44**	**0.89**	**0.74**

2.4.5 CORES SF5A AND SF5C

Cores SF5A and SF5C were collected from the western mudflats, along the northwest side of Newark Bay and south of the I-78/Newark Bay Bridge. Core SF5A comprised 2-3 cm of tan-colored, silt and fine sand on the surface, with darker-colored material at depths of 2-6 cm; and then even darker-colored material visible from 6-24 cm. At 24 cm, the material was tan-colored which persisted to the bottom of the core. There was sand and fine sand throughout the core. The tan-colored material at a depth of 24 cm was very stiff material, sufficient to cause bending of the metal sampling spoon during sampling.

The surface of core SF5C consisted of 3-4 cm of tan-colored silt and fine sand with worms or stringy organic material visible at, and immediately beneath the surface layer. Dark gray-colored silty material existed beneath the surface, and a tan-colored clayey material existed at depths deeper than this, similarly to core SF5A. Material in both cores became stiffer and more difficult to erode with depth.

A photograph of the cores aligned with each other is presented in Figure 27. Their respective erosion rate data are plotted in Figure 28. Shear stresses ranging between 0.1 and 6.4 Pa were applied to these cores. The intra-core variation of the depth intervals evaluated in each core are shown in Figure 29. In general, the erosion rates and ratios decreased with depth into the cores.

The power law regression fit within each depth interval of the cores is illustrated in Figure 30. Coefficients and regression statistics from the power law analysis are presented in Table 20 and Table 21 for the cores, respectively. The measured median grain sizes, and the computed wet bulk densities and critical shear stresses for each depth interval are provided in Table 22 and Table 23.

The vertical profiles of d_{50} and ρ_b from each core are shown in Figure 31. The median grain size in SF5A varied between 33.56 µm (coarse silt) at a depth of 3.90 cm and 15.06 µm (fine silt) at a depth of 15.70 cm. The median grain size in SF5C decreased with depth from 31.87 µm (coarse silt) at the surface to 14.32 µm (fine silt) at a depth of 12.20 cm. The core-averaged d_{50} in SF5A and SF5C was 22.36 µm and 21.11 µm (medium silt for both cores), respectively.

The wet bulk density in SF5A varied between 1.45 g/cm^3 at the surface and 1.67 g/cm^3 at a depth of 15.70 cm. The wet bulk density in SF5C was 1.38 g/cm^3 at the surface and 1.80 g/cm^3 at a depth of 15.30 cm. The core-averaged wet bulk density in SF5A was 1.57 g/cm^3 and 1.60 g/cm^3, respectively.

The critical shear stress estimates in each core increased with increasing depth into the core. The overall core-averages were similar between SF5A and SF5C: The linearly interpolated critical shear stress estimate core-averages were 0.80 Pa and 0.91 Pa, respectively; the power law estimates were 0.80 Pa and 0.99 Pa, respectively.

Figure 27. Pre-processing photo of cores SF5A (left) and SF5C (right).

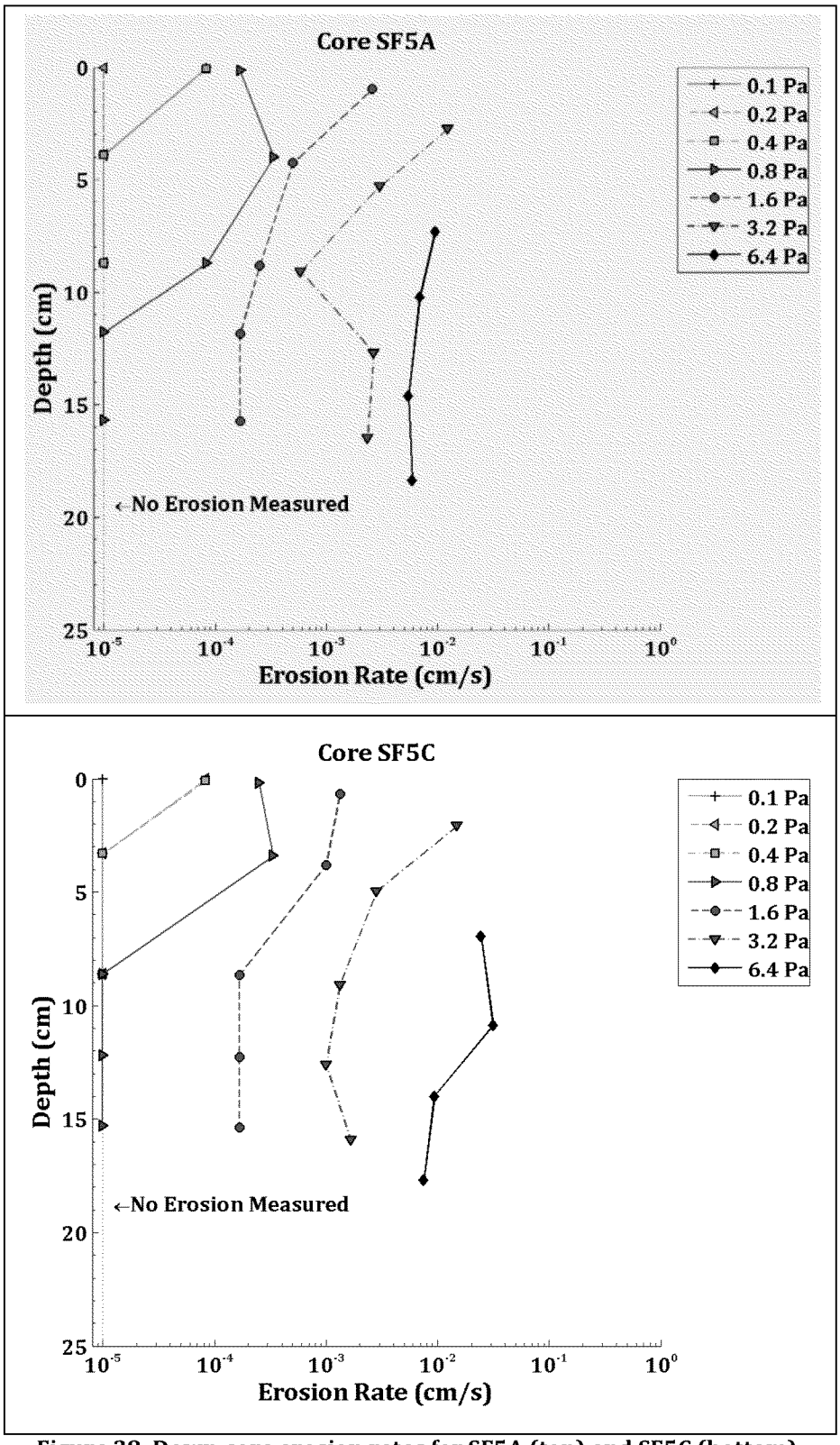

Figure 28. Down-core erosion rates for SF5A (top) and SF5C (bottom).

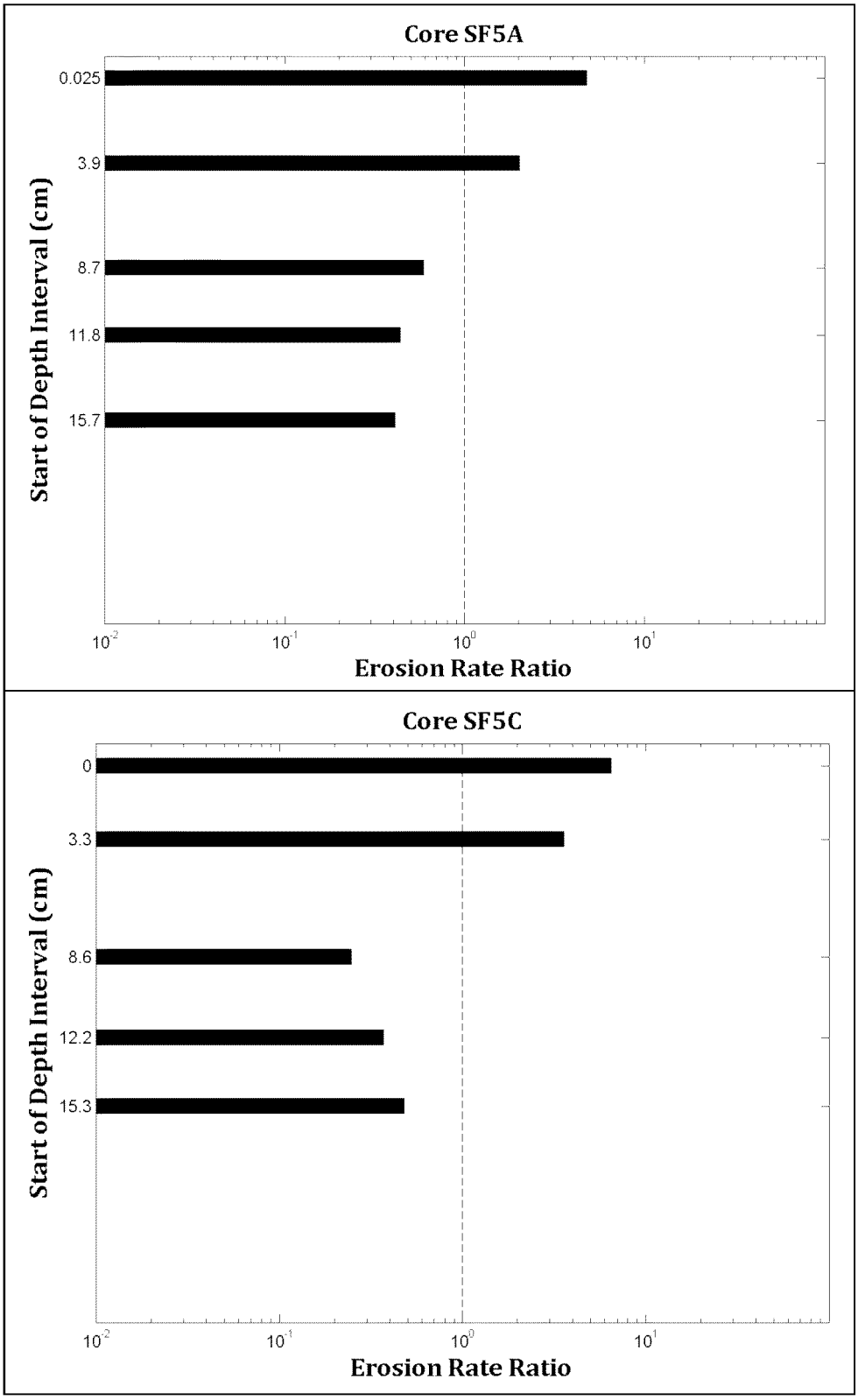

Figure 29. Intra-core erosion rate ratios for SF5A (top) and SF5C (bottom).

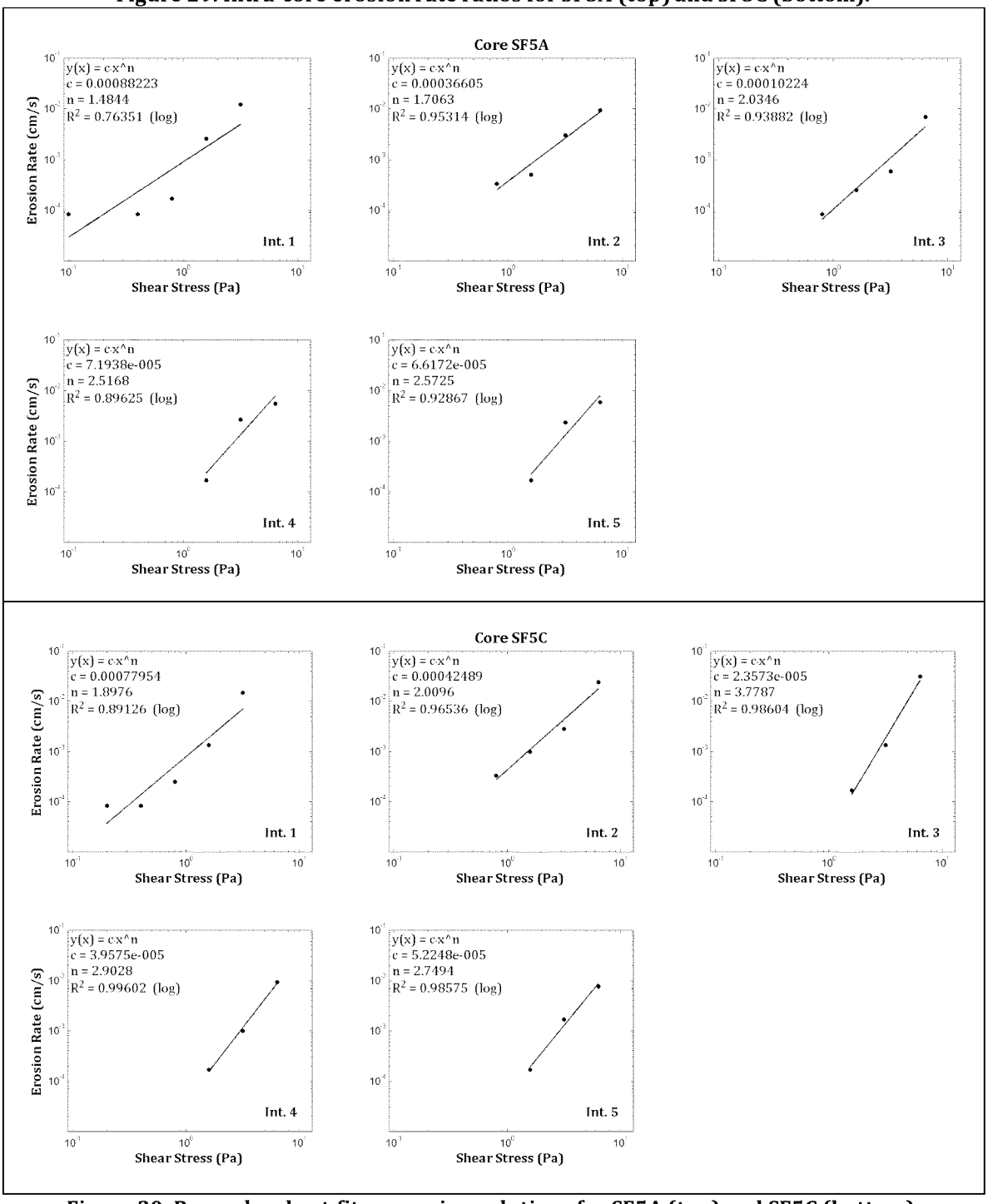

Figure 30. Power law best-fit regression solutions for SF5A (top) and SF5C (bottom).

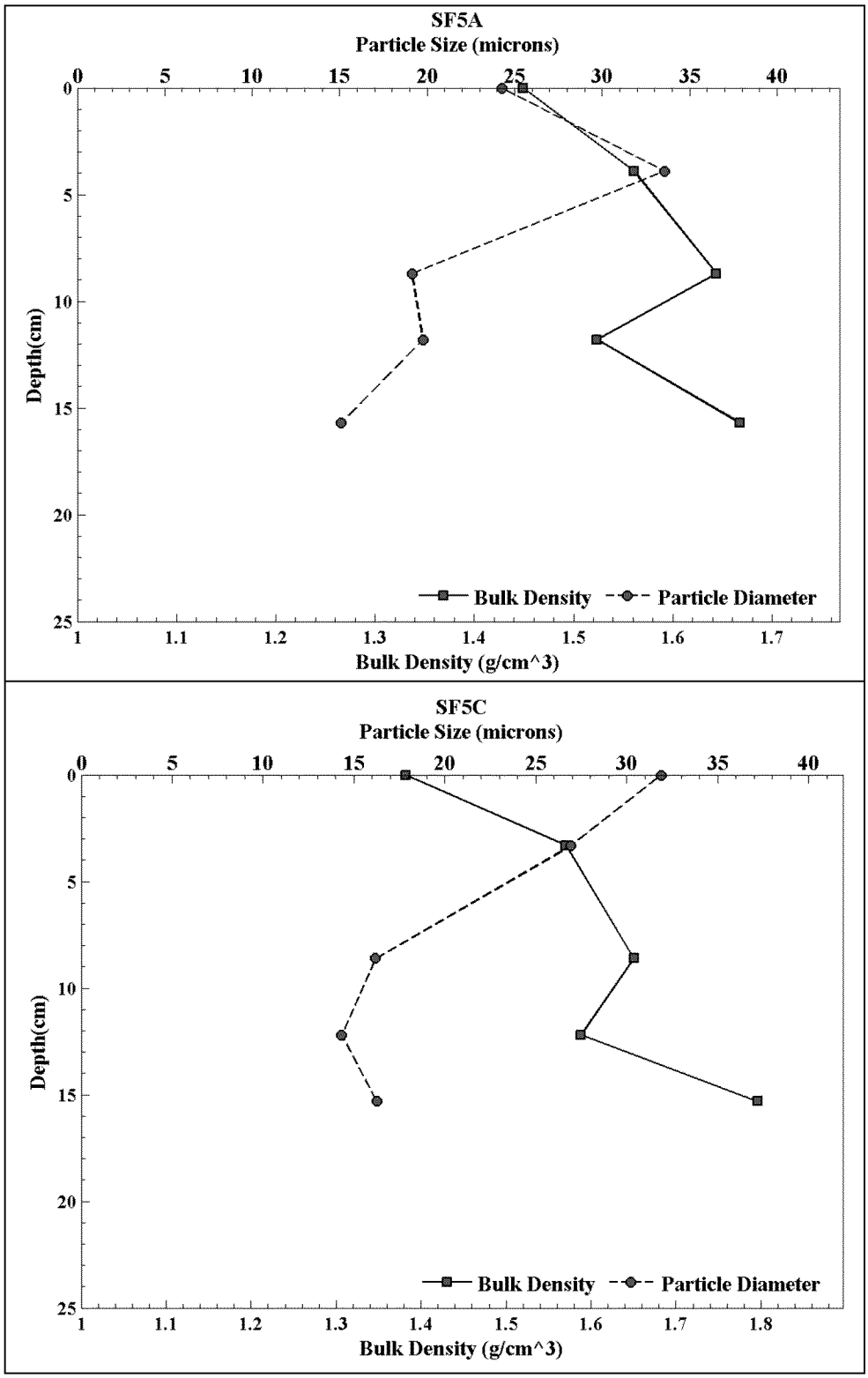

Figure 31. Down-core wet bulk density and median grain size for SF5A (top) and SF5C (bottom).

Table 20. Power law best-fit variables for the measured depth intervals in SF5A.

Depth Interval	Interval Start Depth (cm)	Interval End Depth (cm)	A	n	r^2
1	0.00	3.75	0.000882	1.48	0.76
2	3.90	8.45	0.000366	1.71	0.95
3	8.70	11.20	0.000102	2.03	0.94
4	11.80	15.70	0.000072	2.52	0.90
5	15.70	19.50	0.000066	2.57	0.93

Table 21. Power law best-fit variables for the measured depth intervals in SF5C.

Depth Interval	Interval Start Depth (cm)	Interval End Depth (cm)	A	n	r^2
1	0.00	3.10	0.000780	1.90	0.89
2	3.30	8.10	0.000425	2.01	0.97
3	8.60	12.20	0.000024	3.78	0.99
4	12.20	15.10	0.000040	2.90	1.00
5	15.30	19.00	0.000052	2.75	0.99

Table 22. Median grain size, wet bulk density, fraction LOI and critical shear stress estimates for SF5A.

Sample Depth (cm)	Grain Size (μm)	Wet Bulk Density (g/cm^3)	Fraction LOI	τ_0 (Pa)	τ_1 (Pa)	τ_{linear} (Pa)	τ_{power} (Pa)
0.00	24.27	1.45	0.05	0.05	0.10	0.10	0.23
3.90	33.56	1.56	0.05	0.40	0.80	0.52	0.47
8.70	19.14	1.64	0.03	0.40	0.80	0.80	0.99
11.80	19.75	1.52	0.03	0.80	1.60	1.28	1.14
15.70	15.06	1.67	0.03	0.80	1.60	1.28	1.17
Mean	**22.36**	**1.57**	**0.04**	**0.49**	**0.98**	**0.80**	**0.80**

Table 23. Median grain size, wet bulk density, fraction LOI and critical shear stress estimates for SF5C.

Sample Depth (cm)	Grain Size (μm)	Wet Bulk Density (g/cm^3)	Fraction LOI	τ_0 (Pa)	τ_1 (Pa)	τ_{linear} (Pa)	τ_{power} (Pa)
0.00	31.87	1.38	0.05	0.10	0.20	0.20	0.34
3.30	26.93	1.57	0.03	0.40	0.80	0.52	0.49
8.60	16.17	1.65	0.04	0.80	1.60	1.28	1.47
12.20	14.32	1.59	0.04	0.80	1.60	1.28	1.38
15.30	16.24	1.80	0.03	0.80	1.60	1.28	1.27
Mean	**21.11**	**1.60**	**0.04**	**0.58**	**1.16**	**0.91**	**0.99**

2.4.6 CORES SF6A, SF6B, AND SF6C

Cores SF6A, SF6B, and SF6C were collected from within the navigation channel east of the Port of Newark, just south of the I-78/Newark Bay Bridge. Core SF6A comprised 4-5 cm of loose, clumpy silt and sand mixed with a large amount of organic material (leaves and twigs). The material at deeper depths consisted of silt, sand and shell hash, and became stiffer with depth, containing stiff clayey-silt and coarse sand. Core SF6B consisted of a 1 cm tan-colored low-density silt layer overlying darker-colored coarse sand, shell hash and organic material. The material became stiffer and more difficult to erode with depth, and comprised clayey-silt and coarse sand.

The surface of core SF6C comprised 3-4 cm of tan-colored sediment and a large amount of shells and organic detritus on the surface. One 15-cm long void and large pieces of shells and woody debris were removed prior to the analysis. Below the surface, the general, the core contained darker-colored coarse sand and shell hash. Shells, organic material and coarse sand were encountered throughout the core, some larger pieces requiring removal before continuing with the analysis. A petroleum odor was sensed at the bottom of SF6C.

A photograph of the cores aligned with each other is presented in Figure 32. Their respective erosion rate data are plotted in Figure 33. Shear stresses ranging between 0.1 and 3.2 Pa were applied to these cores. The intra-core erosion rate trends of the depth intervals evaluated in each core are shown in Figure 34. The trends were different within each core: In core SF6A, the erosion rates decreased slightly with depth; in core SF6B, the erosion rates increased with depth; and in SF6C, the erosion rates remained relatively constant with depth. The erosion rate ratio trends of each core followed the same trends as the erosion rates.

The power law regression fit within each depth interval of the cores is illustrated in Figure 35. Coefficients and regression statistics from the power law analysis are presented in Table 24, Table 25, and Table 26 for the cores, respectively. The measured median grain sizes, and the computed wet bulk densities and critical shear stresses for each depth interval are provided in Table 27, Table 28, and Table 29.

The vertical profiles of d_{50} and ρ_b from each core are presented in Figure 36. The median grain size in SF6A decreased from a maximum of 49.39 µm (coarse silt) at a depth of 2.60 cm to a minimum of 10.53 µm (fine silt) at a depth of 11.50 cm. The median grain size in SF6B varied between a minimum of 8.21 µm (fine silt) at the surface and a maximum of 194.30 µm (fine sand) at a depth of 13.40 cm. The median grain size in SF6C varied between a maximum of 158.70 µm (fine sand) at the surface and a minimum of 42.51 µm (coarse silt) at a depth of 5.00 cm. The core-averaged d_{50} in cores SF6A, SF6B, and SF6C was 26.16 µm, 60.82 µm, and 87.90 µm, respectively.

The wet bulk density in SF6A varied between a minimum of 1.31 g/cm^3 at the surface and a maximum of 1.47 g/cm^3 at a depth of 11.60 cm. The wet bulk density in SF6B was a minimum of 1.27 g/cm^3 at the surface and a maximum of 1.92 g/cm^3 at a depth of 13.40 cm. The wet bulk density in SF6C varied between a minimum of 1.34 g/cm^3 at a depth of 5.00

cm and a maximum of 1.90 g/cm³ at a depth of 13.80 cm. The core-averaged wet bulk density in the cores was 1.36 g/cm³, 1.57 g/cm³, and 1.87 g/cm³, respectively.

The critical shear stress estimates in each core were of low magnitudes with little down-core variation. The overall core-averages were similar between all cores though: The linearly interpolated critical shear stress estimate core-averages were 0.29 Pa, 0.41 Pa and 0.34 Pa for the cores, respectively; the power law estimates were 0.30 Pa, 0.31 Pa and 0.33 Pa, respectively.

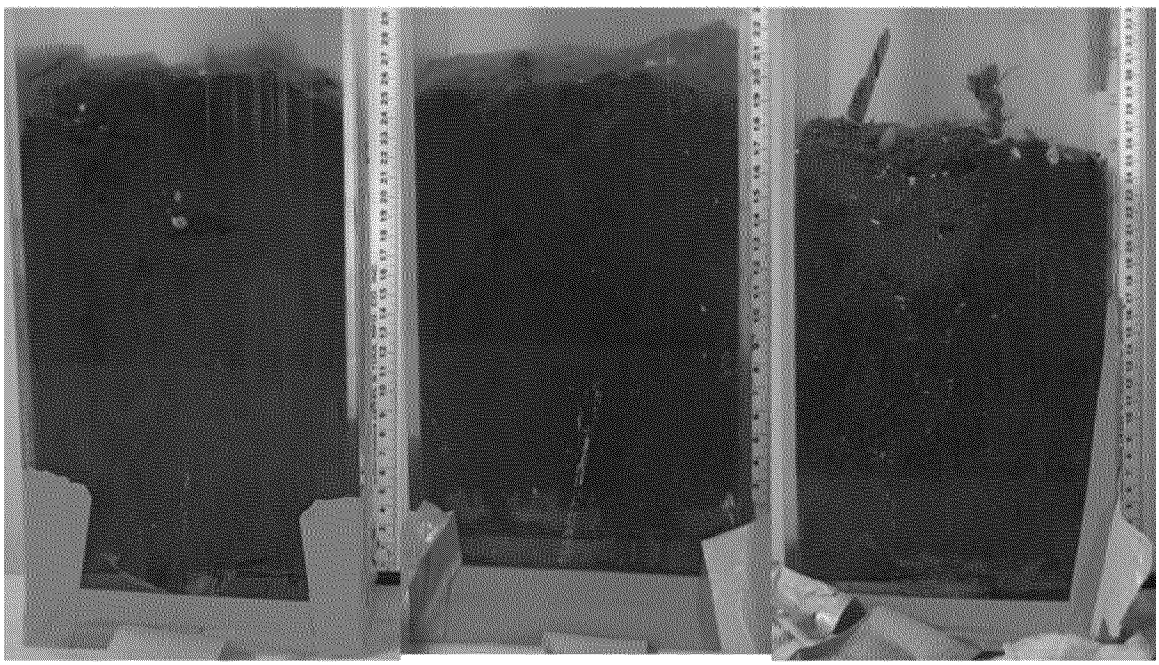

Figure 32. Pre-processing photo of cores SF6A (left), SF6B (middle), SF6C (right).

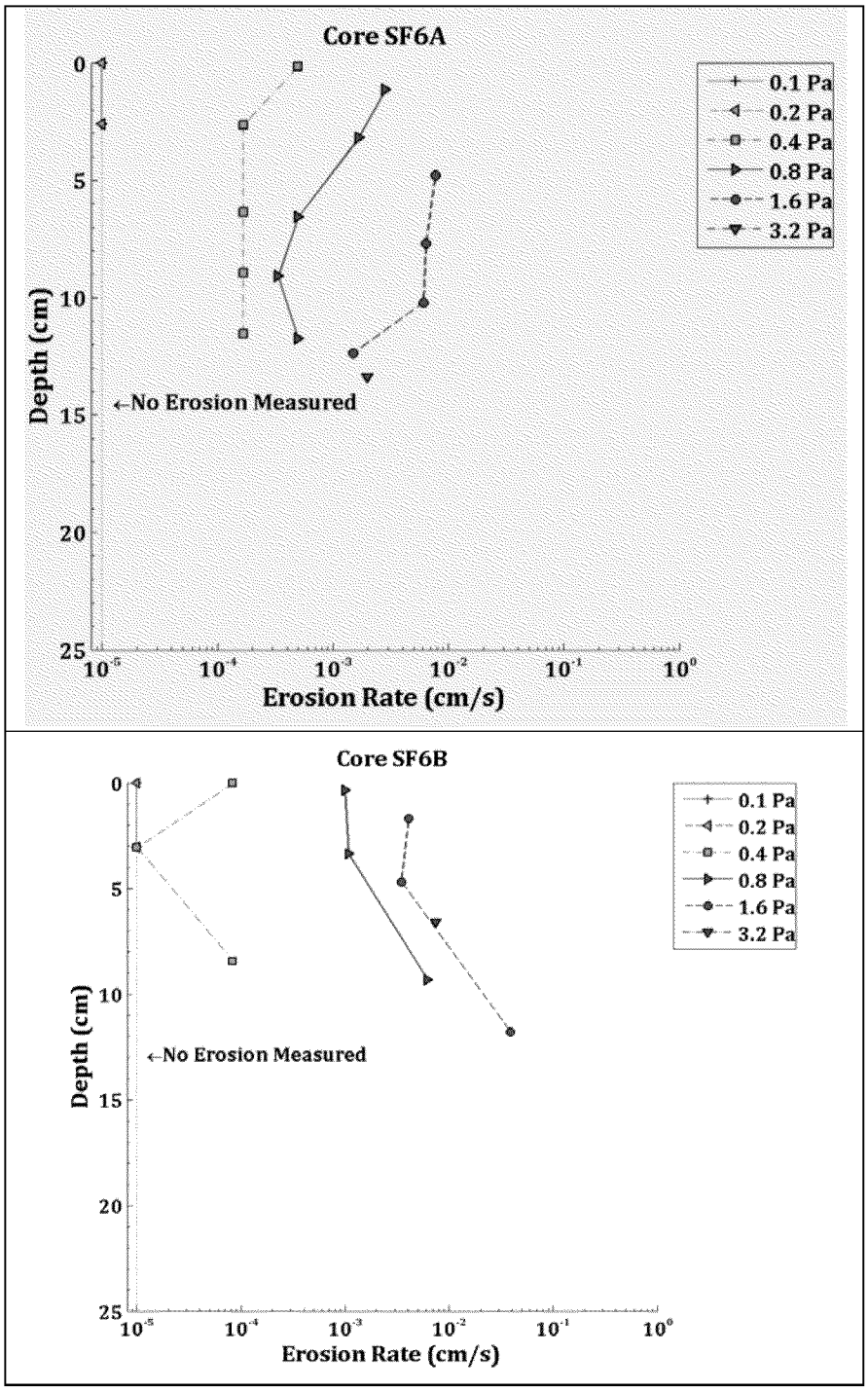

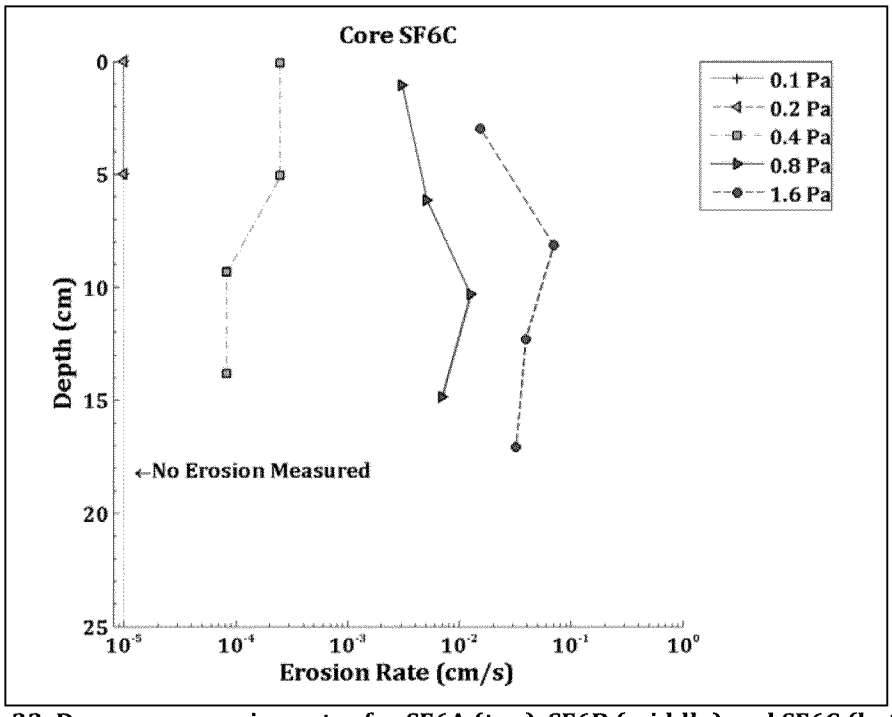

Figure 33. Down-core erosion rates for SF6A (top), SF6B (middle) and SF6C (bottom).

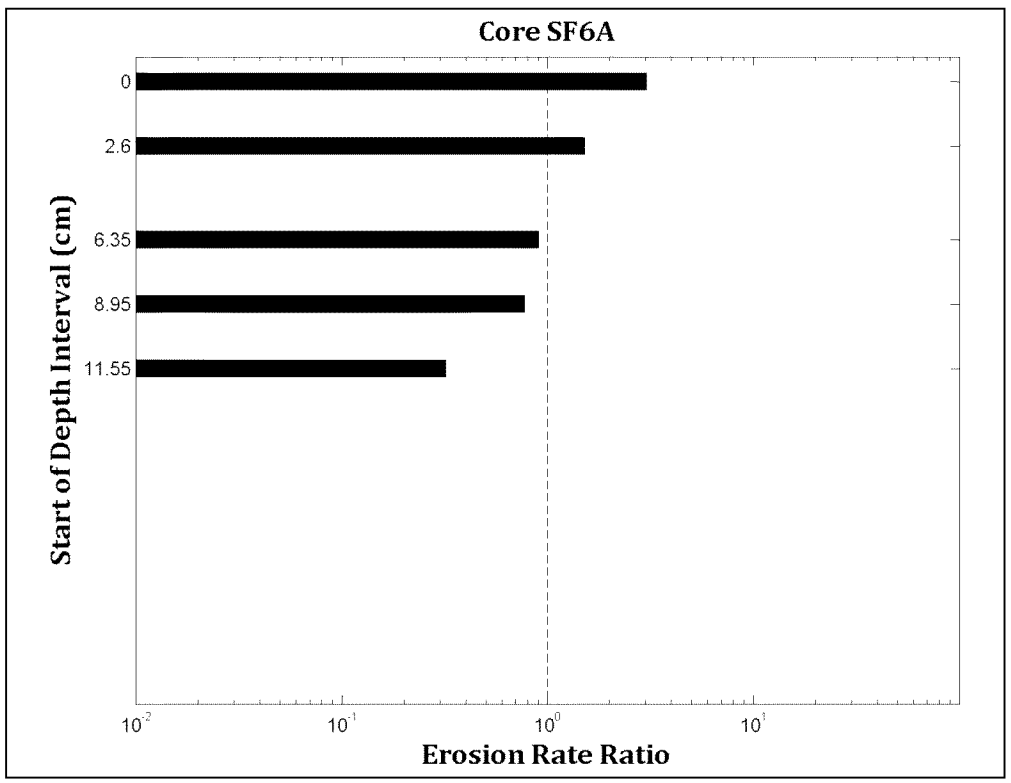

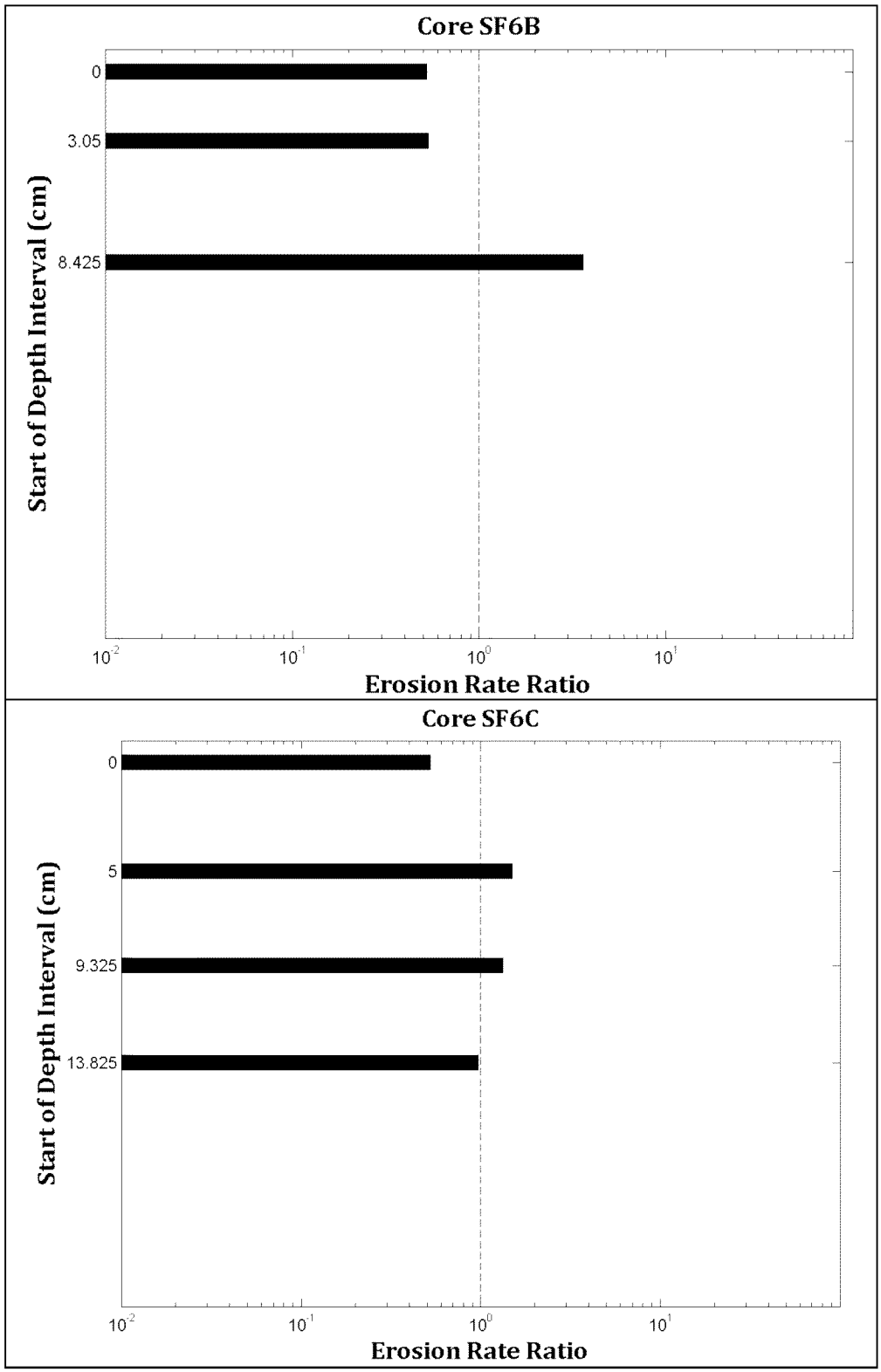

Figure 34. Intra-core erosion rate ratios for SF6A (top), SF6B (middle) and SF6C (bottom).

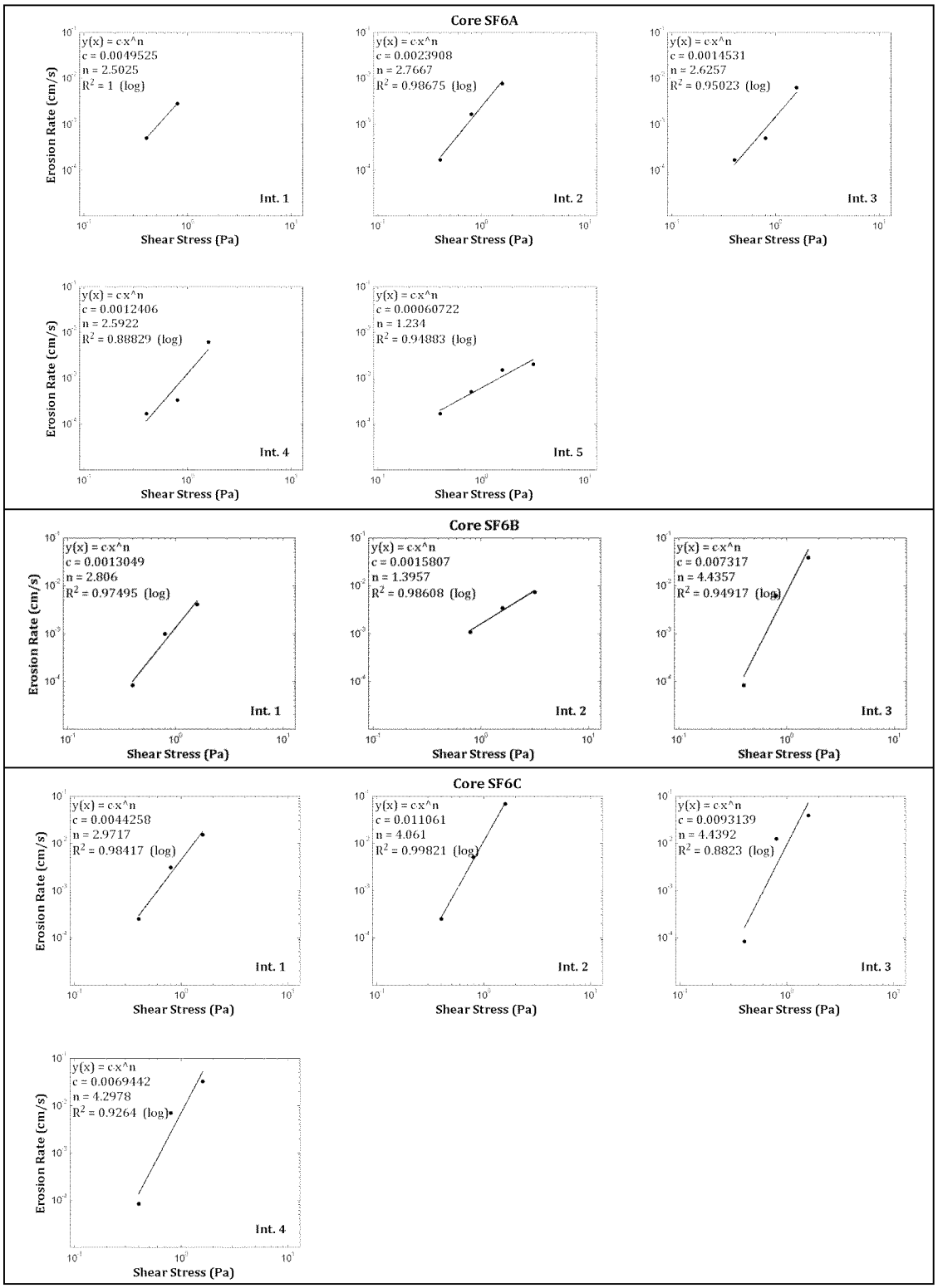

Figure 35. Power law best-fit regression solutions for SF6A (top), SF6B (middle) and SF6C (bottom).

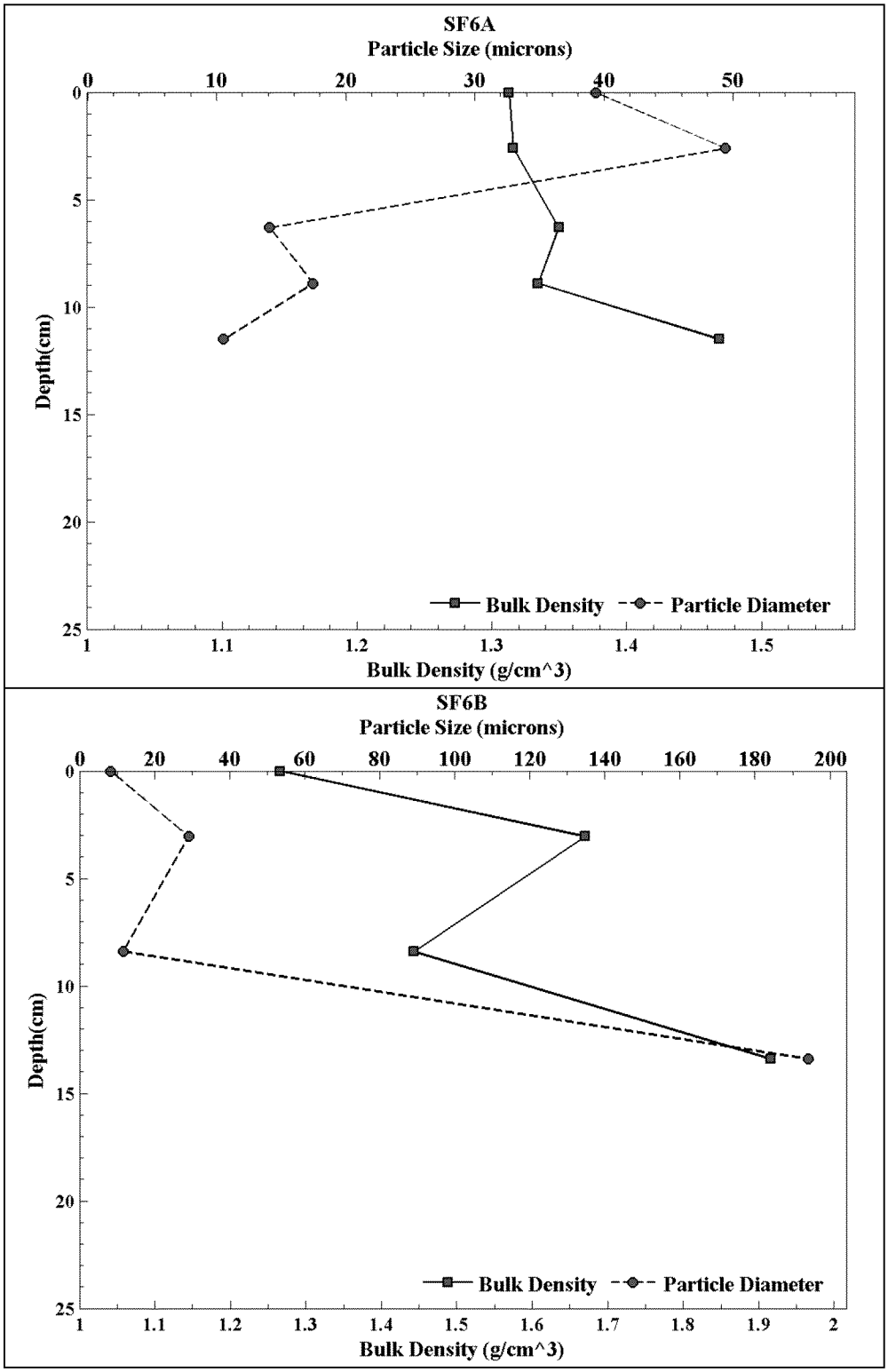

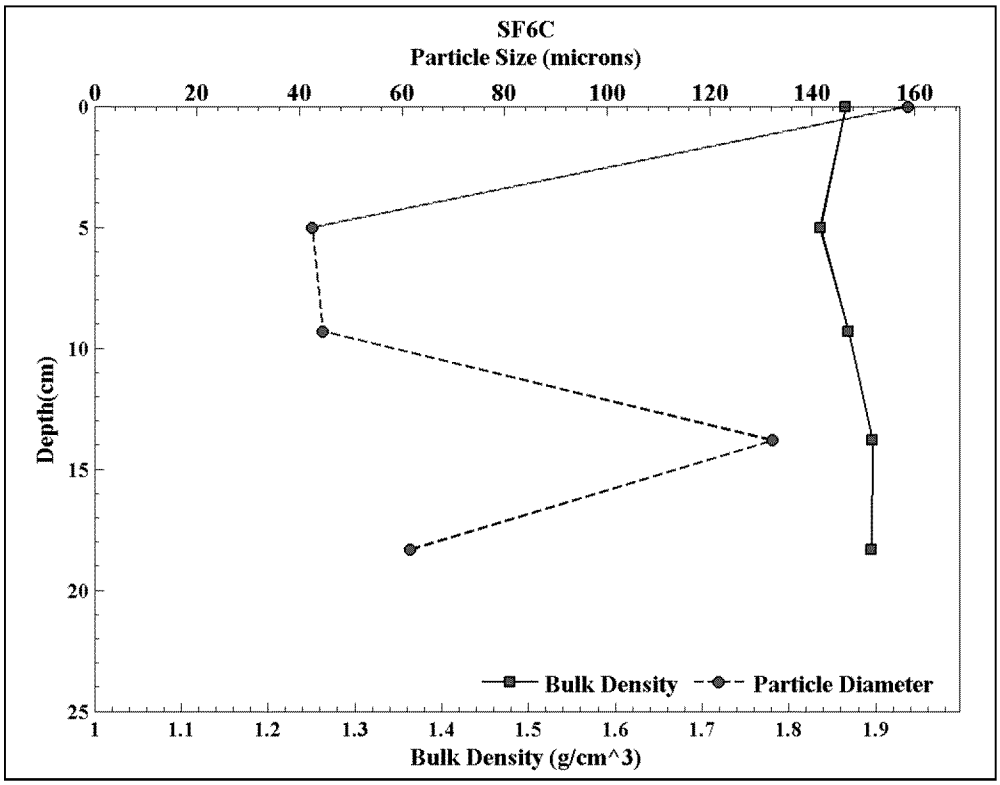

Figure 36. Down-core wet bulk density and median grain size for SF6A (top), SF6B (middle) and SF6C (bottom).

Table 24. Power law best-fit variables for the measured depth intervals in SF6A.

Depth Interval	Interval Start Depth (cm)	Interval End Depth (cm)	A	n	r^2
1	0.00	2.00	0.004953	2.50	1.00
2	2.60	5.90	0.002391	2.77	0.99
3	6.30	8.70	0.001453	2.63	0.95
4	8.90	11.20	0.001241	2.59	0.89
5	11.50	14.00	0.000607	1.23	0.95

Table 25. Power law best-fit variables for the measured depth intervals in SF6B.

Depth Interval	Interval Start Depth (cm)	Interval End Depth (cm)	A	n	r^2
1	0.00	2.70	0.001305	2.81	0.97
2	3.05	7.50	0.001581	1.40	0.99
3	8.40	13.40	0.007317	4.44	0.95

Table 26. Power law best-fit variables for the measured depth intervals in SF6C.

Depth Interval	Interval Start Depth (cm)	Interval End Depth (cm)	A	n	r^2
1	0.00	4.00	0.004426	2.97	0.98
2	5.00	9.10	0.011061	4.06	1.00
3	9.30	13.30	0.009314	4.44	0.88
4	13.80	18.30	0.006944	4.30	0.93

Table 27. Median grain size, wet bulk density, fraction LOI and critical shear stress for SF6A.

Sample Depth (cm)	Grain Size (µm)	Wet Bulk Density (g/cm³)	Fraction LOI	τ_0 (Pa)	τ_1 (Pa)	τ_{linear} (Pa)	τ_{power} (Pa)
0.00	39.33	1.31	0.06	0.20	0.40	0.24	0.21
2.60	49.39	1.32	0.12	0.20	0.40	0.32	0.32
6.30	14.12	1.35	0.07	0.20	0.40	0.30	0.36
8.90	17.45	1.33	0.06	0.20	0.40	0.30	0.38
11.50	10.53	1.47	0.07	0.20	0.40	0.30	0.23
Mean	**26.16**	**1.36**	**0.08**	**0.20**	**0.40**	**0.29**	**0.30**

Table 28. Median grain size, wet bulk density, fraction LOI and critical shear stress for SF6B.

Sample Depth (cm)	Grain Size (µm)	Wet Bulk Density (g/cm³)	Fraction LOI	τ_0 (Pa)	τ_1 (Pa)	τ_{linear} (Pa)	τ_{power} (Pa)
0.00	8.21	1.27	0.04	0.20	0.40	0.40	0.40
3.05	29.12	1.67	0.02	0.40	0.80	0.44	0.14
8.40	11.63	1.44	0.04	0.20	0.40	0.40	0.38
13.40	194.30	1.92	0.01	*n/a*	*n/a*	*n/a*	*n/a*
Mean	**60.82**	**1.57**	**0.03**	**0.27**	**0.53**	**0.41**	**0.31**

Table 29. Median grain size, wet bulk density, fraction LOI and critical shear stress for SF6C.

Sample Depth (cm)	Grain Size (µm)	Wet Bulk Density (g/cm³)	Fraction LOI	τ_0 (Pa)	τ_1 (Pa)	τ_{linear} (Pa)	τ_{power} (Pa)
0.00	158.70	1.87	0.03	0.20	0.40	0.28	0.28
5.00	42.51	1.84	0.02	0.20	0.40	0.28	0.31
9.30	44.57	1.87	0.02	0.20	0.40	0.40	0.36
13.80	132.20	1.90	0.02	0.20	0.40	0.40	0.37
18.30	61.51	1.90	0.01	*n/a*	*n/a*	*n/a*	*n/a*
Mean	**87.90**	**1.87**	**0.02**	**0.20**	**0.40**	**0.34**	**0.33**

2.4.7 CORES SF7A AND SF7C

Cores SF7A and SF7C were collected from the eastern mudflats, east of the Port of Newark. Core SF7A comprised 1-2 cm of tan-colored, low-density silt and fine sand layer overlying 6-8 cm of a tan-colored, higher density silt and sand layer. Small worms and stringy organics were visible on the surface. Deeper than this, the material was dark brown-colored and became stiffer with depth. The surface of core SF7C consisted of 1-2 cm of tan-colored silt and sand of lower density than layers beneath. The material was darker-colored at deeper depths with the exception of a light gray-colored silt and sand layer at approximately 32 cm. One large (1 cm x 2 cm dimension) clam was removed from the surface prior to analysis. Small worms were visible on the core surface. Several clams and some shells and shell hash were observed at deeper depths.

A photograph of the cores aligned with each other is presented in Figure 37. Their respective erosion rate data are plotted in Figure 38. Shear stresses ranging between 0.1 and 6.4 Pa were applied to these cores. The intra-core variation of the depth intervals evaluated in each core are shown in Figure 39. In general, the erosion rates and ratios decreased with depth into the cores.

The power law regression fit within each depth interval of the cores is illustrated in Figure 40. Coefficients and regression statistics from the power law analysis are presented in Table 30 and Table 31 for the cores, respectively. The measured median grain sizes, and the computed wet bulk densities and critical shear stresses for each depth interval are provided in Table 32 and Table 33.

The vertical profiles of d_{50} and ρ_b from each core are presented in Figure 41. The median grain size in SF7A varied between a minimum of 24.22 µm (medium silt) at the surface to a maximum of 65.40 µm (very fine sand) at a depth of 7.00 cm. The median grain size in SF7C varied down-core from a maximum of 60.11 µm (coarse silt) at the surface to a minimum of 33.18 µm (coarse silt) at a depth of 6.60 cm. The core-averaged d_{50} in SF7A and SF7C was 43.05 µm and 48.89 µm, respectively (coarse silt for both cores).

The wet bulk density in SF7A varied between a minimum of 1.35 g/cm^3 at the surface and a maximum of 1.61 g/cm^3 at a depth of 7.00 cm. The wet bulk density in SF7C increased with depth from a minimum of 1.43 g/cm^3 at the surface to a maximum of 1.58 g/cm^3 at a depth of 11.80 cm. The core-averaged wet bulk density in the cores was 1.53 g/cm^3 and 1.50 g/cm^3, respectively.

The critical shear stress estimates in each core generally increased with down-core depth. The overall core-averages were similar between all cores: The linearly interpolated critical shear stress estimate core-averages were 1.04 Pa and 1.15 Pa, respectively; the power law estimates were 1.18 Pa and 1.37 Pa, respectively.

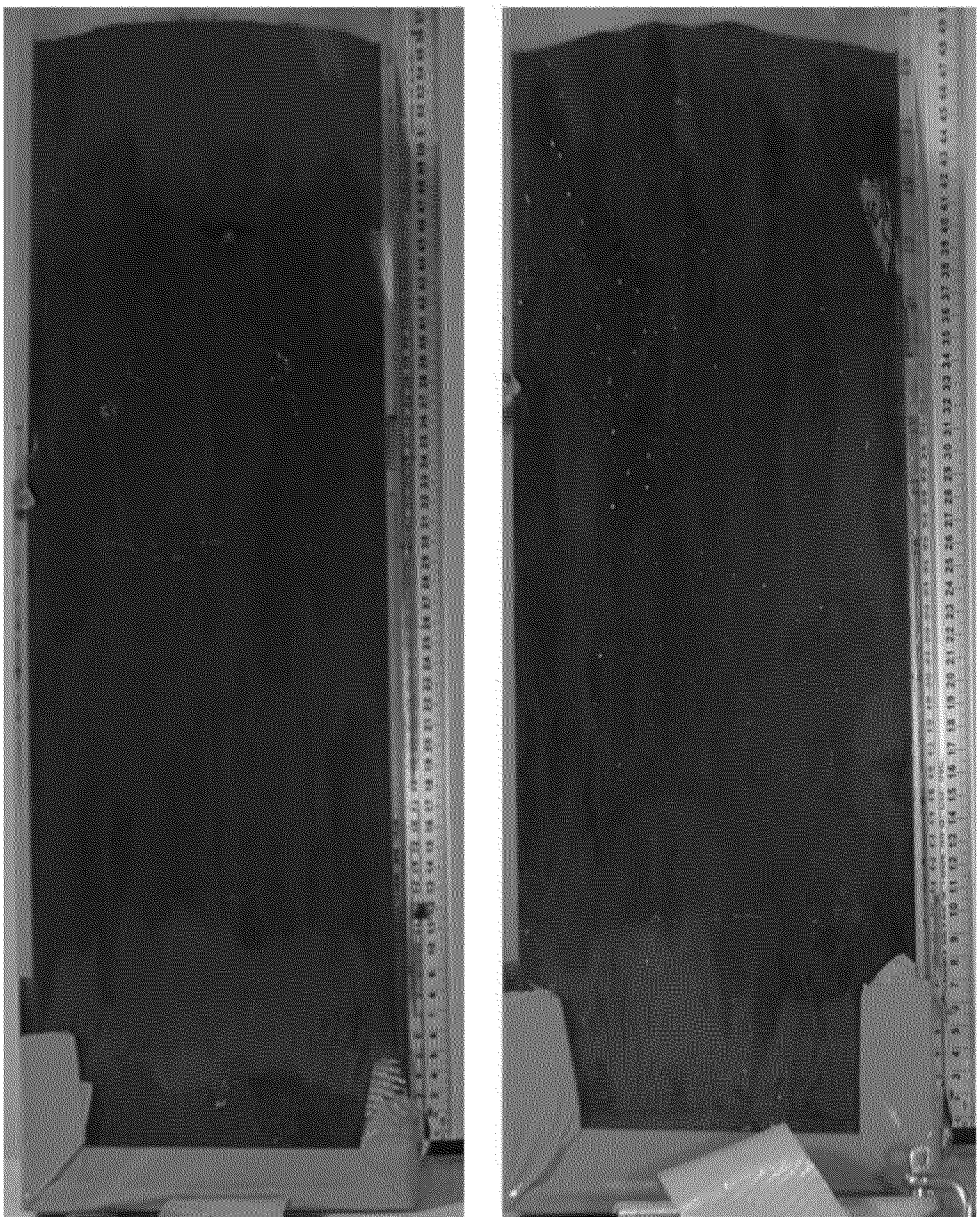

Figure 37. Pre-processing photo of cores SF7A (left) and SF7C (right).

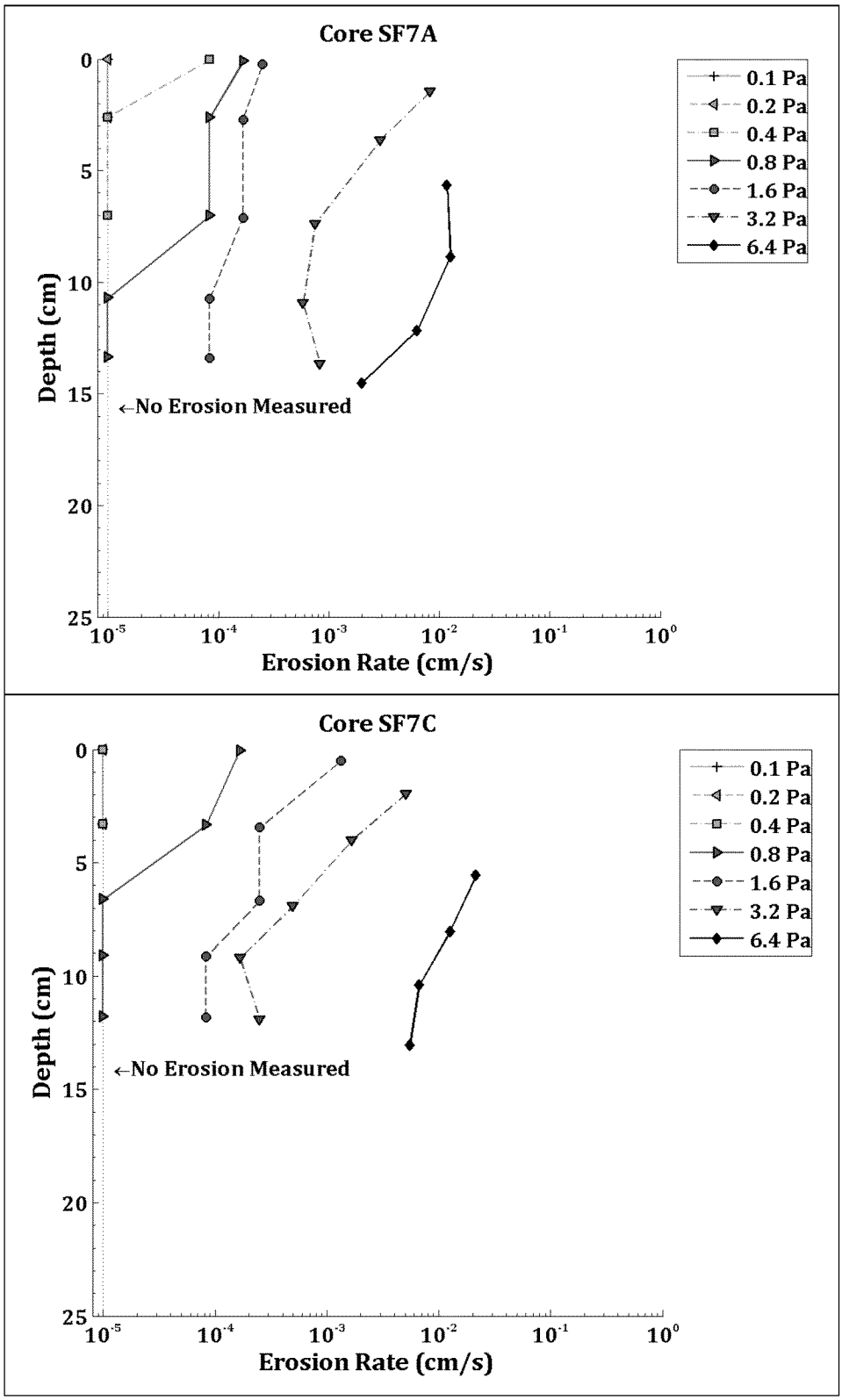

Figure 38. Down-core erosion rates for SF7A (top) and SF7C (bottom).

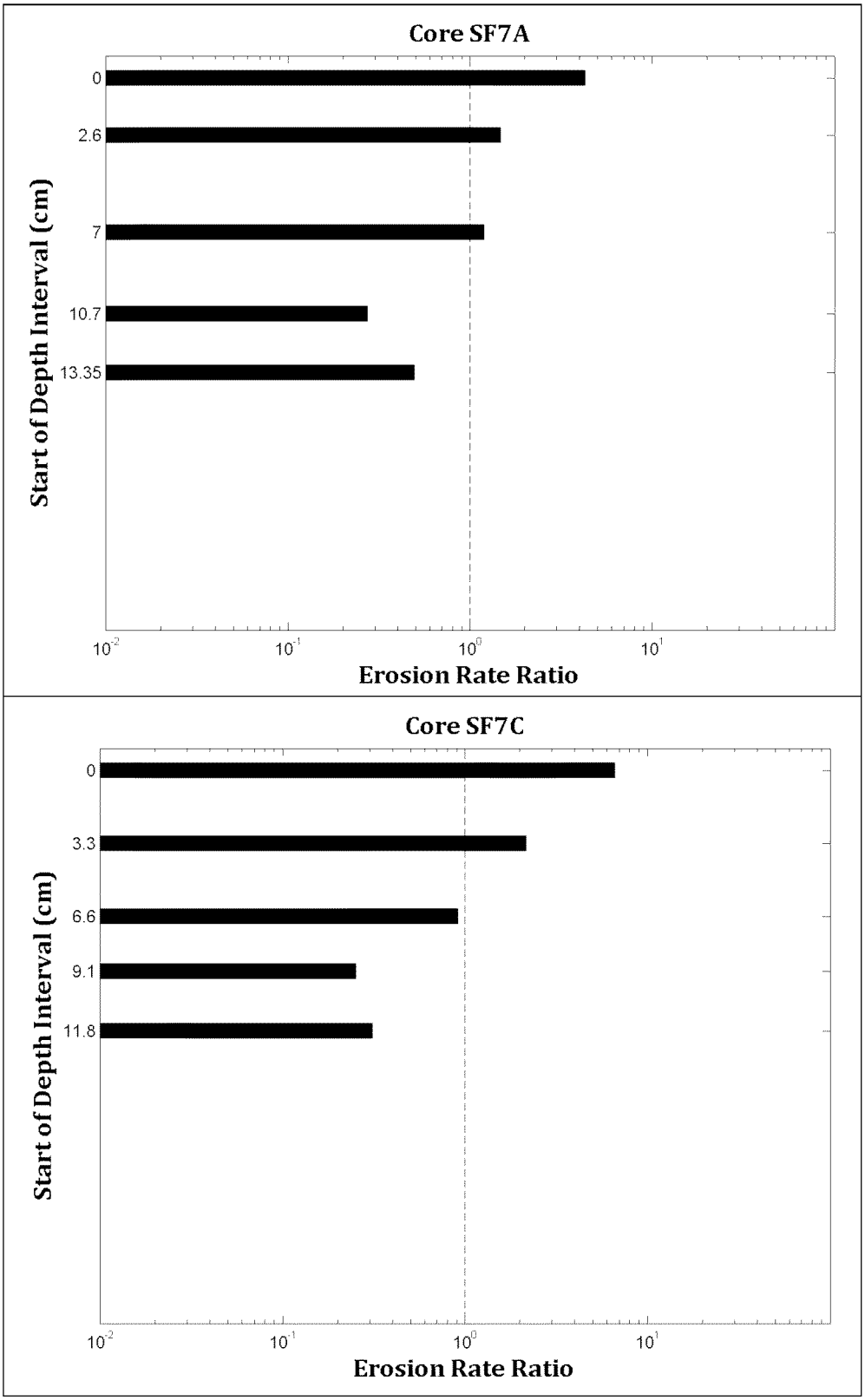

Figure 39. Intra-core erosion rate ratios for SF7A (top) and SF7C (bottom).

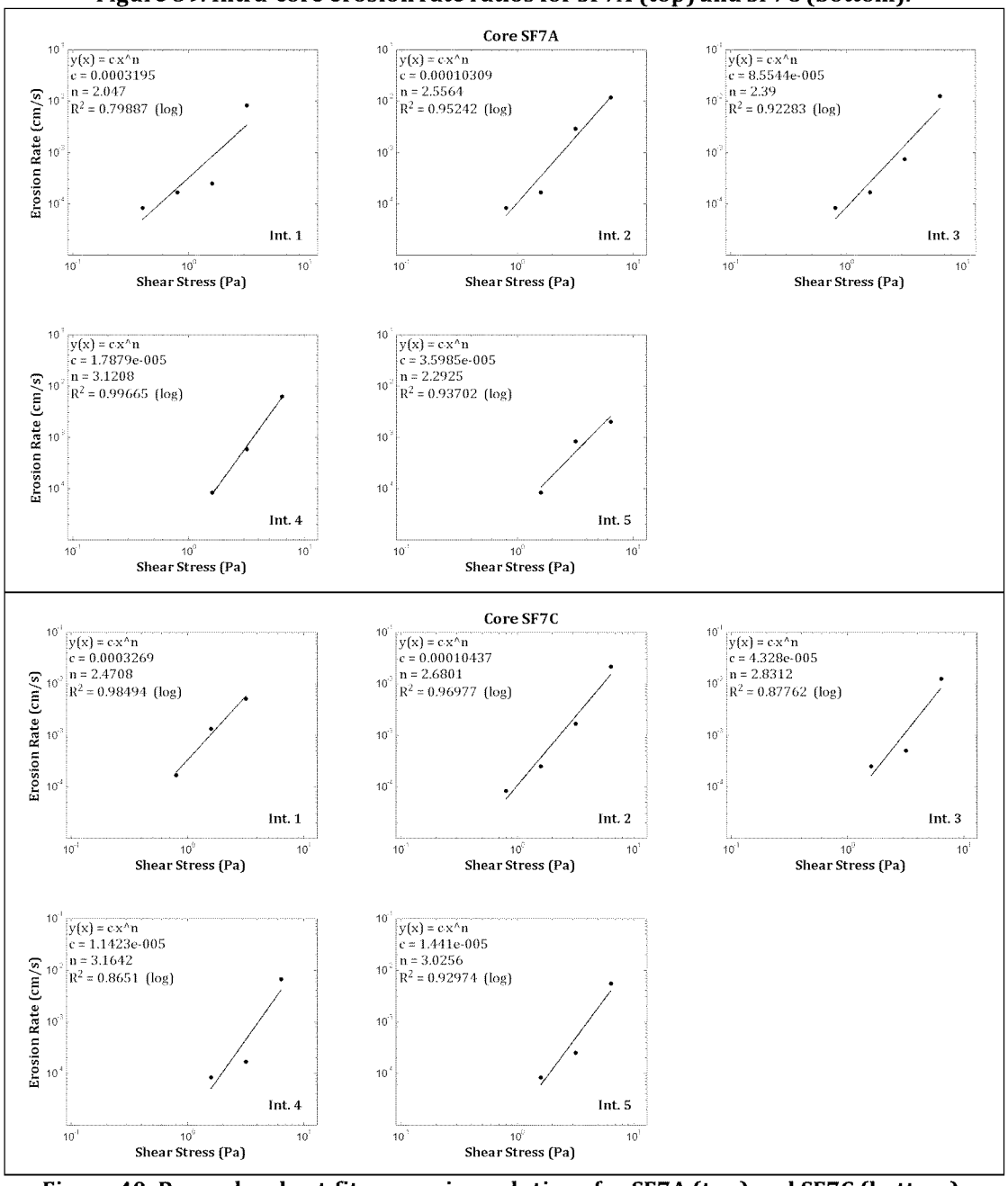

Figure 40. Power law best-fit regression solutions for SF7A (top) and SF7C (bottom).

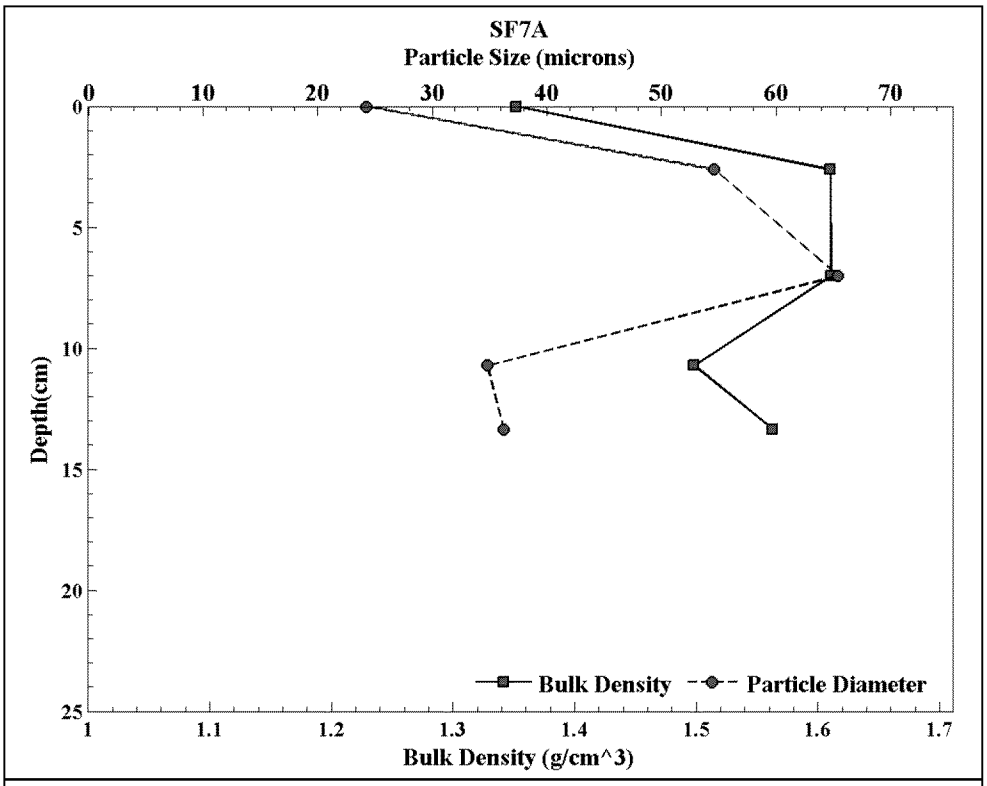

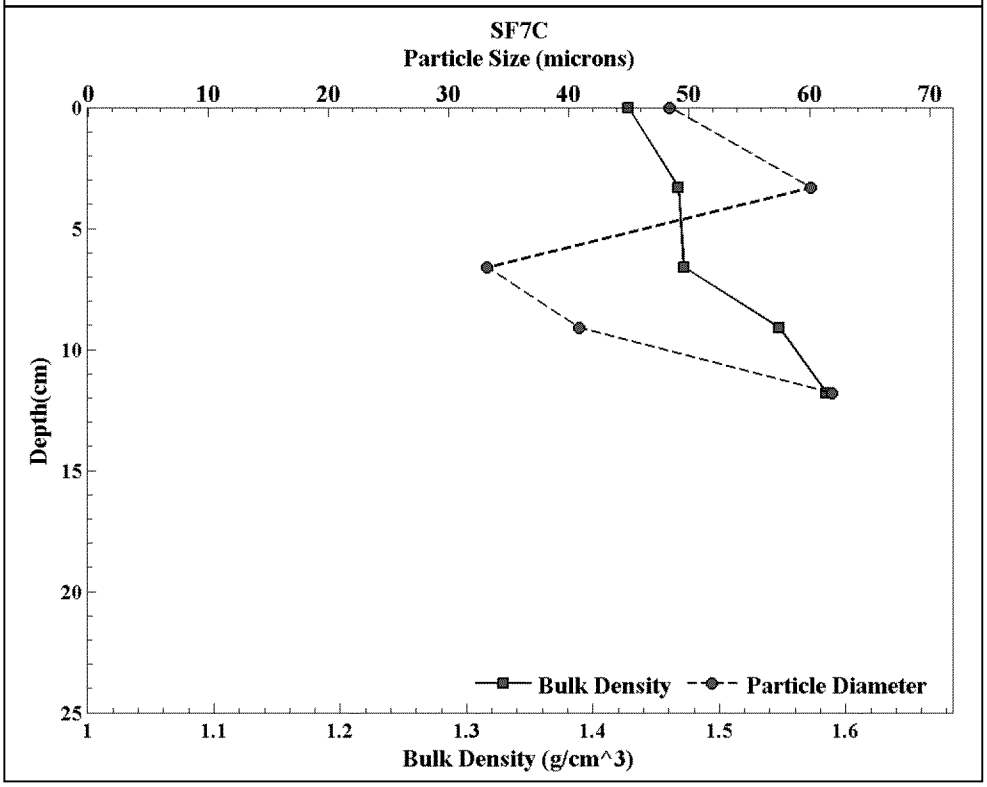

Figure 41. Down-core wet bulk density and median grain size for SF7A (top) and SF7C (bottom).

Table 30. Power law best-fit variables for the measured depth intervals in SF7A.

Depth Interval	Interval Start Depth (cm)	Interval End Depth (cm)	A	n	r^2
1	0.00	2.60	0.000320	2.05	0.80
2	2.60	6.80	0.000103	2.56	0.95
3	7.00	10.10	0.000086	2.39	0.92
4	10.70	13.20	0.000018	3.12	1.00
5	13.35	15.10	0.000036	2.29	0.94

Table 31. Power law best-fit variables for the measured depth intervals in SF7C.

Depth Interval	Interval Start Depth (cm)	Interval End Depth (cm)	A	n	r^2
1	0.00	3.00	0.000327	2.47	0.98
2	3.30	6.60	0.000104	2.68	0.97
3	6.60	9.00	0.000043	2.83	0.88
4	9.10	11.50	0.000011	3.16	0.87
5	11.80	14.10	0.000014	3.03	0.93

Table 32. Median grain size, wet bulk density, fraction LOI and critical shear stress for SF7A.

Sample Depth (cm)	Grain Size (μm)	Wet Bulk Density (g/cm³)	Fraction LOI	τ_0 (Pa)	τ_1 (Pa)	τ_{linear} (Pa)	τ_{power} (Pa)
0.00	24.22	1.35	0.05	0.20	0.40	0.40	0.57
2.60	54.58	1.61	0.04	0.40	0.80	0.80	0.99
7.00	65.40	1.61	0.04	0.40	0.80	0.80	1.07
10.70	34.80	1.50	0.05	0.80	1.60	1.60	1.74
13.35	36.26	1.56	0.06	0.80	1.60	1.60	1.56
Mean	**43.05**	**1.53**	**0.05**	**0.52**	**1.04**	**1.04**	**1.18**

Table 33. Median grain size, wet bulk density, fraction LOI and critical shear stress for SF7C.

Sample Depth (cm)	Grain Size (μm)	Wet Bulk Density (g/cm³)	Fraction LOI	τ_0 (Pa)	τ_1 (Pa)	τ_{linear} (Pa)	τ_{power} (Pa)
0.00	48.41	1.43	0.04	0.40	0.80	0.64	0.62
3.30	60.11	1.47	0.05	0.40	0.80	0.80	0.98
6.60	33.18	1.47	0.06	0.80	1.60	1.12	1.34
9.10	40.83	1.55	0.05	0.80	1.60	1.60	1.99
11.80	61.90	1.58	0.06	0.80	1.60	1.60	1.90
Mean	**48.89**	**1.50**	**0.05**	**0.64**	**1.28**	**1.15**	**1.37**

2.4.8 CORES SF8A AND SF8B

Cores SF8A and SF8B were collected from the navigation channel east of the Confined Disposal Facility (CDF). Core SF8A comprised 10-12 cm of tan-colored silt and fine sand layer on the surface. At deeper depths, the material was darker-colored and stiffer, containing clayey-silt and sand. The surface of core SF8B consisted of 10 cm of tan-colored silt and fine sand with darker-colored silt and clay layers. The material became stiffer with depth. Some red/brown-colored clayey material was observed at a depth of 22 cm, approximately. Some gas pockets or gas bubbles were visible down-core in both cores.

A photograph of the cores aligned with each other is presented in Figure 42. Their respective erosion rate data are plotted in Figure 43. Shear stresses ranging between 0.1 and 6.4 Pa were applied to these cores. The intra-core erosion of the depth intervals evaluated in each core are shown in Figure 44. The SF8A erosion rates varied with depth, first decreasing and then increasing at deeper depths. The SF8B erosion rates also varied with depth, decreasing slightly at the deepest depths. For both cores, erosion susceptibility varied with depth, remaining relatively consistent down-core.

The power law regression fit within each depth interval of the cores is illustrated in Figure 45. Coefficients and regression statistics from the power law analysis are presented in Table 34 and Table 35 for the cores, respectively. The measured median grain sizes, and the computed wet bulk densities and critical shear stresses for each depth interval are provided in Table 36 and Table 37.

The vertical profiles of d_{50} and ρ_b from each core are presented in Figure 46. The median grain size in SF8A varied between a maximum of 15.13 µm (fine silt) at the surface to a minimum of 9.26 µm (fine silt) at a depth of 7.00 cm. The median grain size in SF8B varied between a minimum of 10.24 µm (fine silt) at a depth of 3.00 cm to a maximum of 13.92 µm (fine silt) at a depth of 6.20 cm. The core-averaged d_{50} in SF8A and SF8B was 12.74 µm and 11.71 µm, respectively (fine silt for both cores).

The wet bulk density in SF8A varied between 1.29 g/cm^3 at the surface and 1.38 g/cm^3 at a depth of 15.60 cm. The wet bulk density in SF8B was 1.29 g/cm^3 at the surface and 1.50 g/cm^3 at a depth of 12.00 cm. The core-averaged wet bulk density in each core was 1.34 g/cm^3 and 1.37 g/cm^3, respectively.

The critical shear stress estimates in each core slightly increased with down-core depth, though the magnitudes were larger in SF8B than SF8A. The interpolated critical shear stress estimate core-averages were 0.50 Pa and 0.75 Pa for SF8A and SF8B, respectively; the power law estimates were 0.58 Pa and 0.76 Pa, respectively.

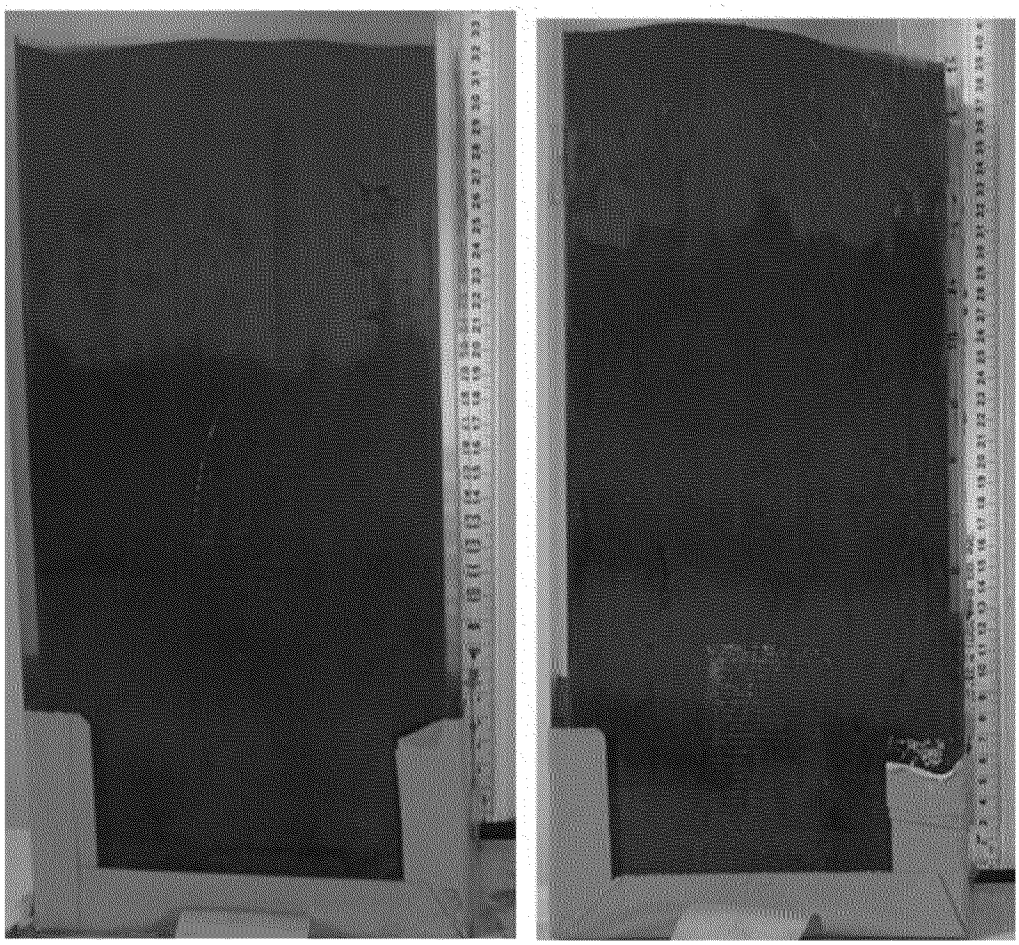

Figure 42. Pre-processing photo of cores SF8A (left) and SF8B (right).

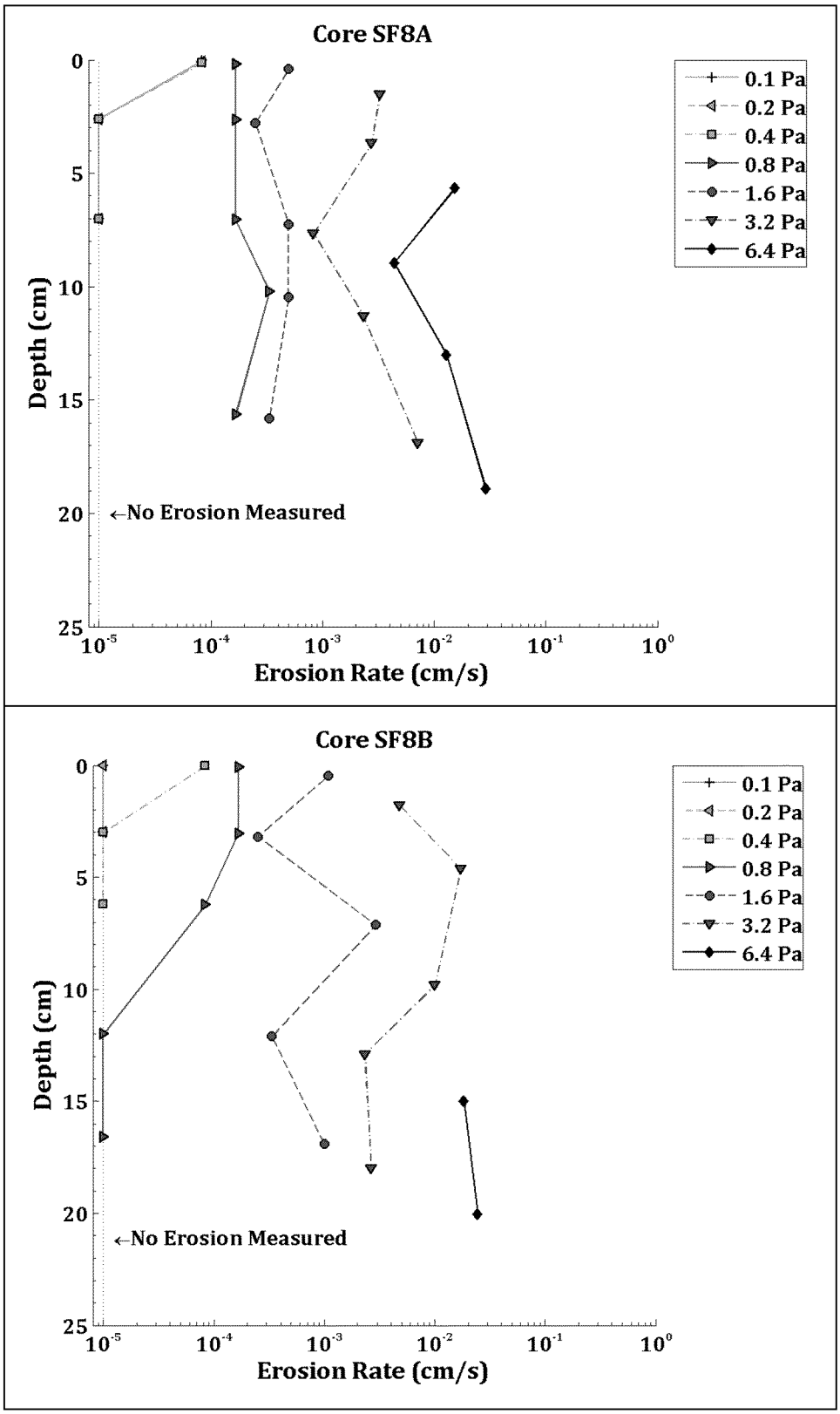

Figure 43. Down-core erosion rates for SF8A (top) and SF8B (bottom).

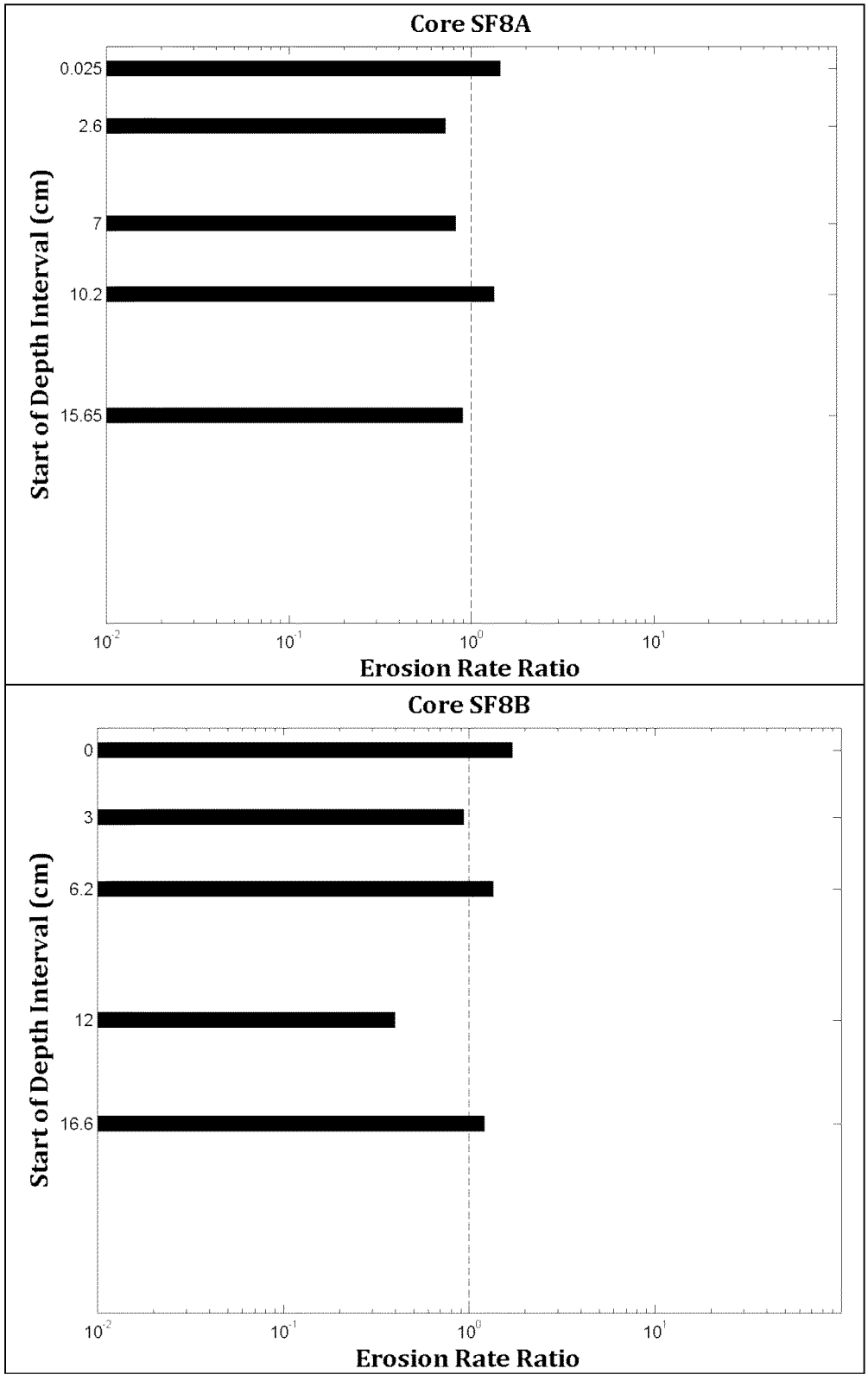

Figure 44. Intra-core erosion rate ratios for SF8A (top) and SF8B (bottom).

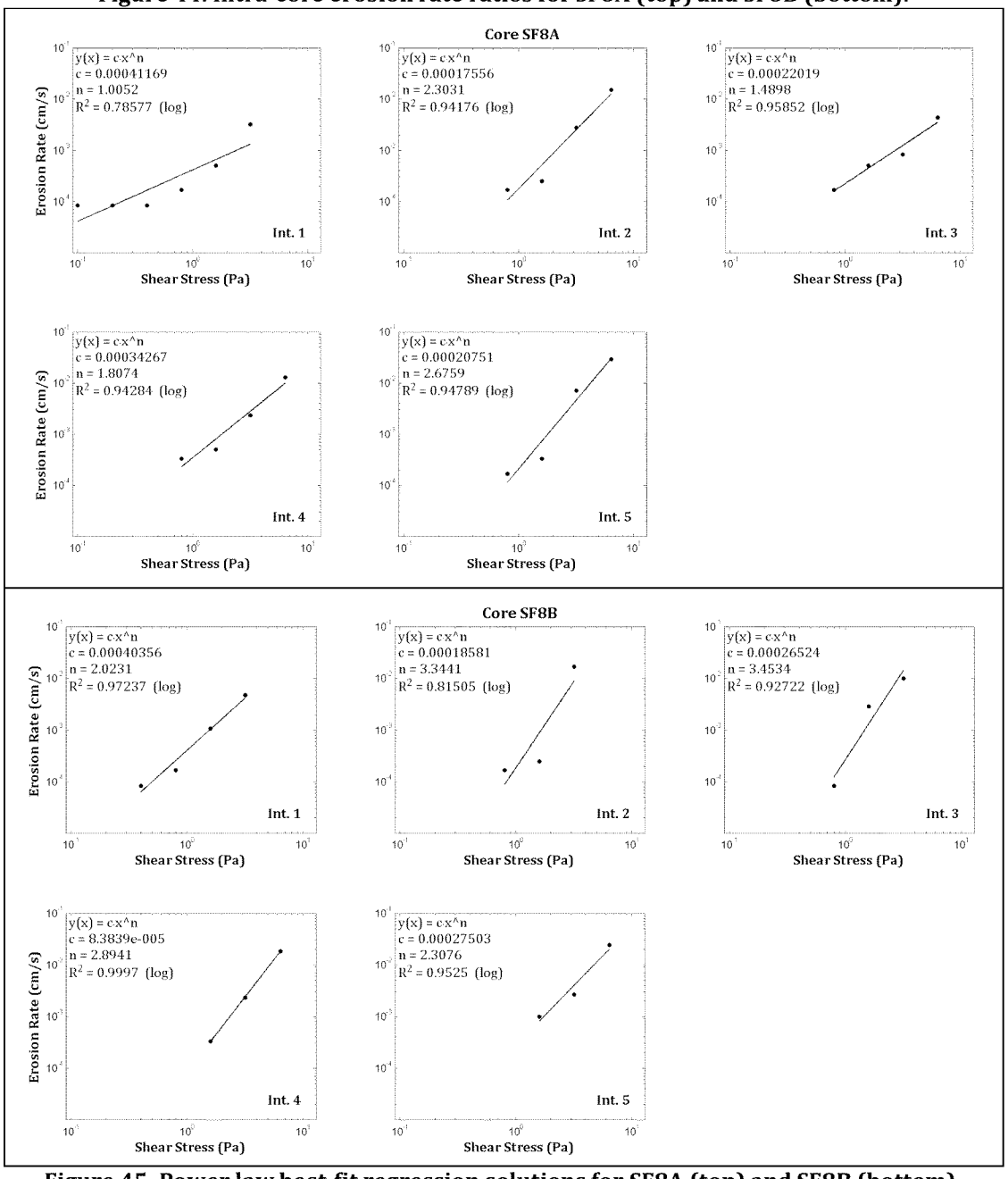

Figure 45. Power law best-fit regression solutions for SF8A (top) and SF8B (bottom).

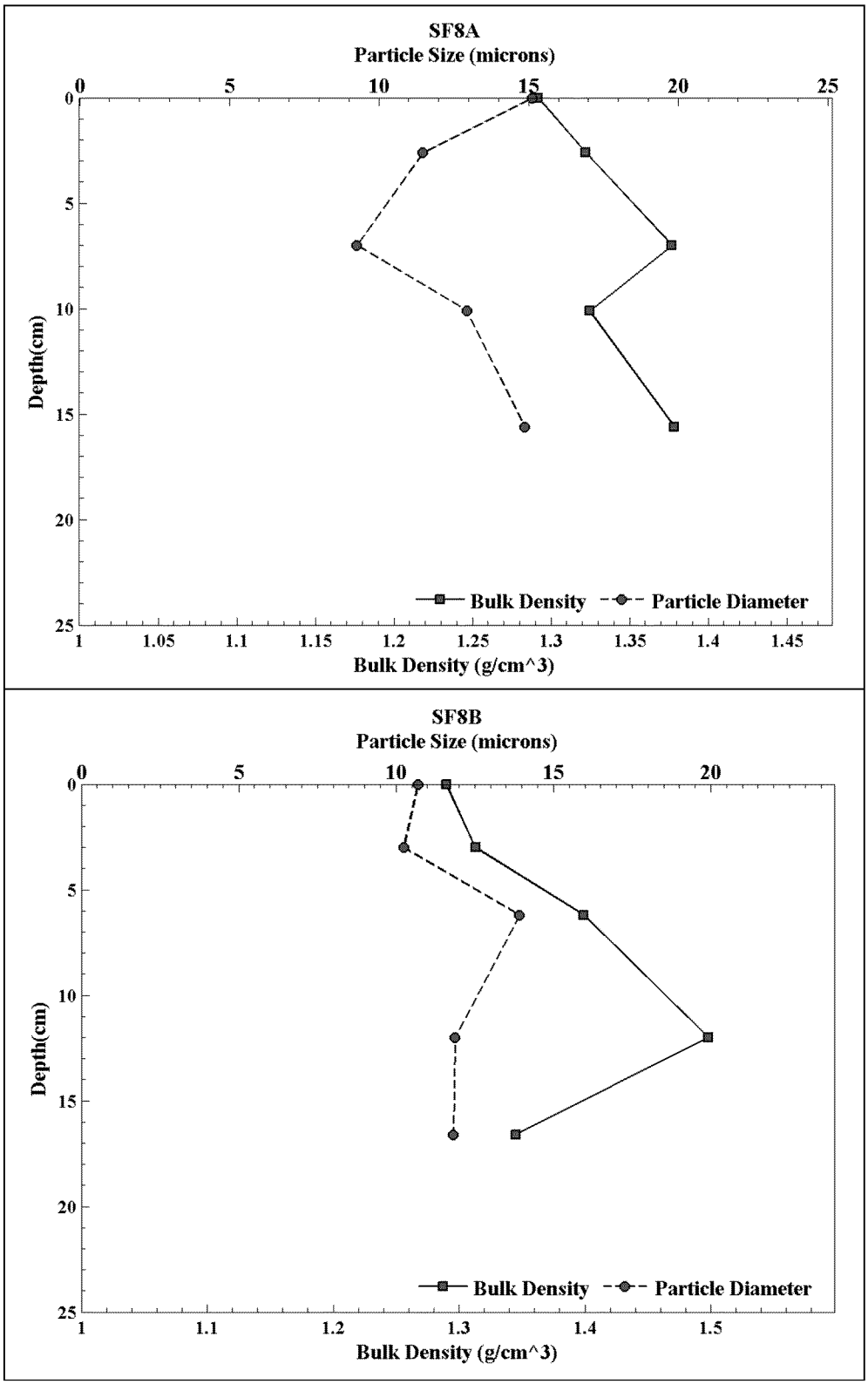

Figure 46. Down-core wet bulk density and median grain size for SF8A (top) and SF8B (bottom).

Table 34. Power law best-fit variables for the measured depth intervals in SF8A.

Depth Interval	Interval Start Depth (cm)	Interval End Depth (cm)	A	n	r^2
1	0.00	2.50	0.000412	1.01	0.79
2	2.60	6.80	0.000176	2.30	0.94
3	7.00	10.00	0.000220	1.49	0.96
4	10.10	14.00	0.000343	1.81	0.94
5	15.60	19.90	0.000208	2.68	0.95

Table 35. Power law best-fit variables for the measured depth intervals in SF8B.

Depth Interval	Interval Start Depth (cm)	Interval End Depth (cm)	A	n	r^2
1	0.00	2.80	0.000404	2.02	0.97
2	3.00	6.00	0.000186	3.34	0.82
3	6.20	11.60	0.000265	3.45	0.93
4	12.00	16.40	0.000084	2.89	1.00
5	16.60	21.30	0.000275	2.31	0.95

Table 36. Median grain size, wet bulk density, fraction LOI and critical shear stress for SF8A.

Sample Depth (cm)	Grain Size (µm)	Wet Bulk Density (g/cm³)	Fraction LOI	τ_0 (Pa)	τ_1 (Pa)	τ_{linear} (Pa)	τ_{power} (Pa)
0.00	15.13	1.29	0.06	0.05	0.10	0.10	0.24
2.60	11.47	1.32	0.07	0.40	0.80	0.64	0.78
7.00	9.26	1.38	0.06	0.40	0.80	0.64	0.59
10.10	12.94	1.32	0.08	0.40	0.80	0.51	0.51
15.60	14.88	1.38	0.05	0.40	0.80	0.60	0.76
Mean	**12.74**	**1.34**	**0.06**	**0.33**	**0.66**	**0.50**	**0.58**

Table 37. Median grain size, wet bulk density, fraction LOI and critical shear stress for SF8B.

Sample Depth (cm)	Grain Size (µm)	Wet Bulk Density (g/cm³)	Fraction LOI	τ_0 (Pa)	τ_1 (Pa)	τ_{linear} (Pa)	τ_{power} (Pa)
0.00	10.70	1.29	0.06	0.20	0.40	0.40	0.50
3.00	10.24	1.31	0.07	0.40	0.80	0.64	0.83
6.20	13.92	1.40	0.07	0.40	0.80	0.80	0.75
12.00	11.88	1.50	0.07	0.80	1.60	1.04	1.06
16.60	11.82	1.35	0.06	0.80	1.60	0.89	0.65
Mean	**11.71**	**1.37**	**0.07**	**0.52**	**1.04**	**0.75**	**0.76**

2.4.9 CORES SF9A AND SF9B

Cores SF9A and SF9B were collected from the eastern mudflats, east of coring location SF8 and the CDF. Core SF9A comprised 1-2 cm tan-colored silt and fine sand over darker colored silt and fine sand. Small worms and organic detritus were sticking up from the surface. The surface of core SF9B, as well, consisted of 1-2 cm of tan-colored silt and fine sand. One small worm was observed on the surface, and organic material was visible immediately beneath the surface layer. Both cores became stiffer with depth, containing clayey-silt and fine sand.

A photograph of the cores aligned with each other is presented in Figure 47. Their respective erosion rate data are plotted in Figure 48. Shear stresses ranging between 0.1 and 12.8 Pa were applied to these cores. The intra-core erosion rate ratios of the depth intervals evaluated in each core are shown in Figure 49. For both cores, erosion rates and ratios generally decreased with depth.

The power law regression fit within each depth interval of the cores is illustrated in Figure 50. Coefficients and regression statistics from the power law analysis are presented in Table 38 and Table 39 for the cores, respectively. The measured median grain sizes, and the computed wet bulk densities and critical shear stresses for each depth interval are provided in Table 40 and Table 41.

The vertical profiles of d_{50} and ρ_b from each core are presented in Figure 51. The median grain size in SF9A varied very little with depth, from a minimum of 8.05 µm (fine silt) at a depth of 5.15 cm to a maximum of 13.93 µm (fine silt) at a depth of 7.50 cm. The median grain size in SF9B also showed little variation: between 8.74 µm (fine silt) at the surface to 16.62 µm (medium silt) at a depth of 7.70 cm. The core-averaged d_{50} in SF9A and SF9B was 11.53 µm and 11.62 µm, respectively (fine silt in both cores).

The wet bulk density in SF9A varied between a minimum of 1.23 g/cm^3 at the surface and a maximum of 1.44 g/cm^3 at a depth of 2.70 cm. The wet bulk density in SF9B was a maximum of 1.41 g/cm^3 at a depth of 7.70 cm and a minimum of 1.37 g/cm^3 at a depth of 8.40 cm. The core-averaged wet bulk density in the cores was 1.37 g/cm^3 and 1.38 g/cm^3, respectively.

The critical shear stress estimates in each core increased with down-core depth; the magnitudes were slightly larger at depth in core SF9A than SF9B. The linearly interpolated critical shear stress estimate core-averages were 1.45 Pa and 1.33 Pa for SF9A and SF9B, respectively; the power law estimates were 1.58 Pa and 1.52 Pa, respectively.

Figure 47. Pre-processing photo of cores SF9A (left) and SF9B (right).

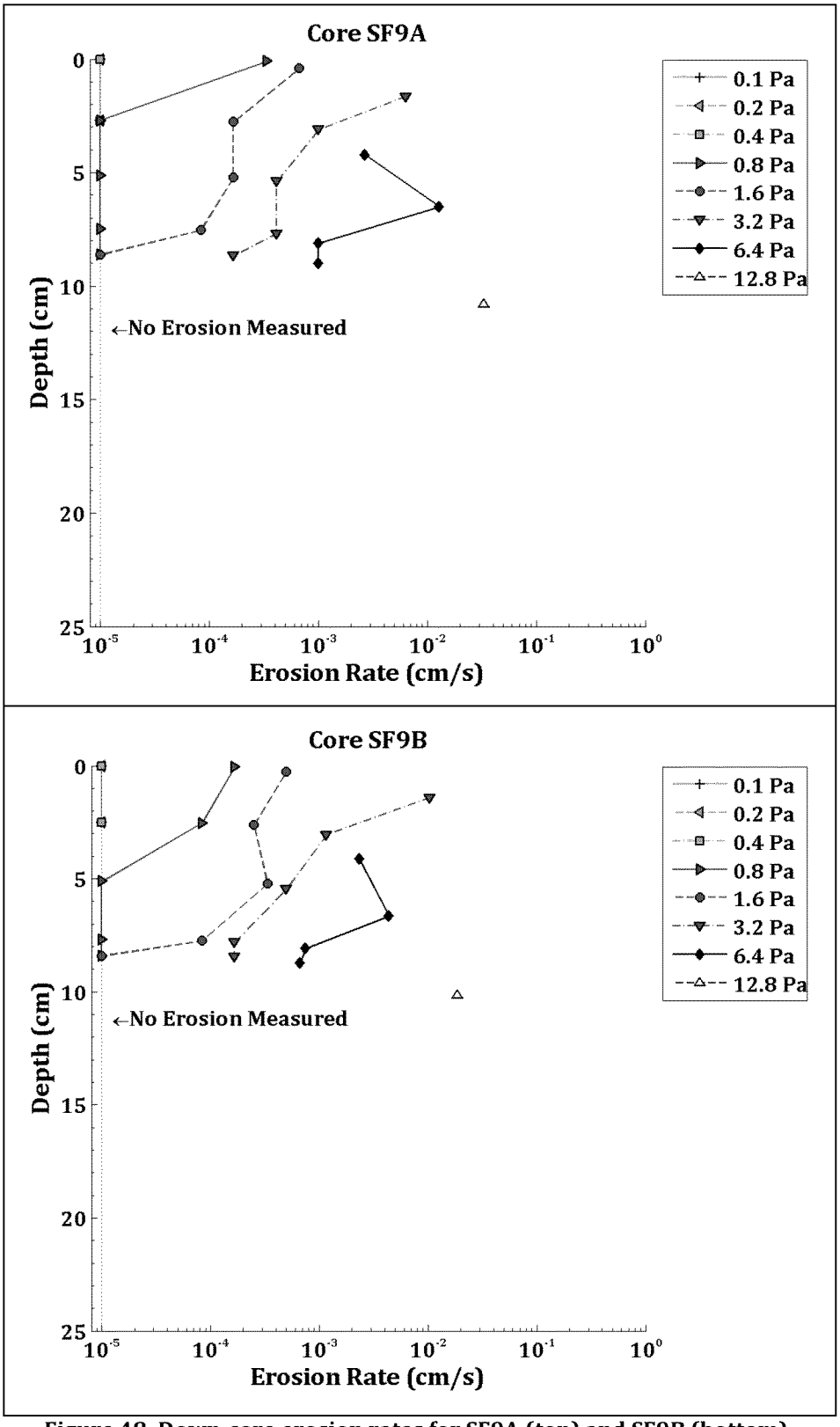

Figure 48. Down-core erosion rates for SF9A (top) and SF9B (bottom).

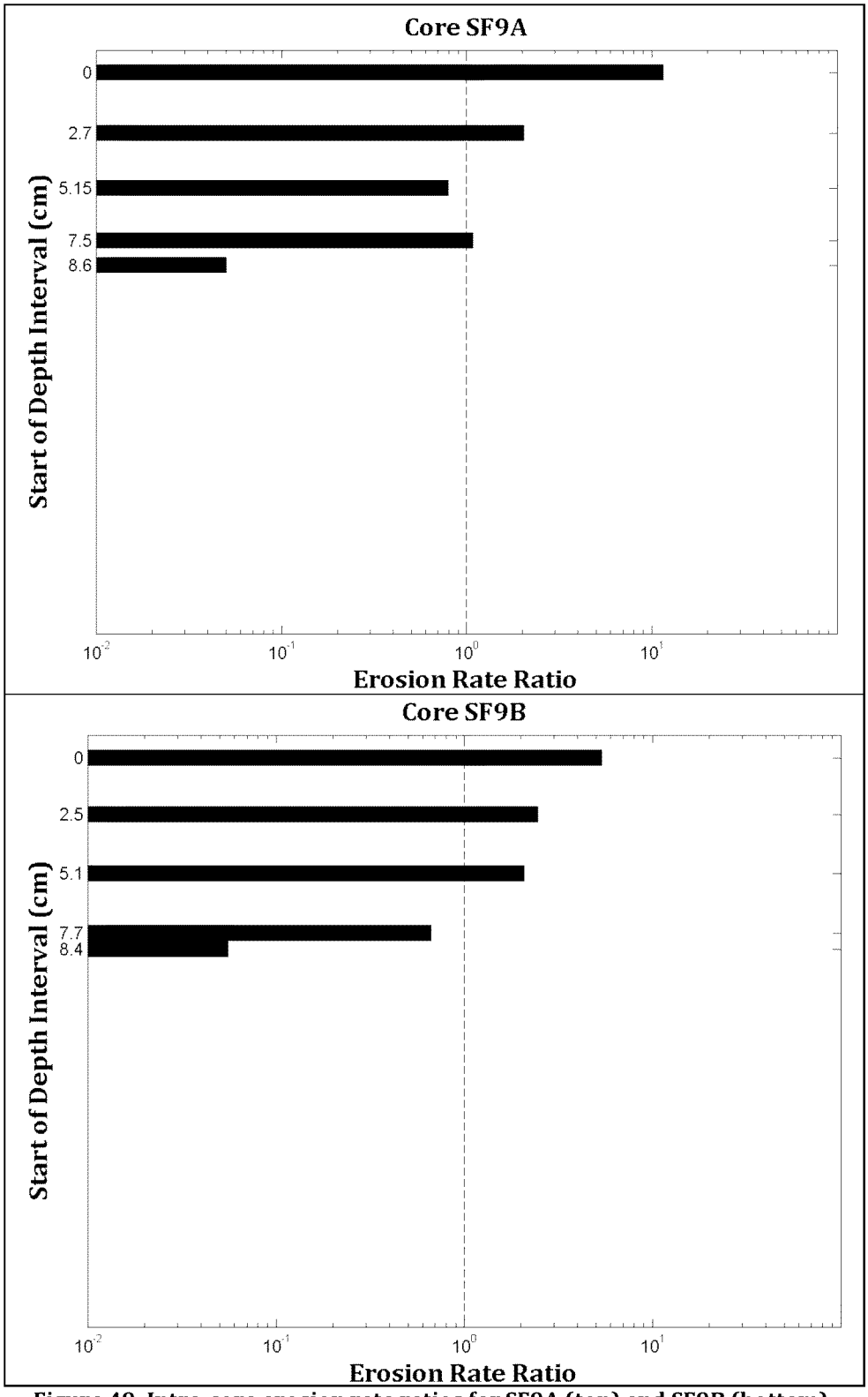

Figure 49. Intra-core erosion rate ratios for SF9A (top) and SF9B (bottom).

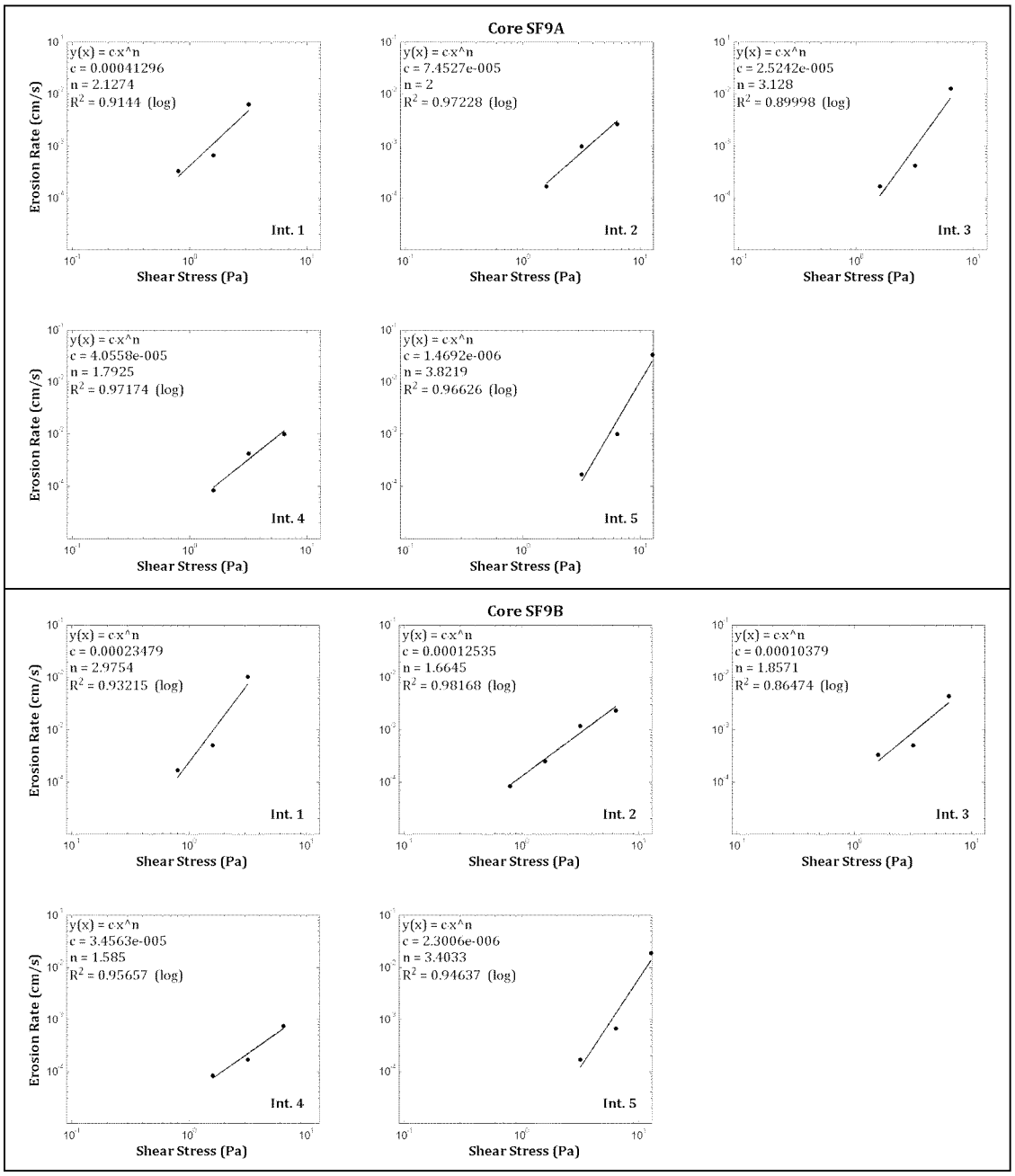

Figure 50. Power law best-fit regression solutions for SF9A (top) and SF9B (bottom).

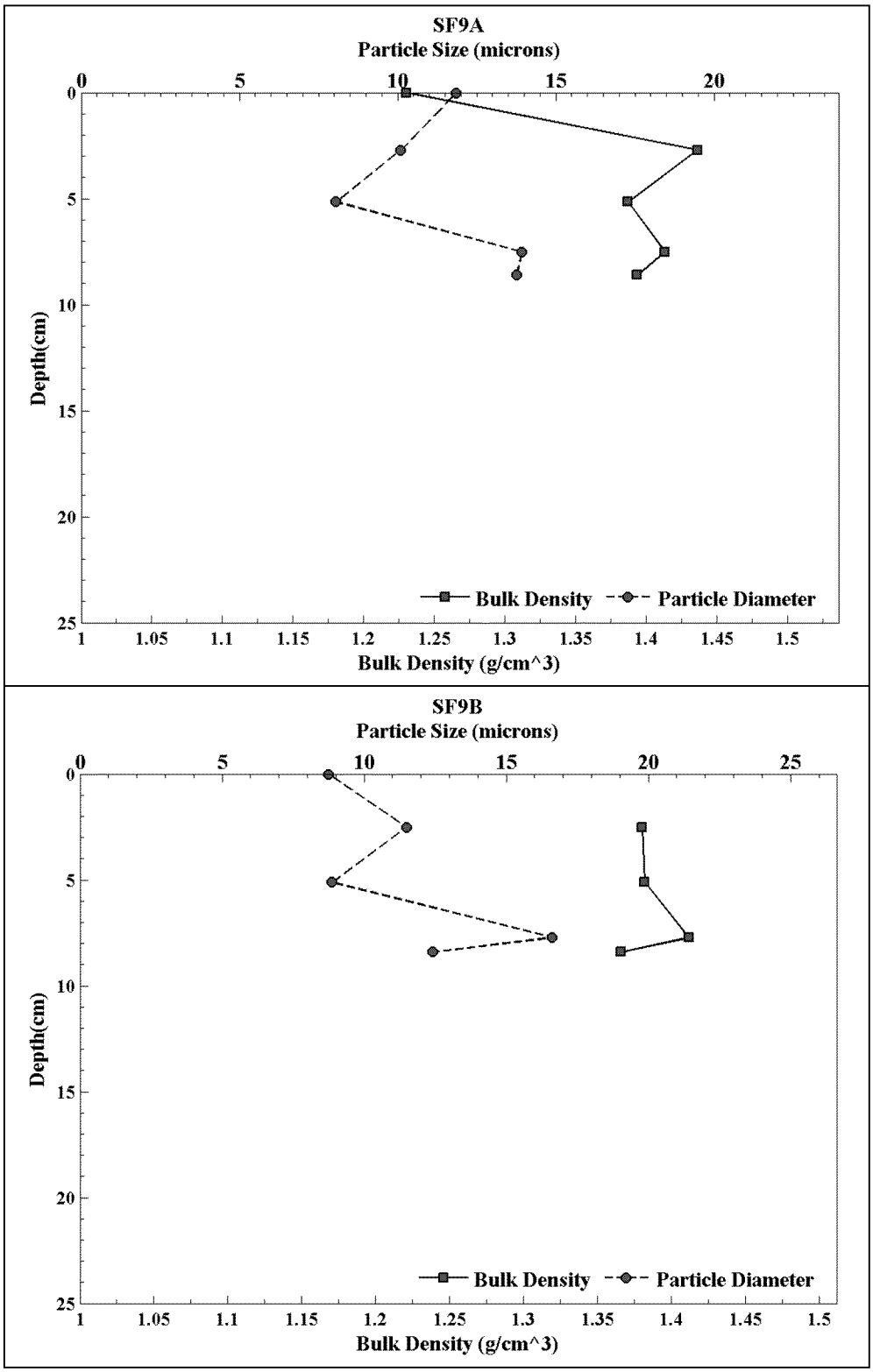

Figure 51. Down-core wet bulk density and median grain size for SF9A (top) and SF9B (bottom).

Table 38. Power law best-fit variables for the measured depth intervals in SF9A.

Depth Interval	Interval Start Depth (cm)	Interval End Depth (cm)	A	n	r^2
1	0.00	2.70	0.000413	2.13	0.91
2	2.70	5.00	0.000075	2.00	0.97
3	5.15	7.50	0.000025	3.13	0.90
4	7.50	8.40	0.000041	1.79	0.97
5	8.60	12.30	0.000001	3.82	0.97

Table 39. Power law best-fit variables for the measured depth intervals in SF9B.

Depth Interval	Interval Start Depth (cm)	Interval End Depth (cm)	A	n	r^2
1	0.00	2.40	0.000235	2.98	0.93
2	2.50	4.80	0.000125	1.66	0.98
3	5.10	7.70	0.000104	1.86	0.86
4	7.70	8.30	0.000035	1.58	0.96
5	8.40	11.40	0.000002	3.40	0.95

Table 40. Median grain size, wet bulk density, fraction LOI and critical shear stress for SF9A.

Sample Depth (cm)	Grain Size (μm)	Wet Bulk Density (g/cm³)	Fraction LOI	τ_0 (Pa)	τ_1 (Pa)	τ_{linear} (Pa)	τ_{power} (Pa)
0.00	11.84	1.23	0.06	0.40	0.80	0.52	0.51
2.70	10.09	1.44	0.06	0.80	1.60	1.28	1.16
5.15	8.05	1.39	0.07	0.80	1.60	1.28	1.55
7.50	13.93	1.41	0.06	0.80	1.60	1.60	1.65
8.60	13.75	1.39	0.06	1.60	3.20	2.56	3.02
Mean	**11.53**	**1.37**	**0.06**	**0.88**	**1.76**	**1.45**	**1.58**

Table 41. Median grain size, wet bulk density, fraction LOI and critical shear stress for SF9B.

Sample Depth (cm)	Grain Size (μm)	Wet Bulk Density (g/cm³)	Fraction LOI	τ_0 (Pa)	τ_1 (Pa)	τ_{linear} (Pa)	τ_{power} (Pa)
0.00	8.74	-	0.05	0.40	0.80	0.64	0.75
2.50	11.48	1.38	0.06	0.40	0.80	0.80	0.87
5.10	8.86	1.38	0.06	0.80	1.60	1.04	0.98
7.70	16.62	1.41	0.06	0.80	1.60	1.60	1.95
8.40	12.42	1.37	0.05	1.60	3.20	2.56	3.03
Mean	**11.62**	**1.38**	**0.06**	**0.80**	**1.60**	**1.33**	**1.52**

2.4.10 CORES SF10A AND SF10B

Cores SF10A and SF10B were collected from the eastern mudflats east of the Port of Elizabeth. Core SF10A comprised 2-3 cm of tan-colored silt and sandy-silt overlying brown-colored silt and sand beneath. Small benthic organisms (0.5 cm dimension) were visible on the surface. The surface of core SF10B consisted of a 2-3 cm thick, low-density silt and fine sand surface. Material beneath was darker-colored. Fine, stringy organics were visible on the surface. Deeper material in both cores was higher in density and contained small visible gas bubbles.

A photograph of the cores aligned with each other is presented in Figure 52. Their respective erosion rate data are plotted in Figure 53. Shear stresses ranging between 0.1 and 6.4 Pa were applied to these cores. The intra-core variation of the depth intervals evaluated in each core are shown in Figure 54. The rates in core SF10A remained relatively constant with depth, increasing slightly at the deepest depths. The erosion rates in core SF10B decreased beneath the surface layer. For both cores, erosion susceptibility did not vary much with depth.

The power law regression fit within each depth interval of the cores is illustrated in Figure 55. Coefficients and regression statistics from the power law analysis are presented in Table 42 and Table 43 for the cores, respectively. The measured median grain sizes, and the computed wet bulk densities and critical shear stresses for each depth interval are provided in Table 44 and Table 45.

The vertical profiles of d_{50} and ρ_b from each core are presented in Figure 56. The median grain size in SF10A varied very little with depth: between a minimum of 8.57 µm (fine silt) at a depth of 4.60 cm and a maximum of 11.08 µm (fine silt) at a depth of 9.30 cm. The median grain size in SF10B also varied little with depth: a minimum of 8.71 µm (fine silt) at a depth of 7.30 cm and a maximum of 10.38 µm (fine silt) at a depth of 3.70 cm. The core-averaged d_{50} in SF10A and SF10B was 9.68 µm and 9.42 µm, respectively (fine silt for both cores).

The wet bulk density in SF10A varied between a minimum of 1.20 g/cm^3 at the surface and a maximum of 1.37 g/cm^3 at a depth of 19.10 cm. The wet bulk density in SF10B varied between a minimum of 1.20 g/cm^3 at the surface and a maximum of 1.36 g/cm^3 at a depth of 16.00 cm. The core-averaged wet bulk density in the cores was 1.33 g/cm^3 and 1.32 g/cm^3, respectively.

The critical shear stress estimates in SF10A vary little down-core; those in SF10B increase slightly with depth. In general, those computed in SF10B are larger: The linearly interpolated critical shear stress estimate core-averages were 0.48 Pa and 0.62 Pa, respectively; the power law estimates were 0.44 Pa and 0.64 Pa, respectively.

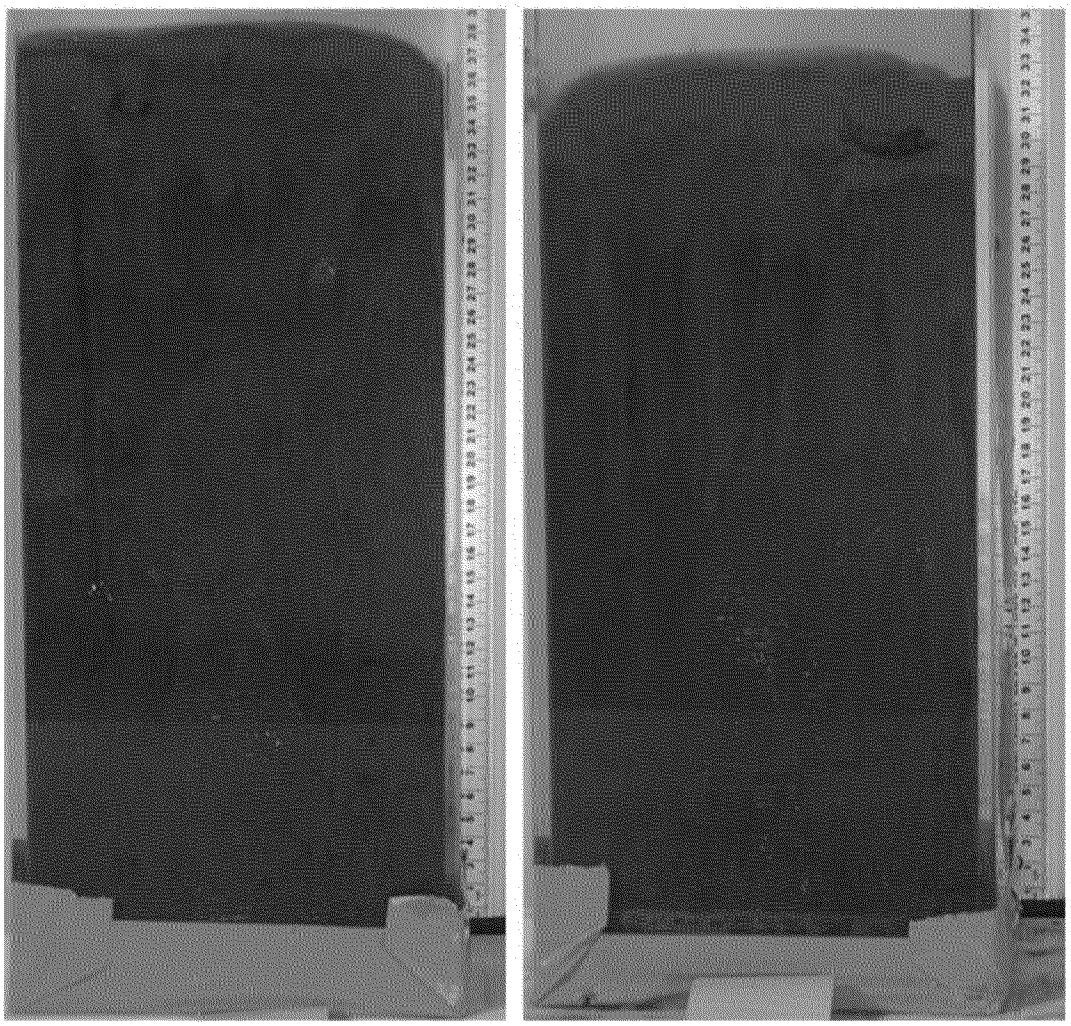

Figure 52. Pre-processing photo of cores SF10A (left) and SF10B (right).

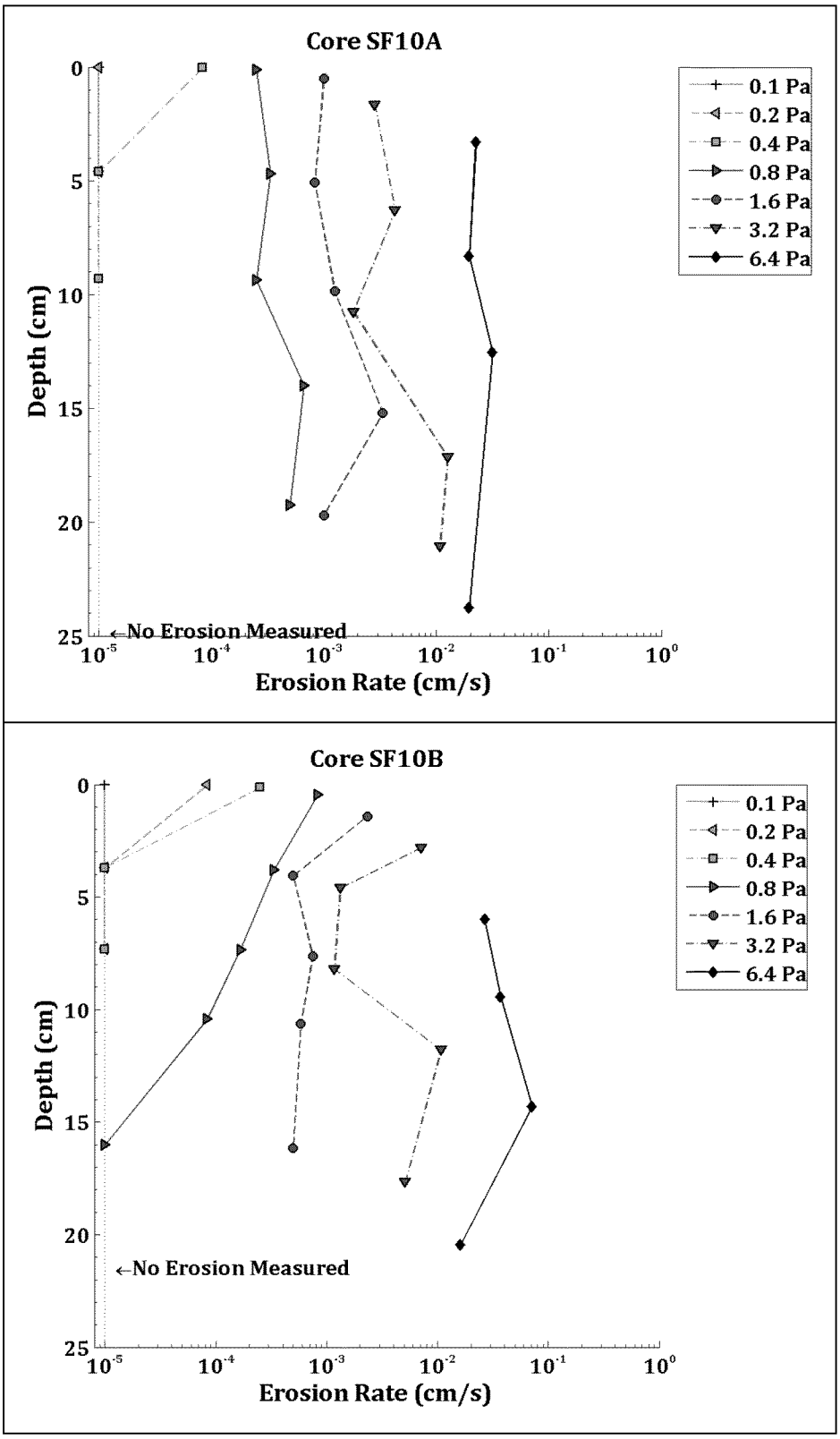

Figure 53. Down-core erosion rates for SF10A (top) and SF10B (bottom).

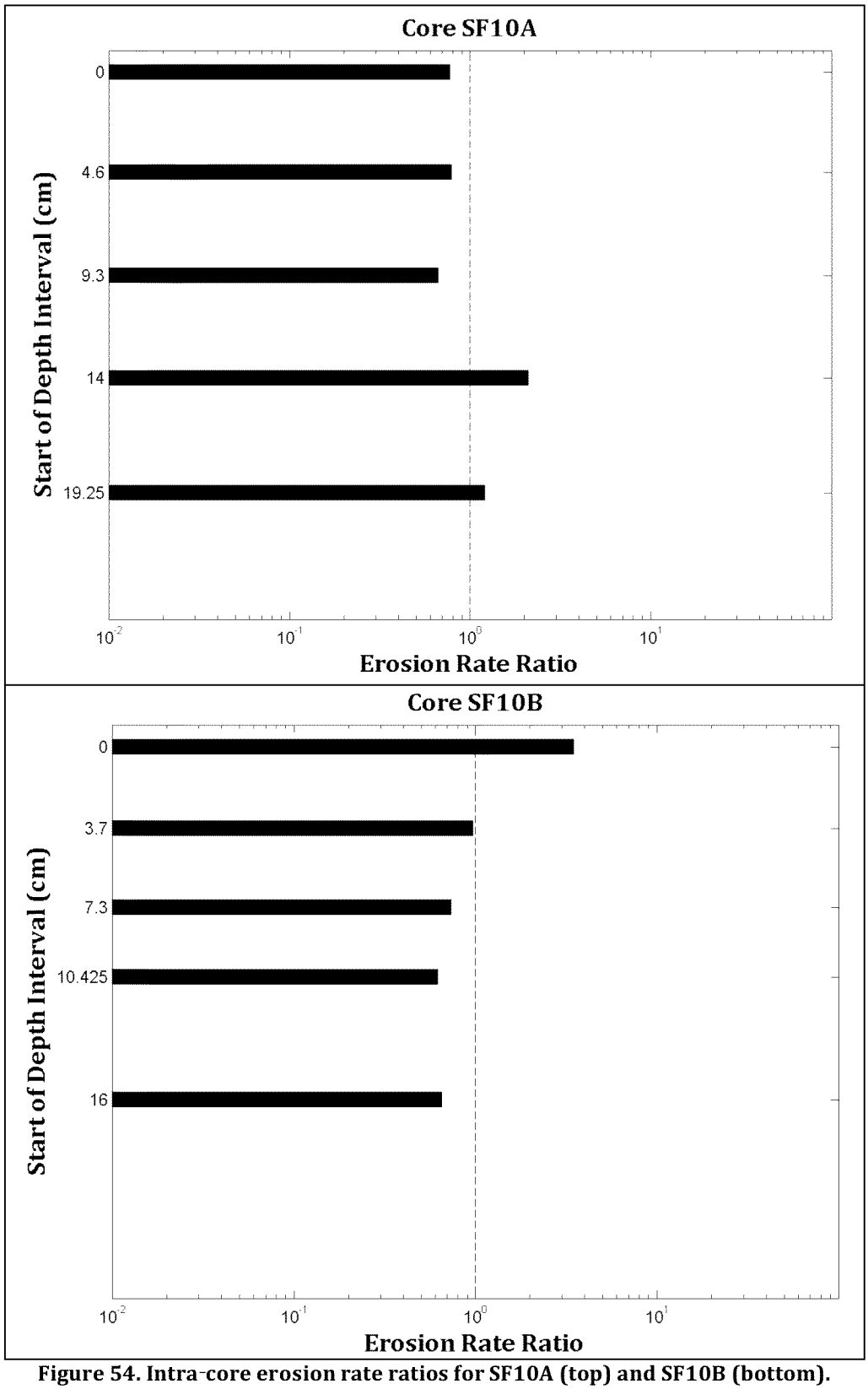

Figure 54. Intra-core erosion rate ratios for SF10A (top) and SF10B (bottom).

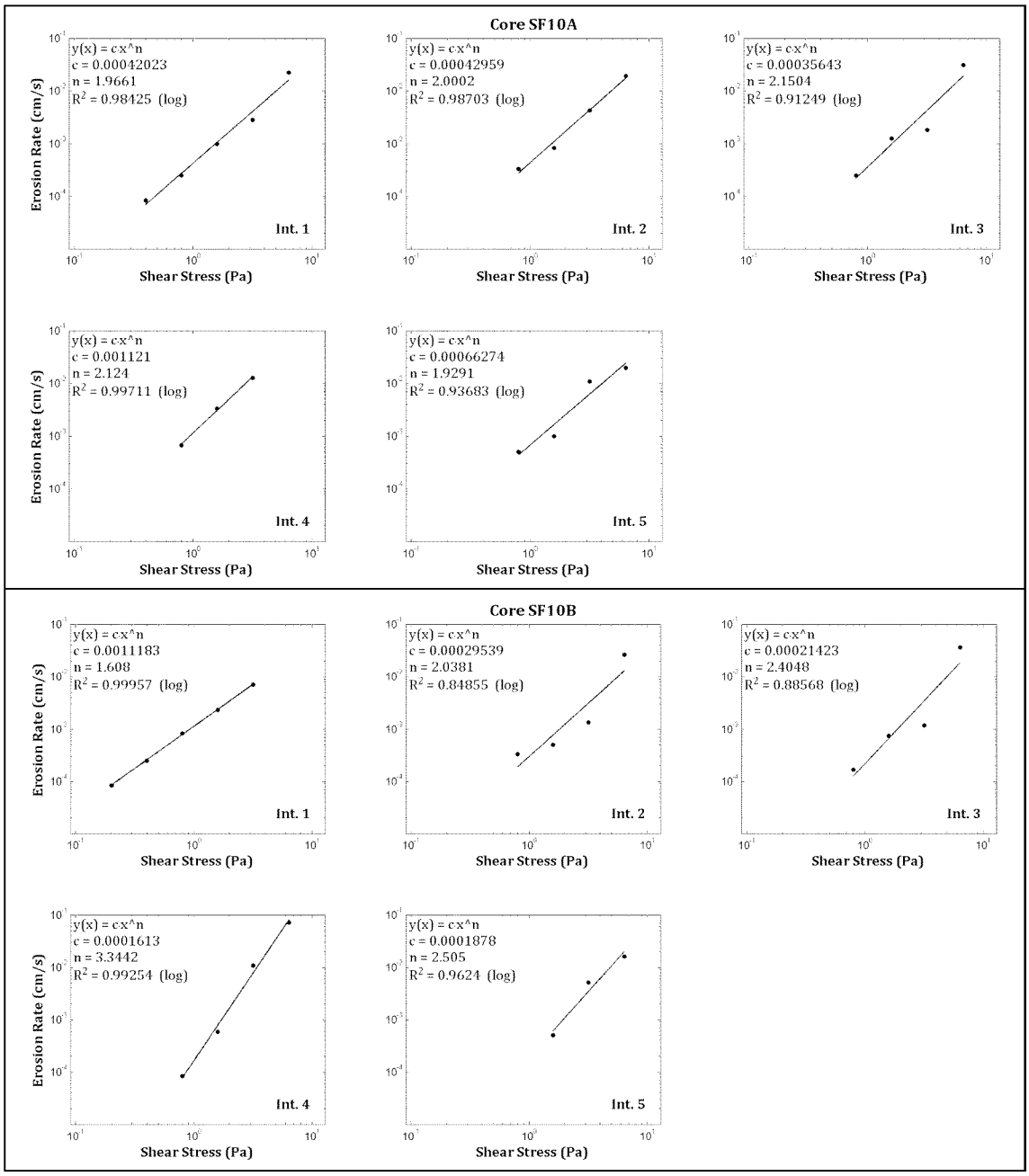

Figure 55. Power law best-fit regression solutions for SF10A (top) and SF10B (bottom).

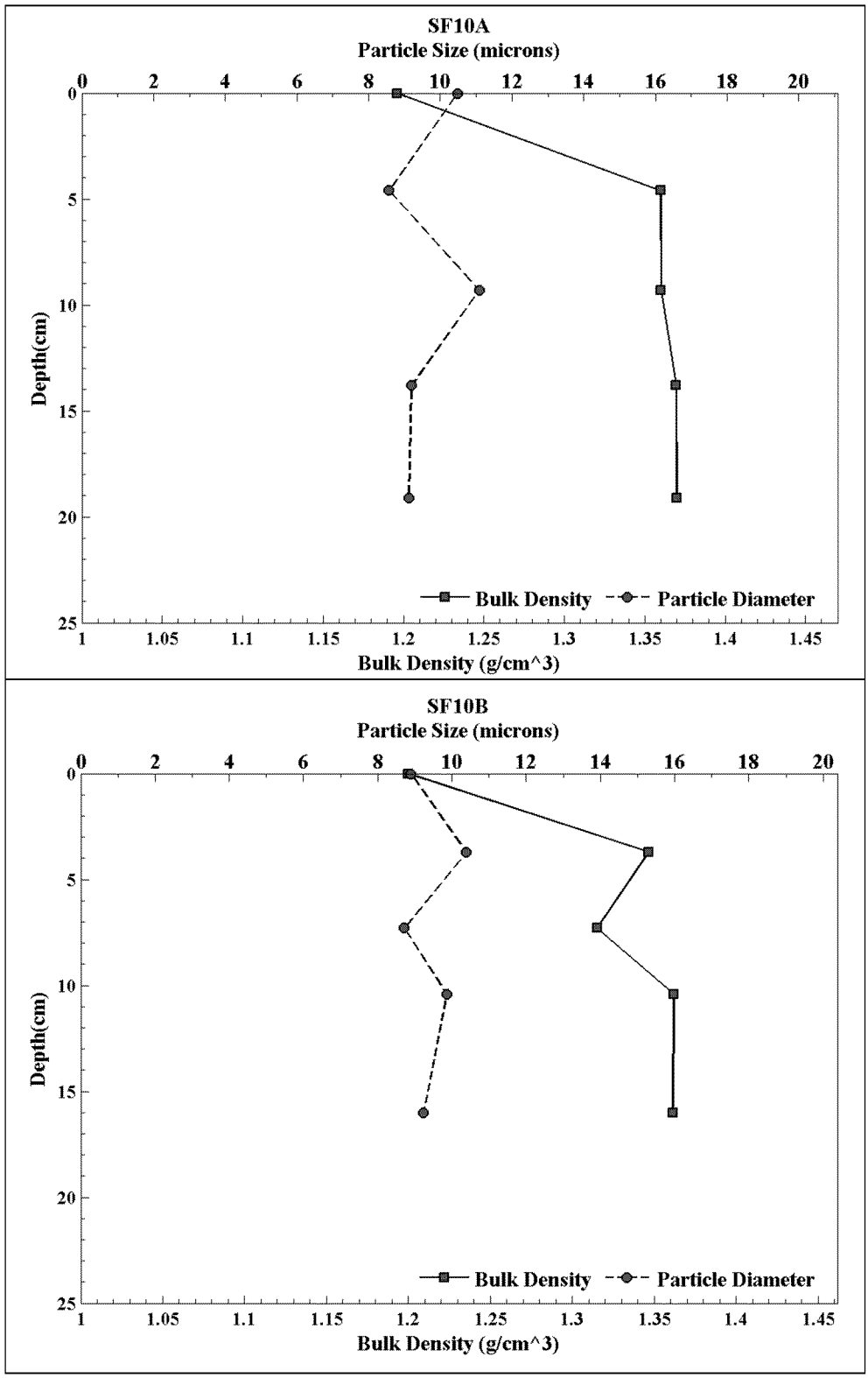

Figure 56. Down-core wet bulk density and median grain size for SF10A (top) and SF10B (bottom).

Table 42. Power law best-fit variables for the measured depth intervals in SF10A.

Depth Interval	Interval Start Depth (cm)	Interval End Depth (cm)	A	n	r^2
1	0.00	4.10	0.000420	1.97	0.98
2	4.60	9.30	0.000430	2.00	0.99
3	9.30	13.80	0.000356	2.15	0.91
4	13.80	18.10	0.001121	2.12	1.00
5	19.10	25.40	0.000663	1.93	0.94

Table 43. Power law best-fit variables for the measured depth intervals in SF10B.

Depth Interval	Interval Start Depth (cm)	Interval End Depth (cm)	A	n	r^2
1	0.00	3.50	0.001118	1.61	1.00
2	3.70	7.00	0.000295	2.04	0.85
3	7.30	10.30	0.000214	2.40	0.89
4	10.40	15.80	0.000161	3.34	0.99
5	16.00	21.90	0.000188	2.51	0.96

Table 44. Median grain size, wet bulk density, fraction LOI and critical shear stress for SF10A.

Sample Depth (cm)	Grain Size (μm)	Wet Bulk Density (g/cm^3)	Fraction LOI	τ_0 (Pa)	τ_1 (Pa)	τ_{linear} (Pa)	τ_{power} (Pa)
0.00	10.47	1.20	0.07	0.20	0.40	0.40	0.48
4.60	8.57	1.36	0.07	0.40	0.80	0.52	0.48
9.30	11.08	1.36	0.06	0.40	0.80	0.56	0.55
13.80	9.19	1.37	0.06	0.40	0.80	0.46	0.32
19.10	9.12	1.37	0.06	0.40	0.80	0.47	0.38
Mean	**9.68**	**1.33**	**0.07**	**0.36**	**0.72**	**0.48**	**0.44**

Table 45. Median grain size, wet bulk density, fraction LOI and critical shear stress for SF10B.

Sample Depth (cm)	Grain Size (μm)	Wet Bulk Density (g/cm^3)	Fraction LOI	τ_0 (Pa)	τ_1 (Pa)	τ_{linear} (Pa)	τ_{power} (Pa)
0.00	8.89	1.20	0.08	0.10	0.20	0.20	0.22
3.70	10.38	1.35	0.07	0.40	0.80	0.52	0.59
7.30	8.71	1.32	0.08	0.40	0.80	0.64	0.73
10.40	9.86	1.36	0.07	0.40	0.80	0.80	0.87
16.00	9.24	1.36	0.07	0.80	1.60	0.96	0.78
Mean	**9.42**	**1.32**	**0.08**	**0.42**	**0.84**	**0.62**	**0.64**

2.4.11 CORES SF11B AND SF11C

Cores SF11B and SF11C were collected from the western mouth of the Port of Elizabeth and in proximity to the western shoreline. Core SF11B comprised 1-2 cm of tan-colored, low-density silt and sand over dark gray- and tan-colored silt and clayey-silt. At a depth of 25 cm, a light gray-colored silt and clayey-silt layer existed and persisted for the remainder of the core. The surface of core SF11C consisted of a 2-3 cm tan-colored layer of silt and sand overlying 20-22 cm of dark-colored silt and sand. Some coarse sand lenses were visible down-core and at the bottom of the core. Both cores became stiffer with depth, and a strong petroleum odor was sensed throughout both cores.

A photograph of the cores aligned with each other is presented in Figure 57. Their respective erosion rate data are plotted in Figure 58. Shear stresses ranging between 0.1 and 6.4 Pa were applied to these cores. The intra-core erosion of the depth intervals evaluated in each core are shown in Figure 59. In general, core SF11B featured a decrease in erosion rate with depth; however, at a depth of 10 cm, the erosion rate increased significantly (order of magnitude or more). The explanation for this is unknown at present. The down-core erosion rates in core SF11C were variable, indicating layers of easier- and more-difficult-to-erode sediments. Akin to the down-core erosion rate trends, the erosion susceptibility varied with depth in both cores.

The power law regression fit within each depth interval of the cores is illustrated in Figure 60. Coefficients and regression statistics from the power law analysis are presented in Table 46 and Table 47 for the cores, respectively. The measured median grain sizes, and the computed wet bulk densities and critical shear stresses for each depth interval are provided in Table 48 and Table 49.

The vertical profiles of d_{50} and ρ_b from each core are presented in Figure 61. The median grain size in SF11B varied between very fine and fine silt: from a maximum of 10.24 µm at a depth of 2.70 cm to a minimum of 5.35 µm at a depth of 5.80 cm. The median grain size in SF11C generally increased with depth from a minimum of 5.23 µm (very fine silt) at a depth of 6.90 cm to a maximum of 16.04 µm (medium silt) at a depth of 12.80 cm. The core-averaged d_{50} in SF11B and SF11C was 6.90 µm and 8.82 µm, respectively (very fine to medium silt).

The wet bulk density in SF11B increased from a minimum of 1.30 g/cm^3 at a depth of 2.70 cm to a maximum of 1.45 g/cm^3 at a depth of 10.20 cm. The wet bulk density in SF11C varied down-core between a minimum of 1.26 g/cm^3 at a depth of 11.20 cm and a maximum of 1.44 g/cm^3 at a depth of 6.90 cm. The core-averaged wet bulk density in each core was 1.35 g/cm^3 and 1.33 g/cm^3, respectively.

The critical shear stress estimates in both cores increase with down-core depth. The overall core-averages were similar: The linearly interpolated critical shear stress estimates were 1.08 Pa and 1.18 Pa, respectively; the power law estimates were 1.20 Pa and 1.13 Pa, respectively.

Figure 57. Pre-processing photo of cores SF11B (left) and SF11C (right).

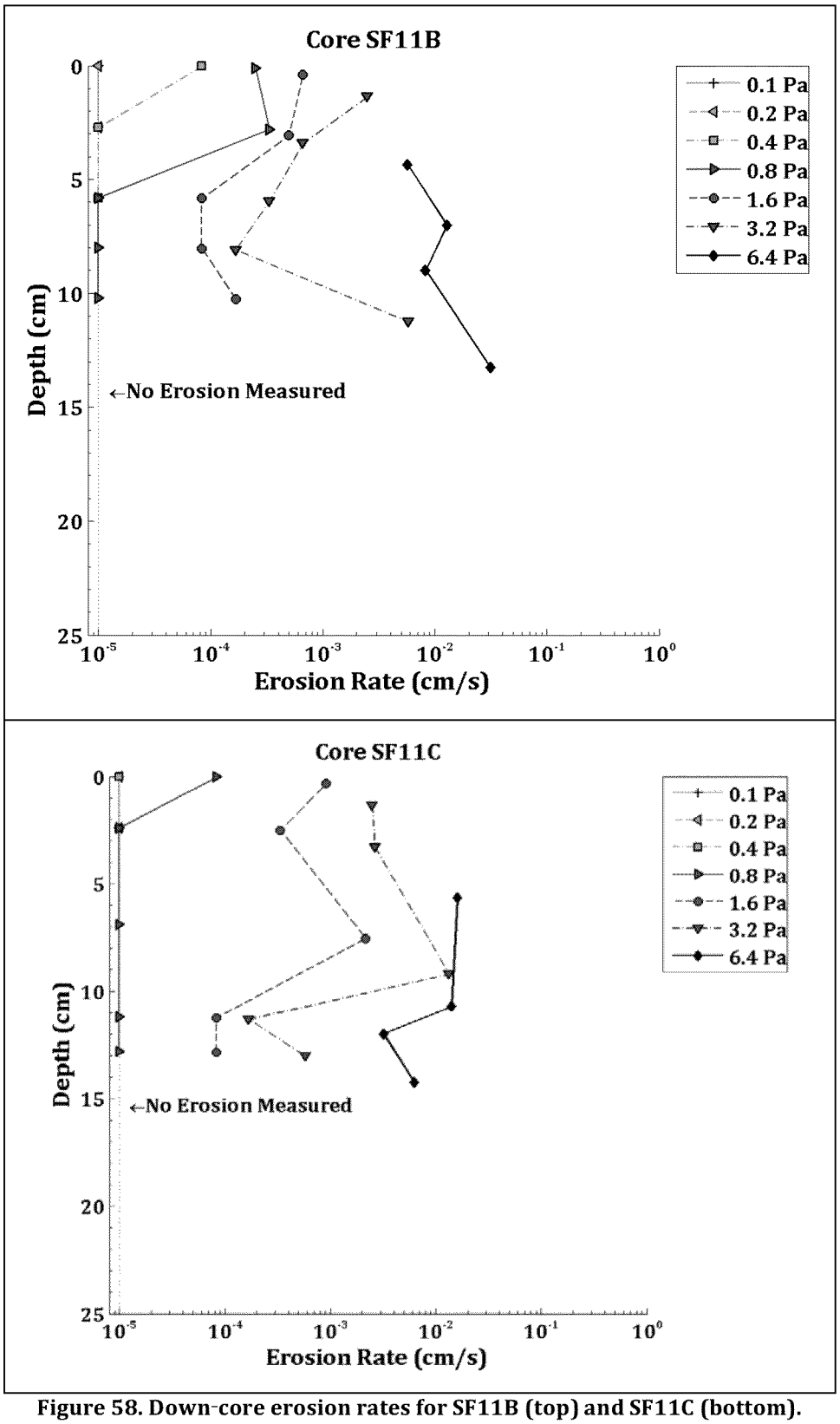

Figure 58. Down-core erosion rates for SF11B (top) and SF11C (bottom).

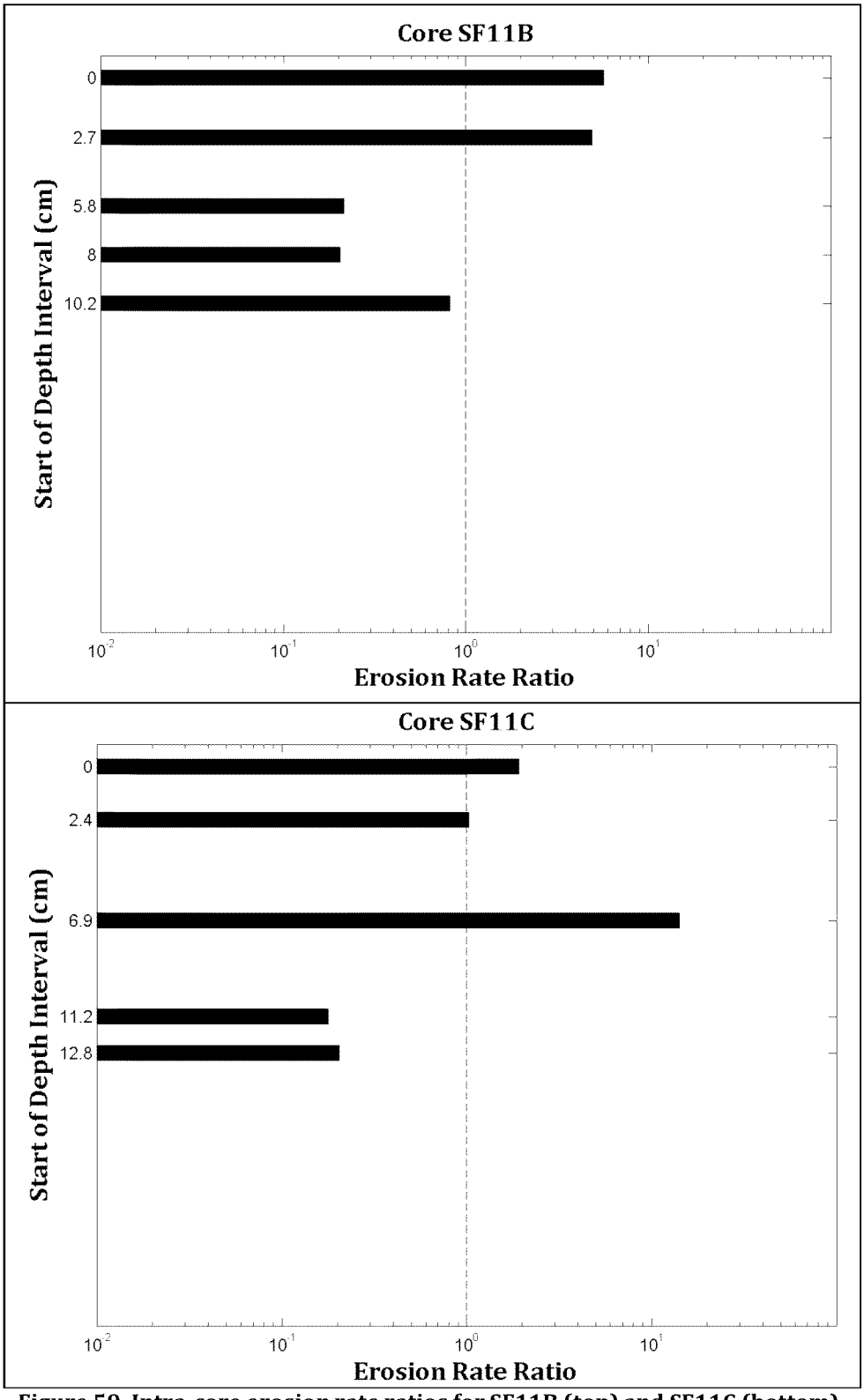

Figure 59. Intra-core erosion rate ratios for SF11B (top) and SF11C (bottom).

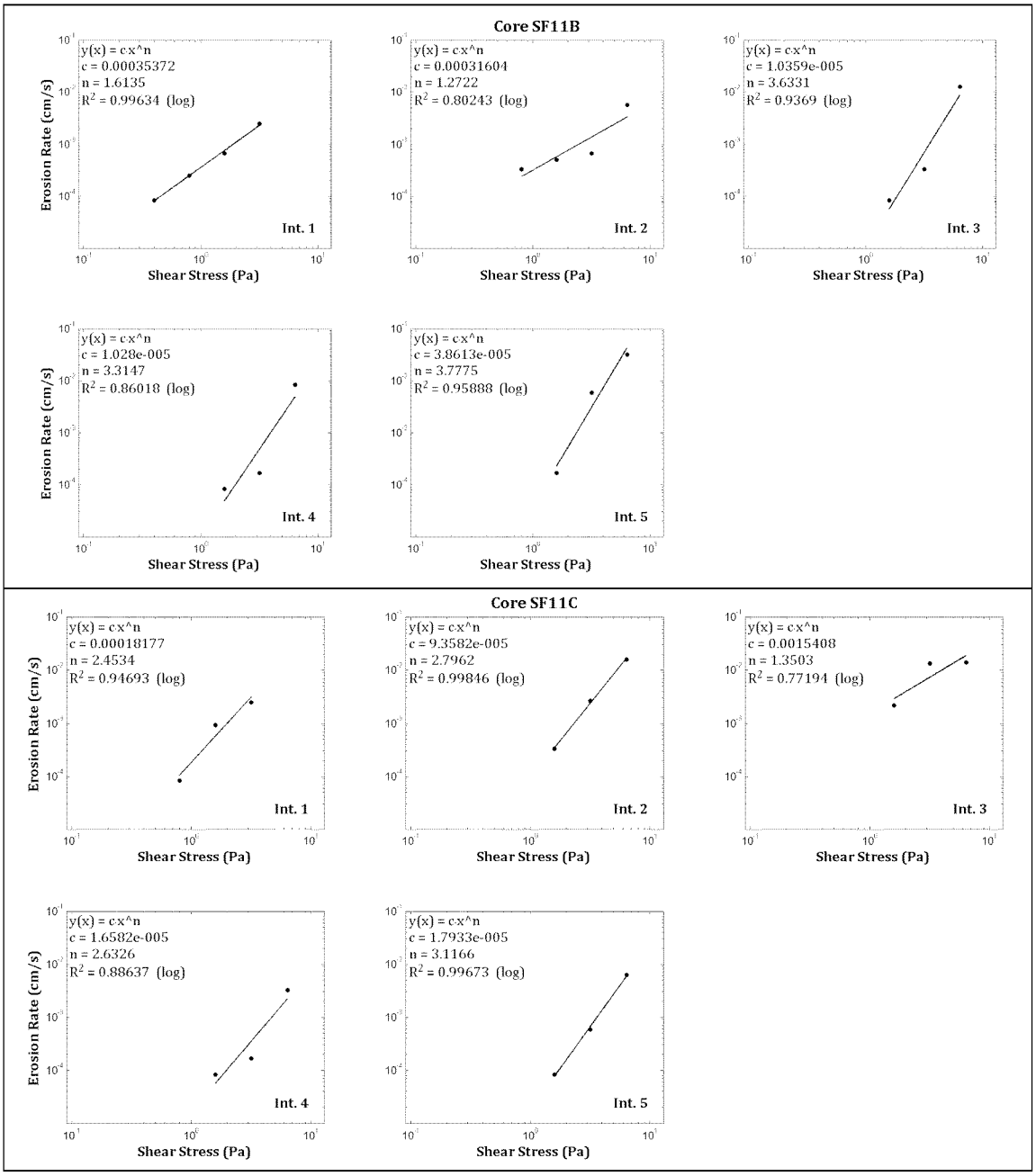

Figure 60. Power law best-fit regression solutions for SF11B (top) and SF11C (bottom).

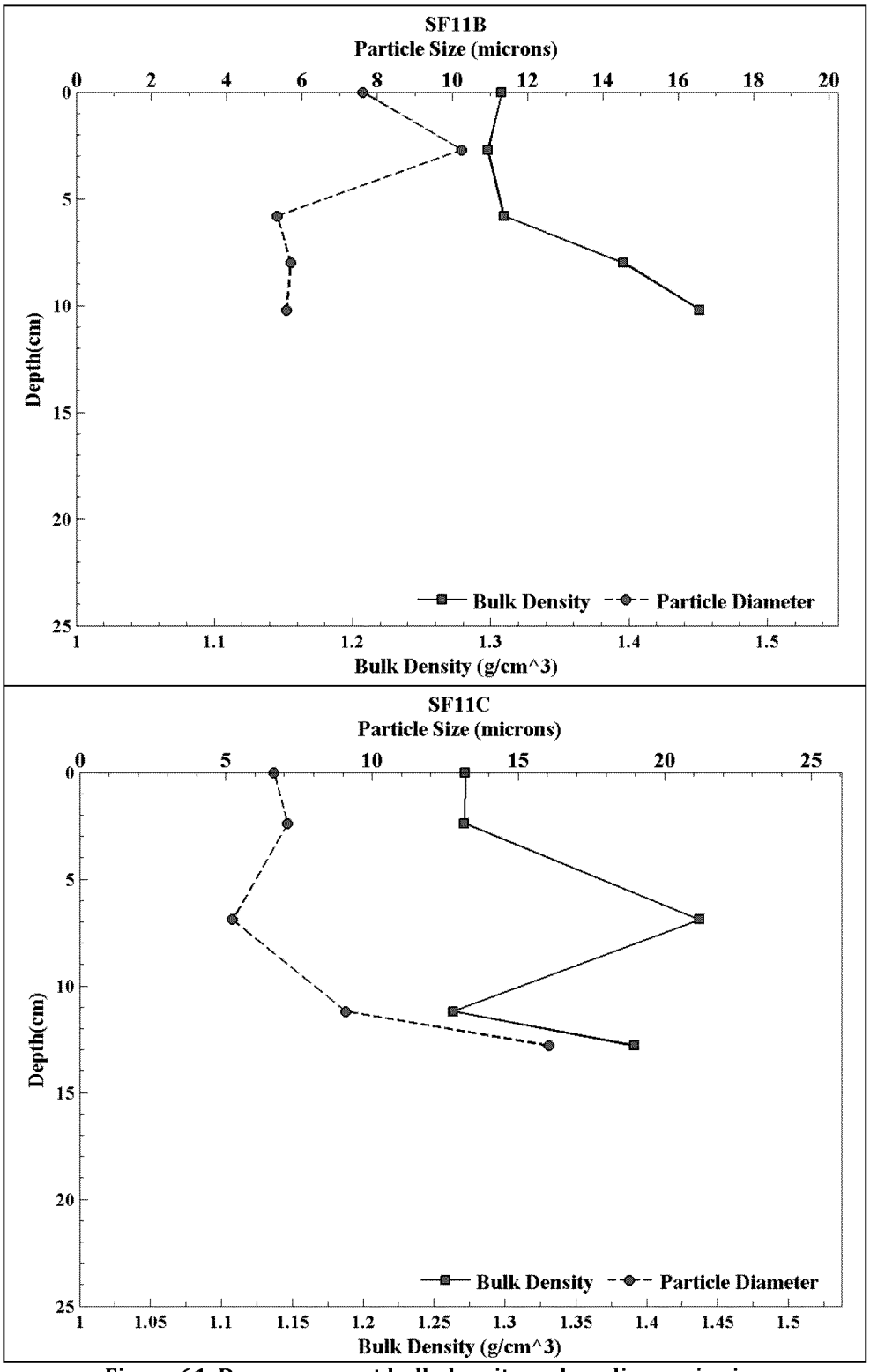

Figure 61. Down-core wet bulk density and median grain size for SF11B (top) and SF11C (bottom).

Table 46. Power law best-fit variables for the measured depth intervals in SF11B.

Depth Interval	Interval Start Depth (cm)	Interval End Depth (cm)	A	n	r^2
1	0.00	2.10	0.000354	1.61	1.00
2	2.70	5.10	0.000316	1.27	0.80
3	5.80	8.00	0.000010	3.63	0.94
4	8.00	9.80	0.000010	3.31	0.86
5	10.20	14.30	0.000039	3.78	0.96

Table 47. Power law best-fit variables for the measured depth intervals in SF11C.

Depth Interval	Interval Start Depth (cm)	Interval End Depth (cm)	A	n	r^2
1	0.00	2.10	0.000182	2.45	0.95
2	2.40	6.80	0.000094	2.80	1.00
3	6.90	11.20	0.001541	1.35	0.77
4	11.20	12.60	0.000017	2.63	0.89
5	12.80	15.30	0.000018	3.12	1.00

Table 48. Median grain size, wet bulk density, fraction LOI and critical shear stress for SF11B.

Sample Depth (cm)	Grain Size (μm)	Wet Bulk Density (g/cm³)	Fraction LOI	τ_0 (Pa)	τ_1 (Pa)	τ_{linear} (Pa)	τ_{power} (Pa)
0.00	7.62	1.31	0.06	0.20	0.40	0.40	0.46
2.70	10.24	1.30	0.11	0.40	0.80	0.52	0.40
5.80	5.35	1.31	0.06	0.80	1.60	1.60	1.87
8.00	5.69	1.40	0.05	0.80	1.60	1.60	1.99
10.20	5.58	1.45	0.05	0.80	1.60	1.28	1.29
Mean	**6.90**	**1.35**	**0.07**	**0.60**	**1.20**	**1.08**	**1.20**

Table 49. Median grain size, wet bulk density, fraction LOI and critical shear stress for SF11C.

Sample Depth (cm)	Grain Size (μm)	Wet Bulk Density (g/cm³)	Fraction LOI	τ_0 (Pa)	τ_1 (Pa)	τ_{linear} (Pa)	τ_{power} (Pa)
0.00	6.64	1.27	0.08	0.40	0.80	0.80	0.78
2.40	7.11	1.27	0.08	0.80	1.60	1.04	1.02
6.90	5.23	1.44	0.05	0.80	1.60	0.84	0.13
11.20	9.09	1.26	0.13	0.80	1.60	1.60	1.98
12.80	16.04	1.39	0.10	0.80	1.60	1.60	1.74
Mean	**8.82**	**1.33**	**0.09**	**0.72**	**1.44**	**1.18**	**1.13**

2.4.12 CORES SF12A AND SF12B

Cores SF12A and SF12B were collected from the western mudflats, south of the Port of Elizabeth and along the eastern edge of the mudflats. Core SF12A comprised 1 cm of a tan-colored fluff layer of sand and silt over 10 cm of light tan-colored sand and silt. A few small benthic organisms were visible on the surface. Deeper material was darker brown-colored clayey-silt and sand of increasing stiffness. The surface of core SF12B consisted of 1-2 cm of tan-colored silt and fine sand over darker-colored, and increasingly stiffer, clayey-silt and sand. A few small worms were visible on the surface.

A photograph of the cores aligned with each other is presented in Figure 62. Their respective erosion rate data are plotted in Figure 63. Shear stresses ranging between 0.1 and 12.8 Pa were applied to these cores. The intra-core erosion rate ratios of the depth intervals evaluated in each core are shown in Figure 64. For both cores, erosion rate generally decreased with depth. Core SF12B, however, showed an increase in erosion rate at depths of approximately 8-10 cm before erosion rates continued to decrease. For both, erosion susceptibility followed similar patterns to that of the respective down-core erosion rates.

The power law regression fit within each depth interval of the cores is illustrated in Figure 65. Coefficients and regression statistics from the power law analysis are presented in Table 50 and Table 51 for the cores, respectively. The measured median grain sizes, and the computed wet bulk densities and critical shear stresses for each depth interval are provided in Table 52 and Table 53.

The vertical profiles of d_{50} and ρ_b from each core are presented in Figure 66. Both cores had variable median grain sizes with depth including a spike in grain size beneath the surface. The median grain size in SF12A varied between a minimum of 5.96 µm (very fine silt) at the surface and a maximum of 33.55 µm (coarse silt) at a depth of 8.85 cm. The median grain size in SF12B varied between a maximum of 43.56 µm (coarse silt) at a depth of 5.20 cm to a minimum of 17.78 µm (medium silt) at a depth of 8.10 cm. The core-averaged d_{50} in SF12A and SF12B was 17.16 µm and 24.96 µm, respectively (medium silt for both cores).

The wet bulk density in SF12A varied between a minimum of 1.42 g/cm^3 at the surface and a maximum of 1.65 g/cm^3 at a depth of 6.85 cm. The wet bulk density in SF12B varied between a minimum of 1.43 g/cm^3 at the surface and a maximum of 1.63 g/cm^3 at a depth of 5.20 cm. The core-averaged wet bulk density in the cores was 1.54 g/cm^3 and 1.56 g/cm^3, respectively.

The critical shear stress estimates in both cores generally increased with down-core depth. The overall core-averages were similar: The linearly interpolated critical shear stress estimates were 1.30 Pa and 1.34 Pa, respectively; the power law estimates were 1.29 Pa and 1.37 Pa, respectively.

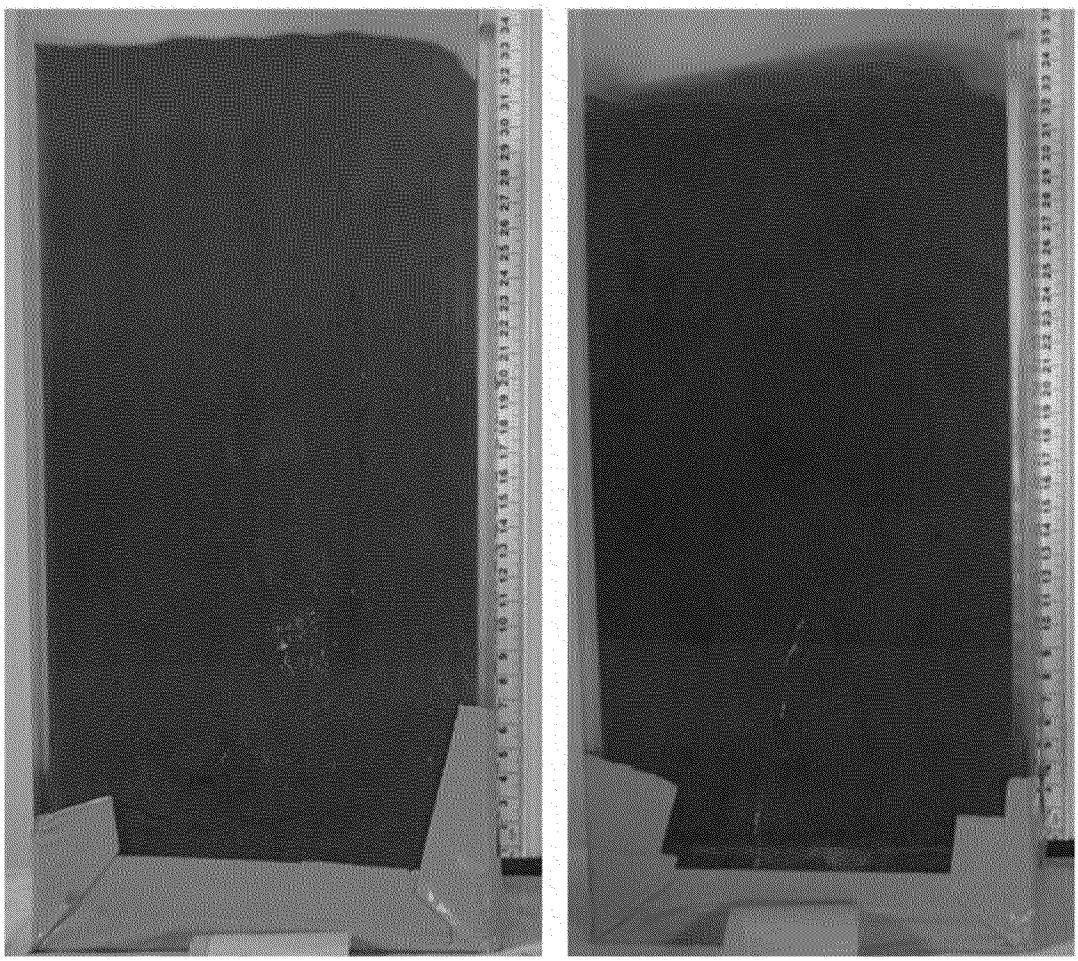

Figure 62. Pre-processing photo of cores SF12A (left) and SF12B (right).

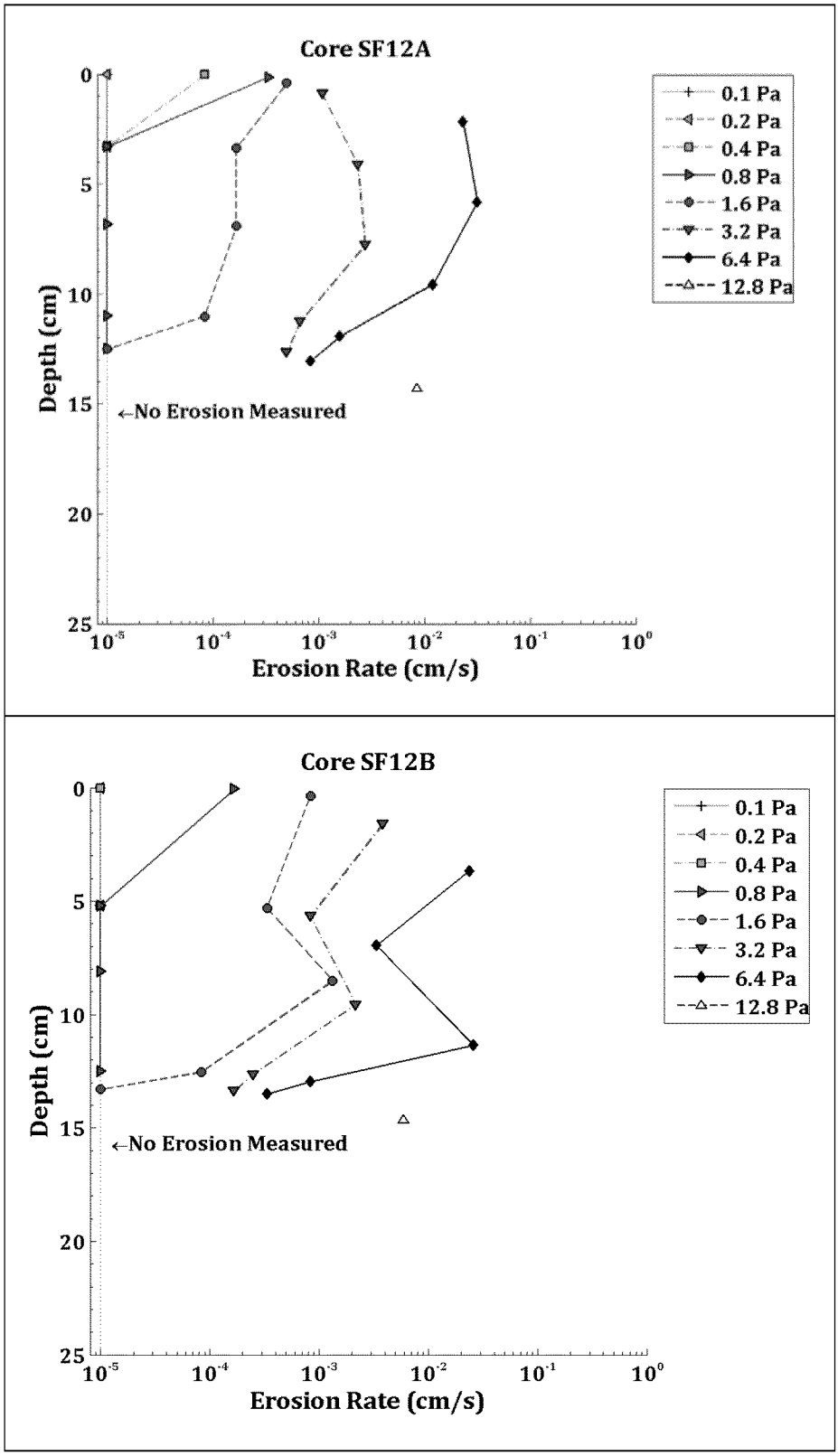

Figure 63. Down-core erosion rates for SF12A (top) and SF12B (bottom).

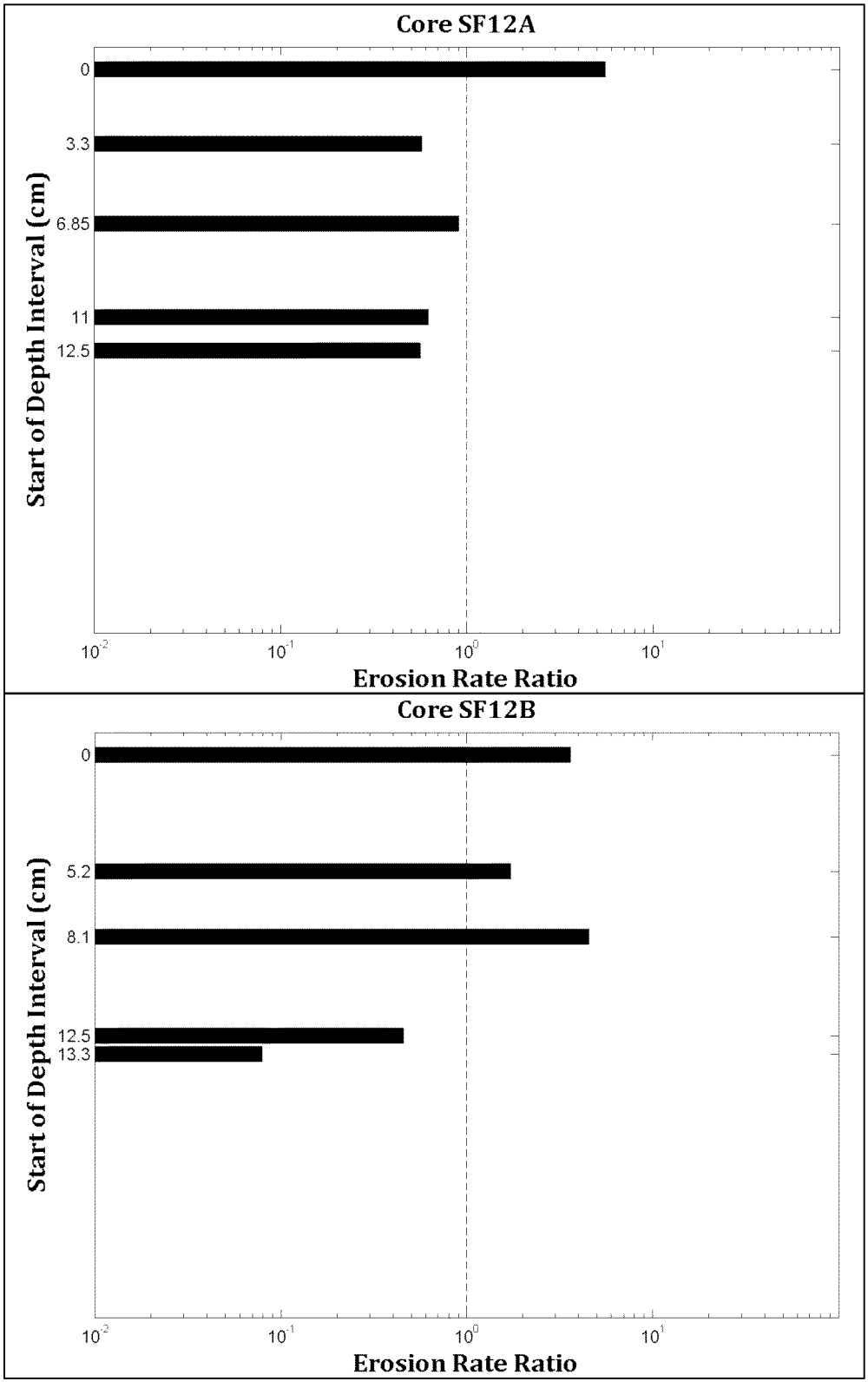

Figure 64. Intra-core erosion rate ratios for SF12A (top) and SF12B (bottom).

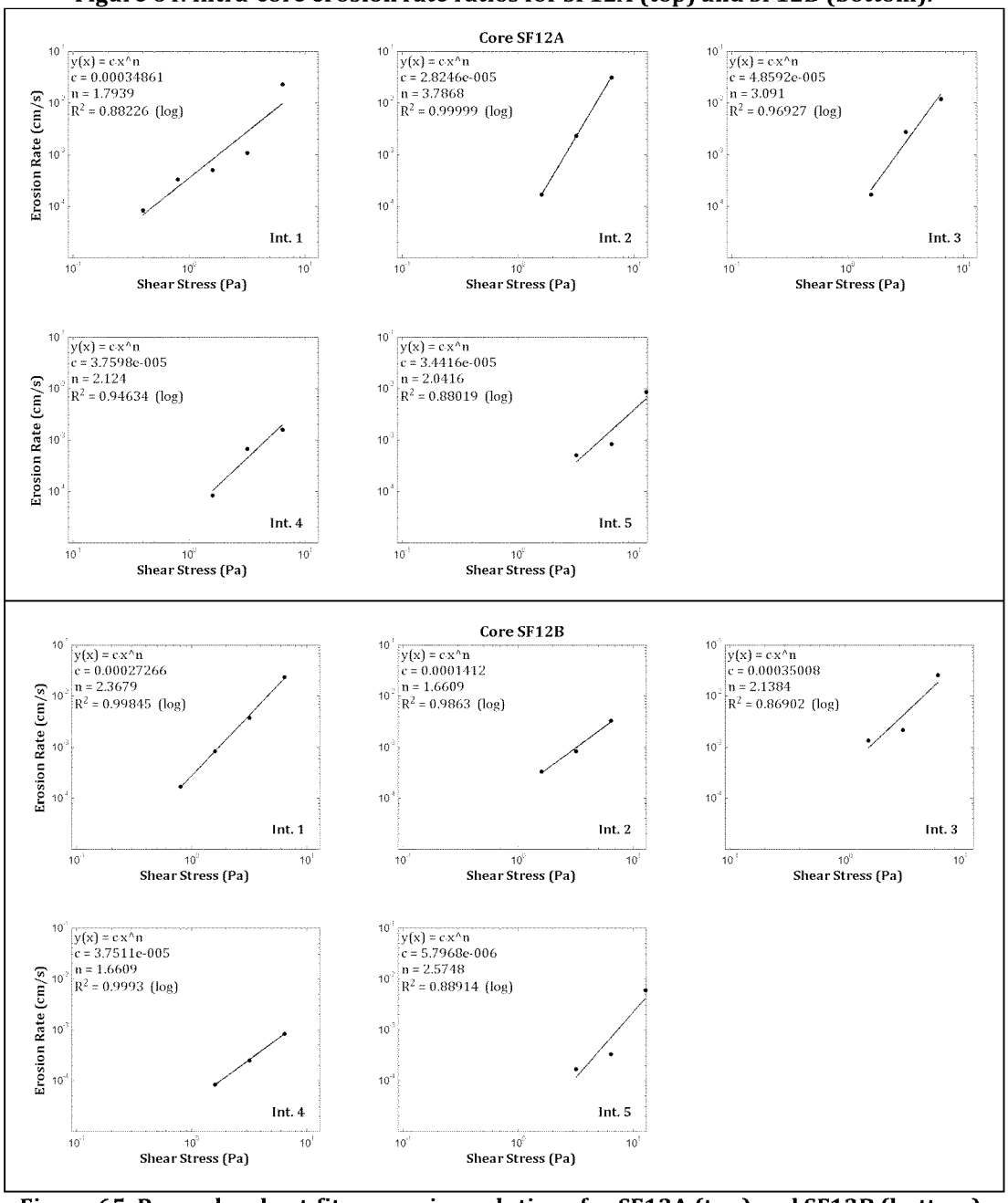

Figure 65. Power law best-fit regression solutions for SF12A (top) and SF12B (bottom).

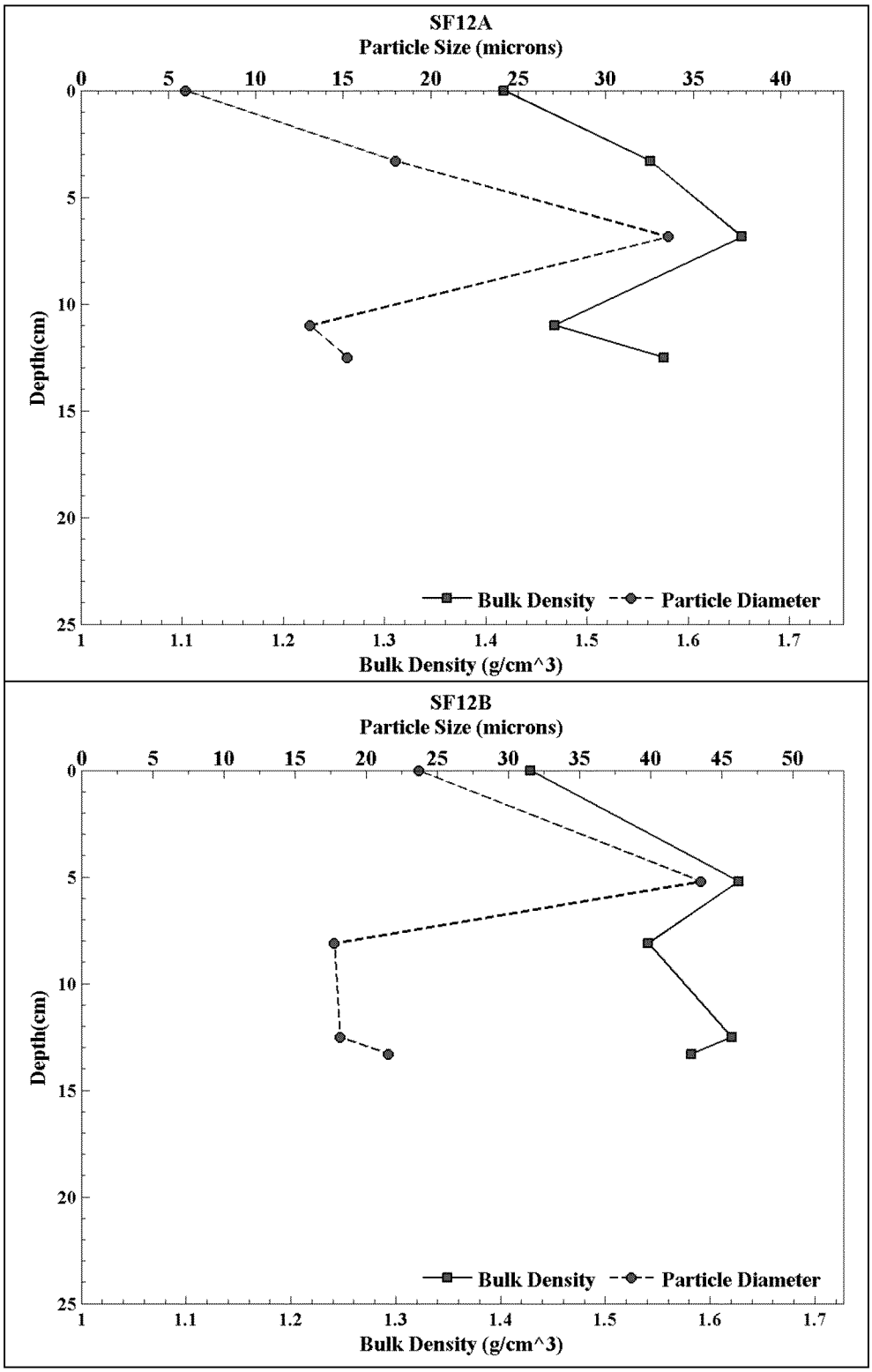

Figure 66. Down-core wet bulk density and median grain size for SF12A (top) and SF12B (bottom).

Table 50. Power law best-fit variables for the measured depth intervals in SF12A.

Depth Interval	Interval Start Depth (cm)	Interval End Depth (cm)	A	n	r^2
1	0.00	3.10	0.000349	1.79	0.88
2	3.30	6.80	0.000028	3.79	1.00
3	6.85	10.50	0.000049	3.09	0.97
4	11.00	12.40	0.000038	2.12	0.95
5	12.50	15.30	0.000034	2.04	0.88

Table 51. Power law best-fit variables for the measured depth intervals in SF12B.

Depth Interval	Interval Start Depth (cm)	Interval End Depth (cm)	A	n	r^2
1	0.00	4.70	0.000273	2.37	1.00
2	5.20	8.00	0.000141	1.66	0.99
3	8.10	12.50	0.000350	2.14	0.87
4	12.50	13.20	0.000038	1.66	1.00
5	13.30	15.70	0.000006	2.57	0.89

Table 52. Median grain size, wet bulk density, fraction LOI and critical shear stress for SF12A.

Sample Depth (cm)	Grain Size (μm)	Wet Bulk Density (g/cm^3)	Fraction LOI	τ_0 (Pa)	τ_1 (Pa)	τ_{linear} (Pa)	τ_{power} (Pa)
0.00	5.96	1.42	0.05	0.20	0.40	0.40	0.50
3.30	17.96	1.56	0.04	0.80	1.60	1.28	1.40
6.85	33.55	1.65	0.03	0.80	1.60	1.28	1.26
11.00	13.08	1.47	0.04	0.80	1.60	1.60	1.58
12.50	15.23	1.58	0.04	1.60	3.20	1.92	1.69
Mean	**17.16**	**1.54**	**0.04**	**0.84**	**1.68**	**1.30**	**1.29**

Table 53. Median grain size, wet bulk density, fraction LOI and critical shear stress for SF12B.

Sample Depth (cm)	Grain Size (μm)	Wet Bulk Density (g/cm^3)	Fraction LOI	τ_0 (Pa)	τ_1 (Pa)	τ_{linear} (Pa)	τ_{power} (Pa)
0.00	23.69	1.43	0.05	0.40	0.80	0.64	0.65
5.20	43.56	1.63	0.04	0.80	1.60	1.04	0.81
8.10	17.78	1.54	0.04	0.80	1.60	0.86	0.56
12.50	18.20	1.62	0.04	0.80	1.60	1.60	1.80
13.30	21.59	1.58	0.04	1.60	3.20	2.55	3.02
Mean	**24.96**	**1.56**	**0.04**	**0.88**	**1.76**	**1.34**	**1.37**

2.4.13 CORES SF13A AND SF13B

Cores SF13A and SF13B were collected from within the navigation channel, southeast of the Port of Elizabeth, in the south end of Newark Bay. Initial attempts to core at the pre-project selected coordinates were unsuccessful[18]. Core barrels returned to the surface full of clear water and, at times, cracked, indicating that the seafloor was not being penetrated and possibly consisting of a hard substrate. This is an area blasted and dredged; it is possible that the material comprised rock. The coring location was shifted due east to the opposite side of the navigation channel where fine sediment, capable of being cored, was discovered.

Core SF13A comprised 10 cm of silt and sandy silt over a dark-colored silt layer. The surface layer was very low-density and the low-density[19] material beneath this surface layer persisted to a depth of at least 25 cm (the depth at which the analysis reached). Some small benthic organisms and fine organic material were observed on the surface. The surface of core SF13B consisted of 1-2 cm of a tan-colored fluff layer of silt and fine sand encompassed within a 10 cm tan-colored layer of silt and sand. Material at greater depths was darker-colored silt and sand. Similarly to core SF13A, the material remained of low-density throughout the processing depth.

A photograph of the cores aligned with each other is presented in Figure 67. Their respective erosion rate data are plotted in Figure 68. Shear stresses ranging between 0.1 and 6.4 Pa were applied to these cores. Figure 69 displays the intra-core erosion rate ratios of the depth intervals evaluated in each core. Erosion rates and ratios generally decreased with depth.

The power law regression fit within each depth interval of the cores is illustrated in Figure 70. Coefficients and regression statistics from the power law analysis are presented in Table 54 and Table 55 for the cores, respectively. The measured median grain sizes, and the computed wet bulk densities and critical shear stresses for each depth interval are provided in Table 56 and Table 57.

The vertical profiles of d_{50} and ρ_b from each core are presented in Figure 71. The median grain size in SF13A varied little with depth, between 5.64 µm (very fine silt) and 9.84 µm (fine silt). The median grain size in SF13B also varied little with depth between 5.94 µm (very fine silt) to 10.66 µm (fine silt). The core-averaged d_{50} in SF13A and SF13B was 8.32 µm and 7.49 µm, respectively (at the threshold of very fine to fine silt for both cores).

The wet bulk density in SF13A varied between a minimum of 1.22 g/cm^3 at the surface and a maximum of 1.33 g/cm^3 at a depth of 11.50 cm. The wet bulk density in SF13B varied between a minimum of 1.22 g/cm^3 at the surface and a maximum of 1.32 g/cm^3 at a depth of 13.20 cm. The core-averaged wet bulk density in the cores was 1.30 g/cm^3 in both cores.

[18] Initial attempts were along the western edge of the navigation channel in this reach.

[19] Low-density characterization is qualitative, and is due to the much softer material sampled beneath surface layers in other cores (namely, the mudflat cores).

The critical shear stress estimates in both cores increased with depth. The two linearly interpolated critical shear stress estimate core-averages were 0.62 Pa for both cores; the power law estimates were 0.65 Pa and 0.76 Pa, for SF13A and SF13B, respectively.

Figure 67. Pre-processing photo of cores SF13A (left) and SF13B (right).

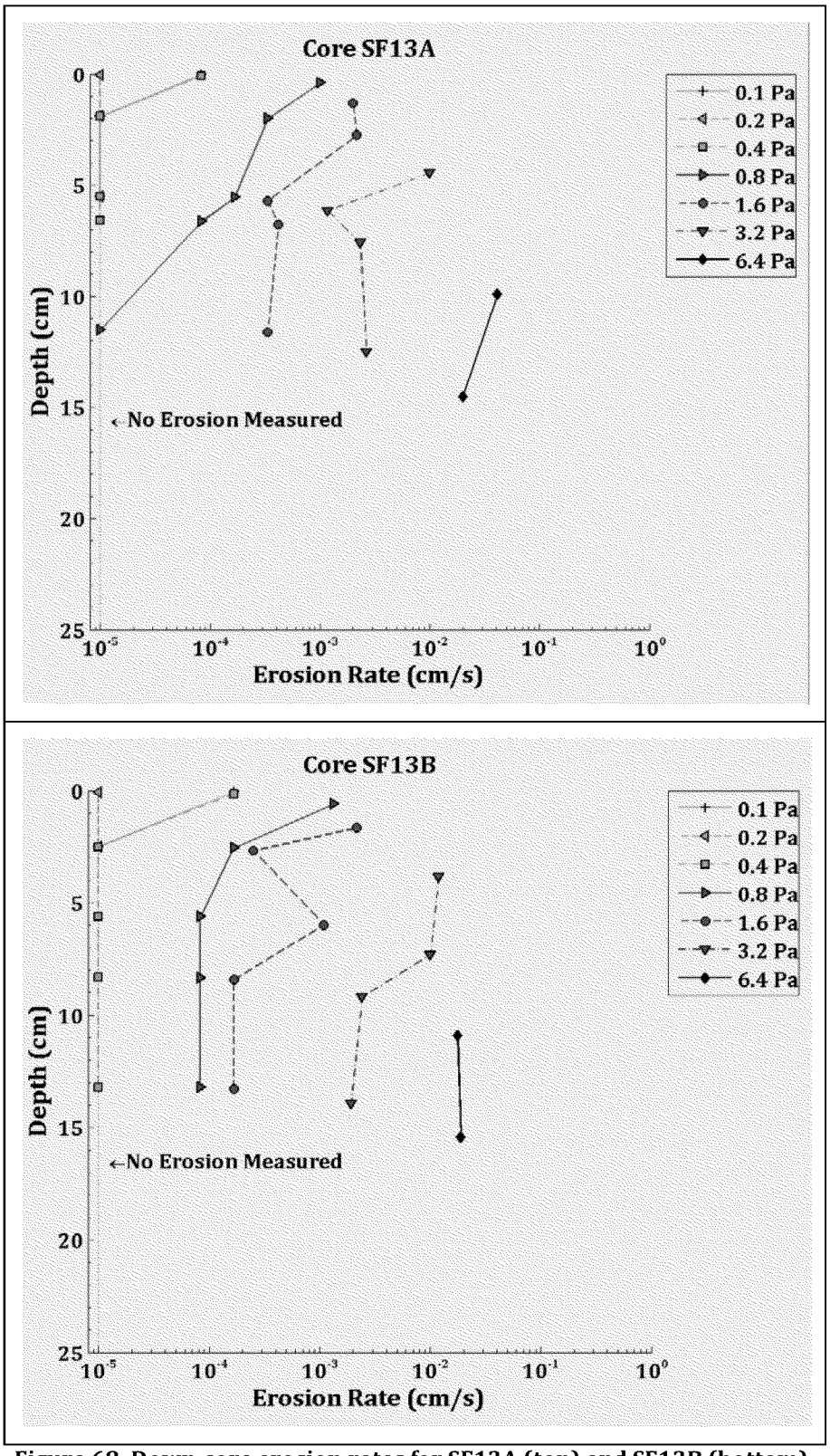

Figure 68. Down-core erosion rates for SF13A (top) and SF13B (bottom).

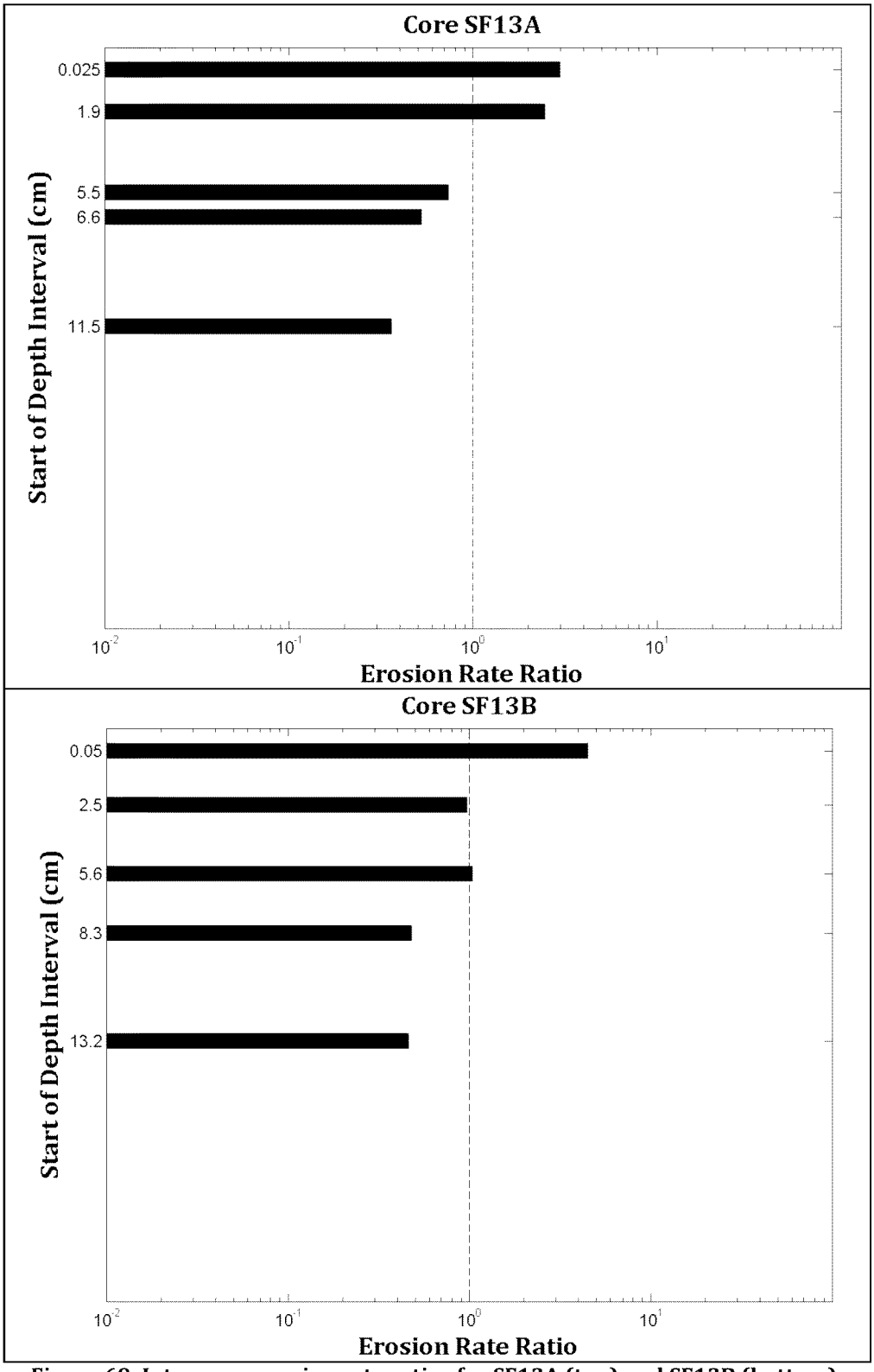

Figure 69. Intra-core erosion rate ratios for SF13A (top) and SF13B (bottom).

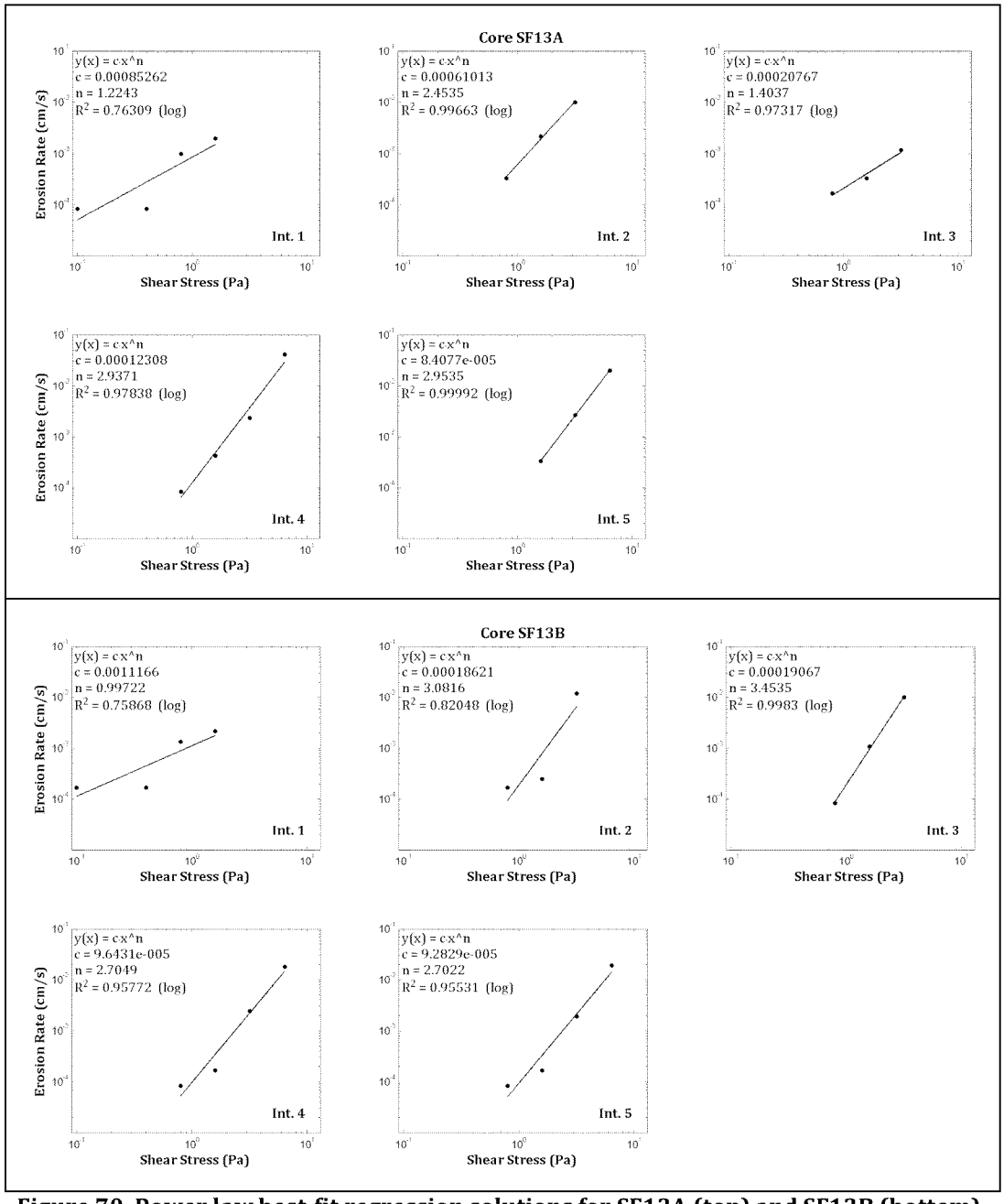

Figure 70. Power law best-fit regression solutions for SF13A (top) and SF13B (bottom).

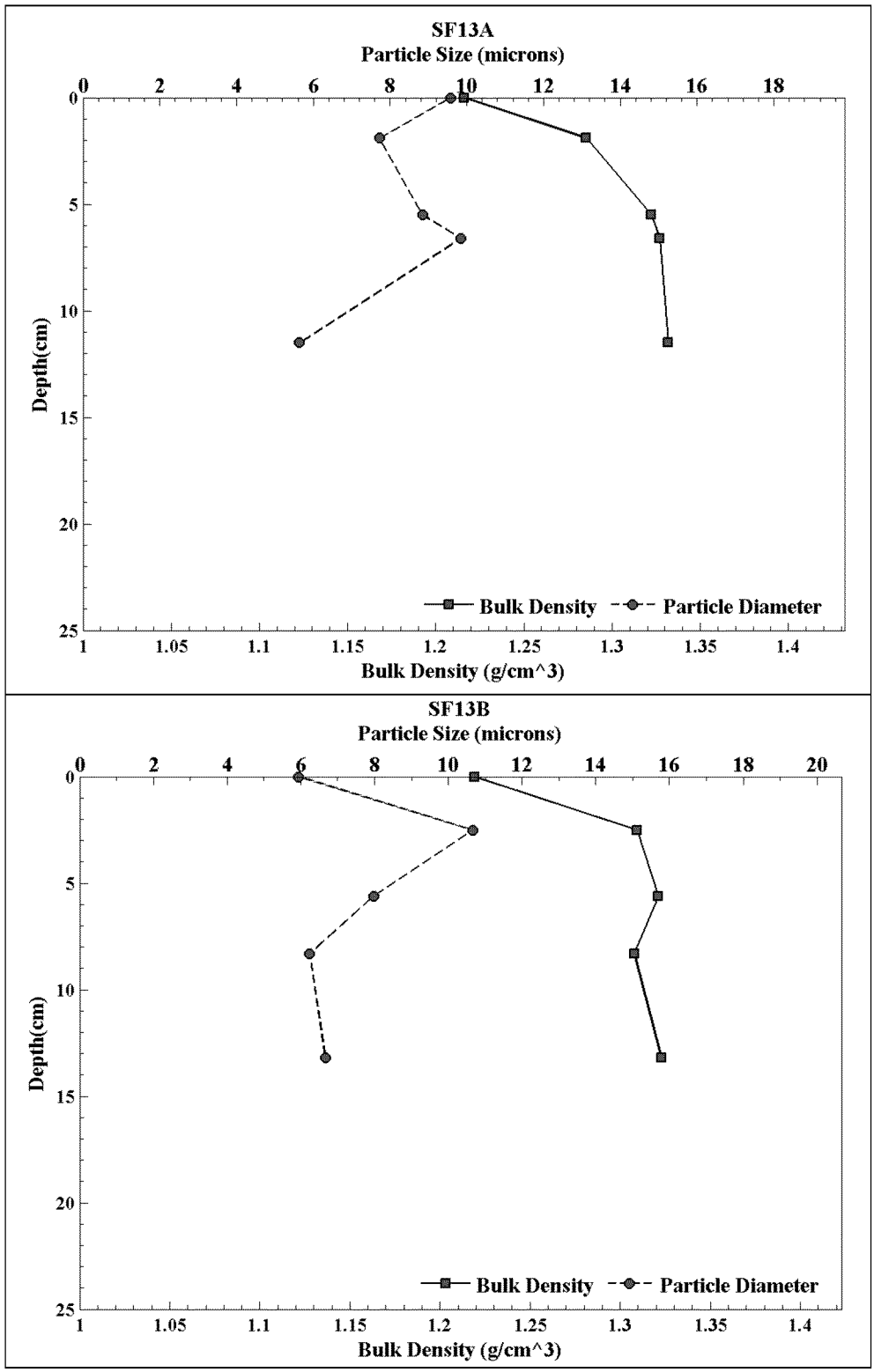

Figure 71. Down-core wet bulk density and median grain size for SF13A (top) and SF13B (bottom).

Table 54. Power law best-fit variables for the measured depth intervals in SF13A.

Depth Interval	Interval Start Depth (cm)	Interval End Depth (cm)	A	n	r^2
1	0.00	1.90	0.000853	1.22	0.76
2	1.90	5.50	0.000610	2.45	1.00
3	5.50	6.50	0.000208	1.40	0.97
4	6.60	11.50	0.000123	2.94	0.98
5	11.50	15.70	0.000084	2.95	1.00

Table 55. Power law best-fit variables for the measured depth intervals in SF13B.

Depth Interval	Interval Start Depth (cm)	Interval End Depth (cm)	A	n	r^2
1	0.00	2.30	0.001117	1.00	0.76
2	2.50	4.90	0.000186	3.08	0.82
3	5.60	8.30	0.000191	3.45	1.00
4	8.30	11.90	0.000096	2.70	0.96
5	13.20	16.40	0.000093	2.70	0.96

Table 56. Median grain size, wet bulk density, fraction LOI and critical shear stress for SF13A.

Sample Depth (cm)	Grain Size (μm)	Wet Bulk Density (g/cm³)	Fraction LOI	τ_0 (Pa)	τ_1 (Pa)	τ_{linear} (Pa)	τ_{power} (Pa)
0.00	9.58	1.22	0.08	0.05	0.10	0.10	0.17
1.90	7.72	1.29	0.06	0.40	0.80	0.52	0.48
5.50	8.84	1.32	0.07	0.40	0.80	0.64	0.59
6.60	9.84	1.33	0.07	0.40	0.80	0.80	0.93
11.50	5.64	1.33	0.07	0.80	1.60	1.04	1.06
Mean	**8.32**	**1.30**	**0.07**	**0.41**	**0.82**	**0.62**	**0.65**

Table 57. Median grain size, wet bulk density, fraction LOI and critical shear stress for SF13B.

Sample Depth (cm)	Grain Size (μm)	Wet Bulk Density (g/cm³)	Fraction LOI	τ_0 (Pa)	τ_1 (Pa)	τ_{linear} (Pa)	τ_{power} (Pa)
0.00	5.94	1.22	0.07	0.05	0.10	0.05	0.09
2.50	10.66	1.31	0.06	0.40	0.80	0.64	0.82
5.60	7.97	1.32	0.07	0.40	0.80	0.80	0.83
8.30	6.24	1.31	0.07	0.40	0.80	0.80	1.01
13.20	6.66	1.32	0.07	0.40	0.80	0.80	1.03
Mean	**7.49**	**1.30**	**0.07**	**0.33**	**0.66**	**0.62**	**0.76**

2.4.14 CORES SF14A AND SF14B

Cores SF14A and SF14B were collected from the eastern mudflats in the southeast end of Newark Bay, east of coring location SF13. Core SF14A comprised 1-2 cm of tan-colored, low-density silt and sand overlying darker-colored, higher density silt and sand. The surface of core SF14B consisted of 1-2 cm of tan-colored, low-density silt and sand. One small orange-colored worm was visible on the surface and stringy organic material was observed immediately beneath the surface. At deeper depths, the material became stiffer and comprised clayey-silt and fine sand. The analysis of both of these cores was halted after the fourth depth interval because there was no erosion occurring at an applied shear stress of 1.6 Pa[20].

A photograph of the cores aligned with each other is presented in Figure 72. Their respective erosion rate data are plotted in Figure 73. Shear stresses ranging between 0.1 and 12.8 Pa were applied to these cores. The intra-core erosion rate ratios of the depth intervals evaluated in each core are shown in Figure 74. Throughout the cores, erosion rates and ratios generally decreased with depth.

The power law regression fit within each depth interval of the cores is illustrated in Figure 75. Coefficients and regression statistics from the power law analysis are presented in Table 58 and Table 59 for the cores, respectively. The measured median grain sizes, and the computed wet bulk densities and critical shear stresses for each depth interval are provided in Table 60 and Table 61.

The vertical profiles of d_{50} and ρ_b from each core are presented in Figure 76. The median grain size in SF14A varied around the very fine / fine silt size threshold: 7.58 µm to 8.71 µm. The median grain size in SF14B also varied around the same threshold: fluctuating between 7.49 µm and 10.08 µm. The core-averaged d_{50} in SF14A and SF14B was 8.22 µm and 8.84 µm, respectively (fine silt for both cores).

The wet bulk density in SF14A varied between a minimum of 1.21 g/cm^3 at the surface and a maximum of 1.38 g/cm^3 at a depth of 6.80 cm. The wet bulk density in SF14B varied between a minimum of 1.21 g/cm^3 at the surface and a maximum of 1.45 g/cm^3 at a depth of 9.20 cm. The core-averaged wet bulk density in the cores was 1.32 g/cm^3 and 1.37 g/cm^3, respectively.

The critical shear stress estimates in both cores increased with down-core depth, though those computed in SF14B at deeper depths were larger than those computed in SF14A at similar depths. The linearly interpolated critical shear stress estimate core-averages were 1.26 Pa and 1.50 for SF14A and SF14B, respectively; the power law estimates were 1.35 Pa and 1.66 Pa, respectively.

[20] Based on hydrodynamic modeling conducted by HDR|HydroQual, a Field Modification was approved October 29, 2012 that allowed stopping the analysis if no erosion was observed at an applied shear stress of 1.6 Pa, which is thought to exceed typical shear stresses that would occur at the mudflats within Newark Bay.

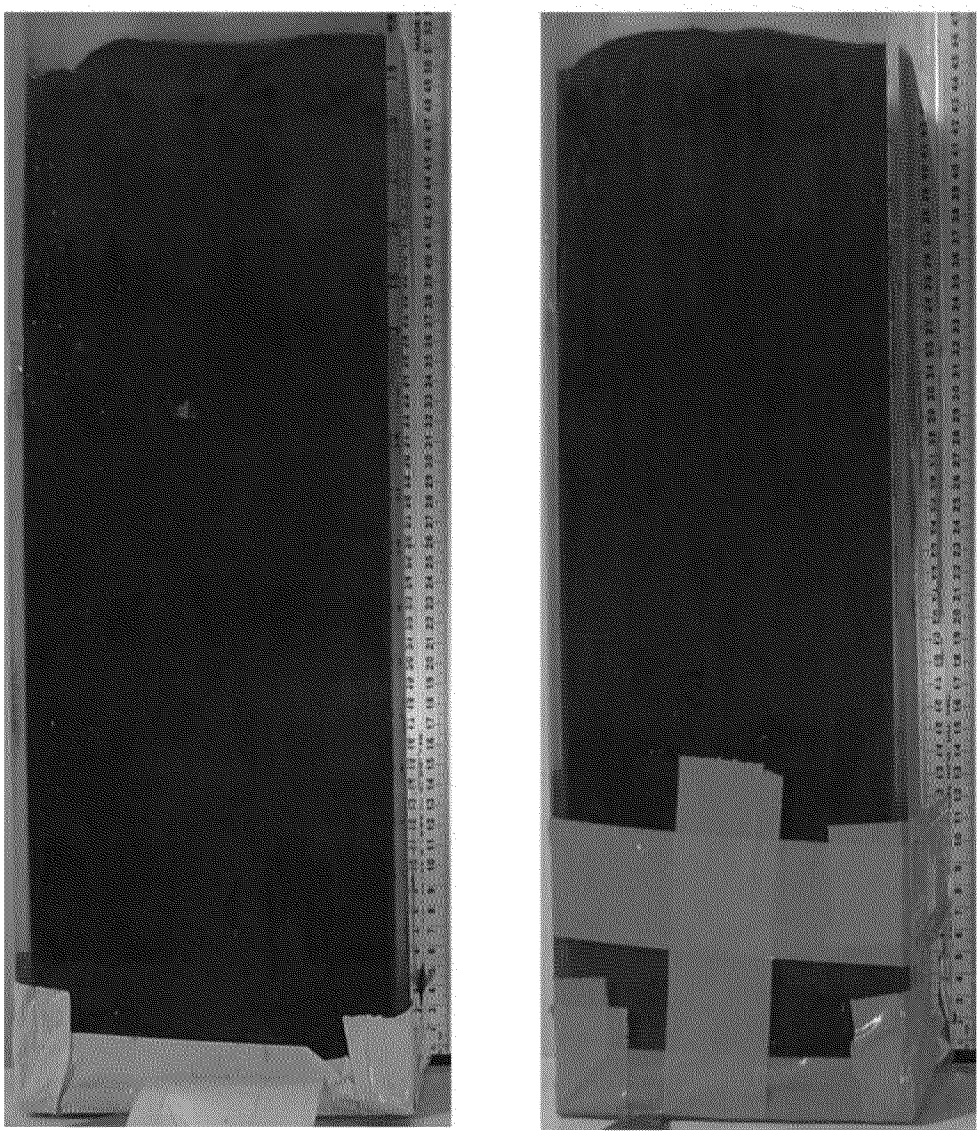

Figure 72. Pre-processing photo of cores SF14A (left) and SF14B (right).

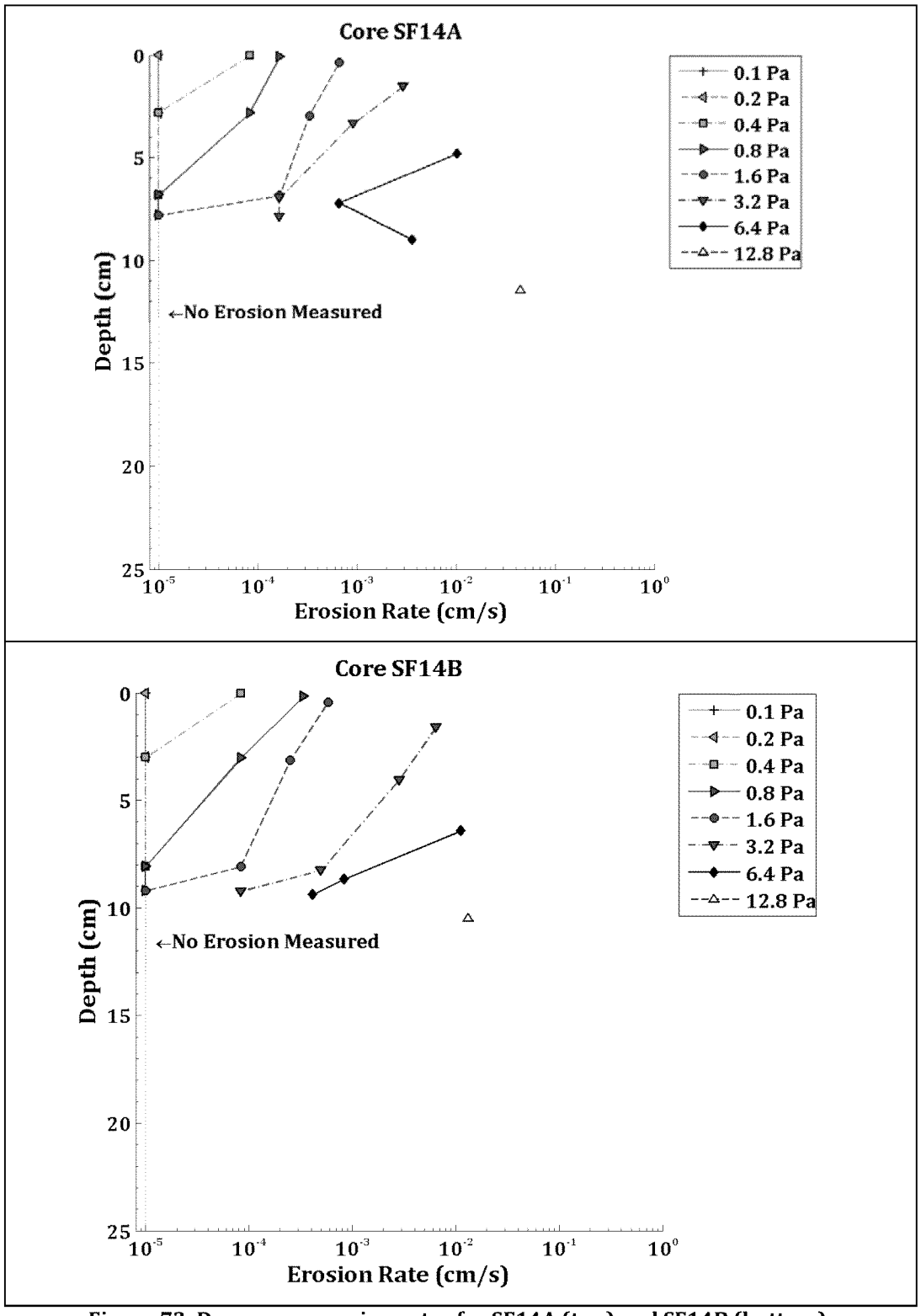

Figure 73. Down-core erosion rates for SF14A (top) and SF14B (bottom).

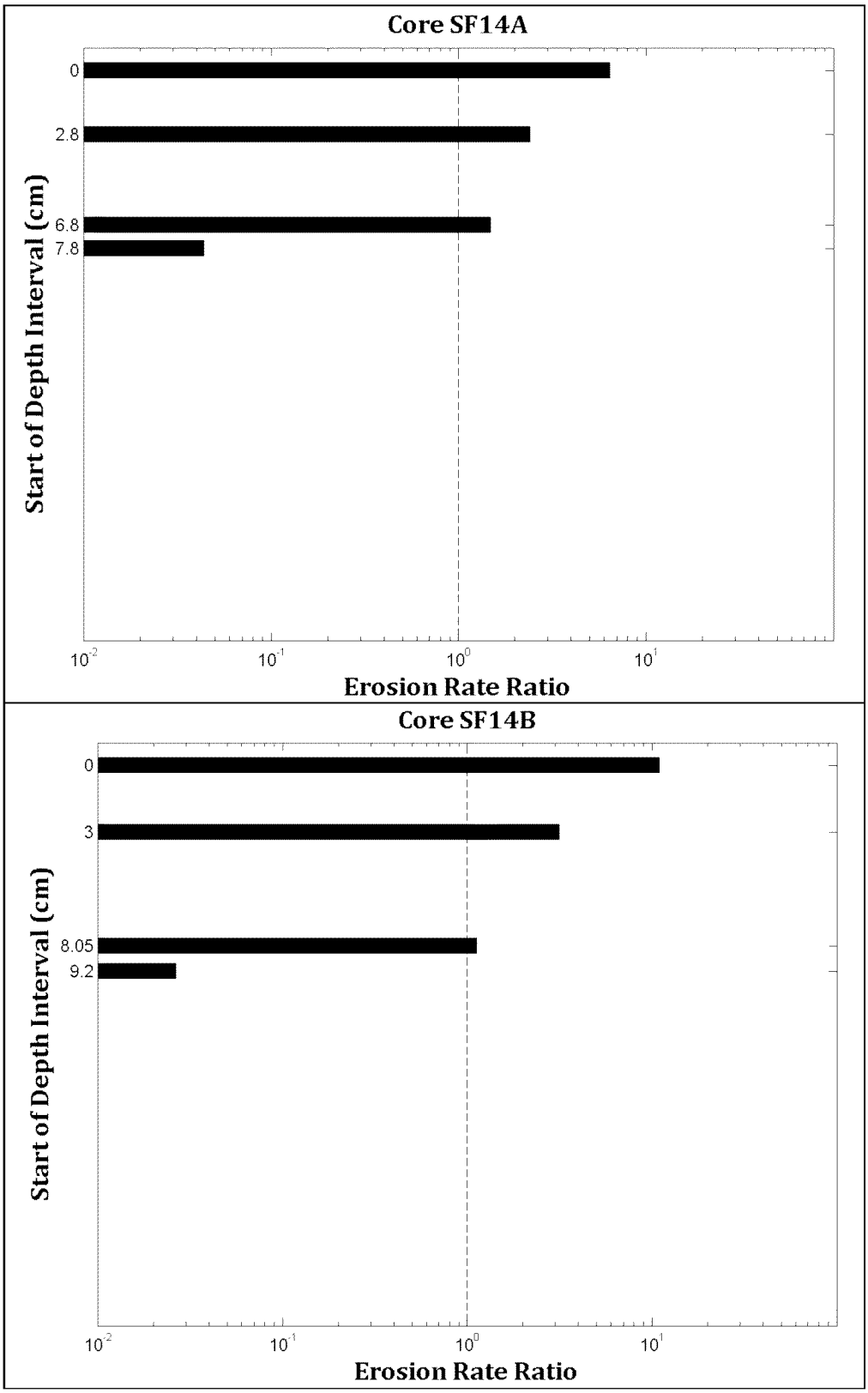

Figure 74. Intra-core erosion rate ratios for SF14A (top) and SF14B (bottom).

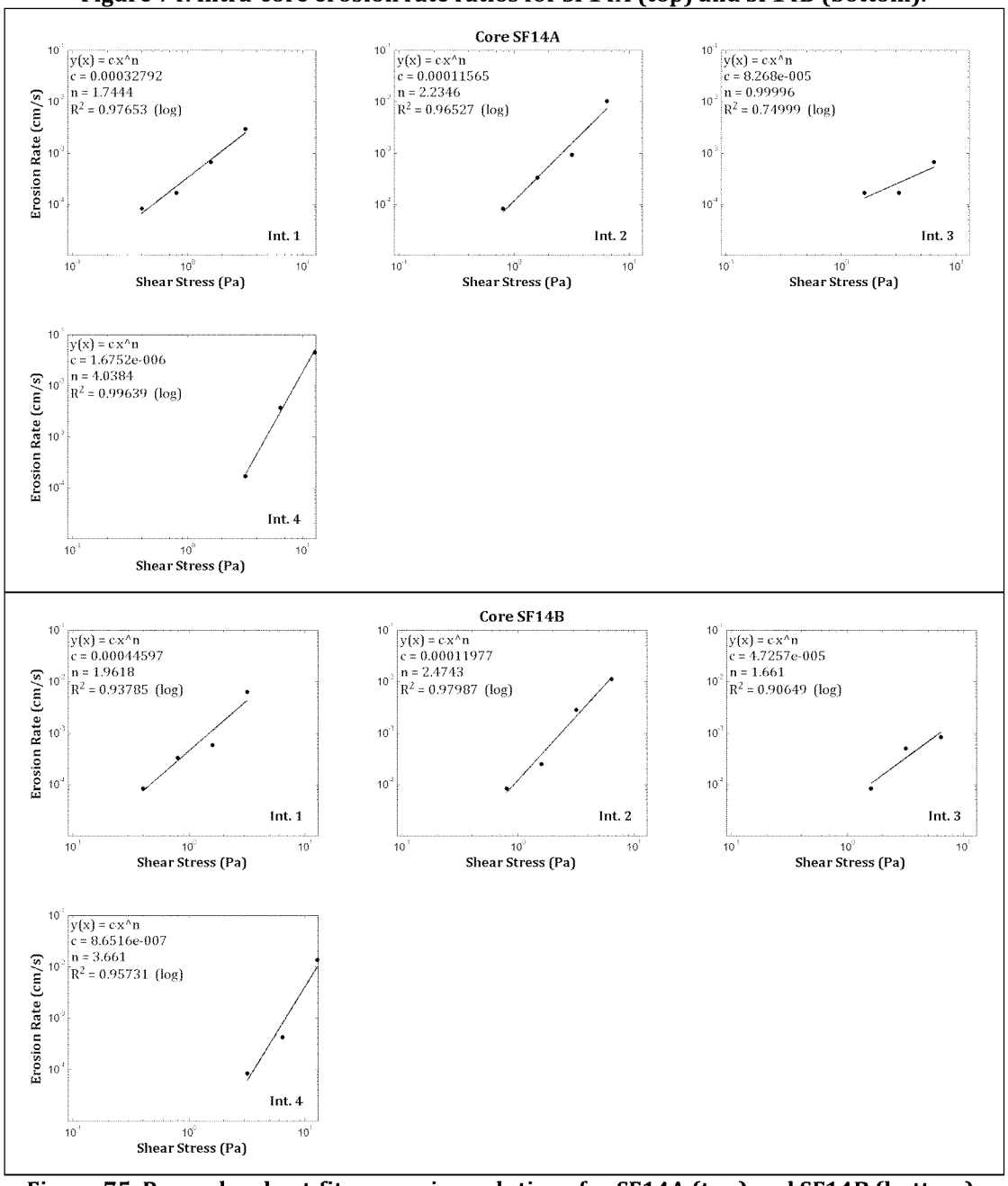

Figure 75. Power law best-fit regression solutions for SF14A (top) and SF14B (bottom).

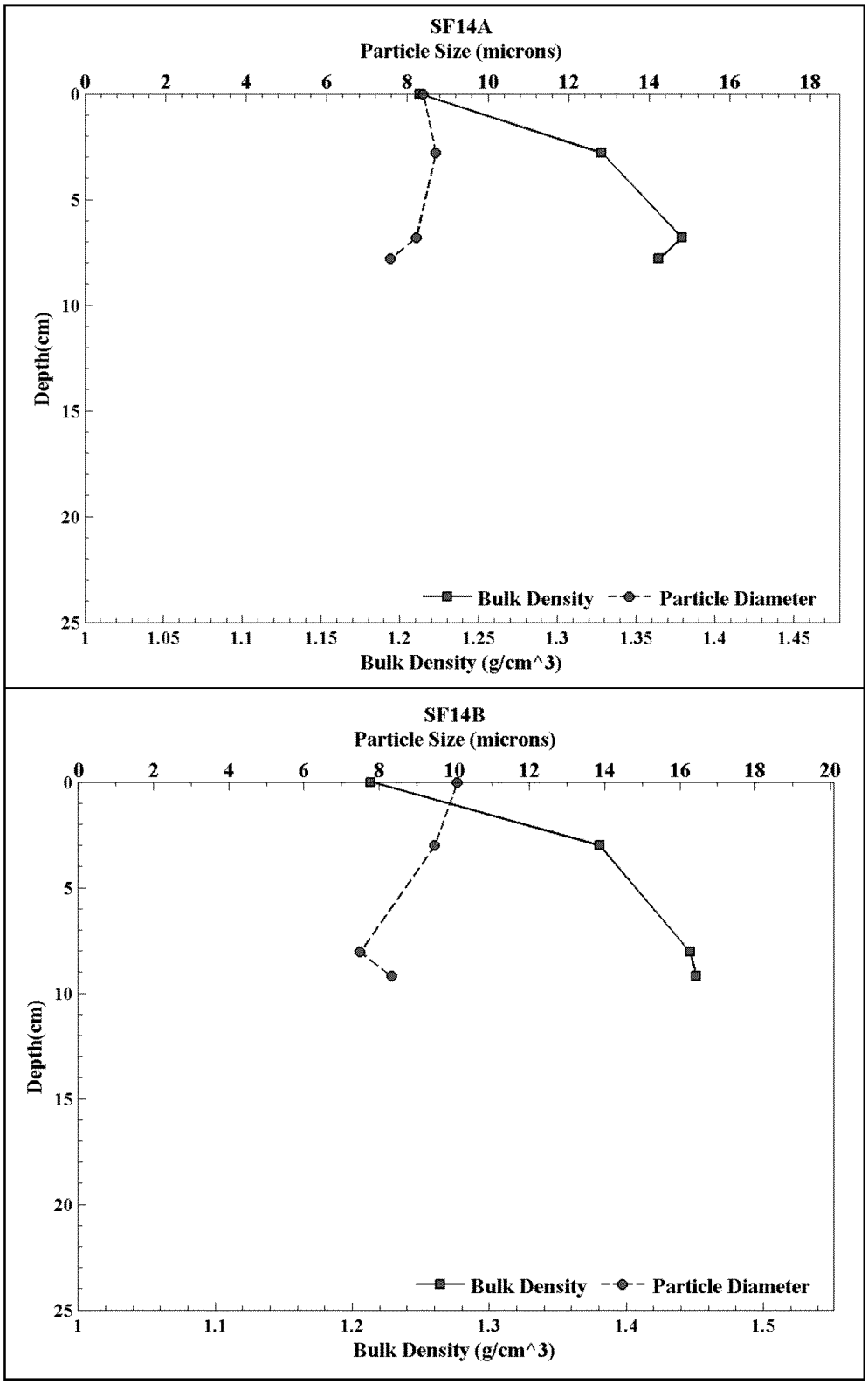

Figure 76. Down-core wet bulk density and median grain size for SF14A (top) and SF14B (bottom).

Table 58. Power law best-fit variables for the measured depth intervals in SF14A.

Depth Interval	Interval Start Depth (cm)	Interval End Depth (cm)	A	n	r^2
1	0.00	2.50	0.000328	1.74	0.98
2	2.80	6.00	0.000116	2.23	0.97
3	6.80	7.40	0.000083	1.00	0.75
4	7.80	12.80	0.000002	4.04	1.00

Table 59. Power law best-fit variables for the measured depth intervals in SF14B.

Depth Interval	Interval Start Depth (cm)	Interval End Depth (cm)	A	n	r^2
1	0.00	2.60	0.000446	1.96	0.94
2	3.00	7.90	0.000120	2.47	0.98
3	8.05	8.90	0.000047	1.66	0.91
4	9.20	11.50	0.000001	3.66	0.96

Table 60. Median grain size, wet bulk density, fraction LOI and critical shear stress for SF14A.

Sample Depth (cm)	Grain Size (μm)	Wet Bulk Density (g/cm^3)	Fraction LOI	τ_0 (Pa)	τ_1 (Pa)	τ_{linear} (Pa)	τ_{power} (Pa)
0.00	8.39	1.21	0.08	0.20	0.40	0.40	0.51
2.80	8.71	1.33	0.07	0.40	0.80	0.80	0.94
6.80	8.21	1.38	0.06	0.80	1.60	1.28	1.21
7.80	7.58	1.36	0.06	1.60	3.20	2.56	2.75
Mean	**8.22**	**1.32**	**0.07**	**0.75**	**1.50**	**1.26**	**1.35**

Table 61. Median grain size, wet bulk density, fraction LOI and critical shear stress for SF14B.

Sample Depth (cm)	Grain Size (μm)	Wet Bulk Density (g/cm^3)	Fraction LOI	τ_0 (Pa)	τ_1 (Pa)	τ_{linear} (Pa)	τ_{power} (Pa)
0.00	10.08	1.21	0.07	0.20	0.40	0.40	0.47
3.00	9.48	1.38	0.06	0.40	0.80	0.80	0.93
8.05	7.49	1.45	0.06	0.80	1.60	1.60	1.57
9.20	8.33	1.45	0.06	1.60	3.20	3.20	3.66
Mean	**8.84**	**1.37**	**0.06**	**0.75**	**1.50**	**1.50**	**1.66**

SECTION 3 – PHASE II LABORATORY EFFORT

3.1 LABORATORY ACTIVITIES

The laboratory effort phase of this project took place between November 2012 and March 2013. The effort comprised preparation and setup of SEDFlume core barrels for seven sets of consolidation cores, sediment settling measurements and erosion rate testing with the SEDFlume. Prior to consolidation, the moisture contents of the preliminary (as sampled and shipped) slurries were determined and then mixed with the proper ratio of saline water to achieve targeted initial slurry concentrations. These slurries were mixed and poured into the core barrels and allowed to consolidate for the predetermined duration before processing[21].

In all, thirty-five sediment cores were reconstructed using the surface sediment grab material recovered from the NBSA (see Figure 4 for locations). A targeted initial concentration of 350 g/L was established from each of the five NBSA sampling locations (SF3-C, SF6-C, SF8-C, SF9-C and SF13-C); two additional concentrations (100 g/L and 125 g/L) were also created from the SF8-C sediments to evaluate the effects of dilution on the sediment settlement and consolidation process. The core preparation methods and procedures are described in detail in the following sections.

3.2 LABORATORY EFFORT METHODS

3.2.1 PREPARATION METHODS

To prepare the slurries for consolidation, it was necessary to first homogenize the sediment material collected from each sampling station location and determine the preliminary slurry density. The sediment from each location was placed in a separate, large aluminum container, and mixed[22]. A cordless drill and paint stirrer was used to mix the slurries.

A sample of each preliminary slurry mixture was collected and weighed for moisture content analysis (following the equations in Table 1). The result yielded the preliminary moisture content (i.e. bulk density) of each mixture, and allowed computation of the proper sediment-water ratios necessary for each mixture to attain the target initial concentration for the consolidation SEDFlume analysis. Table 62 lists the preliminary slurry wet bulk densities. It should be noted that the slurry wet bulk densities, and resultant dry solids masses, are based on assumptions about the particle density of the material (2.60 g/ cm^3) and do not include the organic content (i.e. organic content was considered 0% at this stage to simplify the estimates).

[21] 1-, 4-, 7-, 14- and 28-day durations.

[22] The preliminary mixing period was typically 5-10 minutes and determined complete when the material was visually homogenous.

Table 62. Moisture content (BD) results of the preliminaryslurry mixtures (used to determine mixing ratios to reach target initial concentrations).

Sample ID	Date	Tray Wt. (g)	Wet Wt. (g)	Dry Wt. (g)	Water Content	Wet Bulk Density (g/cm³)[23]
SF8-C(1)	11/9/2012	1.324	29.408	15.456	0.50	1.45
SF8-C(2)	11/9/2012	1.332	23.088	12.085	0.51	1.44
SF9-C	11/10/2012	1.332	20.014	10.387	0.52	1.43
SF13-C	11/10/2012	1.311	27.115	12.429	0.57	1.36
SF3-C	11/10/2012	1.329	27.059	11.965	0.59	1.34
SF6-C	11/10/2012	1.307	31.629	21.504	0.33	1.69
SF8-C(1) - 1 Day Re-pour	12/8/2012	1.316	28.233	7.958	0.75	1.18
SF8-C(1) - 4 Day Re-pour	12/8/2012	1.310	20.036	6.109	0.74	1.19
SF13-C - 1 Day Re-pour	12/8/2012	1.318	24.162	8.336	0.69	1.23
SF13-C - 4 Day Re-pour	12/8/2012	1.321	18.512	6.398	0.70	1.22
SF8-C(3)	2/12/2013	1.300	28.092	14.590	0.50	1.44

3.2.2 DETERMINING MIXING RATIOS

The following procedure was used to determine the sediment-water ratios from the measured preliminary wet bulk densities:

1) Assume the following parameter definitions are valid:
   a. The water density is ρ_w = 1.00 g/cm³
   b. The sediment dry density is ρ_s = 2.60 g/cm³
   c. φ_s = the solids volume fraction
   d. $\varphi = 1 - \varphi_s$ porosity or pore space fraction
   e. ρ_d = the dry density or sediment mass concentration (g/cm³)
   f. ρ_{bo} = the preliminary slurry wet bulk density (g/cm³)
      i. *This is the density of the slurries mixed from the NBSA grab samples*
   g. $\rho_s \varphi_{s0}$ = the preliminary slurry concentration (dry bulk density, g/cm³)
   h. $\rho_s \varphi_{st}$ = the targeted initial slurry concentration (dry bulk density, g/cm³)
   i. f_d = the dilution fraction

2) The solids volume fraction of the preliminary slurries can be represented as:

$$\varphi_s = \frac{\rho_{bo} - \rho_w}{\rho_s - \rho_w} = \frac{\rho_{bo} - 1}{1.65} \qquad [8]$$

3) The preliminary sediment dry bulk density, $\rho_s \varphi_{so}$, can be represented as:

$$\rho_s \varphi_{s0} = \rho_s \frac{\rho_{bo} - 1}{1.65} \qquad [9]$$

[23] Computed per Equation 5.

4) Establish the target initial slurry sediment concentration for the SEDFlume analysis. During this analysis, the following values were used as target initial concentrations:
   a. 100 g/L (0.100 g/cm^3)
   b. 125 g/L (0.125 g/cm^3)
   c. 350 g/L (0.350 g/cm^3)

5) The dilution fraction was determined as:

$$f_d = 1 - \frac{\rho_s - \rho_{st}}{\rho_s - \rho_{so}} \quad [10]$$

6) The dilution ratio, r, was determined as:

$$r = \frac{f_d}{1 - f_d} \quad [11]$$

where r is the water volume per sediment volume: to make X volumetric units of a slurry at the targeted initial concentration, mix r volume units of water with $(X-r)$ volume units of sediment. The targeted initial concentrations prepared for each sampling station location and results of applying equations 8-11 are listed in Table 63.

Table 63. Phase II Laboratory Effort targeted initial concentrations and mixing ratios.

Sample ID	Prelim. Slurry Wet Bulk Density (g/cm^3)	Prelim. Slurry Dry Bulk Density g/cm^3*	Target Initial Slurry Conc. (g/cm^3)**	Dilute frac., f_d	Dilute ratio, r	Water Volume per Sed. Volume	Sed. Amount (gal)	Water Amount (gal)	Total Slurry Vol. (gal)
SF8-C(1)	1.46	0.73	**0.125**	0.83	4.80	4.80	0.86	4.14	5.00
SF8-C(2)	1.44	0.70	**0.100**	0.86	5.93	5.93	0.72	4.28	5.00
SF3-C	1.35	0.55	**0.350**	0.37	0.58	0.58	1.59	0.91	2.50
SF6-C	1.71	1.12	**0.350**	0.69	2.20	2.20	0.78	1.72	2.50
SF9-C	1.43	0.68	**0.350**	0.48	0.94	0.94	1.29	1.21	2.50
SF13-C	1.37	0.58	**0.350**	0.40	0.67	0.67	1.50	1.00	2.50
SF8-C(3)	1.45	0.71	**0.350**	0.51	1.03	1.03	1.23	1.27	2.50
Re-pour Cores (Dec 2012)									
SF8-C(1) 1 Day	1.18	0.28	0.125	0.56	1.27	1.27	1.12	2.80	2.50
SF13-C (1 Day)	1.24	0.38	0.350	0.07	0.08	0.08	2.31	0.19	2.50
SF8-C(1) 4 Day	1.19	0.30	0.125	0.58	1.40	1.40	1.04	2.91	2.50
SF13-C (4 Day)	1.23	0.36	0.350	0.03	0.04	0.04	2.41	0.09	2.50

*Dry bulk density is the mass of the dry solids divided by the volume of the sample.
**1000 g/cm^3 = 1 g/L

To mimic the natural aquatic state of Newark Bay, saline water was used when creating sediment slurries instead of freshwater from the tap. The saline water either comprised Newark Bay seawater (collected during the field effort and stored at the SEI Santa Cruz, CA laboratory) or manufactured salt water created with Instant Ocean® aquarium salt. CTD

(conductivity-temperature-depth) water profile measurements were collected of the Newark Bay seawater at the time of water sample collection (Oct 19, 2012); therefore, when preparing saline water with Insta-Ocean®, the target salinity of the water was known. Insta-Ocean® solutions were measured with a calibrated CTD in the SEI Santa Cruz, CA, laboratory to verify proper salinity.

3.2.3 POUR AND CONSOLIDATION PROCEDURE

The consolidation cores were poured according to the schedule in Table 64. Six sets of cores were prepared and processed between November and December 2012. An additional set of cores was prepared and processed between February and March 2013.

For the cores prepared and processed in November and December 2012, sediment and water were added in the proper ratios (established in Table 63) to five buckets from each NBSA sampling station location, slurried, poured into the corresponding core barrels sequentially and then allowed to consolidate.

The SF8-C(3) core preparation in February and March 2013 differed only in the schedule in which the cores were poured: each SF8-C(3) core was poured on a *different* day (instead of sequentially) and allowed to consolidate for the prescribed number of days before analyzing, allowing for all five cores to be processed on two consecutive days.

All other slurrying and pouring processes remained the same for all cores. Prior to pouring the targeted concentration slurry into each core, the material in the buckets was sufficiently homogenized. A cordless drill with paint stirrer was utilized for a minimum duration of 1 minute[24]. Immediately prior to pouring into a SEDFlume core barrel, a sample was collected from the mixture for moisture content analysis [25]. When the mixing was stopped, the slurry was poured into its respective core barrel as quickly as possible to minimize sediment settling within the bucket. Slurries were poured through a funnel to prevent spilling and adhesion of the slurry to the core barrel walls (which would make visual observations difficult).

Immediately upon pouring each slurry into a core, a measurement of the initial slurry height was recorded to establish the baseline for settlement measurements. Subsequently, measurements of the settlement of the sediment-water interface were recorded according to the following schedule for the November and December 2012 cores:

1) *Measurements were collected every minute for the first 30 minutes after pouring.*
2) *Measurements continued every 10 minutes for the next 30 minutes.*
    a. *These procedures were altered for the 350 g/L target initial concentrations because the amount of rapid settlement was much less than observed in the lower concentration slurries (100 g/L and 125 g/L).*

[24] Less mixing time was required immediately prior to pouring because the targeted concentration slurries were of significantly lower density than the preliminary slurries (i.e. the material mixed much more rapidly).

[25] A moisture content measurement from each slurry allowed estimation of the actual concentration of slurry in each core barrel, accounting for potentially small differences between slurry concentrations from the same sampling station location.

b. *The settlement of the 350 g/L concentration slurries was measured at least hourly during the first day.*

3) *Measurements continued hourly through the remainder of the work day.*
4) *Measurements continued daily through settlement day 7.*
5) *Measurements were also collected on day 14 and 28 prior to processing.*

As mentioned, the visual sediment settling occurred much more rapidly for the lower concentration slurries (100 g/L and 125 g/L), necessitating measurements every minute or 10 minutes (Steps 1 and 2). For the 350 g/L concentrations, however, settling was visually slow, prompting SEI personnel to measure settling every 15 minutes (instead of every minute or 10 minutes) for the first hour. Steps 3-5 were followed for all cores.

Qualitative photographs were taken throughout the first day of core settling. Further, daily photographs were taken of each core that had yet to be processed up to settlement day 7. Immediately prior to processing each core with the SEDFlume, cores were photographed per standard SEDFlume procedures.

Settling of the SF8-C(3) cores in February and March 2013 was not measured as described above. Rather, an initial and final slurry level was measured for each core, indicating the total amount of settlement that occurred during the consolidation duration. Photographs were taken immediately after pouring each core and just prior to processing.

3.3 LABORATORY EFFORT SUMMARY

Table 64 provides a breakdown of the daily laboratory activity during the Laboratory effort.

Table 64. Phase II Laboratory Effort daily activity breakdown.

Date	Cores Slurried	Cores Processed	Description
11/9/2012	–	–	Mixed sediments into as-is slurries (in large tin buckets) for locations SF8-C(1), 125 g/L target initial concentration, and SF8-C(2), 100 g/L target initial concentration. Samples of the initial slurries were dried in the oven overnight to determine initial moisture concentrations. Then, sediment to water ratios were determined for targeted initial concentrations, assuming a sediment density of 2.60 kg/m^3.
11/10/2012	–	–	Mixed sediments into as-is slurries (in large tin buckets) for locations SF3-C, SF6-C, SF9-C and SF13-C. Samples of the initial slurries were dried in the oven overnight to determine initial moisture concentrations. Then, sediment to water ratios were determined for targeted initial concentrations.
11/11/2012	SF8-C(1) (125 g/L) and SF8-C(2) (100 g/L)	–	Slurried and poured consolidation core sets for two dilutions from location 8: target initial concentrations of 125 g/L (for SF8-C(1)) and 100 g/L (for SF8-C(2)).
11/12/2012	SF9-C (350 g/L) and SF13-C (350 g/L)	1 Day Cores: SF8-C(2) (100 g/L); SF8-C(1) (125 g/L) leaked and was not processed	The SF13-C cores were initially slurried and poured to a targeted initial concentration of 125 g/L. However, when Core SF8-C(1) (125 g/L) 1 Day was being processed in SEDFlume, the sediment was still so liquid-like that it leaked around the core piston, losing all material through the bottom of the core. Therefore, it was decided that all future slurries would target 350 g/L in an attempt to avoid losing more unconsolidated

			sediment material. The location SF8-C cores at lower concentrations would remain as-is (at 125 g/L and 100 g/L) for this experiment. Consolidation core sets (5 cores in each set) were poured for locations SF9-C and SF13-C: target initial concentrations of 350 g/L. Core SF8-C(2), 100 g/L, was successfully processed.
11/13/2012	SF3-C (350 g/L) and SF6-C (350 g/L); SF8-C(1) (125 g/L) 1-Day core was re-poured for processing the next day.	1 Day Cores: SF9-C (350 g/L); SF13-C (350 g/L) leaked and was not processed	Core SF9-C (350 g/L) 1 Day was successfully processed. Core SF13-C (350 g/L) 1 Day leaked around the bottom of the piston. Most of the sediment slurry was saved in a 5-gallon bucket, sealed with a lid and placed aside for later processing (noted as "re-pour" cores below).
11/14/2012	–	1 Day Cores: SF3-C (350 g/L) and SF6-C (350 g/L)	Core SF8-C(1) (125 g/L) 1 Day (re-pour) leaked around the bottom of the piston, again, and was saved in a 5-gallon bucket, sealed with a lid and placed aside for later processing (as a "re-pour" core). Processed 1 day cores from SF3-C (350 g/L) and SF6-C (350 g/L) successfully.
11/15/2012	–	4 Day Cores: SF8-C(2) 100 g/L; SF8-C(1) 125 g/L leaked and was not processed	Core SF8-C(1) (125 g/L) 4 Day leaked around the bottom of the piston and was saved in a 5-gallon bucket, sealed with a lid, and placed aside for later processing. Core SF8-C(2) 100 g/L was processed successfully.
11/16/2012	–	4 Day Cores: SF9-C (350 g/L); SF13-C (350 g/L) leaked and was not processed	Core SF9-C (350 g/L) 4 Day was successfully processed. Core SF13-C (350 g/L) 4 Day leaked around the bottom of the piston. The sediment slurry was saved in a 5-gallon bucket, sealed with a lid and placed aside for later processing (noted as "re-pour" cores below).
11/17/2012	–	4 Day Cores: SF3-C (350 g/L) and SF6-C (350 g/L)	Successfully processed 4 day cores from SF3-C (350 g/L) and SF6-C (350 g/L).
11/18/2012	–	7 Day Cores: SF8-C(1) (125 g/L) and SF8-C(2) (100 g/L)	Successfully processed 7 day cores from SF8-C(1) (125 g/L) and SF8-C(2) (100 g/L).
11/19/2012	–	7 Day Cores: SF9-C (350 g/L) and SF13-C (350 g/L)	Successfully processed 7 day cores from SF9-C (350 g/L) and SF13-C (350 g/L).
11/20/2012	–	7 Day Cores: SF3-C (350 g/L) and SF6-C (350 g/L)	Successfully processed 7 day cores from SF3-C (350 g/L) and SF6-C (350 g/L).
11/25/2012	–	14 Day Cores: SF8-C(1) (125 g/L) and SF8-C(2) (100 g/L)	Processed 14 day cores from SF8-C(1) (125 g/L) and SF8-C(2) (100 g/L).
11/26/2012	–	14 Day Cores: SF9-C (350 g/L) and SF13-C (350 g/L)	Processed 14 day cores from SF9-C (350 g/L) and SF13-C (350 g/L).
11/27/2012	–	14 Day Cores: SF3-C (350 g/L) and SF6-C (350 g/L)	Processed 14 day cores from SF3-C (350 g/L) and SF6-C (350 g/L).
12/9/2012	4 Day Re-pour Cores: Locations SF8-C(1) (125 g/L) Re-pour and SF13-C (350 g/L) Re-pour	28 Day Cores: SF8-C(1) (125 g/L) and SF8-C(2) (100 g/L)	Slurried 4 day re-pour cores from SF8-C(1) (125 g/L) and SF13-C (350 g/L). Successfully processed 28 day cores from SF8-C(1) (125 g/L) and SF8-C(2) (100 g/L).
12/10/2012	–	28 Day Cores: SC9-C (350 g/L) and SF13-C	Successfully processed 28 day cores from SF9-C (350 g/L) and SF13-C (350 g/L).

		(350 g/L)	
12/11/2012	1 Day Re-pour Cores: Locations SF8-C(1) (125 g/L) Re-pour and SF13-C (350 g/L) Re-pour	28 Day Cores: SF3-C (350 g/L) and SF6-C (350 g/L)	Slurried 1 day re-pour cores from SF8-C(1) (125 g/L) and SF13-C (350 g/L). Successfully processed 28 day cores from SF3-C (350 g/L) and SF6-C (350 g/L).
12/12/2012	–	1 Day Re-pour Cores: Locations SF8-C(1) (125 g/L) Re-pour and SF13-C (350 g/L) Re-pour	Successfully processed 1 day re-pour cores from SF8-C(1) (125 g/L) and SF13-C (350 g/L).
12/13/2012	–	4 Day Re-pour Cores: Locations SF8-C(1) (125 g/L) Re-pour and SF13-C (350 g/L) Re-pour	Successfully processed 4 day re-pour cores from SF8-C(1) (125 g/L) and SF13-C (350 g/L).
2/15/2013	28 Day Core: SF8-C(3) (350 g/L)	–	Slurried and poured the 28 day consolidation core from SF8-C(3) (350 g/L) .
3/1/2013	14 Day Core: SF8-C(3) (350 g/L)	–	Slurried and poured the 14 day consolidation core from SF8-C(3) (350 g/L) .
3/7/2013	7 Day Core: SF8-C(3) (350 g/L)	–	Slurried and poured the 7 day consolidation core from SF8-C(3) (350 g/L) .
3/10/2013	4 Day Core: SF8-C(3) (350 g/L)	–	Slurried and poured the 4 day consolidation core from SF8-C(3) (350 g/L) .
3/13/2013	1 Day Core: SF8-C(3) (350 g/L)	–	Slurried and poured the 1 day consolidation core from SF8-C(3) (350 g/L) .
3/14/2013	1 Day Re-pour Core: SF8-C(3) (350 g/L) Re-pour	Cores: SF8-C(3) (350 g/L) 4 and 7 day; Core SF8-C(3) (350 g/L) 1 day leaked and was not processed.	Processed 4 and 7 day cores from SF8-C(3) (350 g/L); Core SF8-C(1) (350 g/L) 1 Day core leaked around the bottom of the piston (5 pistons were inside the core attempting to halt the leaking), and was saved in a 5-gallon bucket, re-slurried and re-poured for next-day re-processing (as a "re-pour" core) .
3/15/2013	–	Cores: SF8-C(3) (350 g/L) 1, 14 and 28 day	Processed 1 (re-pour), 14 and 28 day cores from SF8-C(3) (350 g/L).

3.4 LABORATORY CORE ANALYSIS

3.4.1 SF3-C CONSOLIDATION CORES (350 G/L TARGET CONCENTRATION)

Individual Consolidation Core Results

The sediment used to construct the SF3-C consolidation cores was collected from the navigation channel at the mouth of the Passaic River. The material comprised silt, sand, a large amount of organic detritus (e.g. leaves, sticks) and various pieces of garbage (e.g. plastic). The surfaces of the SF3-C cores prior to processing were orange-colored, a characteristic not observed in cores from other locations (most were light tan colored, indicating oxidation of the sediments on the surface). The water overlying the sediment surfaces in each SF3-C core remained cloudy through the day of processing (where water in the other cores became clear after sediment settlement). In general, the core descriptions on their respective day of processing were:

- 1 Day: Very low-density, fluidic surface overlying a slightly more dense slurry of silt, sand and organic material.
- 4 Day: Very low-density gelatinous surface consistency that became slightly denser with depth.
- 7 Day: Low-density silt and sand surface. Material became more dense with depth and sand-sized particles were observed at the bottom of the core.
- 14 Day: Low-density silt and sand surface. Organic detritus observed throughout the core. Sand-sized particles were visible at the bottom of the core. Material became slightly denser with depth.
- 28 Day: Low-density silt and sand surface. Organic detritus observed throughout the core. Amount of visible sand particles at the bottom increased. The core material became slightly denser with depth.

Qualitative terms are used throughout the consolidation core discussions and within the raw (handwritten) notes to describe the material consistencies observed during core processing. These are included herein in order to best depict the state of the core at the time of the analysis in a manner other than solely quantitative or qualitative observations. These serve to supplement the measured, quantitative erosion rate and sub-sample sediment property data. Though the expressions are relative, in general:

1) *very low-density* refers to a fluidic consistency of the slurry (slurry moves like water and erodes at the lowest shear stresses).
    a. Oftentimes, the sediment of a very low-density material was of such low resistive strength that the entire surface of the core would be tilted by the flow – lower upstream and higher downstream, as a result of the stress imparted by the flow.
    b. This scenario would typically result in sediment flowing off of the downstream end of the core at very low flow rates.
2) *low-density* refers to a slightly more dense consistency where the material is more cohesive, resists erosion at the very low shear stresses, but is still fluidic and/or gelatinous.

3) *soft (e.g. "soft clayey-silt")* refers to a material consistency of mayonnaise (stiffer material that resists erosion but is still very pliable).
    a. This material was able to be sub-sampled without disturbing adjacent sediment.
4) *stiff (e.g. "stiff clayey-silt")* refers to a material consistency of peanut butter (stiffer material that resists erosion and is of higher density).
    a. This material, when sub-sampled, separated from adjacent sediment in clumps.

For all laboratory consolidation core figures herein, the photographs and plots are arranged sequentially by consolidation duration from left to right (and top to bottom). Photographs of the SF3-C cores are presented in Figure 76[26]. The erosion rate data for the cores are plotted in Figure 78. Shear stresses ranging between 0.1 and 6.4 Pa were applied to these cores. Aside from the 1-day core, which showed little variation with depth, erosion rates generally decreased with depth in the cores.

The intra-core erosion rate ratios of the depth intervals evaluated in each core are shown in Figure 79. Erosion susceptibility increased down-core at 1 day of consolidation. At 4 days of consolidation, the susceptibility varies slightly with depth. After 4 days of consolidation, the erosion susceptibility decreases with depth, in general.

The power law regression fit within each depth interval from the SF3-C consolidation core sets is illustrated in Figure 80. Coefficients and regression statistics from the power law fit analysis, the measured median grain sizes, the computed wet bulk densities and the critical shear stresses for each depth interval, from each core, are presented in Table 65 to Table 74.

Consolidation Core Set Summary

The temporal variation in down-core sediment properties and computed parameters is illustrated in Figure 81 through Figure 83. Figure 81 contains the down-core median grain sizes measured; Figure 82 contains the down-core wet bulk densities computed; and Figure 83 represents the down-core linearly interpolated critical shear stresses[27].

The down-core structure of the median grain size did not indicate much variability over the consolidation duration. Median particle sizes remained in the medium to coarse silt range with a slight trend towards larger grain sizes with depth. The averaged median grain sizes ranged from 40.30 µm to 44.17 µm.

[26] The vertical scale of the photos is not equivalent.

[27] Only the linearly interpolated critical shear stresses are shown here as those values occur between τ_0 and τ_1. Those determined by power law regression introduce additional complexity in understanding and are not plotted.

The down-core wet bulk density profiles indicate a trend of increasing density both with consolidation duration and depth. After 1 day, the wet bulk density on the surface was 1.21 g/cm^3. After 28 days, the wet bulk density at a depth of 23.40 cm was 1.33 g/cm^3.

The linearly interpolated critical shear stresses varied slightly down-core, though indicated an overall increasing trend with depth and time. Aside from an unexplained anomaly in the 14-day core trend, the core-average linearly interpolated critical shear stresses increased from 0.19 Pa after 1 day to 0.39 Pa after 28 days.

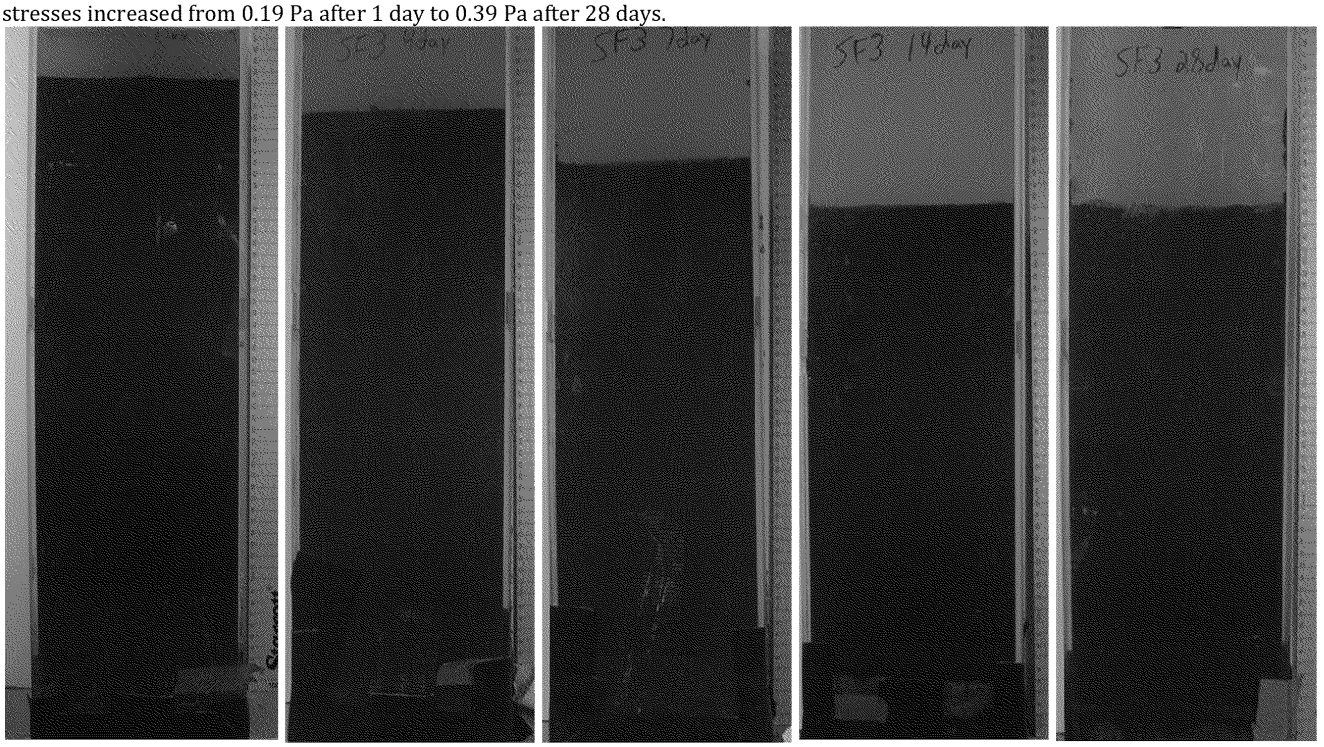

Figure 77. Pre-processing photos for the SF3-C (350 g/L) consolidation core set.

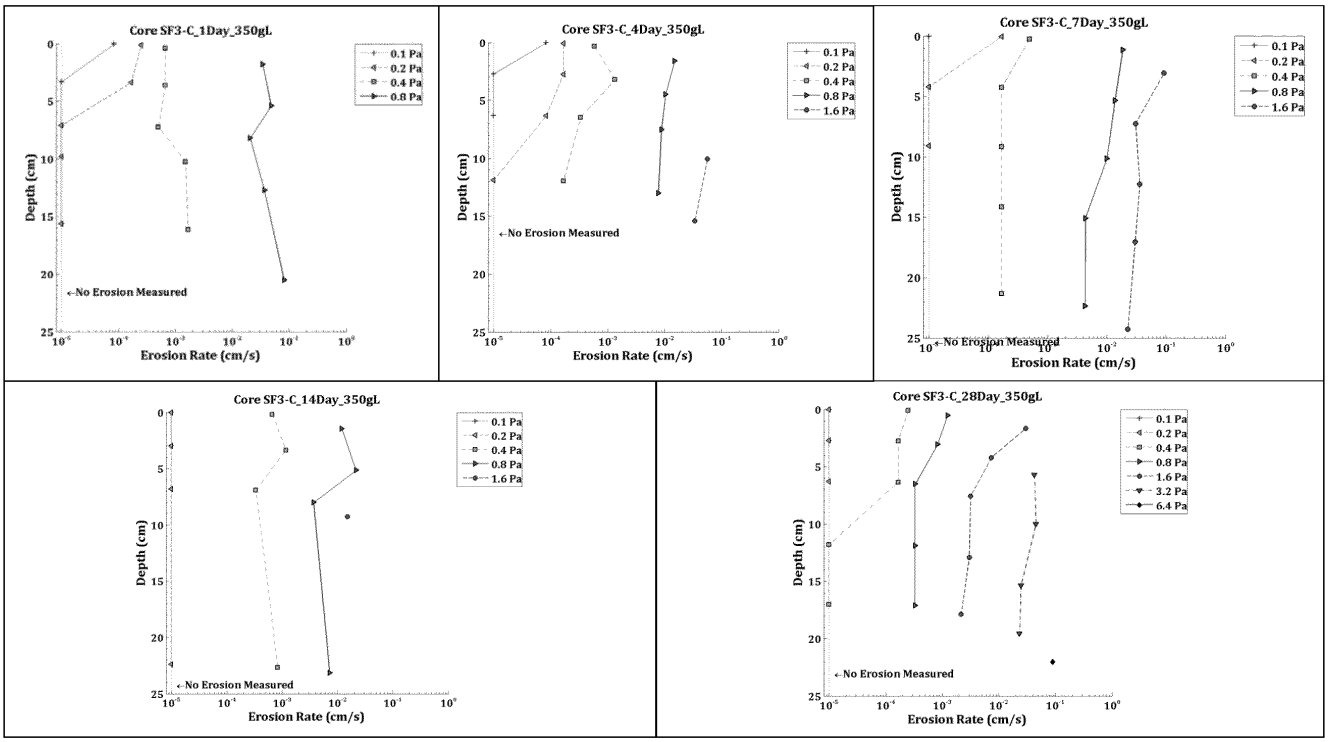

Figure 78. Down-core erosion rates for the SF3-C (350 g/L) consolidation core set.

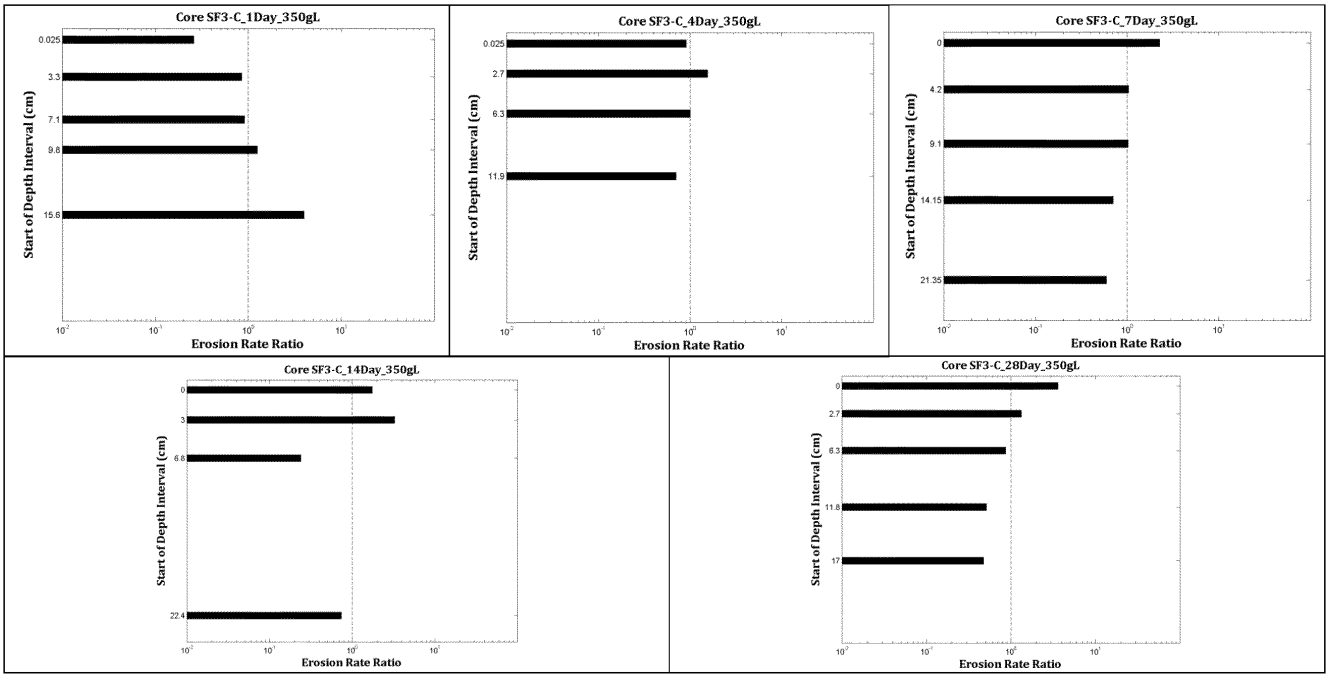

Figure 79. Intra-core erosion rate ratios for the SF3-C (350 g/L) consolidation core set.

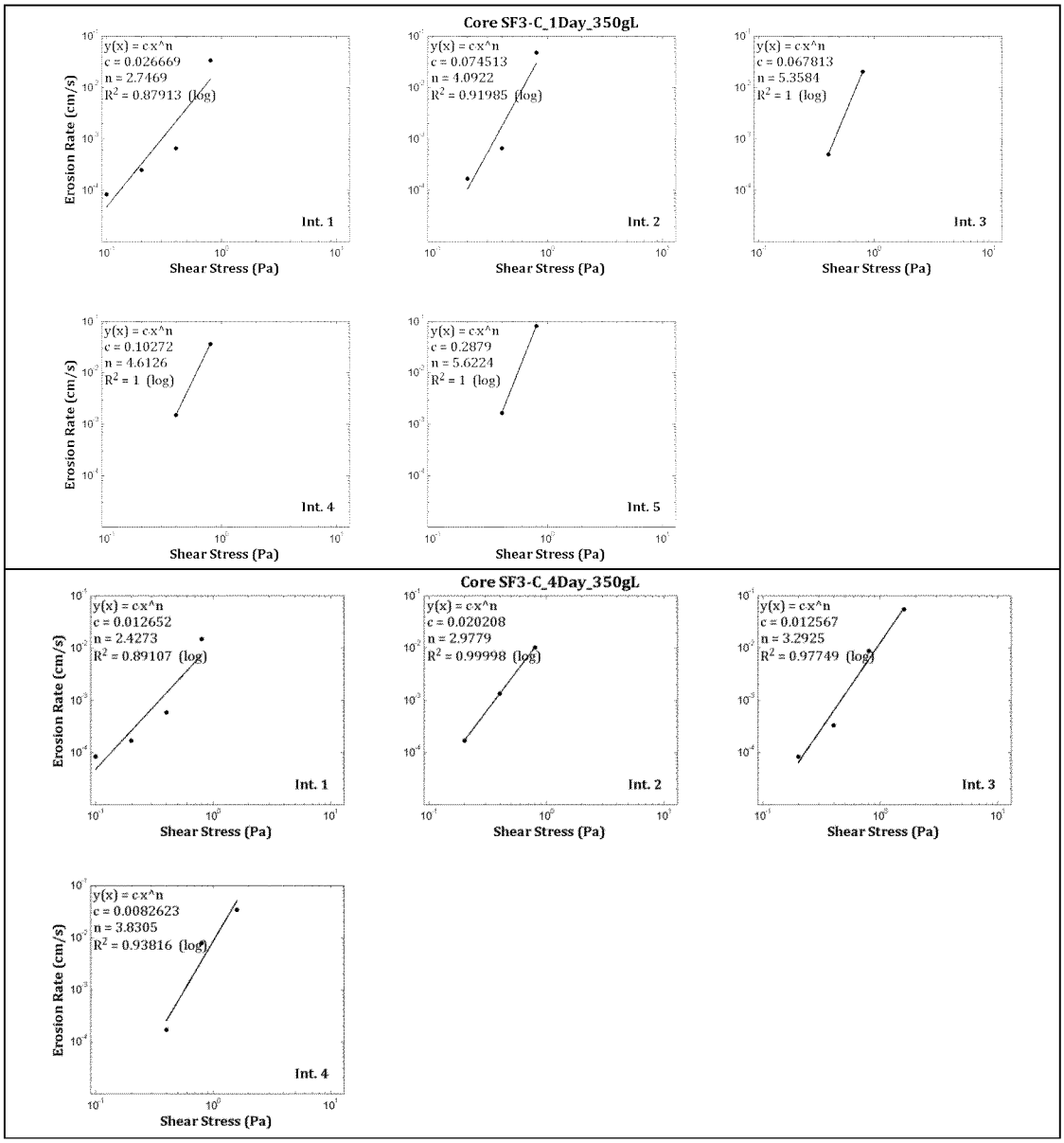

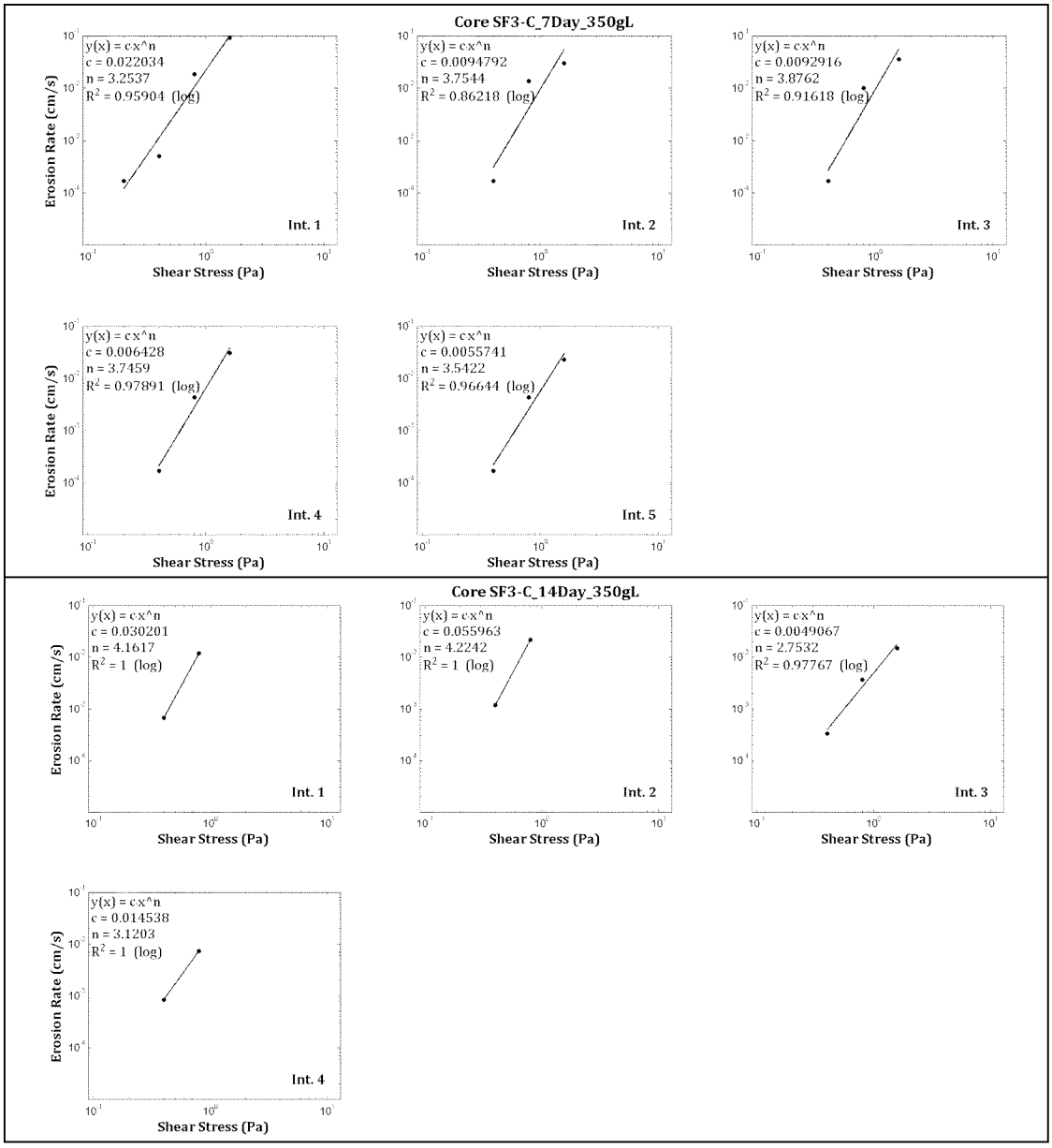

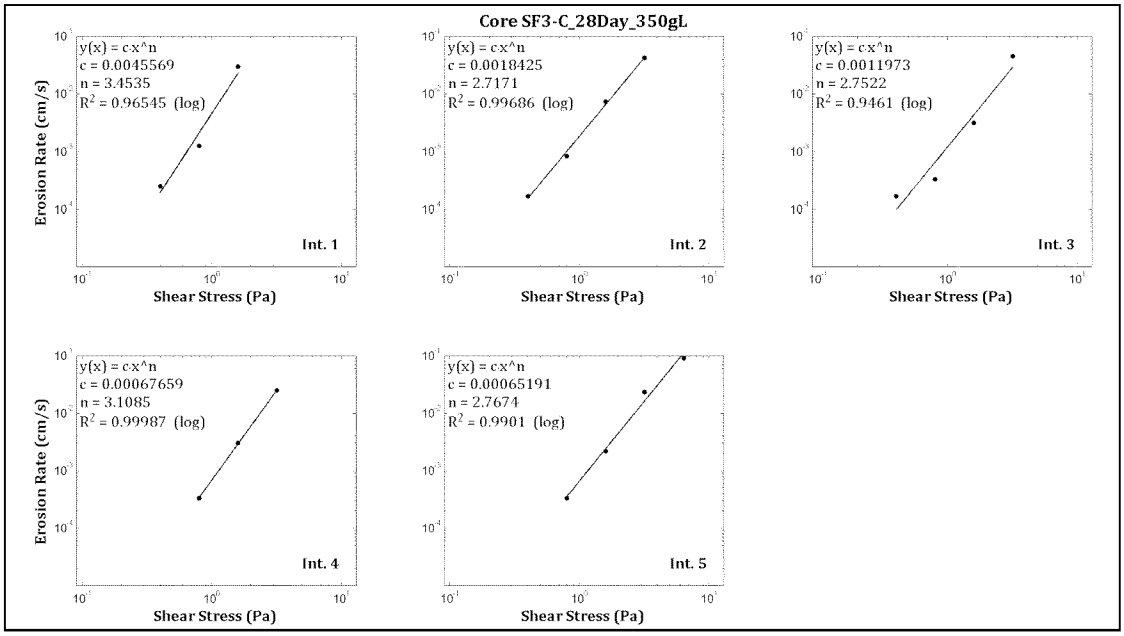

Figure 80. Power law best-fit regression solutions for the SF3-C (350 g/L) consolidation core set (sequential from top to bottom).

Table 65. Power law best-fit variables for specified depth intervals in the SF3-C 1D core.

Depth Interval	Interval Start Depth (cm)	Interval End Depth (cm)	A	n	r^2
1	0.00	3.00	0.026669	2.75	0.88
2	3.30	7.00	0.074513	4.09	0.92
3	7.10	9.00	0.067813	5.36	1.00
4	9.80	14.70	0.102716	4.61	1.00
5	15.60	24.40	0.287895	5.62	1.00

Table 66. Median grain size, wet bulk density, fraction LOI and critical shear stress for SF3-C 1D.

Sample Depth (cm)	Grain Size (μm)	Wet Bulk Density (g/cm³)	Fraction LOI	τ_0 (Pa)	τ_1 (Pa)	τ_{linear} (Pa)	τ_{power} (Pa)
0.00	28.85	1.21	0.14	0.05	0.10	0.10	0.13
3.30	39.10	1.20	0.13	0.10	0.20	0.16	0.20
7.10	35.24	1.22	0.15	0.20	0.40	0.24	0.30
9.80	51.95	1.21	0.14	0.20	0.40	0.22	0.22
15.60	47.38	1.22	0.13	0.20	0.40	0.22	0.24
24.40	47.39	1.22	0.13	*n/a*	*n/a*	*n/a*	*n/a**
Mean	**41.65**	**1.21**	**0.14**	**0.15**	**0.30**	**0.19**	**0.22**

*No erosion rate measurements made at this sample depth; there fore, no critical shear stress determinations are listed.

Table 67. Power law best-fit variables for specified depth intervals in the SF3-C 4D core.

Depth Interval	Interval Start Depth (cm)	Interval End Depth (cm)	A	n	r^2
1	0.00	2.70	0.012652	2.43	0.89
2	2.70	5.40	0.020208	2.98	1.00
3	6.30	11.60	0.012567	3.29	0.98
4	11.90	16.80	0.008262	3.83	0.94

Table 68. Median grain size, wet bulk density, fraction LOI and critical shear stress for SF3-C 4D.

Sample Depth (cm)	Grain Size (μm)	Wet Bulk Density (g/cm³)	Fraction LOI	τ_0 (Pa)	τ_1 (Pa)	τ_{linear} (Pa)	τ_{power} (Pa)
0.00	46.64	1.22	0.15	0.05	0.10	0.10	0.14
2.70	53.58	1.24	0.14	0.10	0.20	0.16	0.17
6.30	17.06	1.23	0.15	0.10	0.20	0.20	0.23
11.90	43.19	1.24	0.13	0.20	0.40	0.32	0.32
16.80	60.38	1.30	0.13	*n/a*	*n/a*	*n/a*	*n/a**
Mean	**44.17**	**1.24**	**0.14**	**0.11**	**0.23**	**0.20**	**0.21**

*No erosion rate measurements made at this sample depth; therefore, no critical shear stress determinations are listed.

Table 69. Power law best-fit variables for specified depth intervals in the SF3-C 7D core.

Depth Interval	Interval Start Depth (cm)	Interval End Depth (cm)	A	n	r^2
1	0.00	4.20	0.022034	3.25	0.96
2	4.20	8.10	0.009479	3.75	0.86
3	9.10	13.40	0.009292	3.88	0.92
4	14.10	18.10	0.006428	3.75	0.98
5	21.30	25.20	0.005574	3.54	0.97

Table 70. Median grain size, wet bulk density, fraction LOI and critical shear stress for SF3-C 7D.

Sample Depth (cm)	Grain Size (μm)	Wet Bulk Density (g/cm³)	Fraction LOI	τ_0 (Pa)	τ_1 (Pa)	τ_{linear} (Pa)	τ_{power} (Pa)
0.00	36.66	1.22	0.13	0.10	0.20	0.16	0.19
4.20	35.03	1.25	0.13	0.20	0.40	0.32	0.30
9.10	39.75	1.26	0.14	0.20	0.40	0.32	0.31
14.10	47.52	1.27	0.14	0.20	0.40	0.30	0.33
21.30	51.35	1.27	0.14	0.20	0.40	0.30	0.32
25.20	43.71	1.29	0.15	*n/a*	*n/a*	*n/a*	*n/a**
Mean	**42.34**	**1.26**	**0.14**	**0.18**	**0.36**	**0.28**	**0.29**

*No erosion rate measurements made at this sample depth; therefore, no critical shear stress determinations are listed.

Table 71. Power law best-fit variables for specified depth intervals in SF3-C 14D core.

Depth Interval	Interval Start Depth (cm)	Interval End Depth (cm)	A	n	r^2
1	0.00	2.50	0.030201	4.16	1.00
2	3.00	6.60	0.055963	4.22	1.00
3	6.80	9.50	0.004907	2.75	0.98
4	22.40	23.40	0.014538	3.12	1.00

Table 72. Median grain size, wet bulk density, fraction LOI and critical shear stress for SF3-C 14D.

Sample Depth (cm)	Grain Size (μm)	Wet Bulk Density (g/cm³)	Fraction LOI	τ_0 (Pa)	τ_1 (Pa)	τ_{linear} (Pa)	τ_{power} (Pa)
0.00	47.79	1.21	0.13	0.20	0.40	0.23	0.25
3.00	44.68	1.26	0.13	0.20	0.40	0.22	0.22
6.80	39.99	1.28	0.13	0.20	0.40	0.26	0.24
22.40	43.17	1.29	0.13	0.20	0.40	0.23	0.20
23.40	45.54	1.32	0.13	*n/a*	*n/a*	*n/a*	*n/a**
Mean	**44.23**	**1.27**	**0.13**	**0.20**	**0.40**	**0.24**	**0.23**

*No erosion rate measurements made at this sample depth; therefore, no critical shear stress determinations are listed.

Table 73. Power law best-fit variables for specified depth intervals in SF3-C 28D core.

Depth Interval	Interval Start Depth (cm)	Interval End Depth (cm)	A	n	r^2
1	0.00	2.40	0.004557	3.45	0.97
2	2.70	6.30	0.001843	2.72	1.00
3	6.30	11.50	0.001197	2.75	0.95
4	11.80	16.90	0.000677	3.11	1.00
5	17.00	23.40	0.000652	2.77	0.99

Table 74. Median grain size, wet bulk density, fraction LOI and critical shear stress for SF3-C 28D.

Sample Depth (cm)	Grain Size (μm)	Wet Bulk Density (g/cm³)	Fraction LOI	τ_0 (Pa)	τ_1 (Pa)	τ_{linear} (Pa)	τ_{power} (Pa)
0.00	36.70	1.19	0.13	0.20	0.40	0.28	0.33
2.70	40.21	1.27	0.13	0.20	0.40	0.32	0.34
6.30	51.34	1.28	0.14	0.20	0.40	0.32	0.41
11.80	34.93	1.29	0.13	0.40	0.80	0.52	0.54
17.00	38.29	1.31	0.13	0.40	0.80	0.52	0.51
23.40	40.30	1.33	0.13	*n/a*	*n/a*	*n/a*	*n/a**
Mean	**40.30**	**1.28**	**0.13**	**0.28**	**0.56**	**0.39**	**0.43**

*No erosion rate measurements made at this sample depth; therefore, no critical shear stress determinations are listed.

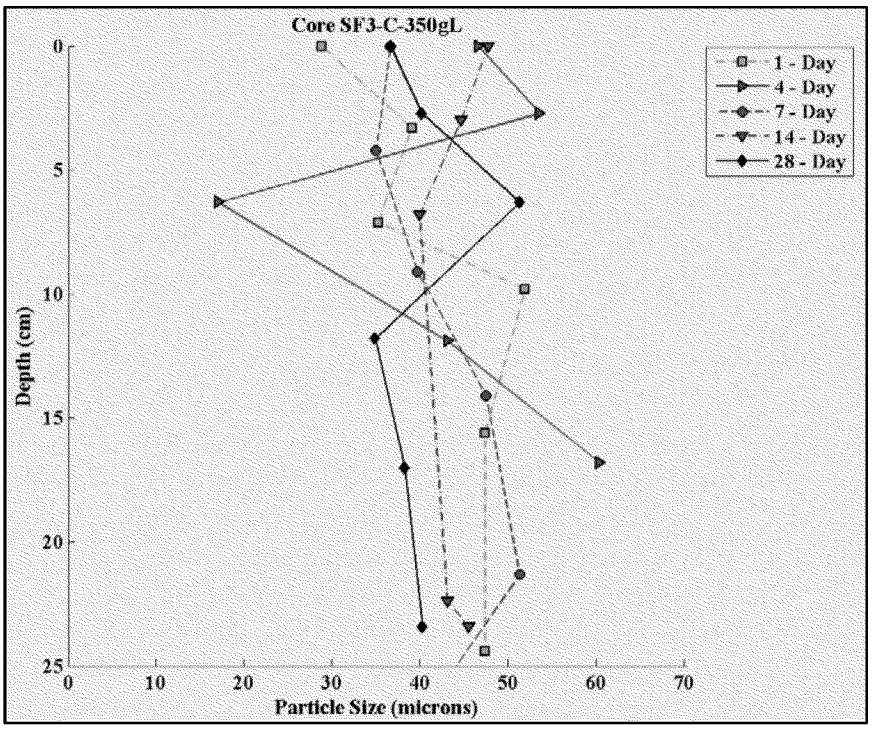

Figure 81. Down-core median grain size for each SF3-C (350 g/L) consolidation core.

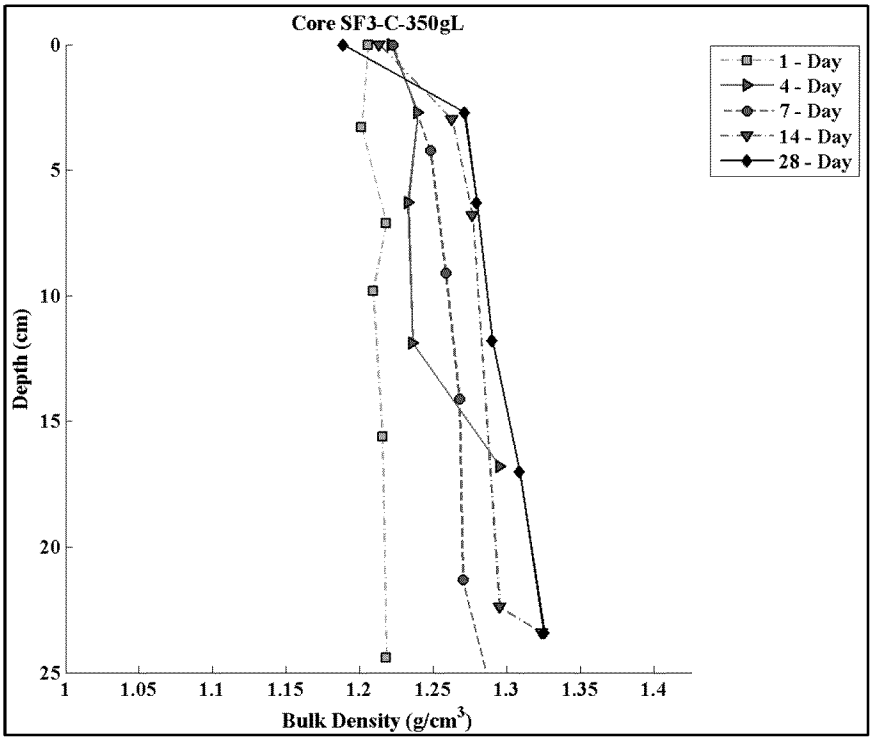

Figure 82. Down-core wet bulk density for each SF3-C (350 g/L) consolidation core.

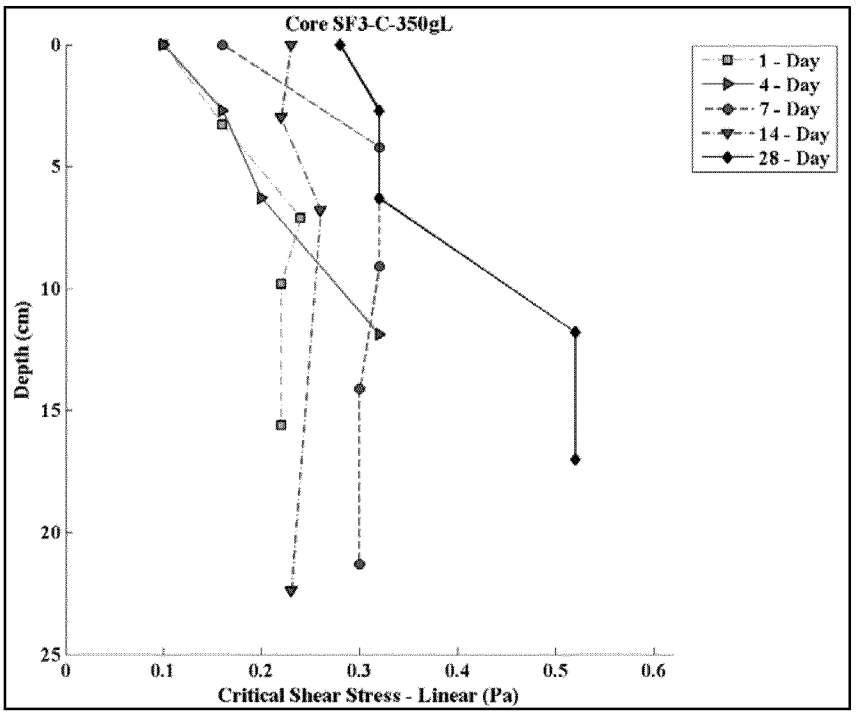

Figure 83. Down core linearly interpolated critical shear stresses for each SF3-C (350 g/L) consolidation core.

3.4.2 SF6-C Consolidation Cores (350 g/L target concentration)

Individual Consolidation Core Results

The sediment used to construct the SF6-C consolidation cores was collected from the navigation channel east of the Port of Newark, just south of the Newark Bay Bridge. The material comprised silt and a large percentage of coarser, sand-sized particles. The material consolidated very rapidly in the cores, faster than material from other locations, resulting in relatively shorter core lengths to analyze. In general, the core descriptions on their respective day of processing were:

- 1 Day: Very low-density, fluidic surface that became denser with depth. Coarser, sand-sized particles were visible at the bottom of the core.
- 4 Day: Low-density surface that became denser with depth. Stiff, clayey-silt and sand observed at the bottom of the core.
- 7 Day: Low-density surface became stiffer with depth. Material was sufficiently low-density and cohesion that it was, at times, vacuumed into the flume during the analysis. At the bottom of the core, the sandy material was visibly porous that water was leaking through the core toward the end of the analysis. Core processing was halted prior to sampling 5 intervals due to shorter length of the core and material disturbance.
- 14 Day: Low-density silt and sand surface that became denser with depth. Clayey-silt and sand was observed at the deeper depths. Material at the bottom was also vacuumed into the flume during the analysis, halting the analysis at a depth of 13 cm.
- 28 Day: Low-density silt and sand surface with coarser particles increasing in number with depth. The material became denser with depth. A coarser sand layer was encountered after a blowout near the bottom of the core.

Photographs of the SF6-C cores are presented in Figure 84. Erosion rate data for the cores are plotted in Figure 85. Shear stresses ranging between 0.1 to 6.4 Pa were applied to these cores. Erosion rates in all cores generally decreased with depth. An *increase* in erosion rate was measured in the final depth interval in the 1-day core, possibly due to the increase in sand content at that depth.

The intra-core erosion rate ratios of the depth intervals evaluated in each core are shown in Figure 86. Erosion susceptibility varied slightly, but in general, decreased with depth.

The power law regression fit within each depth interval for the SF6-C consolidation core sets is illustrated in Figure 87. Coefficients and regression statistics from the power law fit analysis, the measured median grain sizes, the computed wet bulk densities and the critical shear stresses for each depth interval, from each core, are presented in Table 75 to Table 84.

Consolidation Core Set Summary

The temporal variation in down-core sediment properties and computed parameters is illustrated in Figure 88 through Figure 90. Figure 88 contains the down-core median grain sizes measured; Figure 89 contains the down-core wet bulk densities computed; and Figure 90 represents the down-core linearly interpolated critical shear stresses.

The down-core trends of the median grain size did not indicate much variability in each core until the final sub-sample depth, at which point the median grain sizes increased significantly. Above the deepest sampling depths, the median grain sizes in the cores remained in the very fine to fine silt range (6.13 µm to 12.32 µm). At the deepest sampling depths, the median grain size increased sharply, between 36.59 µm and 195.90 µm, which is coarse silt to fine sand. The large range in grain size in the bottom samples is likely a result of random sediment settling processes and dissimilar sub-sampling depths between cores during the analysis.

Similarly, the down-core wet bulk density profiles trended toward rapidly increasing density both with time and depth, punctuated by a sharp increase in wet bulk density at the deepest sampling depth. The data indicate that the material becomes stiffer with depth and over time, which is typical of sediments allowed to consolidate in this manner. Surface wet bulk densities for all the cores ranged between 1.12 g/cm^3 and 1.17 g/cm^3. Wet bulk densities at the deepest sampling depths ranged between 1.57 g/cm^3 and 1.99 g/cm^3.

The linearly interpolated critical shear stresses increased with depth and consolidation duration. In general, the core-averaged linearly interpolated critical shear stresses increased from 0.27 Pa after 1 day to 1.14 Pa after 28 days.

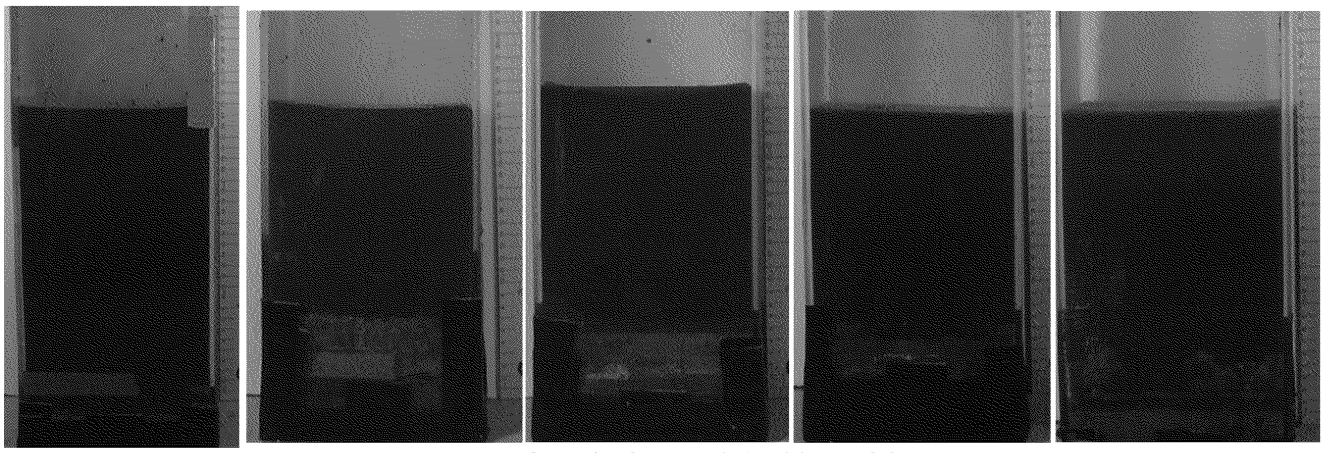

Figure 84. Pre-processing photos for the SF6-C (350 g/L) consolidation core set.

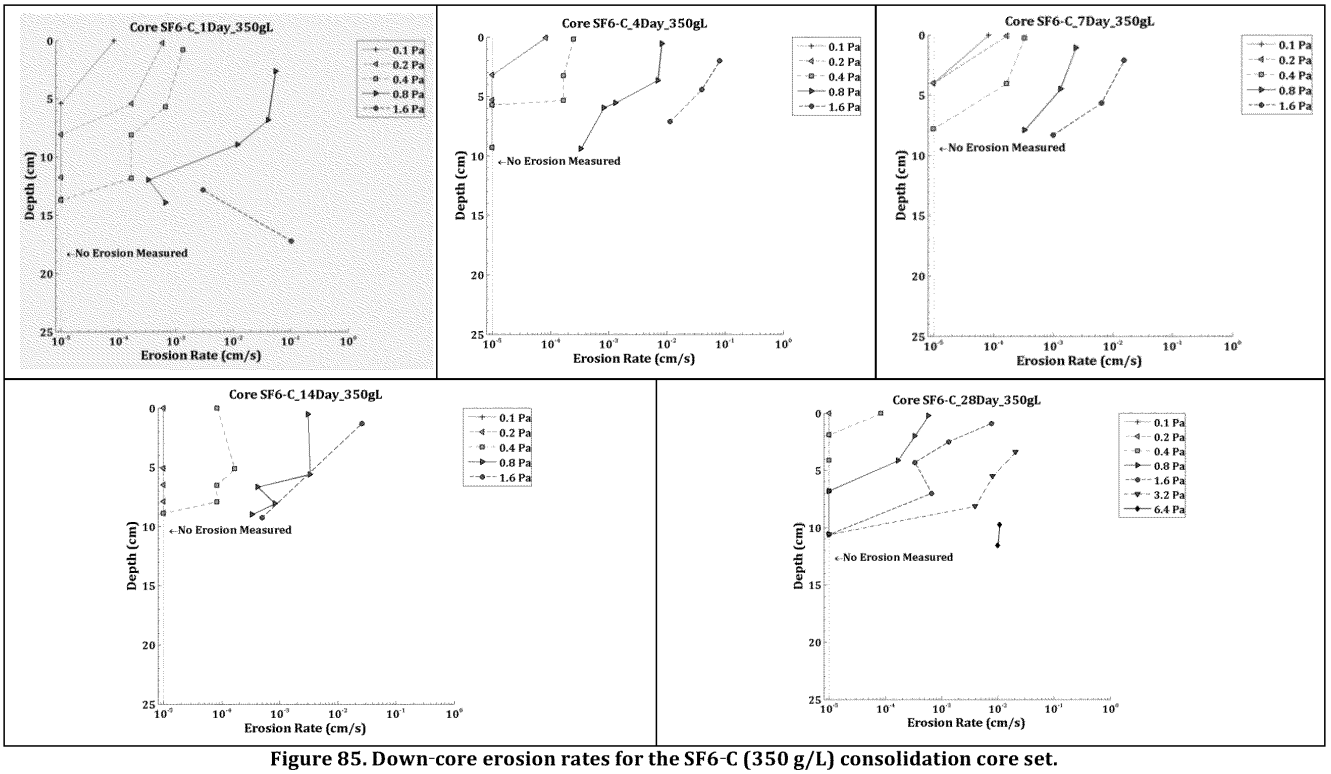

Figure 85. Down-core erosion rates for the SF6-C (350 g/L) consolidation core set.

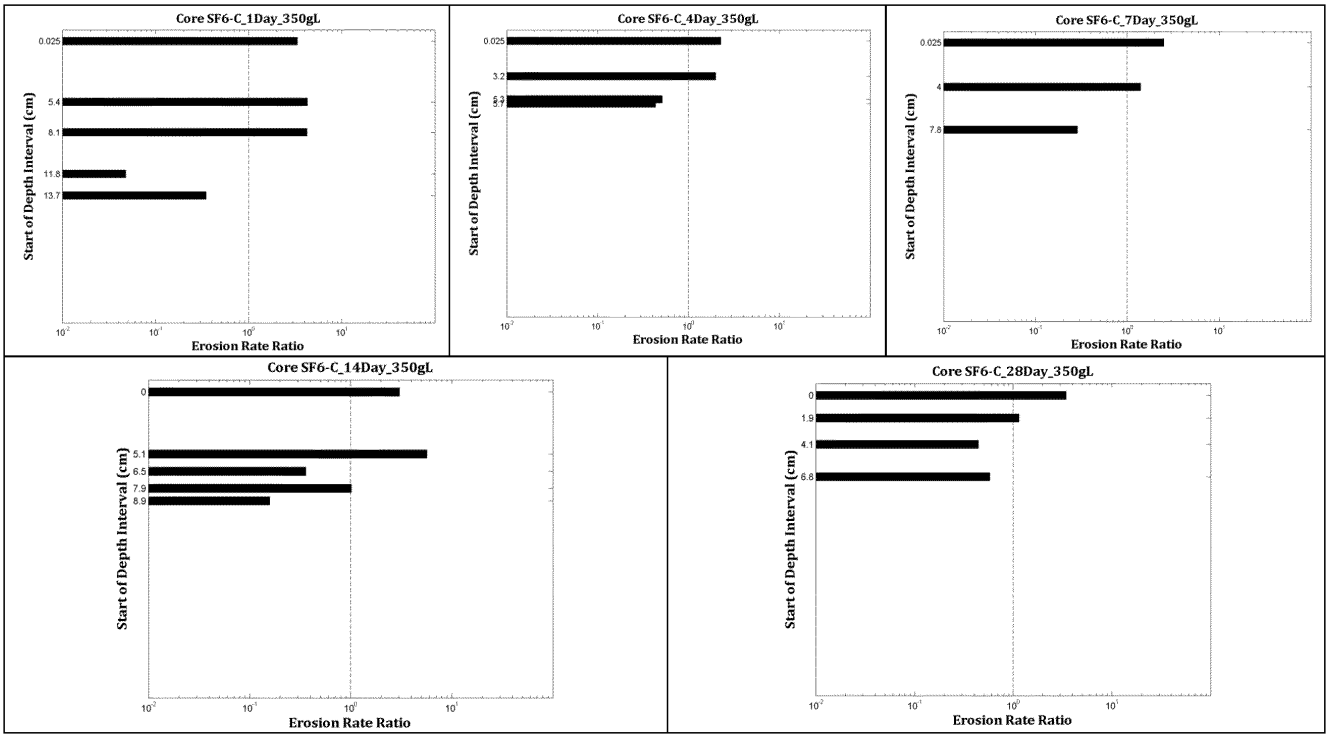

Figure 86. Intra-core erosion rate ratios for the SF6-C (350 g/L) consolidation core set.

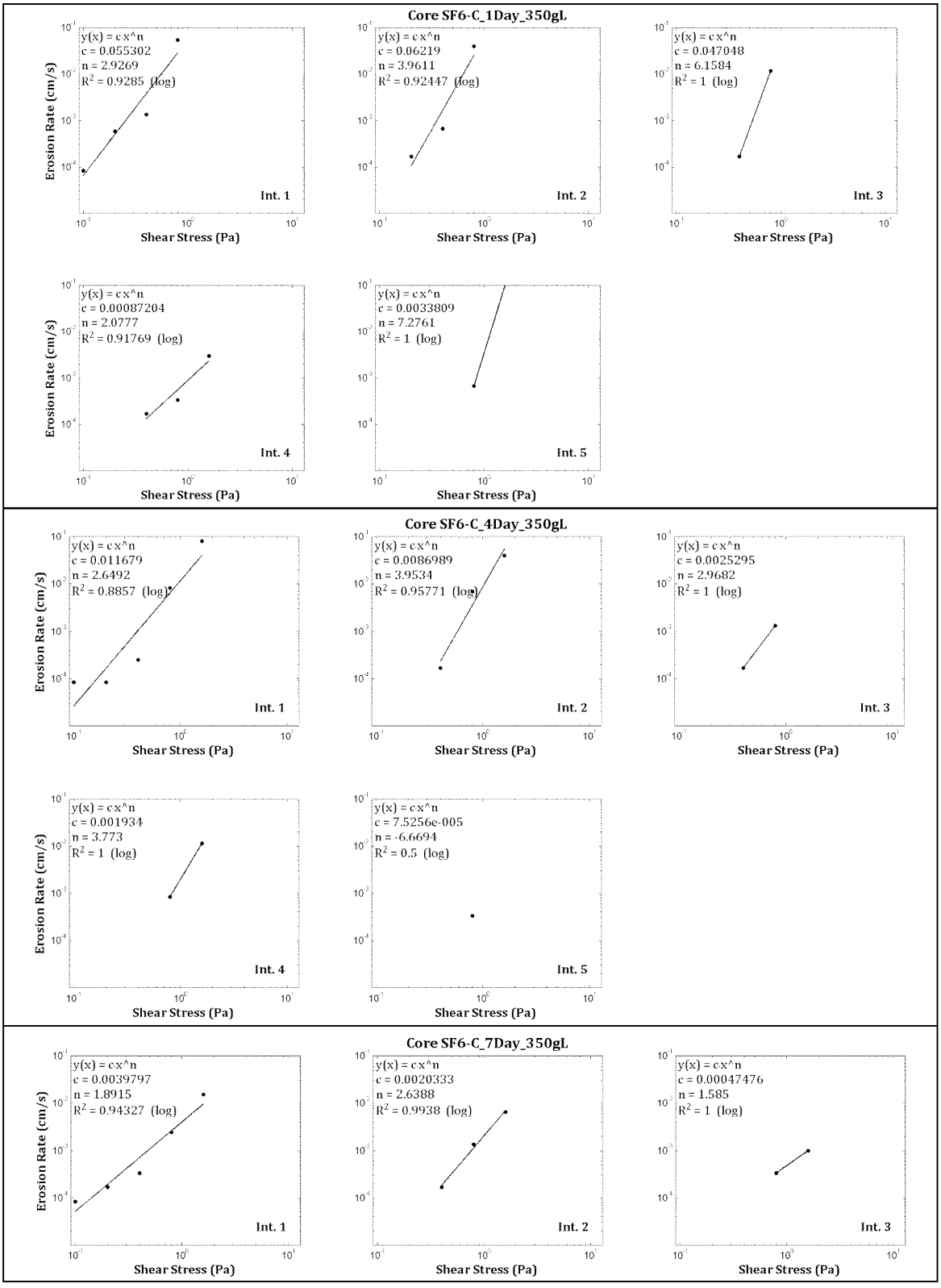

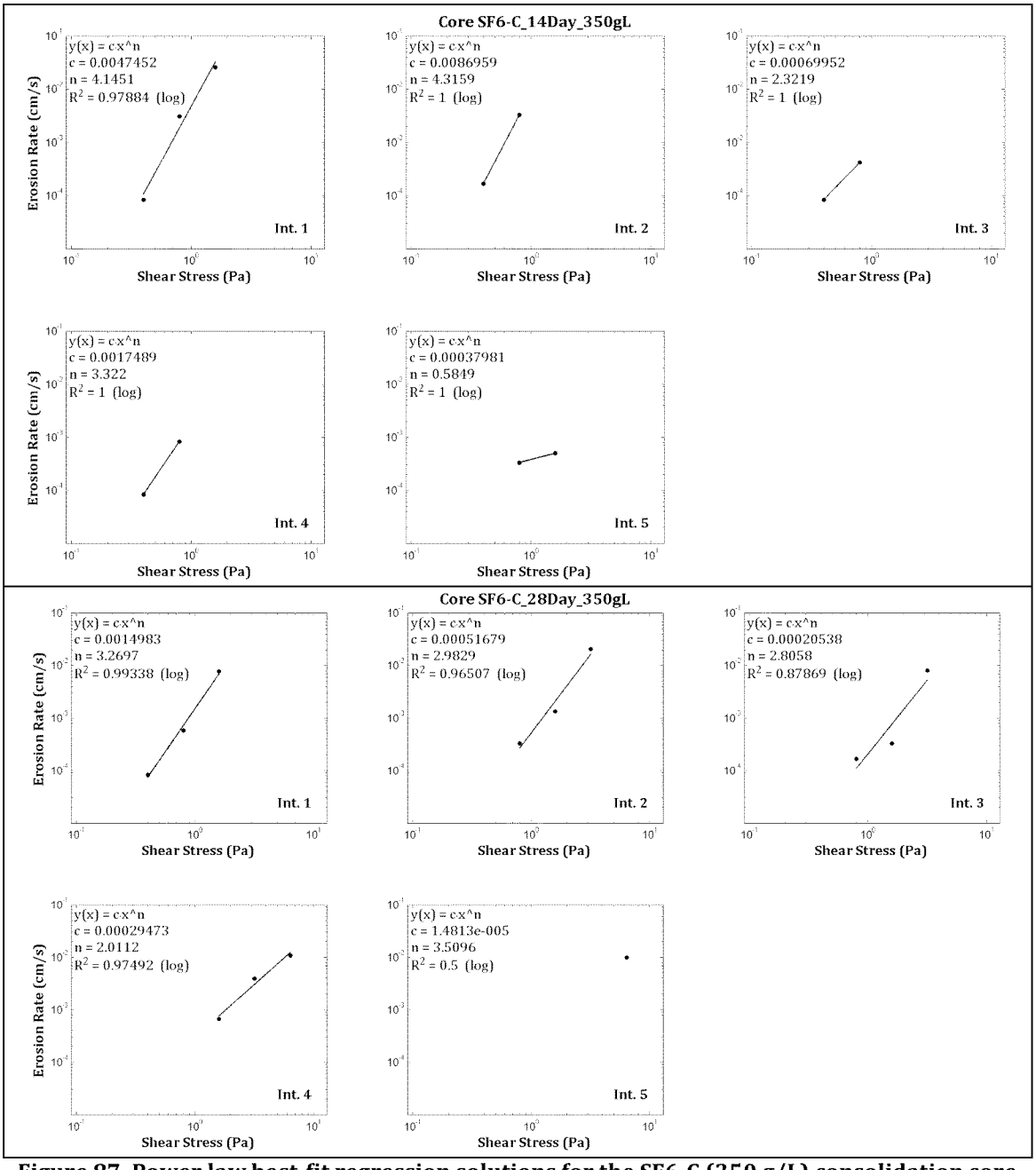

Figure 87. Power law best-fit regression solutions for the SF6-C (350 g/L) consolidation core set (sequential from top to bottom).

Table 75. Power law best-fit variables for specified depth intervals in the SF6-C 1D core.

Depth Interval	Interval Start Depth (cm)	Interval End Depth (cm)	A	n	r^2
1	0.00	4.10	0.055302	2.93	0.93
2	5.40	7.80	0.062190	3.96	0.92
3	8.10	9.70	0.047048	6.16	1.00
4	11.80	13.60	0.000872	2.08	0.92
5	13.70	20.30	0.003381	7.28	1.00

Table 76. Median grain size, wet bulk density, fraction LOI and critical shear stress for SF6-C 1D.

Sample Depth (cm)	Grain Size (μm)	Wet Bulk Density (g/cm^3)	Fraction LOI	τ_0 (Pa)	τ_1 (Pa)	τ_{linear} (Pa)	τ_{power} (Pa)
0.00	6.13	1.12	0.08	0.05	0.10	0.10	0.12
5.40	10.85	1.17	0.08	0.10	0.20	0.16	0.20
8.10	8.40	1.22	0.07	0.20	0.40	0.32	0.37
11.80	9.90	1.33	0.06	0.20	0.40	0.32	0.35
13.70	12.32	1.40	0.06	0.40	0.80	0.46	0.62
20.30	147.90	1.99	0.01	*n/a*	*n/a*	*n/a*	*n/a**
Mean	**32.58**	**1.37**	**0.06**	**0.19**	**0.38**	**0.27**	**0.33**

*No erosion rate measurements made at this sample depth; therefore, no critical shear stress determinations are listed.

Table 77. Power law best-fit variables for specified depth intervals in the SF6-C 4D core.

Depth Interval	Interval Start Depth (cm)	Interval End Depth (cm)	A	n	r^2
1	0.00	3.10	0.011679	2.65	0.89
2	3.20	4.80	0.008699	3.95	0.96
3	5.30	5.70	0.002530	2.97	1.00
4	5.70	8.00	0.001934	3.77	1.00
5	9.30	9.50	*n/a**	*n/a*	0.50

***Insufficient number of erosion rates to calculate via power law regression.**

Table 78. Median grain size, wet bulk density, fraction LOI and critical shear stress for SF6-C 4D.

Sample Depth (cm)	Grain Size (μm)	Wet Bulk Density (g/cm^3)	Fraction LOI	τ_0 (Pa)	τ_1 (Pa)	τ_{linear} (Pa)	τ_{power} (Pa)
0.00	6.33	1.17	0.09	0.05	0.10	0.10	0.17
3.20	8.27	1.27	0.08	0.20	0.40	0.32	0.32
5.30	9.86	1.34	0.07	0.20	0.40	0.32	0.34
5.70	9.63	1.35	0.07	0.40	0.80	0.45	0.46
9.30	12.24	1.42	0.06	0.40	0.80	0.52	*n/a**
9.50	99.73	1.88	0.02	*n/a*	*n/a*	*n/a*	*n/a***
Mean	**24.34**	**1.41**	**0.07**	**0.25**	**0.50**	**0.34**	**0.32**

*Insufficient number of erosion rates to calculate via power law regression.
**No erosion rate measurements made at this sample depth; therefore, no critical shear stress determinations are listed.

Table 79. Power law best-fit variables for specified depth intervals in the SF6-C 7D core.

Depth Interval	Interval Start Depth (cm)	Interval End Depth (cm)	A	n	r^2
1	0.00	2.40	0.003980	1.89	0.94
2	4.00	6.40	0.002033	2.64	0.99
3	7.80	8.60	0.000475	1.58	1.00

Table 80. Median grain size, wet bulk density, fraction LOI and critical shear stress for SF6-C 7D.

Sample Depth (cm)	Grain Size (µm)	Wet Bulk Density (g/cm³)	Fraction LOI	τ_0 (Pa)	τ_1 (Pa)	τ_{linear} (Pa)	τ_{power} (Pa)
0.00	7.72	1.14	0.10	0.05	0.10	0.10	0.14
4.00	7.54	1.26	0.30	0.20	0.40	0.32	0.32
7.80	7.88	1.38	0.06	0.40	0.80	0.52	0.37
8.60	63.36	1.58	0.04	*n/a*	*n/a*	*n/a*	*n/a**
Mean	**21.62**	**1.34**	**0.13**	**0.22**	**0.43**	**0.31**	**0.28**

*No erosion rate measurements made at this sample depth; therefore, no critical shear stress determinations are listed.

Table 81. Power law best-fit variables for specified depth intervals in the SF6-C 14D core.

Depth Interval	Interval Start Depth (cm)	Interval End Depth (cm)	A	n	r^2
1	0.00	1.60	0.004745	4.15	0.98
2	5.10	6.00	0.008696	4.32	1.00
3	6.50	6.80	0.000700	2.32	1.00
4	7.90	8.20	0.001749	3.32	1.00
5	8.90	9.40	0.000380	0.58	1.00

Table 82. Median grain size, wet bulk density, fraction LOI and critical shear stress for SF6-C 14D.

Sample Depth (cm)	Grain Size (µm)	Wet Bulk Density (g/cm³)	Fraction LOI	τ_0 (Pa)	τ_1 (Pa)	τ_{linear} (Pa)	τ_{power} (Pa)
0.00	6.49	1.14	0.09	0.20	0.40	0.40	0.39
5.10	8.94	1.29	0.07	0.20	0.40	0.32	0.36
6.50	8.96	1.33	0.07	0.20	0.40	0.40	0.43
7.90	10.88	1.34	0.07	0.20	0.40	0.40	0.42
8.90	8.56	1.39	0.07	0.40	0.80	0.52	0.10
9.40	36.59	1.57	0.04	*n/a*	*n/a*	*n/a*	*n/a**
Mean	**13.40**	**1.34**	**0.07**	**0.24**	**0.48**	**0.41**	**0.34**

*No erosion rate measurements made at this sample depth; therefore, no critical shear stress determinations are listed.

Table 83. Power law best-fit variables for specified depth intervals in the SF6-C 28D core.

Depth Interval	Interval Start Depth (cm)	Interval End Depth (cm)	A	n	r^2
1	0.00	1.40	0.001498	3.27	0.99
2	1.90	3.90	0.000517	2.98	0.97
3	4.10	6.60	0.000205	2.81	0.88
4	6.80	10.40	0.000295	2.01	0.97
5	10.60	12.50	*n/a**	*n/a*	0.50

*Insufficient number of erosion rates to calculate via power law regression.

Table 84. Median grain size, wet bulk density, fraction LOI and critical shear stress for SF6-C 28D.

Sample Depth (cm)	Grain Size (μm)	Wet Bulk Density (g/cm^3)	Fraction LOI	τ_0 (Pa)	τ_1 (Pa)	τ_{linear} (Pa)	τ_{power} (Pa)
0.00	6.60	1.15	0.07	0.20	0.40	0.40	0.44
1.90	7.50	1.23	0.09	0.40	0.80	0.52	0.58
4.10	9.11	1.28	0.07	0.40	0.80	0.64	0.77
6.80	9.39	1.33	0.07	0.80	1.60	0.92	0.58
10.60	10.90	1.43	0.06	3.20	6.40	3.24	*n/a**
12.50	195.90	1.83	0.01	*n/a*	*n/a*	*n/a*	*n/a***
Mean	**39.90**	**1.37**	**0.06**	**1.00**	**2.00**	**1.14**	**0.59**

*Insufficient number of erosion rates to calculate via power law regression.
**No erosion rate measurements made at this sample depth; therefore, no critical shear stress determinations are listed.

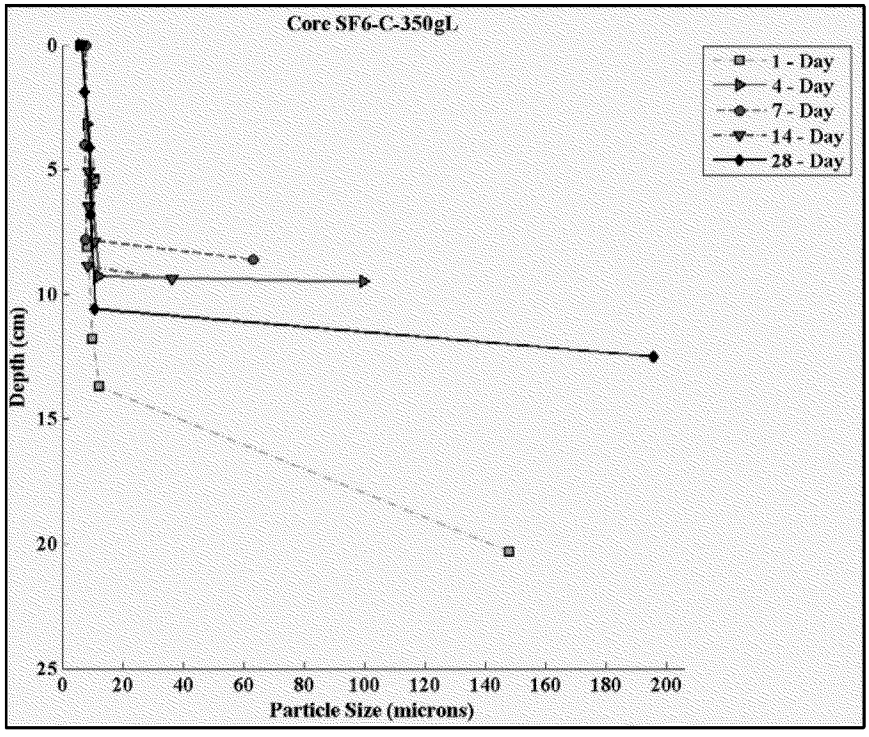

Figure 88. Down-core median grain size for each SF6-C (350 g/L) consolidation core.

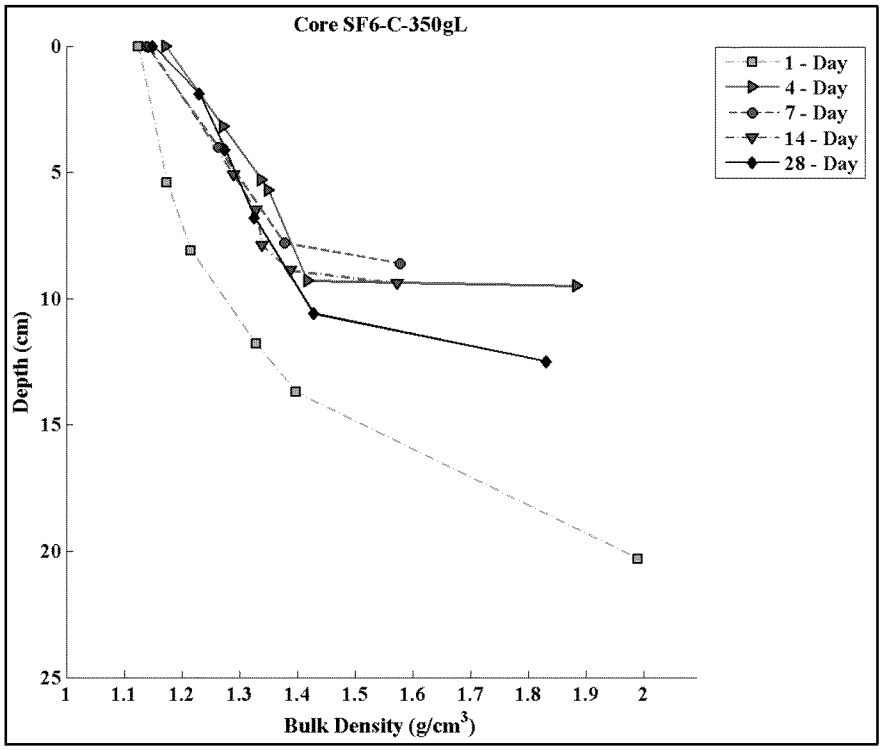

Figure 89. Down-core wet bulk density for each SF6-C (350 g/L) consolidation core.

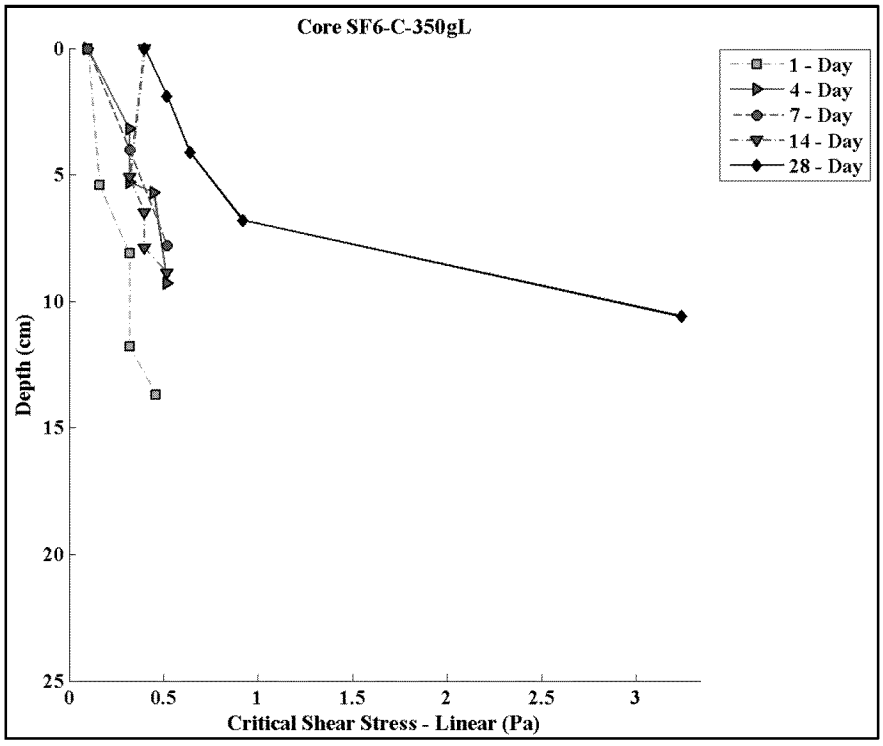

Figure 90. Down core linearly interpolated critical shear stresses for each SF6-C (350 g/L) consolidation core.

3.4.3 SF9-C Consolidation Cores (350 g/L target concentration)

Individual Consolidation Core Results

The sediment used to construct the SF9-C consolidation cores was collected from the eastern mudflats, east of the CDF. The material comprised silt and fine sand throughout. In general, the core descriptions on their respective day of processing were:

- 1 Day: Very low-density, fluidic surface with low-density aggregates floating on the fluid-like surface. Low-density silt and fine sand persisted through the core.
- 4 Day: Very low-density, fluidic surface comprising a tan-colored, fractured, low-density aggregate surface. Material remained fluidic throughout.
- 7 Day: Very low-density, fluidic surface became slightly denser with depth. At the deepest depths, the sediment became gelatinous, but remained of low-density.
- 14 Day: Low-density, fluidic/gelatinous surface. Sediments became slightly denser with depth.
- 28 Day: Low-density silt surface that became denser and soft with depth. Some larger, sand-sized particles were observed at the deepest depths in the core.

Photographs of the SF9-C cores are presented in Figure 91. Erosion rate data for the cores are plotted in Figure 92. Shear stresses ranging between 0.1 to 1.6 Pa were applied to these cores. Erosion rates in all cores generally were variable with depth, fluctuating down-core.

The intra-core erosion rate ratios of the depth intervals evaluated in each core are shown in Figure 93. Generally, down-core erosion susceptibility was variable in all cores.

The power law regression fit within each depth interval for the SF9-C consolidation core sets is illustrated in Figure 94. Coefficients and regression statistics from the power law fit analysis, the measured median grain sizes, the computed wet bulk densities and the critical shear stresses for each depth interval, from each core, are presented in Table 85 to Table 94.

Consolidation Core Set Summary

The temporal variation in down-core sediment properties and computed parameters is illustrated in Figure 95 through Figure 97. Figure 95 contains the down-core median grain sizes measured; Figure 96 contains the down-core wet bulk densities computed; and Figure 97 represents the down-core linearly interpolated critical shear stresses.

The down-core structure of the median grain size did not indicate much variability over the consolidation duration. Median particle sizes remained in the very fine to fine silt range (7.59 µm to12.31 µm) with a slight trend towards increasing grain sizes with depth.

The down-core wet bulk density data indicate that the material becomes stiffer with depth and over time (after 1 day of settlement), which is typical of sediments allowed to consolidate in this manner. The wet bulk density profile for the 1-day core decreased from a surface value of 1.21 g/cm^3 to a value of 1.09 g/cm^3 at a depth of 27.50 cm. After 28

days, however, the wet bulk density profile reversed trend and increased with depth, from 1.22 g/cm^3 at the surface to 1.39 g/cm^3 at a depth of 18.80 cm.

The linearly interpolated critical shear stresses varied downcore and with consolidation duration. There was no easily identifiable trend observed. The lowest core-average values occurred in the 1-, 7- and 14- day cores (0.16-0.22 Pa); the highest core-average values occurred in the 4- and 28-day cores (0.30 Pa). It is evident, though, that these results are all relatively similar and separated by small critical shear stress values.

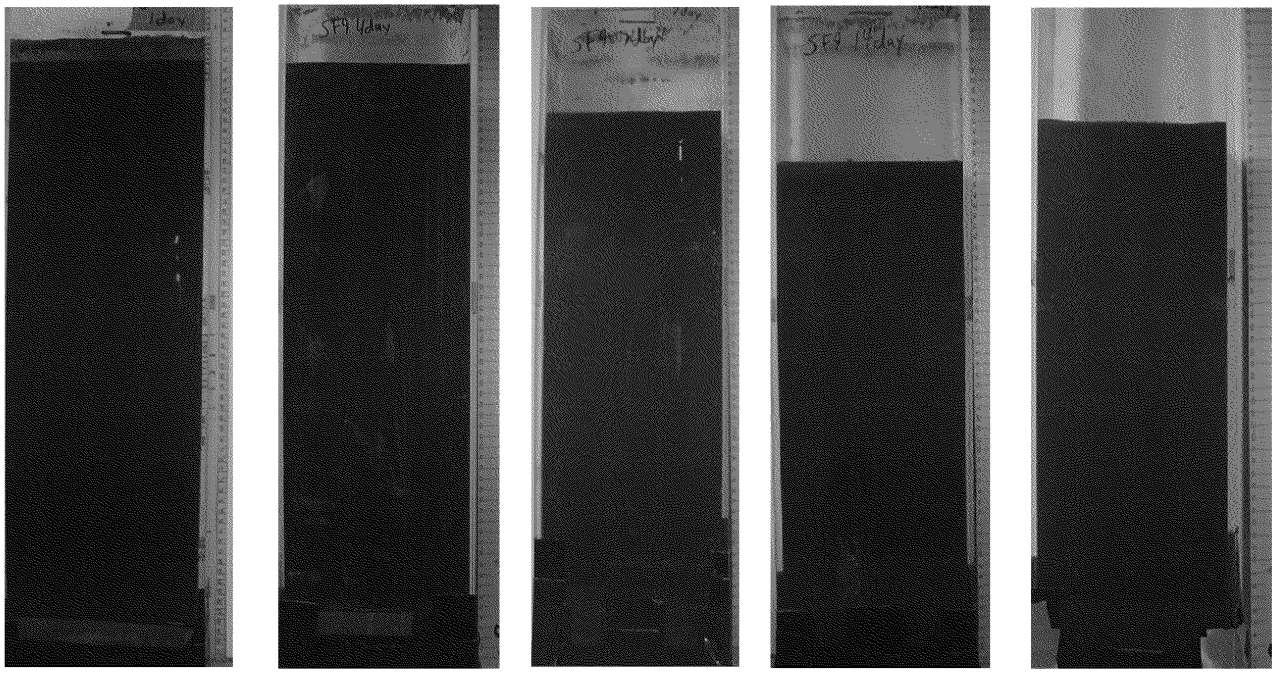

Figure 91. Pre-processing photos for the SF9-C (350 g/L) consolidation core set.

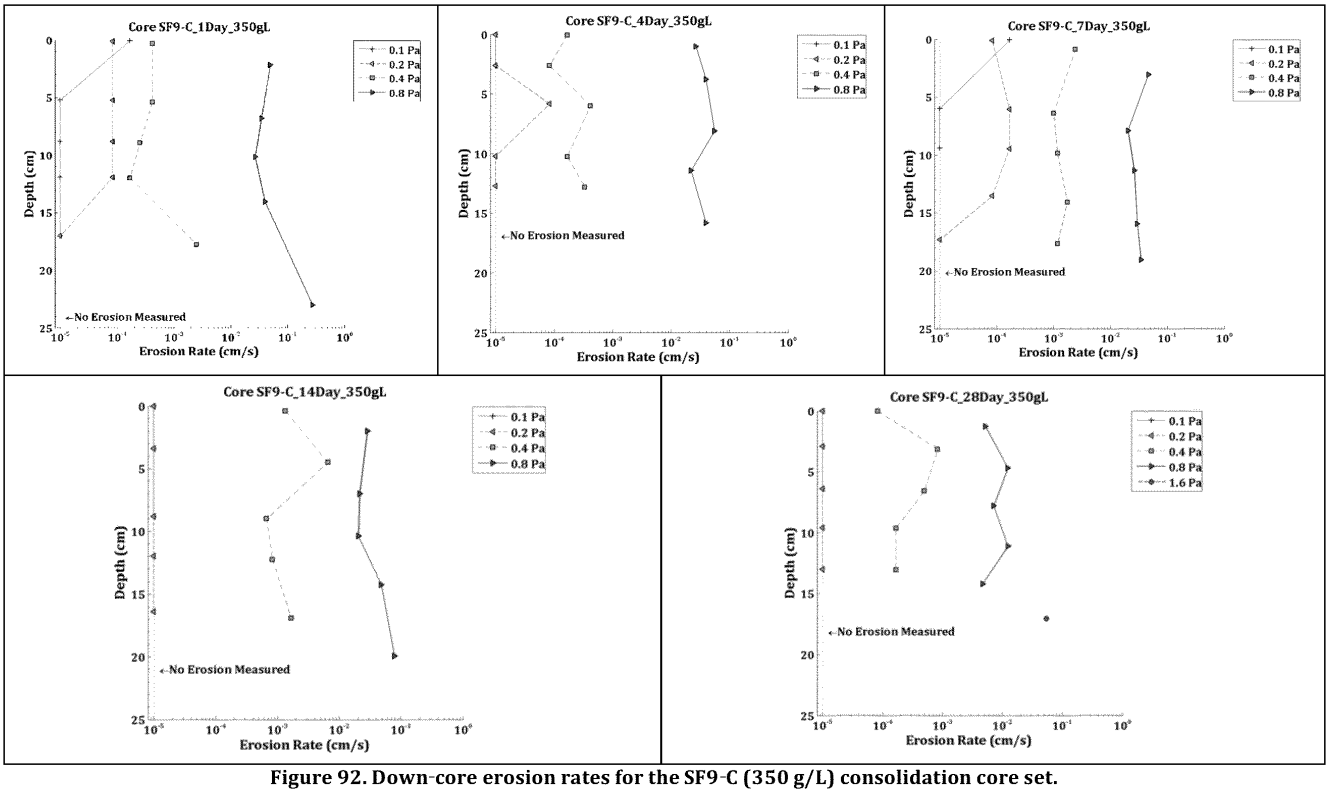

Figure 92. Down-core erosion rates for the SF9-C (350 g/L) consolidation core set.

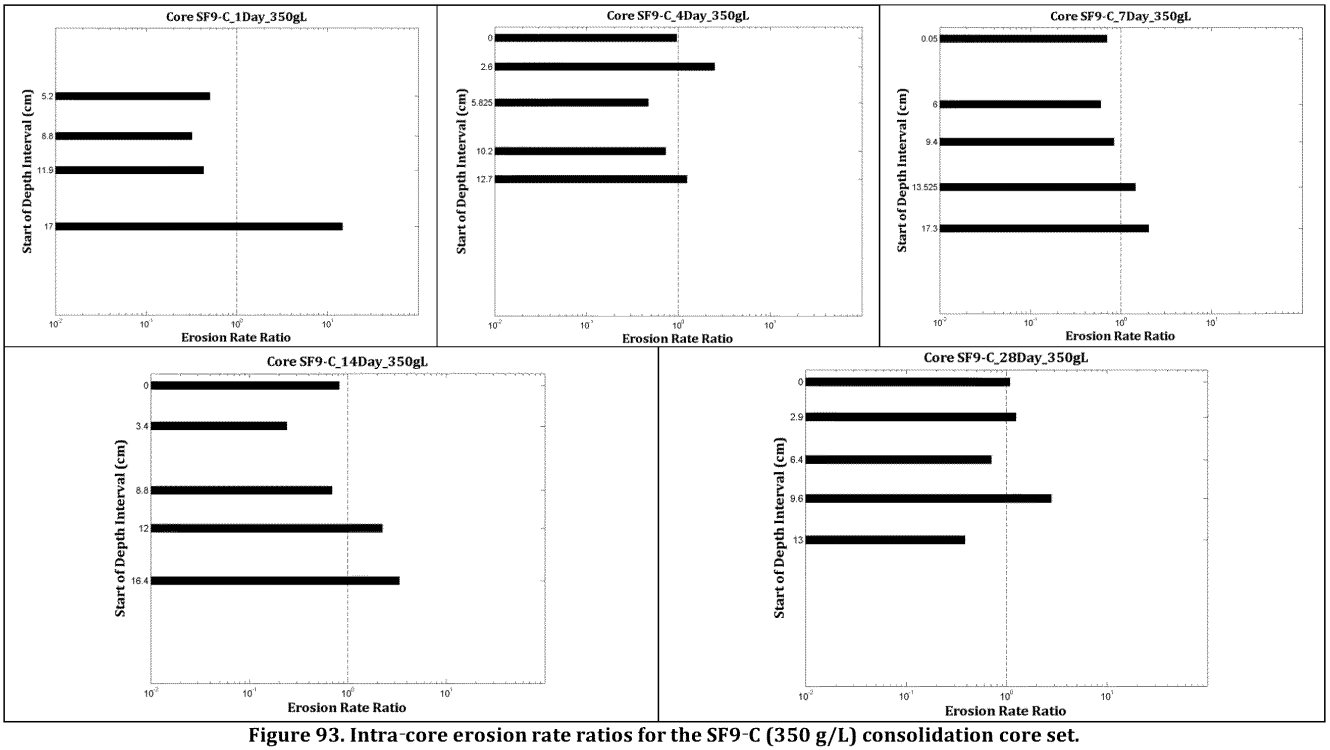

Figure 93. Intra-core erosion rate ratios for the SF9-C (350 g/L) consolidation core set.

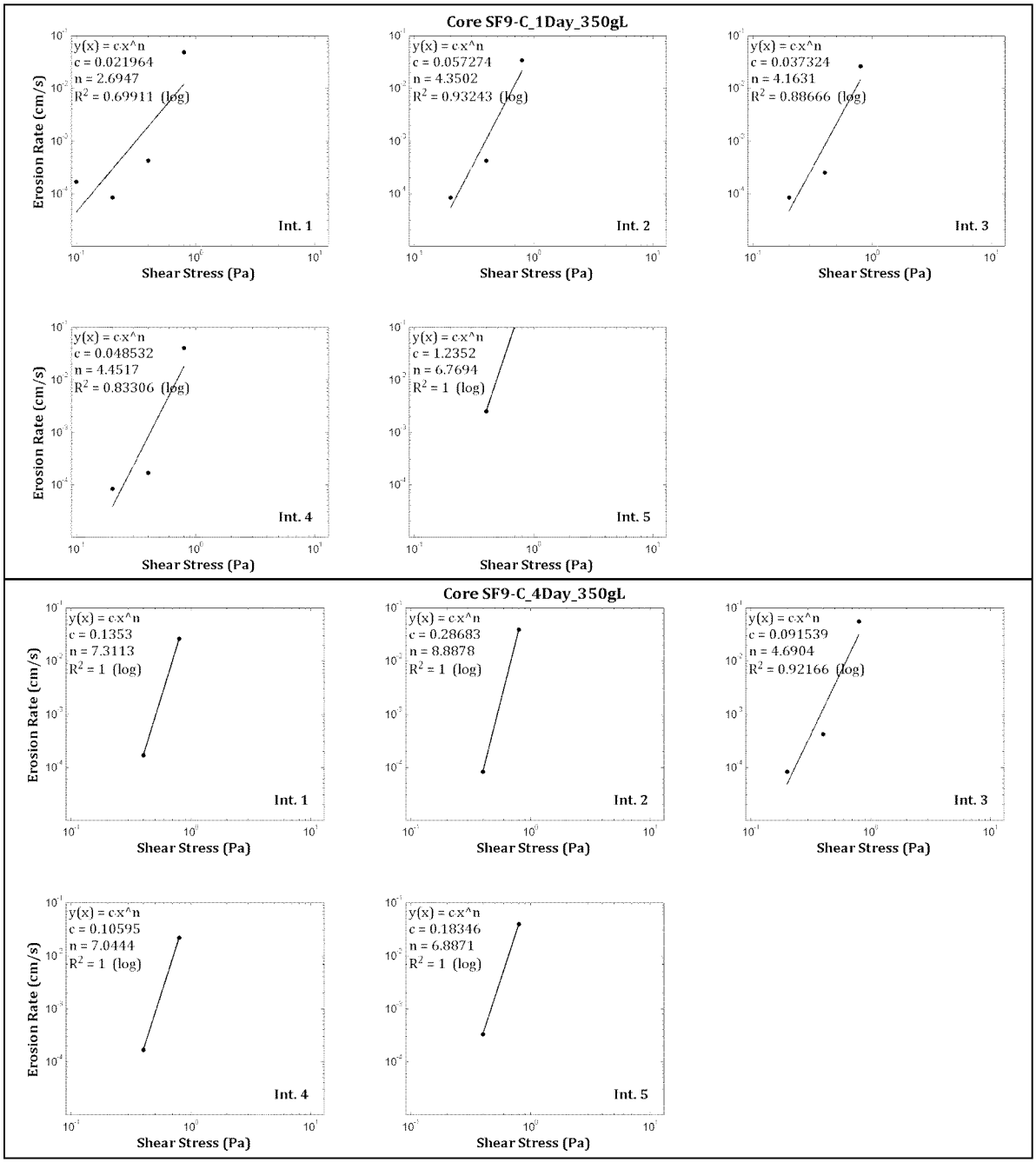

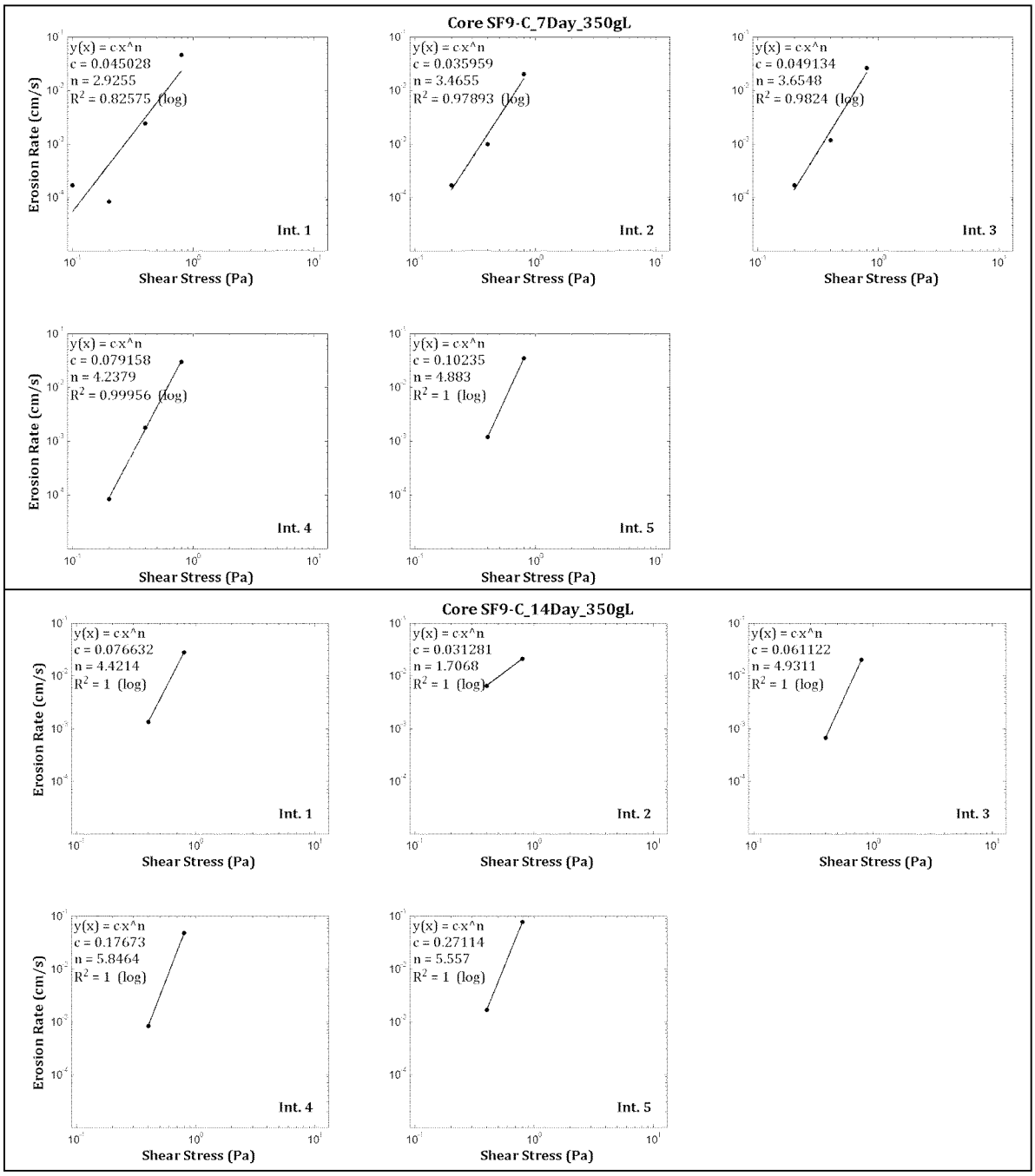

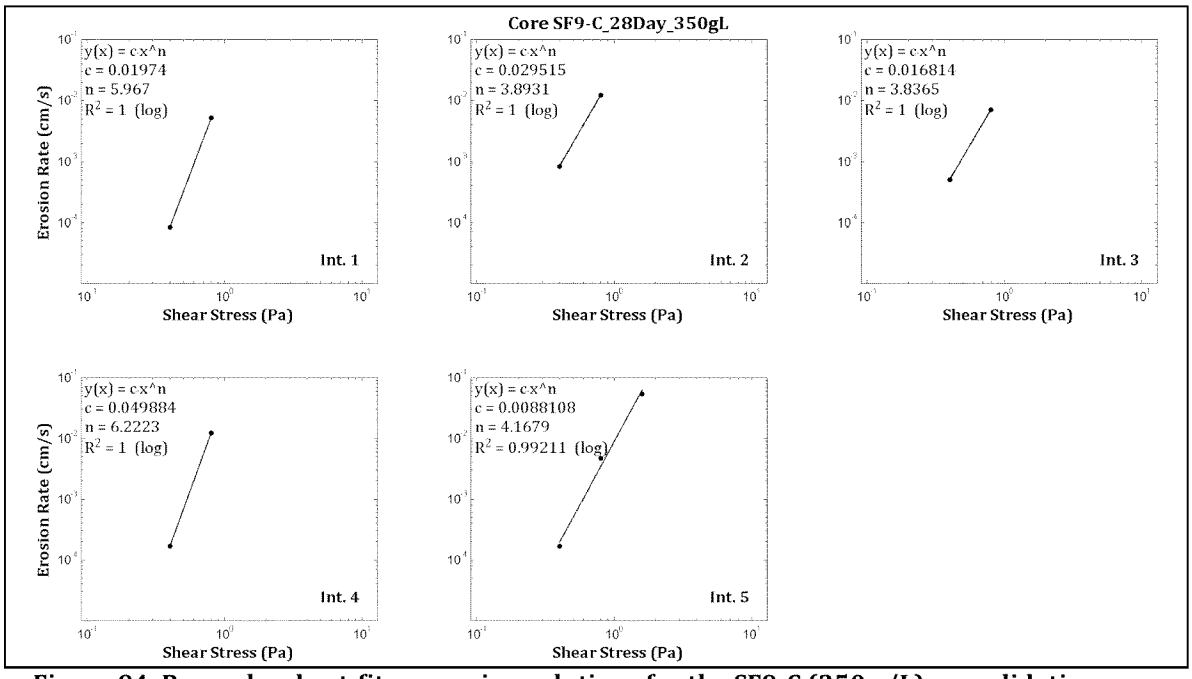

Figure 94. Power law best-fit regression solutions for the SF9-C (350 g/L) consolidation core set (sequential from top to bottom).

Table 85. Power law best-fit variables for specified depth intervals in the SF9-C 1D core.

Depth Interval	Interval Start Depth (cm)	Interval End Depth (cm)	A	n	r^2
1	0.00	3.90	*n/a**	*n/a*	0.70
2	5.20	8.10	0.057274	4.35	0.93
3	8.80	11.30	0.037324	4.16	0.89
4	11.90	16.00	0.048532	4.45	0.83
5	17.00	27.50	1.235215	6.77	1.00

*Insufficient r^2 value from regression.

Table 86. Median grain size, wet bulk density, fraction LOI and critical shear stress for SF9-C 1D.

Sample Depth (cm)	Grain Size (μm)	Wet Bulk Density (g/cm^3)	Fraction LOI	τ_0 (Pa)	τ_1 (Pa)	τ_{linear} (Pa)	τ_{power} (Pa)
0.00	9.31	1.21	0.13	0.05	0.10	0.05	*n/a**
5.20	11.17	1.21	0.06	0.10	0.20	0.20	0.23
8.80	10.04	1.23	0.09	0.10	0.20	0.20	0.24
11.90	11.48	1.23	0.09	0.10	0.20	0.20	0.25
17.00	7.59	1.17	0.12	0.20	0.40	0.21	0.25
27.50	9.70	1.09	0.11	*n/a*	*n/a*	*n/a*	*n/a***
Mean	**9.88**	**1.19**	**0.10**	**0.11**	**0.22**	**0.17**	**0.24**

*Insufficient r^2 value from regression.
**No erosion rate measurements made at this sample depth; therefore, no critical shear stress determinations are listed.

Table 87. Power law best-fit variables for specified depth intervals in the SF9-C 4D core.

Depth Interval	Interval Start Depth (cm)	Interval End Depth (cm)	A	n	r^2
1	0.00	1.90	0.135304	7.31	1.00
2	2.60	4.90	0.286827	8.89	1.00
3	5.80	10.10	0.091539	4.69	0.92
4	10.20	12.50	0.105947	7.04	1.00
5	12.70	18.70	0.183462	6.89	1.00

Table 88. Median grain size, wet bulk density, fraction LOI and critical shear stress for SF9-C 4D.

Sample Depth (cm)	Grain Size (μm)	Wet Bulk Density (g/cm^3)	Fraction LOI	τ_0 (Pa)	τ_1 (Pa)	τ_{linear} (Pa)	τ_{power} (Pa)
0.00	10.81	1.22	0.07	0.20	0.40	0.32	0.37
2.60	12.12	1.23	0.07	0.20	0.40	0.40	0.41
5.80	10.75	1.24	0.07	0.10	0.20	0.20	0.23
10.20	10.80	1.24	0.07	0.20	0.40	0.32	0.37
12.70	10.59	1.24	0.07	0.20	0.40	0.26	0.34
18.70	8.77	1.24	0.07	*n/a*	*n/a*	*n/a*	*n/a**
Mean	**10.64**	**1.23**	**0.07**	**0.18**	**0.36**	**0.30**	**0.34**

*No erosion rate measurements made at this sample depth; therefore, no critical shear stress determinations are listed.

Table 89. Power law best-fit variables for specified depth intervals in the SF9-C 7D core.

Depth Interval	Interval Start Depth (cm)	Interval End Depth (cm)	A	n	r^2
1.00	0.00	4.50	0.045028	2.93	0.83
2.00	6.00	9.10	0.035959	3.47	0.98
3.00	9.40	12.50	0.049134	3.65	0.98
4.00	13.50	17.30	0.079158	4.24	1.00
5.00	17.30	20.10	0.102351	4.88	1.00

Table 90. Median grain size, wet bulk density, fraction LOI and critical shear stress for SF9-C 7D.

Sample Depth (cm)	Grain Size (μm)	Wet Bulk Density (g/cm^3)	Fraction LOI	τ_0 (Pa)	τ_1 (Pa)	τ_{linear} (Pa)	τ_{power} (Pa)
0.00	11.79	1.24	0.06	0.05	0.10	0.05	0.12
6.00	10.39	1.25	0.06	0.10	0.20	0.16	0.18
9.40	11.75	1.26	0.05	0.10	0.20	0.16	0.18
13.50	10.73	1.25	0.05	0.10	0.20	0.20	0.21
17.30	12.21	1.27	0.05	0.20	0.40	0.22	0.24
20.10	11.15	1.28	0.06	*n/a*	*n/a*	*n/a*	*n/a**
Mean	**11.34**	**1.26**	**0.06**	**0.11**	**0.22**	**0.16**	**0.19**

*No erosion rate measurements made at this sample depth; therefore, no critical shear stress determinations are listed.

Table 91. Power law best-fit variables for specified depth intervals in the SF9-C 14D core.

Depth Interval	Interval Start Depth (cm)	Interval End Depth (cm)	A	n	r^2
1	0.00	3.20	0.076632	4.42	1.00
2	3.40	8.40	0.031281	1.71	1.00
3	8.80	11.60	0.061122	4.93	1.00
4	12.00	16.00	0.176732	5.85	1.00
5	16.40	22.50	0.271136	5.56	1.00

Table 92. Median grain size, wet bulk density, fraction LOI and critical shear stress for SF9-C 14D.

Sample Depth (cm)	Grain Size (μm)	Wet Bulk Density (g/cm^3)	Fraction LOI	τ_0 (Pa)	τ_1 (Pa)	τ_{linear} (Pa)	τ_{power} (Pa)
0.00	11.74	1.23	0.08	0.20	0.40	0.22	0.22
3.40	10.94	1.26	0.08	0.20	0.40	0.21	0.03
8.80	10.75	1.29	0.07	0.20	0.40	0.23	0.27
12.00	9.98	1.27	0.08	0.20	0.40	0.23	0.28
16.40	10.27	1.28	0.07	0.20	0.40	0.22	0.24
22.50	10.21	1.29	0.07	*n/a*	*n/a*	*n/a*	*n/a**
Mean	**10.65**	**1.27**	**0.08**	**0.20**	**0.40**	**0.22**	**0.21**

*No erosion rate measurements made at this sample depth; therefore, no critical shear stress determinations are listed.

Table 93. Power law best-fit variables for specified depth intervals in the SF9-C 28D core.

Depth Interval	Interval Start Depth (cm)	Interval End Depth (cm)	A	n	r^2
1	0.00	2.50	0.019740	5.97	1.00
2	2.90	6.00	0.029515	3.89	1.00
3	6.40	8.90	0.016814	3.84	1.00
4	9.60	12.50	0.049884	6.22	1.00
5	13.00	18.80	0.008811	4.17	0.99

Table 94. Median grain size, wet bulk density, fraction LOI and critical shear stress for SF9-C 28D.

Sample Depth (cm)	Grain Size (μm)	Wet Bulk Density (g/cm^3)	Fraction LOI	τ_0 (Pa)	τ_1 (Pa)	τ_{linear} (Pa)	τ_{power} (Pa)
0.00	10.22	1.22	0.07	0.20	0.40	0.40	0.41
2.90	10.77	1.30	0.07	0.20	0.40	0.23	0.23
6.40	11.26	1.30	0.07	0.20	0.40	0.24	0.26
9.60	11.31	1.31	0.07	0.20	0.40	0.32	0.37
13.00	11.58	1.32	0.07	0.20	0.40	0.32	0.34
18.80	12.31	1.39	0.07	*n/a*	*n/a*	*n/a*	*n/a**
Mean	**11.24**	**1.31**	**0.07**	**0.20**	**0.40**	**0.30**	**0.32**

*No erosion rate measurements made at this sample depth; therefore, no critical shear stress determinations are listed.

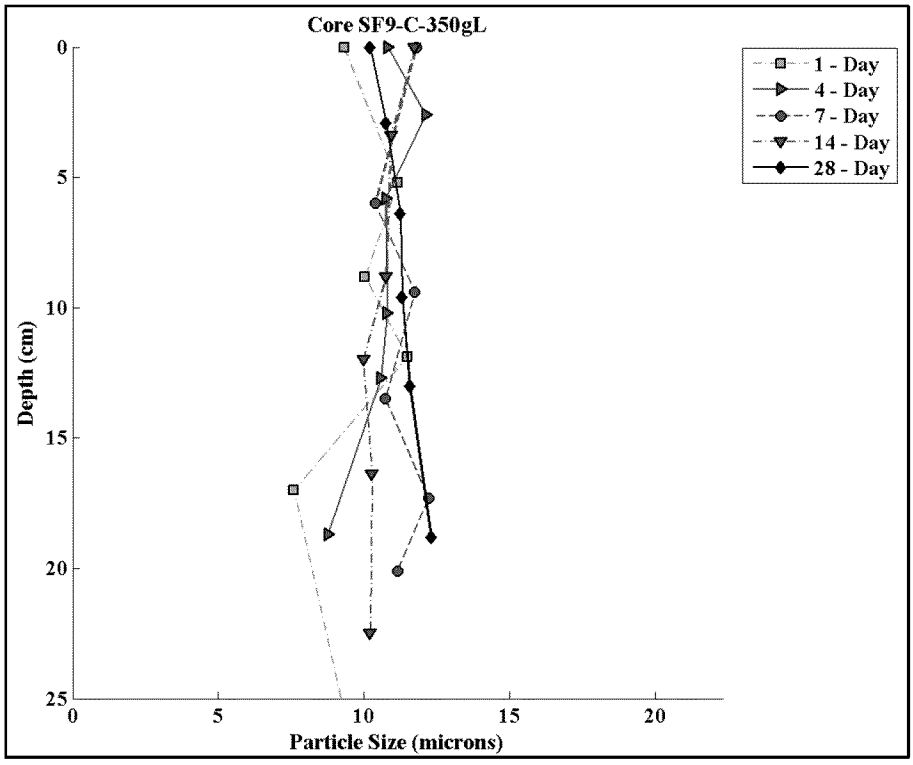

Figure 95. Down-core median grain size for each SF9-C (350 g/L) consolidation core.

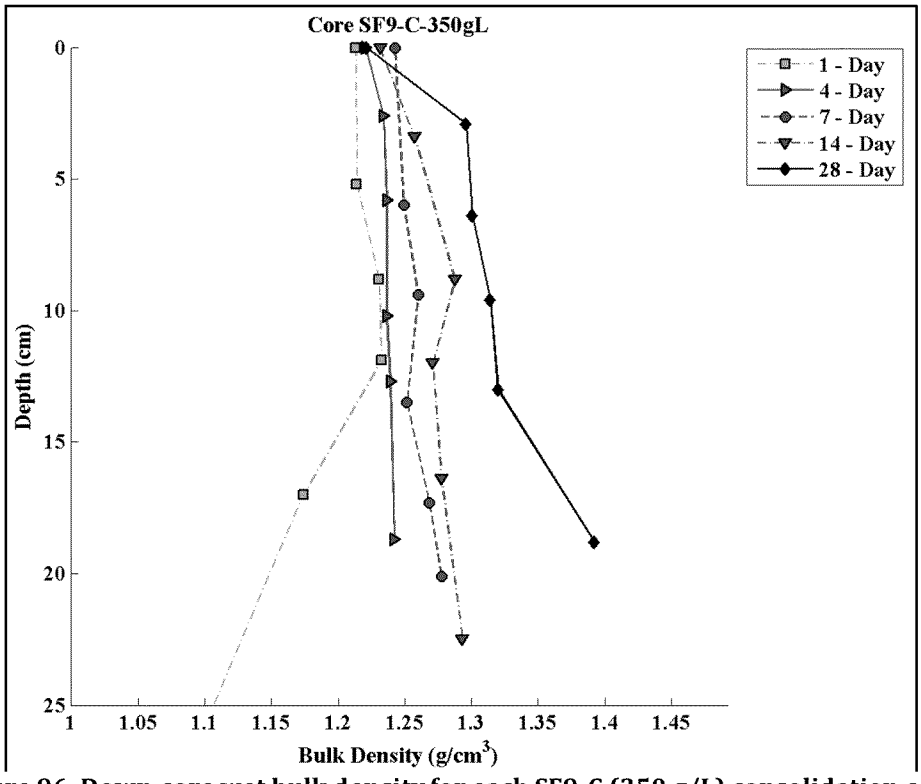

Figure 96. Down-core wet bulk density for each SF9-C (350 g/L) consolidation core.

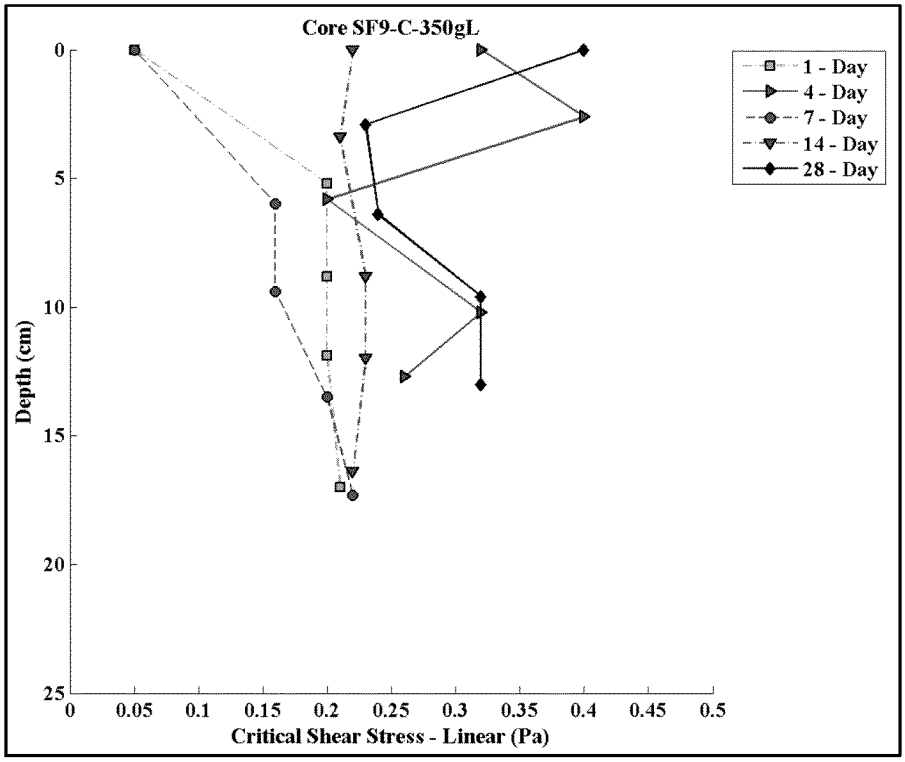

Figure 97. Down core linearly interpolated critical shear stresses for each SF9-C (350 g/L) consolidation core.

3.4.4 SF13-C Consolidation Cores (350 g/L target concentration)

Individual Consolidation Core Results

The sediment used to construct the SF13-C consolidation cores was collected from the east side of the navigation channel, at the south end of Newark Bay. Initial attempts to recover material from the west side of the navigation channel were unsuccessful, likely attributable to the lack of fine sediment at that location[28]. The coring crew moved to the east side of the channel where material was successfully recovered. The sediment comprised mostly silt. In general, the core descriptions on their respective day of processing were:

- 1 Day: Very low-density, fluidic surface that became slightly denser with depth. Low-density silt throughout.
- 4 Day: Very low-density, fluidic surface that became slightly denser with depth. Low-density silt throughout.
- 7 Day: Very low-density, fluidic surface that became slightly denser with depth. Low-density silt throughout.
- 14 Day: Very low-density, fluidic surface that became slightly denser with depth (stiffer at depth than previous cores). Low-density silt throughout.
- 28 Day: Low-density, gelatinous surface that became denser with depth. Low-density silt throughout. Stiffer at depth than previous cores.

Photographs of the SF13-C cores are presented in Figure 98. The erosion rate data for the cores are plotted in Figure 99. Shear stresses ranging between 0.1 to 1.6 Pa were applied to these cores. Erosion rates in all cores generally decreased with depth or remained relatively constant.

The intra-core erosion rate ratios of the depth intervals evaluated in each core are shown in Figure 100. Erosion susceptibility varied slightly with depth, but, in general, decreased with depth down-core.

The power law regression fit within each depth interval for the SF13-C consolidation core sets is illustrated in Figure 101. Coefficients and regression statistics from the power law fit analysis, the measured median grain sizes, the computed wet bulk densities and the critical shear stresses for each depth interval, from each core, are presented in Table 95 to Table 104.

Consolidation Core Set Summary

The temporal variation in down-core sediment properties and computed parameters is illustrated in Figure 102 through Figure 104. Figure 102 contains the down-core median grain sizes measured; Figure 103 contains the down-core wet bulk densities computed; and Figure 104 represents the down-core linearly interpolated critical shear stresses.

[28] The location had been recently blasted and dredged to deepen the navigation channel so it is possible that the bottom substrate comprised hard rock.

The down-core structure of the median grain size did not indicate much variability over the consolidation duration. Median particle sizes remained in the very fine to fine silt range (6.61 µm to 13.42 µm) with no apparent down-core trend.

The down-core wet bulk density profiles were relatively constant with depth early on, but showed increasing trends as consolidation time increased, indicating that the material becomes stiffer with depth and over time. The down-core variation in the 1-day core was 1.21 g/cm^3 to 1.22 g/cm^3. The down-core variation in the 28-day core was 1.20 to 1.29 g/cm^3.

Similar to the SF9-C consolidation core trends, the interpolated critical shear stresses varied down-core and with consolidation duration. The 1-, 4- and 14-day cores had the lowest critical shear stress core-averages and the 7- and 28-day cores had the largest. However, as in the SF9-C cores, the SF13-C critical shear stress core averages had a small shear stress range, between 0.20 Pa and 0.28 Pa.

Figure 98. Pre-processing photos for the SF13-C (350 g/L) consolidation core set.

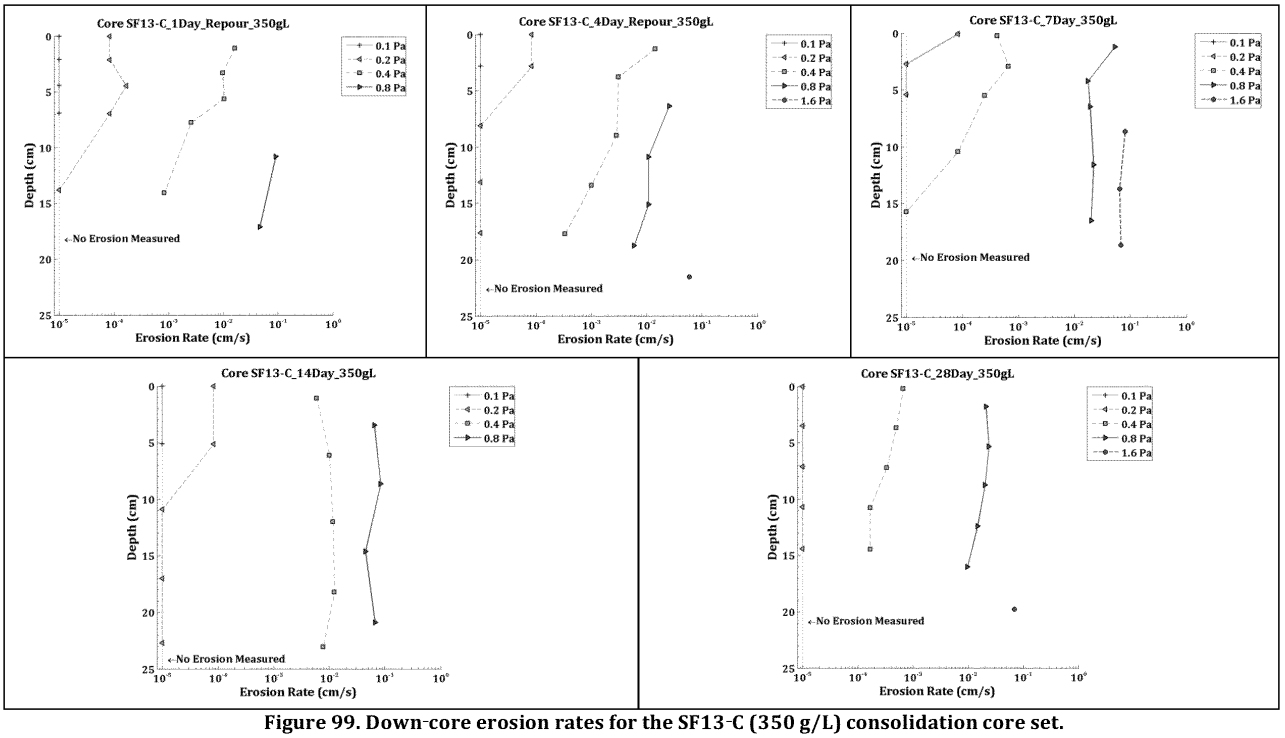

Figure 99. Down-core erosion rates for the SF13-C (350 g/L) consolidation core set.

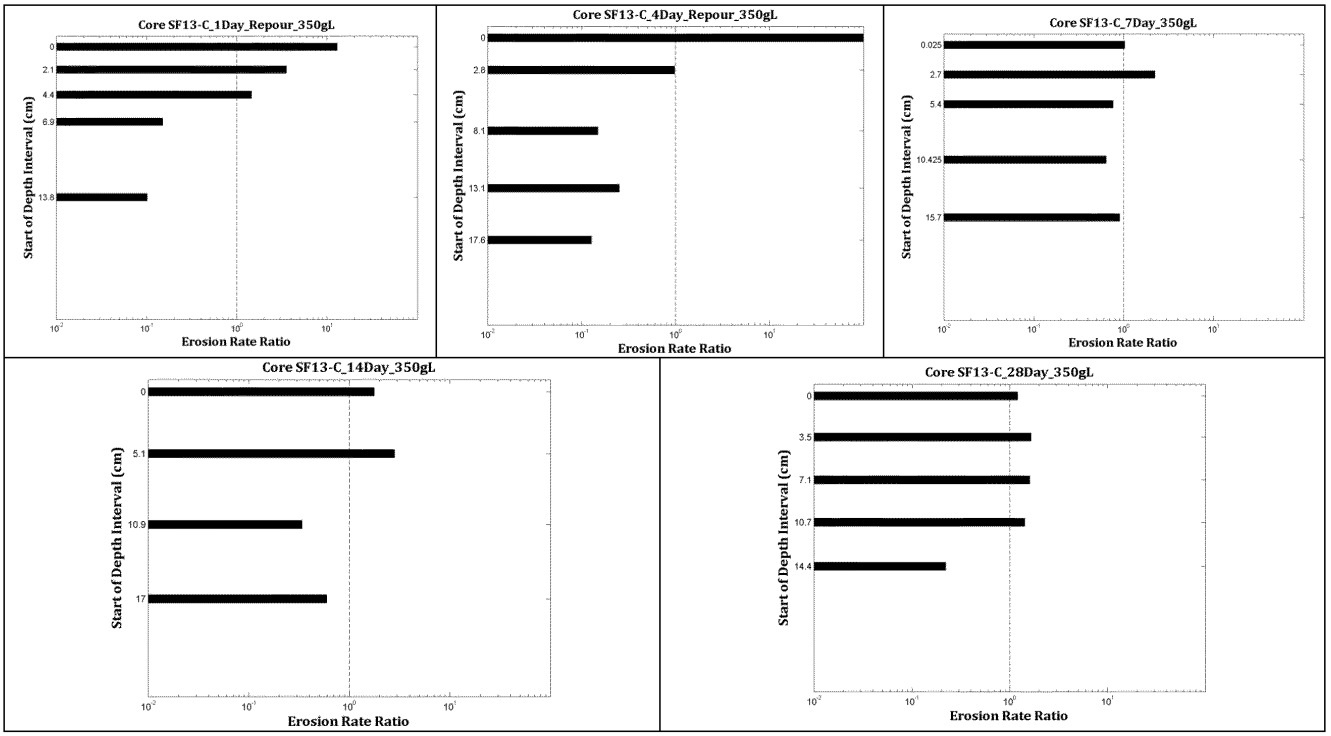

Figure 100. Intra-core erosion rate ratios for the SF13-C (350 g/L) consolidation core set.

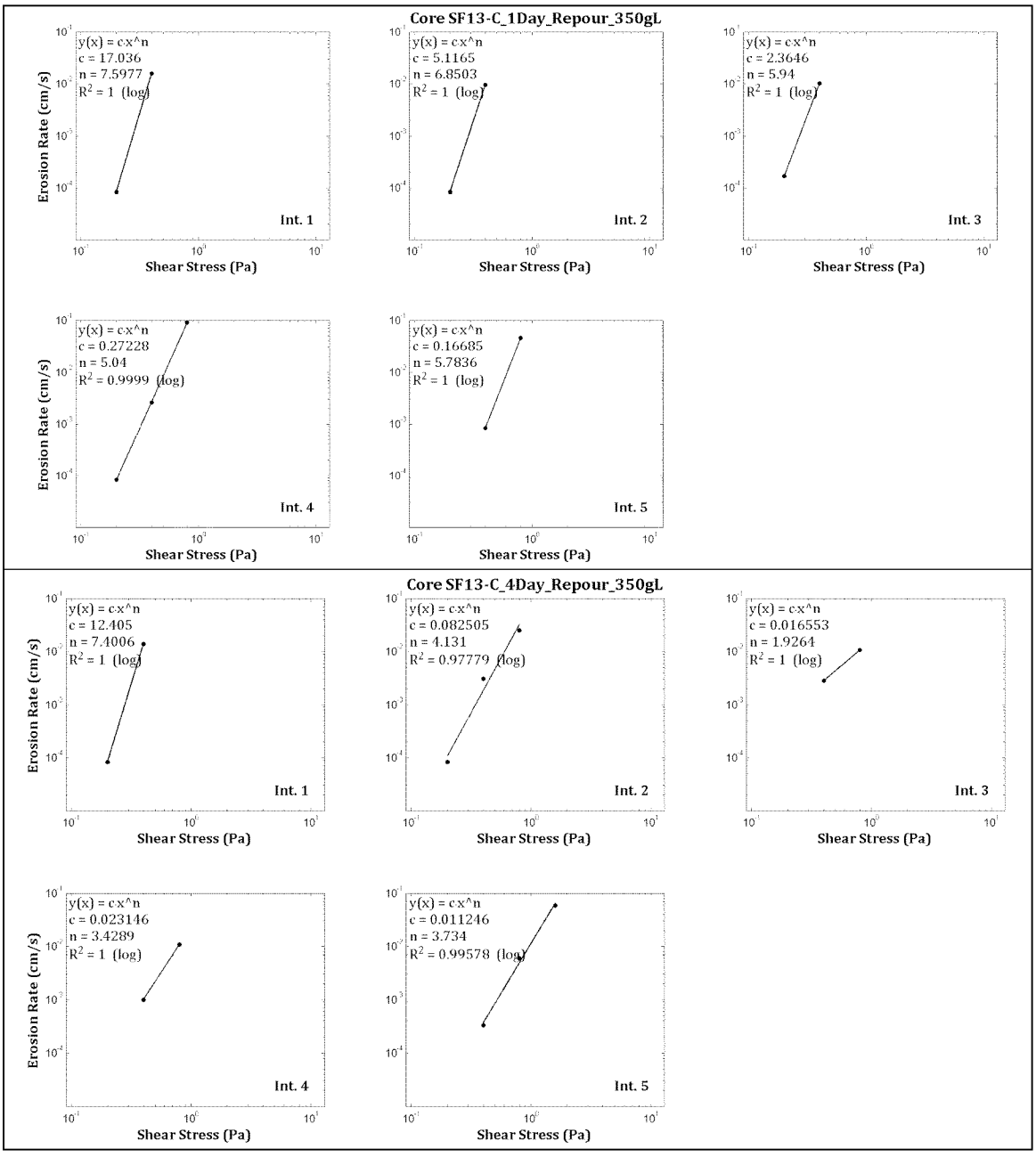

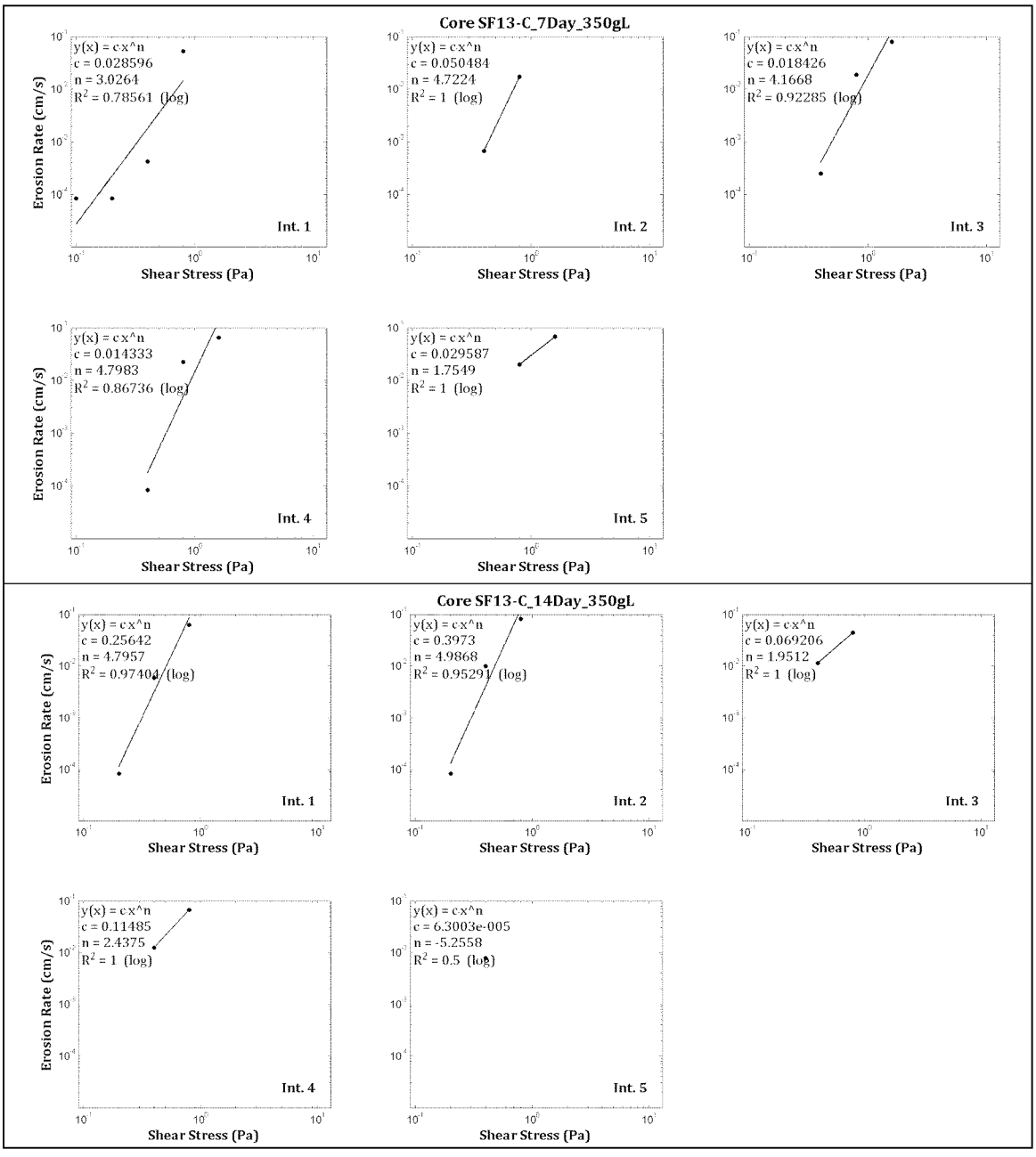

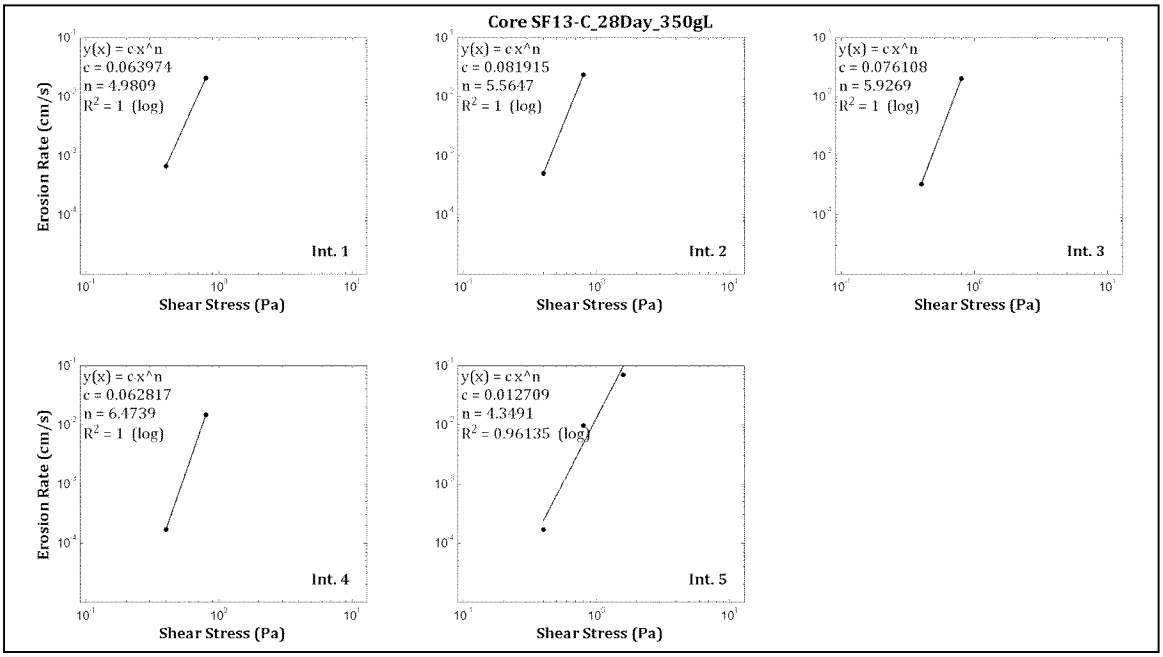

Figure 101. Power law best-fit regression solutions for the SF13-C (350 g/L) consolidation core set (sequential from top to bottom).

Table 95. Power law best-fit variables for specified depth intervals in the SF13-C 1D re-pour core.

Depth Interval	Interval Start Depth (cm)	Interval End Depth (cm)	A	n	r^2
1	0.00	2.10	17.036226	7.60	1.00
2	2.10	4.40	5.116540	6.85	1.00
3	4.40	6.70	2.364640	5.94	1.00
4	6.90	13.10	0.272278	5.04	1.00
5	13.80	19.90	0.166848	5.78	1.00

Table 96. Median grain size, wet bulk density, fraction LOI and critical shear stress for SF13-C 1D re-pour.

Sample Depth (cm)	Grain Size (μm)	Wet Bulk Density (g/cm³)	Fraction LOI	τ_0 (Pa)	τ_1 (Pa)	τ_{linear} (Pa)	τ_{power} (Pa)
0.00	9.72	1.20	0.08	0.10	0.20	0.20	0.20
2.10	10.25	1.21	0.08	0.10	0.20	0.20	0.21
4.40	9.39	1.20	0.08	0.10	0.20	0.16	0.18
6.90	9.57	1.20	0.08	0.10	0.20	0.20	0.21
13.80	8.90	1.22	0.08	0.20	0.40	0.23	0.28
19.90	8.73	1.21	0.08	*n/a*	*n/a*	*n/a*	*n/a**
Mean	**9.43**	**1.21**	**0.08**	**0.12**	**0.24**	**0.20**	**0.22**

*No erosion rate measurements made at this sample depth; therefore, no critical shear stress determinations are listed.

Table 97. Power law best-fit variables for specified depth intervals in the SF13-C 4D re-pour core.

Depth Interval	Interval Start Depth (cm)	Interval End Depth (cm)	A	n	r^2
1	0.00	2.50	12.405275	7.40	1.00
2	2.80	8.00	0.082505	4.13	0.98
3	8.10	11.90	0.016553	1.93	1.00
4	13.10	16.50	0.023146	3.43	1.00
5	17.60	23.30	0.011246	3.73	1.00

Table 98. Median grain size, wet bulk density, fraction LOI and critical shear stress for SF13-C 4D re-pour.

Sample Depth (cm)	Grain Size (μm)	Wet Bulk Density (g/cm^3)	Fraction LOI	τ_0 (Pa)	τ_1 (Pa)	τ_{linear} (Pa)	τ_{power} (Pa)
0.00	6.61	1.20	0.07	0.10	0.20	0.20	0.20
2.80	10.30	1.21	0.07	0.10	0.20	0.20	0.20
8.10	9.44	1.21	0.08	0.20	0.40	0.21	0.07
13.10	9.20	1.21	0.08	0.20	0.40	0.23	0.20
17.60	8.27	1.22	0.06	0.20	0.40	0.26	0.28
23.30	8.48	1.22	0.08	*n/a*	*n/a*	*n/a*	*n/a**
Mean	**8.72**	**1.21**	**0.08**	**0.16**	**0.32**	**0.22**	**0.19**

*No erosion rate measurements made at this sample depth; therefore, no critical shear stress determinations are listed.

Table 99. Power law best-fit variables for specified depth intervals in the SF3-C 7D core.

Depth Interval	Interval Start Depth (cm)	Interval End Depth (cm)	A	n	r^2
1	0.00	2.10	0.028596	3.03	0.79
2	2.70	5.30	0.050484	4.72	1.00
3	5.40	9.90	0.018426	4.17	0.92
4	10.40	14.70	0.014333	4.80	0.87
5	15.70	20.00	0.029587	1.75	1.00

Table 100. Median grain size, wet bulk density, fraction LOI and critical shear stress for SF3-C 7D.

Sample Depth (cm)	Grain Size (μm)	Wet Bulk Density (g/cm³)	Fraction LOI	τ_0 (Pa)	τ_1 (Pa)	τ_{linear} (Pa)	τ_{power} (Pa)
0.00	10.33	1.21	0.07	0.05	0.10	0.10	0.15
2.70	10.49	1.22	0.07	0.20	0.40	0.23	0.27
5.40	7.09	1.23	0.07	0.20	0.40	0.28	0.29
10.40	8.51	1.22	0.06	0.20	0.40	0.40	0.36
15.70	10.65	1.22	0.06	0.40	0.80	0.41	0.04
20.00	10.77	1.23	0.07	*n/a*	*n/a*	*n/a*	*n/a**
Mean	**9.64**	**1.22**	**0.07**	**0.21**	**0.42**	**0.28**	**0.22**

*No erosion rate measurements made at this sample depth; therefore, no critical shear stress determinations are listed.

Table 101. Power law best-fit variables for specified depth intervals in the SF13-C 14D core.

Depth Interval	Interval Start Depth (cm)	Interval End Depth (cm)	A	n	r^2
1	0.00	4.80	0.256419	4.80	0.97
2	5.10	10.20	0.397298	4.99	0.95
3	10.90	16.10	0.069206	1.95	1.00
4	17.00	22.40	0.114850	2.44	1.00
5	22.70	23.40	*n/a**	*n/a*	0.50

*Insufficient number of erosion rates to calculate via power law regression.

Table 102. Median grain size, wet bulk density, fraction LOI and critical shear stress for the SF13-C 14D.

Sample Depth (cm)	Grain Size (μm)	Wet Bulk Density (g/cm³)	Fraction LOI	τ_0 (Pa)	τ_1 (Pa)	τ_{linear} (Pa)	τ_{power} (Pa)
0.00	9.26	1.22	0.09	0.10	0.20	0.20	0.19
5.10	6.55	1.23	0.08	0.10	0.20	0.20	0.19
10.90	8.42	1.24	0.09	0.20	0.40	0.21	0.04
17.00	9.20	1.25	0.09	0.20	0.40	0.21	0.06
22.70	8.93	1.30	0.08	0.20	0.40	0.21	*n/a**
23.40	6.42	1.30	0.08	*n/a*	*n/a*	*n/a*	*n/a***
Mean	**8.13**	**1.26**	**0.08**	**0.16**	**0.32**	**0.21**	**0.12**

*Insufficient number of erosion rates to calculate via power law regression.
**No erosion rate measurements made at this sample depth; therefore, no critical shear stress determinations are listed.

Table 103. Power law best-fit variables for specified depth intervals in the SF13-C 28D core.

Depth Interval	Interval Start Depth (cm)	Interval End Depth (cm)	A	n	r^2
1	0.00	3.20	0.063974	4.98	1.00
2	3.50	6.90	0.081915	5.56	1.00
3	7.10	10.20	0.076108	5.93	1.00
4	10.70	14.00	0.062817	6.47	1.00
5	14.40	22.00	0.012709	4.35	0.96

Table 104. Median grain size, wet bulk density, fraction LOI and critical shear stress for SF13-C 28D.

Sample Depth (cm)	Grain Size (μm)	Wet Bulk Density (g/cm^3)	Fraction LOI	τ_0 (Pa)	τ_1 (Pa)	τ_{linear} (Pa)	τ_{power} (Pa)
0.00	8.92	1.20	0.07	0.20	0.40	0.23	0.27
3.50	10.01	1.25	0.07	0.20	0.40	0.24	0.30
7.10	13.41	1.26	0.08	0.20	0.40	0.26	0.33
10.70	7.67	1.26	0.08	0.20	0.40	0.32	0.37
14.40	6.48	1.27	0.07	0.20	0.40	0.32	0.33
22.00	7.50	1.29	0.08	*n/a*	*n/a*	*n/a*	*n/a**
Mean	**9.00**	**1.25**	**0.08**	**0.20**	**0.40**	**0.27**	**0.32**

**No erosion rate measurements made at this sample depth; therefore, no critical shear stress determinations are listed.

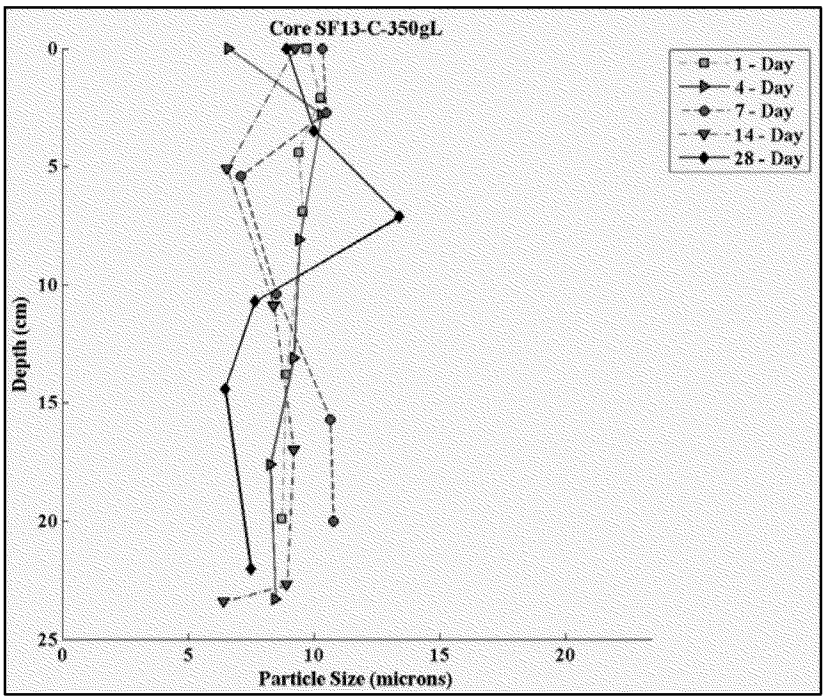

Figure 102. Down-core median grain size for each SF13-C (350 g/L) consolidation core.

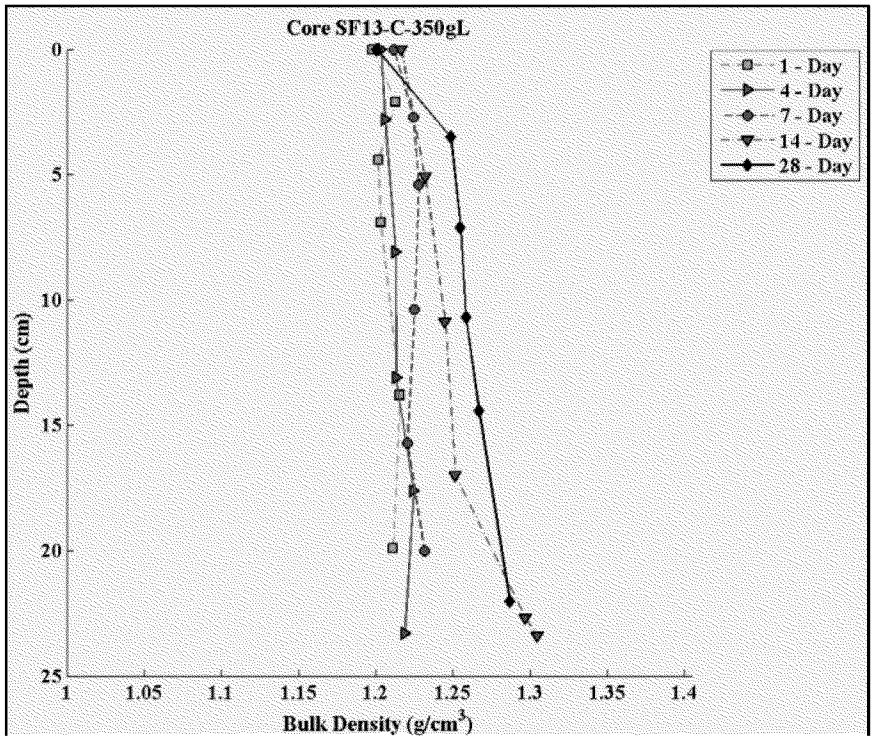

Figure 103. Down-core wet bulk density for each SF13-C (350 g/L) consolidation core.

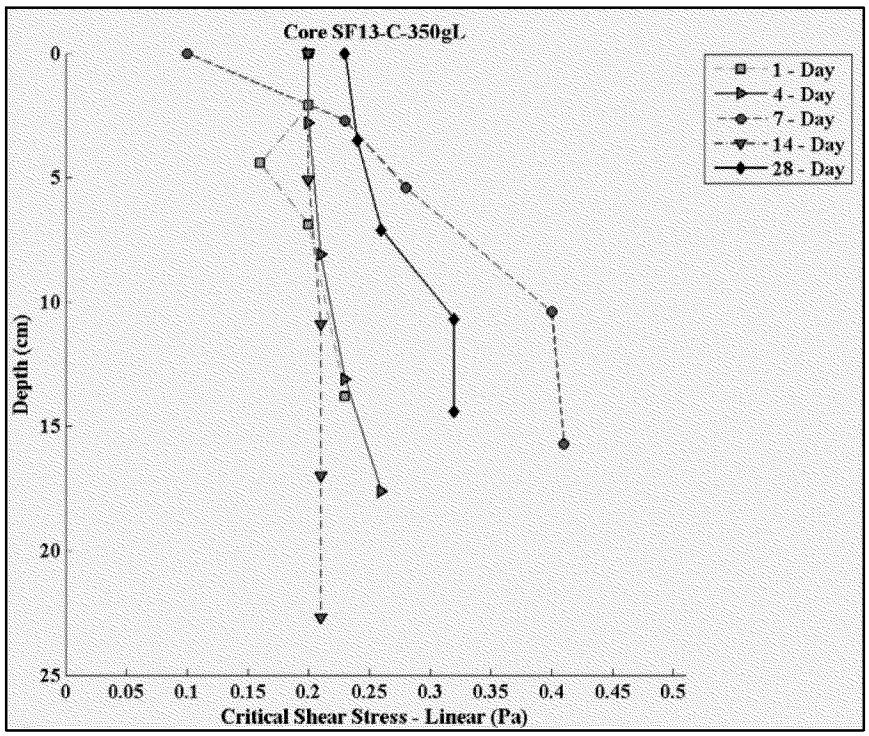

Figure 104. Down core linearly interpolated critical shear stresses for each SF13-C (350 g/L) consolidation core.

3.4.5 SF8-C Consolidation Cores

The sediment used to construct the SF8-C consolidation cores was collected from the navigation channel east of the CDF. The material comprised mostly silt with some fine sand. Three target initial concentrations of slurry were prepared with the SF8-C sediments in order to investigate the effects of initial slurry concentration on erosion rates:

1) SF8-C(1) - 125 g/L
2) SF8-C(2) - 100 g/L
3) SF8-C(3) - 350 g/L

The results of each are described in the following sections.

3.4.6 SF8-C(1) Consolidation Cores (125 g/L target concentration)

Individual Consolidation Core Results

In general, the SF8-C(1) core descriptions on their respective day of processing were:

- 1 Day: Very low-density, fluidic sediment that became slightly denser with depth. The core comprised mostly of fluid-like silt throughout. The initial poured core leaked around the piston like water, as did two additional attempts (re-pours), which required a third re-poured core in order to process successfully.
- 4 Day: Very low-density, fluidic sediment that became slightly denser with depth. The core comprised mostly of fluid-like silt throughout. The initial poured core also leaked around the piston, requiring an additional core (re-pour) to be prepared in order to process successfully.
- 7 Day: Very low-density, fluidic sediment surface that persisted through the core, becoming slightly denser with depth. Material comprised silt throughout.
- 14 Day: Low-density, gelatinous surface with an increase in density with depth.
- 28 Day: Low-density surface that became denser with depth.

Photographs of the SF8-C(1) cores are presented in Figure 105. The erosion rate data for the cores are plotted in Figure 106. Shear stresses ranging between 0.1 to 1.6 Pa were applied to these cores. Erosion rates in all cores generally decreased with depth or remained relatively constant. Near the bottom of the 14-day core, for reasons uncertain at the moment, the erosion rates increased slightly.

The intra-core erosion rate ratios of the depth intervals evaluated in each core are shown in Figure 107. Erosion susceptibility was variable with depth for all cores; though the near-bottom depth intervals in the 7-, 14- and 28-day cores indicated less susceptibility to erosion than the near-surface intervals.

The power law regression fit within each depth interval for the SF8-C(1) consolidation core sets is illustrated in Figure 108. Coefficients and regression statistics from the power law fit analysis, the measured median grain sizes, the computed wet bulk densities and the critical shear stresses for each depth interval, from each core, are presented in Table 105 to Table 114.

Consolidation Core Set Summary

The temporal variation in down-core sediment properties and computed parameters is illustrated in Figure 109 through Figure 111. Figure 109 contains the down-core median grain sizes measured; Figure 110 contains the down-core wet bulk densities computed; and Figure 111 represents the down-core linearly interpolated critical shear stresses.

The down-core structure of the median grain size did not indicate much variability over the consolidation duration, aside from larger grain sizes that were measured at the deepest depth intervals of the 14- and 28-day cores. Median particle sizes remained in the very fine to fine silt range (6.61 µm to 12.05 µm), and increased to coarse silt for the 14- and 28-day cores (49.29 µm and 34.71 µm) at the deepest depth.

The down-core wet bulk density profiles illustrate a trend of increasing density both with consolidation duration and depth, punctuated by a large increase in the deepest samples from the 14- and 28-day cores. Surface bulk densities ranged between 1.11 g/cm^3 and 1.14 g/cm^3 for all cores; and the bulk densities at the deepest depth in each core ranged from 1.24 g/cm^3 to 1.66 g/cm^3.

The linearly interpolated critical shear stresses showed a general increase with depth and consolidation duration. The core-average linearly interpolated critical shear stresses increased from 0.14 Pa after 1 day to 0.38 Pa after 28 days.

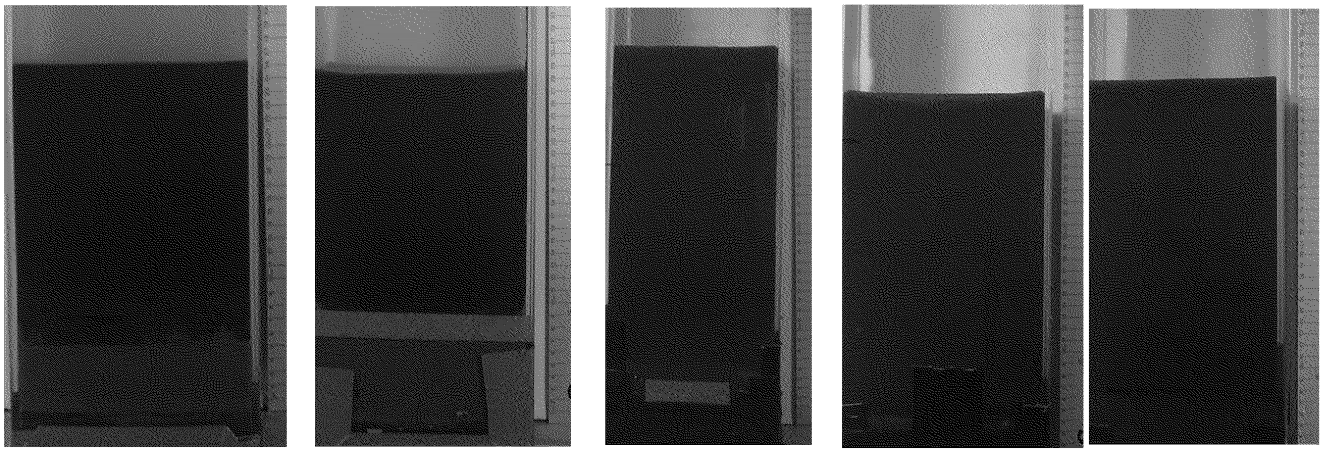

Figure 105. Pre-processing photos for the SF8-C(1) (125 g/L) consolidation core set.

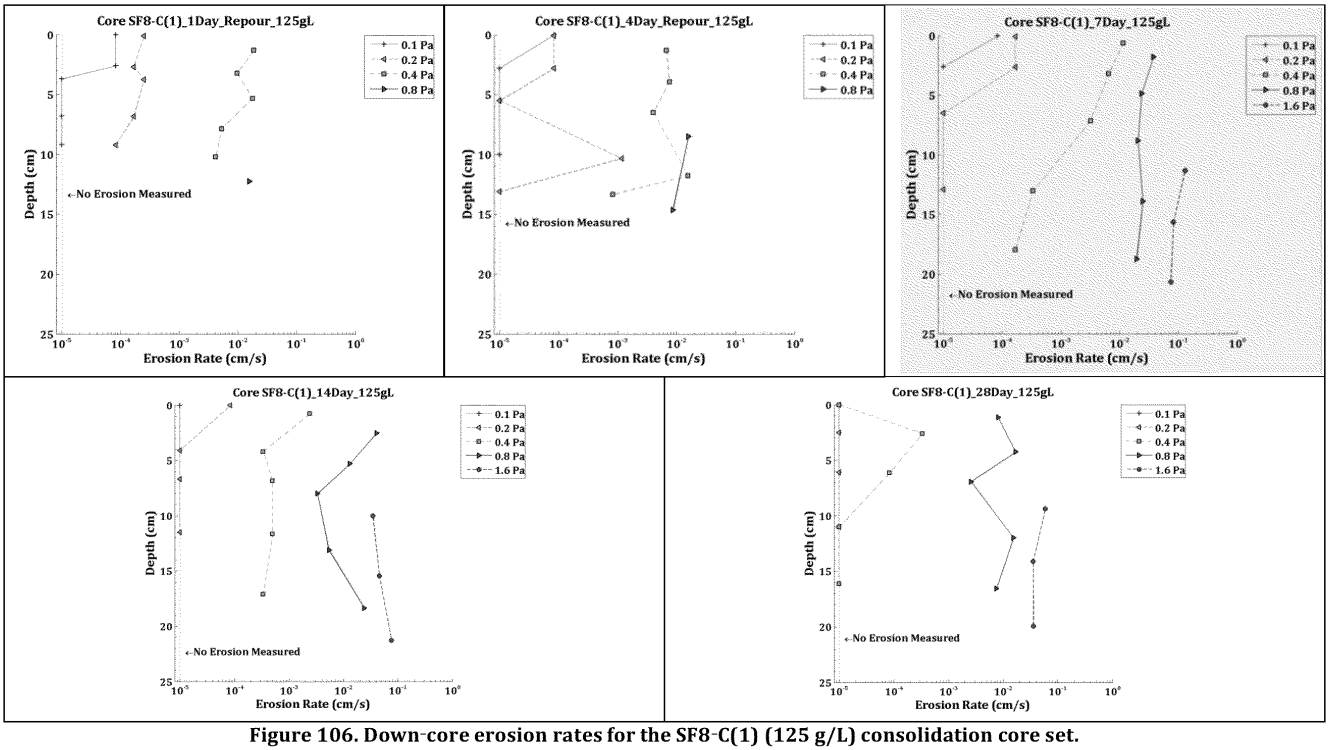

Figure 106. Down-core erosion rates for the SF8-C(1) (125 g/L) consolidation core set.

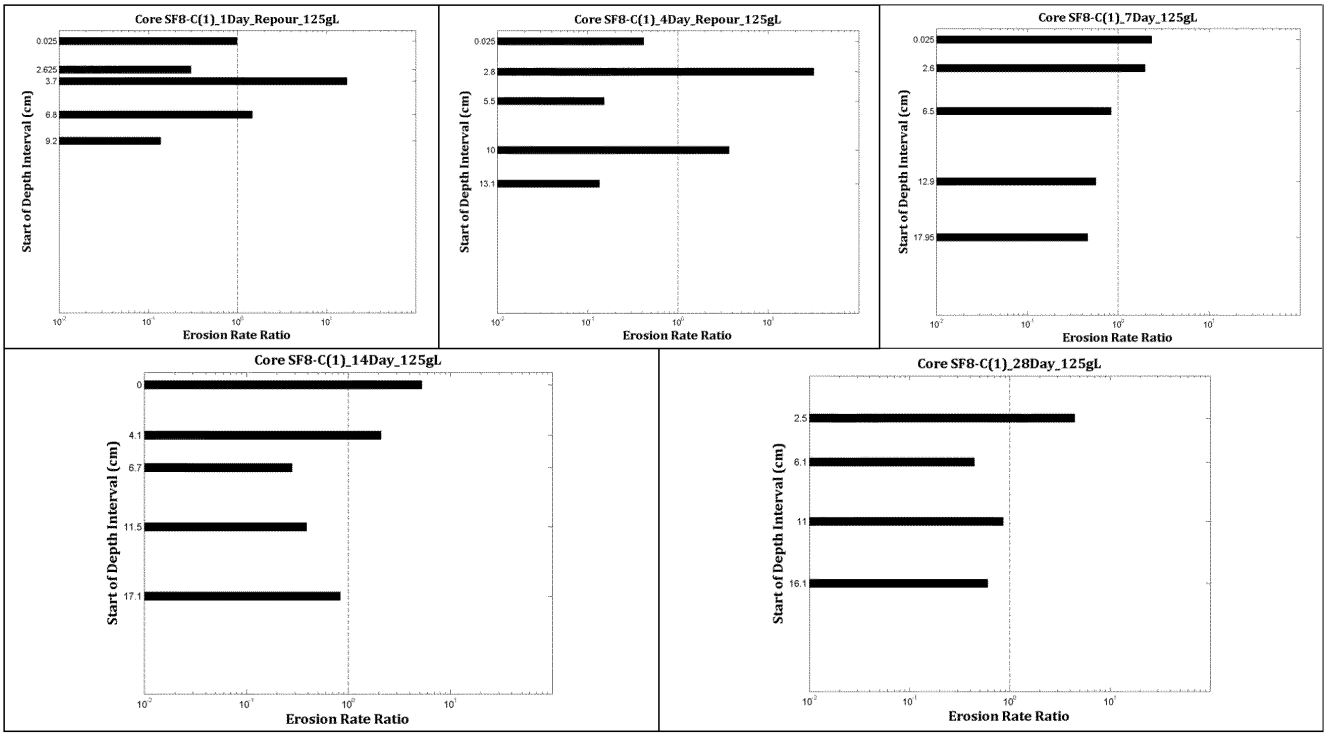

Figure 107. Intra-core erosion rate ratios for the SF8-C(1) (125 g/L) consolidation core set.

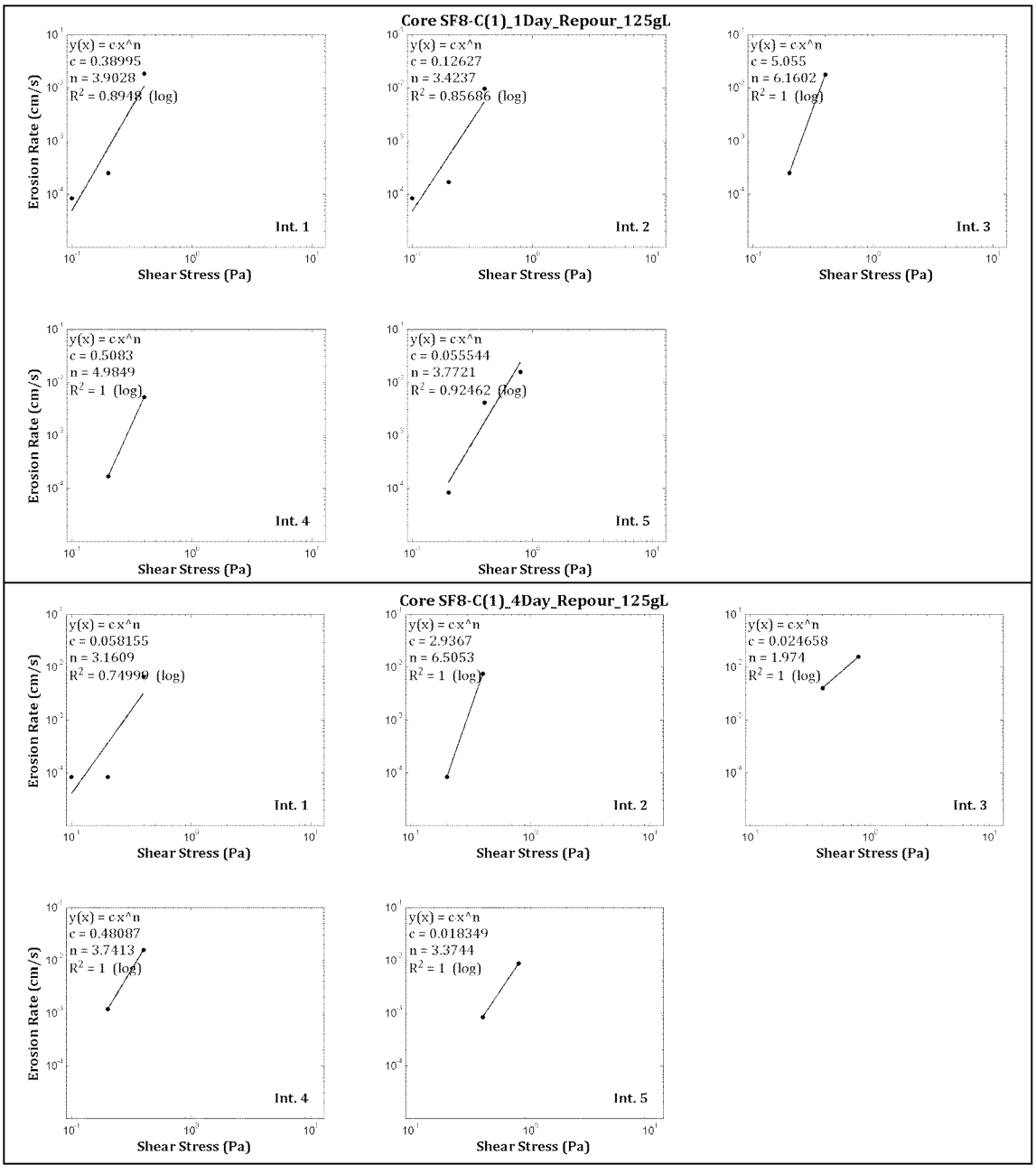

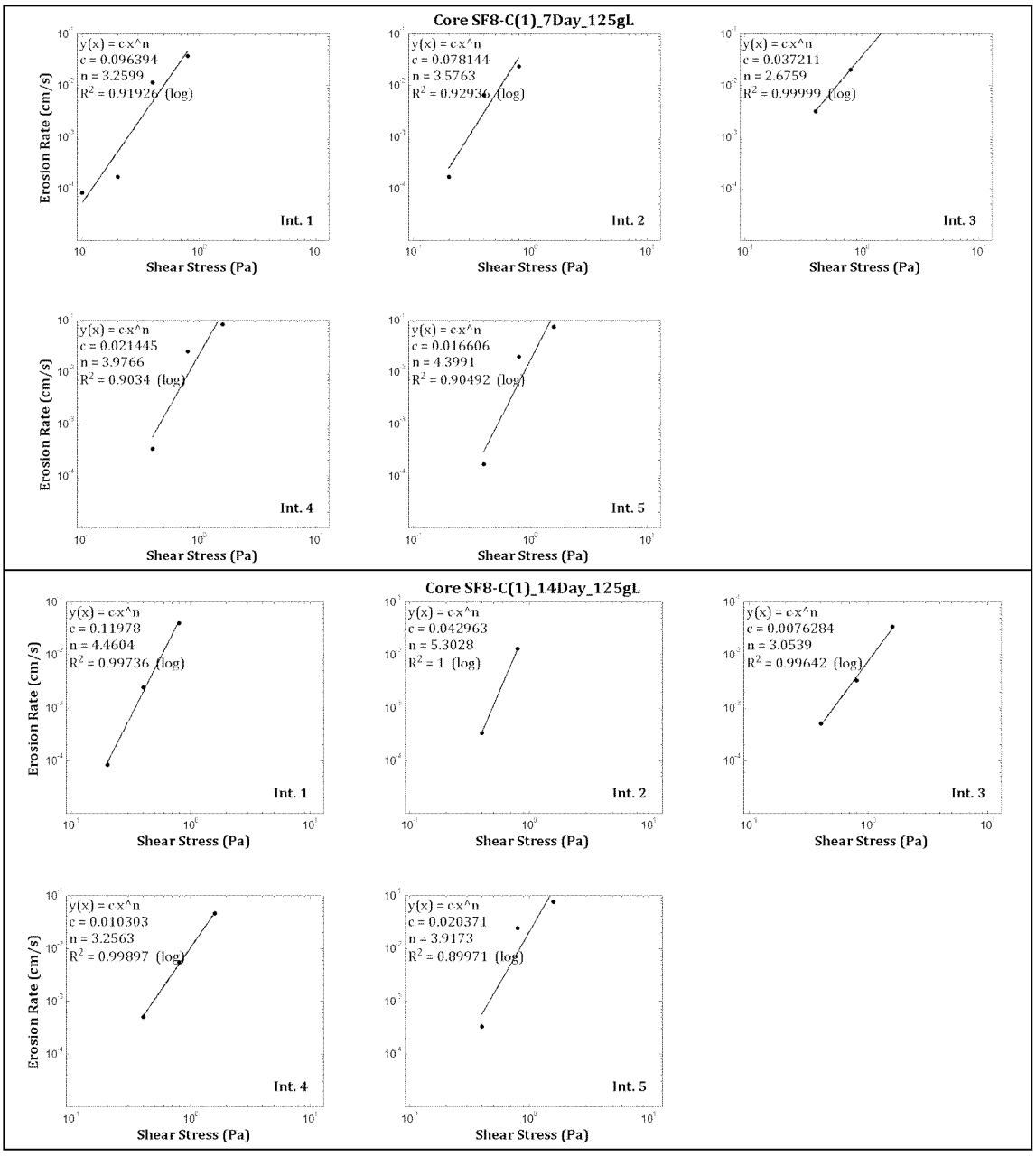

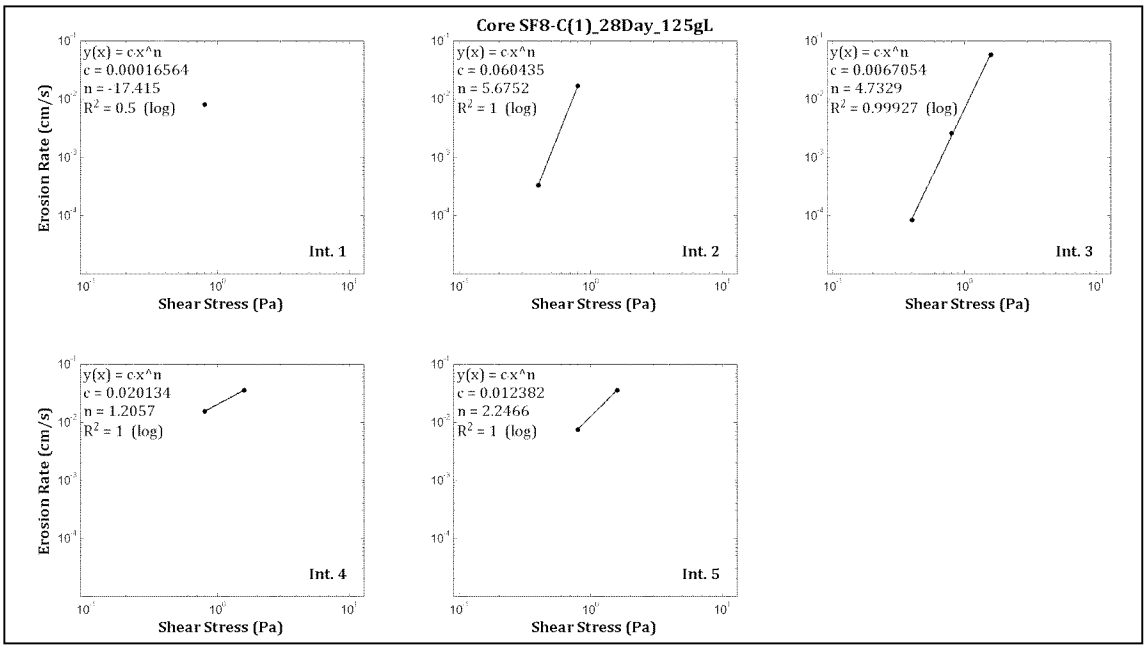

Figure 108. Power law best-fit regression solutions for the SF8-C(1) (125 g/L) consolidation core set (sequential from top to bottom).

Table 105. Power law best-fit variables for specified depth intervals in the SF8-C(1) 1D re-pour core.

Depth Interval	Interval Start Depth (cm)	Interval End Depth (cm)	A	n	r^2
1	0.00	2.40	0.389949	3.90	0.89
2	2.60	3.70	0.126274	3.42	0.86
3	3.70	6.80	5.054991	6.16	1.00
4	6.80	8.80	0.508303	4.98	1.00
5	9.20	13.30	0.055544	3.77	0.92

Table 106. Median grain size, wet bulk density, fraction LOI and critical shear stress for SF8-C(1) 1D re-pour.

Sample Depth (cm)	Grain Size (μm)	Wet Bulk Density (g/cm^3)	Fraction LOI	τ_0 (Pa)	τ_1 (Pa)	τ_{linear} (Pa)	τ_{power} (Pa)
0.00	8.93	1.11	0.09	0.05	0.10	0.10	0.12
2.60	6.73	1.15	0.09	0.05	0.10	0.10	0.12
3.70	7.66	1.15	0.08	0.10	0.20	0.14	0.17
6.80	10.46	1.16	0.08	0.10	0.20	0.16	0.18
9.20	8.51	1.19	0.08	0.10	0.20	0.20	0.19
13.30	11.09	1.30	0.06	*n/a*	*n/a*	*n/a*	*n/a**
Mean	**8.90**	**1.18**	**0.08**	**0.08**	**0.16**	**0.14**	**0.16**

*No erosion rate measurements made at this sample depth; therefore, no critical shear stress determinations are listed.

Table 107. Power law best-fit variables for specified depth intervals in the SF8-C(1) 4D re-pour core.

Depth Interval	Interval Start Depth (cm)	Interval End Depth (cm)	A	n	r^2
1	0.00	2.50	0.058155	3.16	0.75
2	2.80	5.00	2.936698	6.51	1.00
3	5.50	9.50	0.024658	1.97	1.00
4	10.00	12.90	0.480874	3.74	1.00
5	13.10	15.70	0.018349	3.37	1.00

Table 108. Median grain size, wet bulk density, fraction LOI and critical shear stress for SF8-C(1) 4D re-pour.

Sample Depth (cm)	Grain Size (μm)	Wet Bulk Density (g/cm³)	Fraction LOI	τ_0 (Pa)	τ_1 (Pa)	τ_{linear} (Pa)	τ_{power} (Pa)
0.00	8.61	1.11	0.10	0.05	0.10	0.10	0.13
2.80	9.30	1.18	0.09	0.10	0.20	0.20	0.21
5.50	8.74	1.19	0.08	0.20	0.40	0.21	0.06
10.00	9.82	1.20	0.09	0.10	0.20	0.11	0.10
13.10	8.02	1.21	0.09	0.20	0.40	0.23	0.21
15.70	7.66	1.24	0.08	*n/a*	*n/a*	*n/a*	*n/a**
Mean	**8.69**	**1.19**	**0.09**	**0.13**	**0.26**	**0.17**	**0.14**

*No erosion rate measurements made at this sample depth; therefore, no critical shear stress determinations are listed.

Table 109. Power law best-fit variables for specified depth intervals in the SF8-C(1) 7D core.

Depth Interval	Interval Start Depth (cm)	Interval End Depth (cm)	A	n	r^2
1	0.00	2.50	0.096394	3.26	0.92
2	2.60	6.00	0.078144	3.58	0.93
3	6.50	12.80	0.037211	2.68	1.00
4	12.90	16.60	0.021445	3.98	0.90
5	17.90	21.80	0.016606	4.40	0.90

Table 110. Median grain size, wet bulk density, fraction LOI and critical shear stress for SF8-C(1) 7D.

Sample Depth (cm)	Grain Size (μm)	Wet Bulk Density (g/cm³)	Fraction LOI	τ_0 (Pa)	τ_1 (Pa)	τ_{linear} (Pa)	τ_{power} (Pa)
0.00	7.08	1.14	0.09	0.05	0.10	0.10	0.12
2.60	8.17	1.17	0.08	0.10	0.20	0.16	0.16
6.50	8.68	1.17	0.08	0.20	0.40	0.21	0.11
12.90	7.90	1.21	0.08	0.20	0.40	0.26	0.26
17.90	9.86	1.24	0.07	0.20	0.40	0.30	0.31
21.80	12.05	1.32	0.07	*n/a*	*n/a*	*n/a*	*n/a**
Mean	**8.95**	**1.21**	**0.08**	**0.15**	**0.30**	**0.21**	**0.19**

*No erosion rate measurements made at this sample depth; therefore, no critical shear stress determinations are listed.

Table 111. Power law best-fit variables for specified depth intervals in the SF8-C(1) 14D core.

Depth Interval	Interval Start Depth (cm)	Interval End Depth (cm)	A	n	r^2
1	0.00	3.60	0.119782	4.46	1.00
2	4.10	6.30	0.042963	5.30	1.00
3	6.70	11.00	0.007628	3.05	1.00
4	11.50	16.50	0.010303	3.26	1.00
5	17.00	23.00	0.020371	3.92	0.90

Table 112. Median grain size, wet bulk density, fraction LOI and critical shear stress for SF8-C(1) 14D.

Sample Depth (cm)	Grain Size (μm)	Wet Bulk Density (g/cm³)	Fraction LOI	τ_0 (Pa)	τ_1 (Pa)	τ_{linear} (Pa)	τ_{power} (Pa)
0.00	6.61	1.13	0.09	0.10	0.20	0.20	0.20
4.10	7.93	1.21	0.08	0.20	0.40	0.26	0.32
6.70	8.16	1.23	0.08	0.20	0.40	0.24	0.24
11.50	8.32	1.25	0.08	0.20	0.40	0.24	0.24
17.00	10.69	1.30	0.09	0.20	0.40	0.26	0.26
23.00	49.29	1.66	0.03	*n/a*	*n/a*	*n/a*	*n/a**
Mean	**15.17**	**1.30**	**0.08**	**0.18**	**0.36**	**0.24**	**0.25**

*No erosion rate measurements made at this sample depth; therefore, no critical shear stress determinations are listed.

Table 113. Power law best-fit variables for specified depth intervals in the SF8-C(1) 28D core.

Depth Interval	Interval Start Depth (cm)	Interval End Depth (cm)	A	n	r^2
1	0.00	2.30	*n/a**	*n/a*	0.50
2	2.50	5.80	0.060435	5.68	1.00
3	6.10	11.00	0.006705	4.73	1.00
4	11.00	15.20	0.020134	1.21	1.00
5	16.10	21.00	0.012382	2.25	1.00

*Insufficient number of erosion rates to calculate via power law regression.

Table 114. Median grain size, wet bulk density, fraction LOI and critical shear stress for core SF8-C(1) 28D.

Sample Depth (cm)	Grain Size (µm)	Wet Bulk Density (g/cm³)	Fraction LOI	τ_0 (Pa)	τ_1 (Pa)	τ_{linear} (Pa)	τ_{power} (Pa)
0.00	6.91	1.13	0.09	0.40	0.80	0.41	*n/a**
2.50	7.89	1.20	0.09	0.20	0.40	0.26	0.32
6.10	7.51	1.23	0.09	0.20	0.40	0.40	0.41
11.00	8.64	1.26	0.08	0.40	0.80	0.41	0.01
16.10	8.32	1.28	0.08	0.40	0.80	0.41	0.12
21.00	34.71	1.59	0.04	*n/a*	*n/a*	*n/a*	*n/a***
Mean	**12.33**	**1.28**	**0.08**	**0.32**	**0.64**	**0.38**	**0.22**

*Insufficient number of erosion rates to calculate via power law regression.
*No erosion rate measurements made at this sample depth; therefore, no critical shear stress determinations are listed.

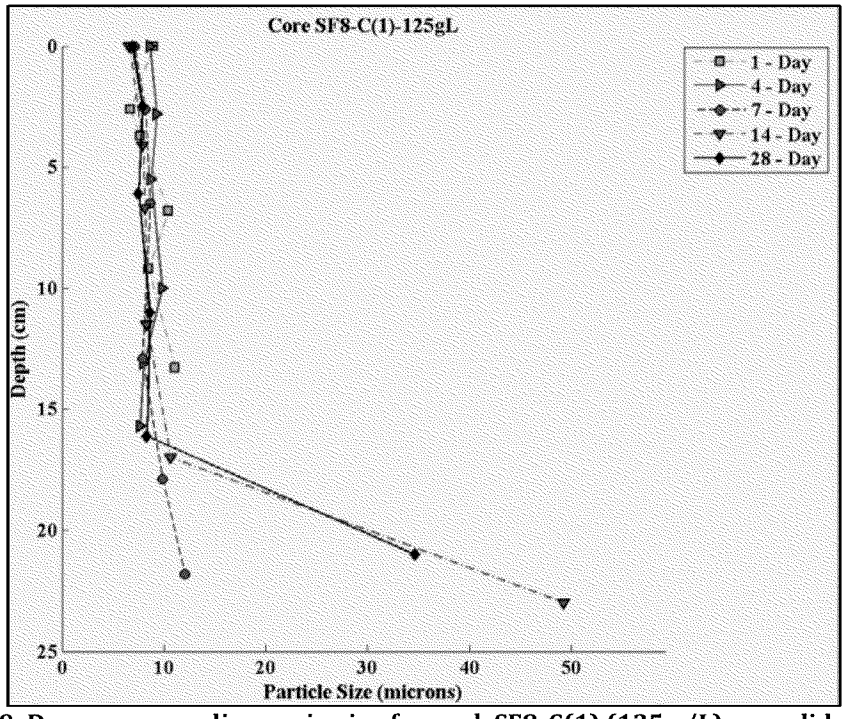

Figure 109. Down-core median grain size for each SF8-C(1) (125 g/L) consolidation core.

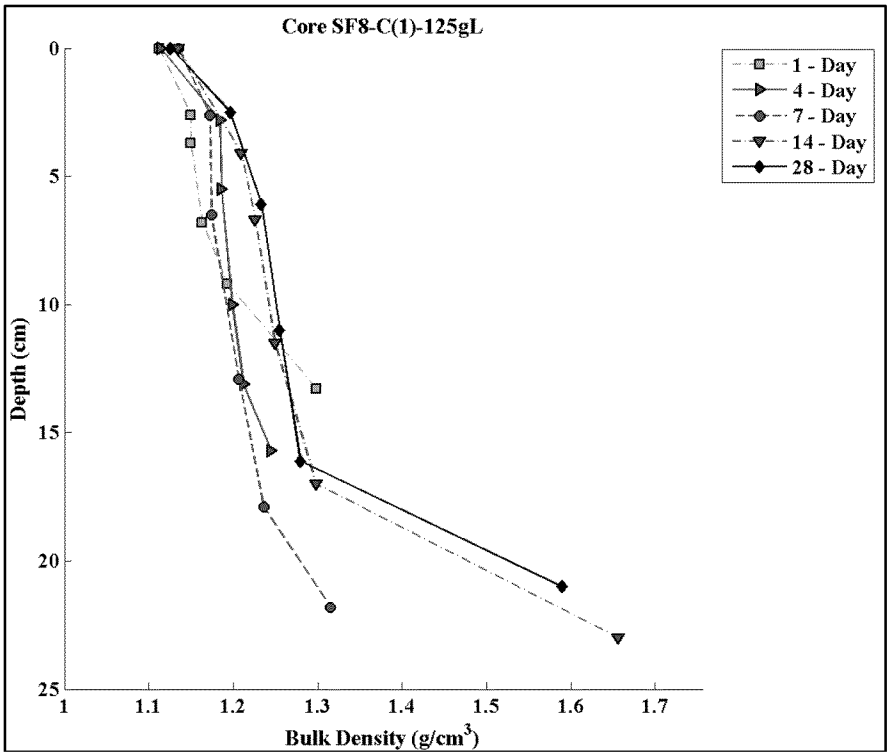

Figure 110. Down-core wet bulk density for each SF8-C(1) (125 g/L) consolidation core.

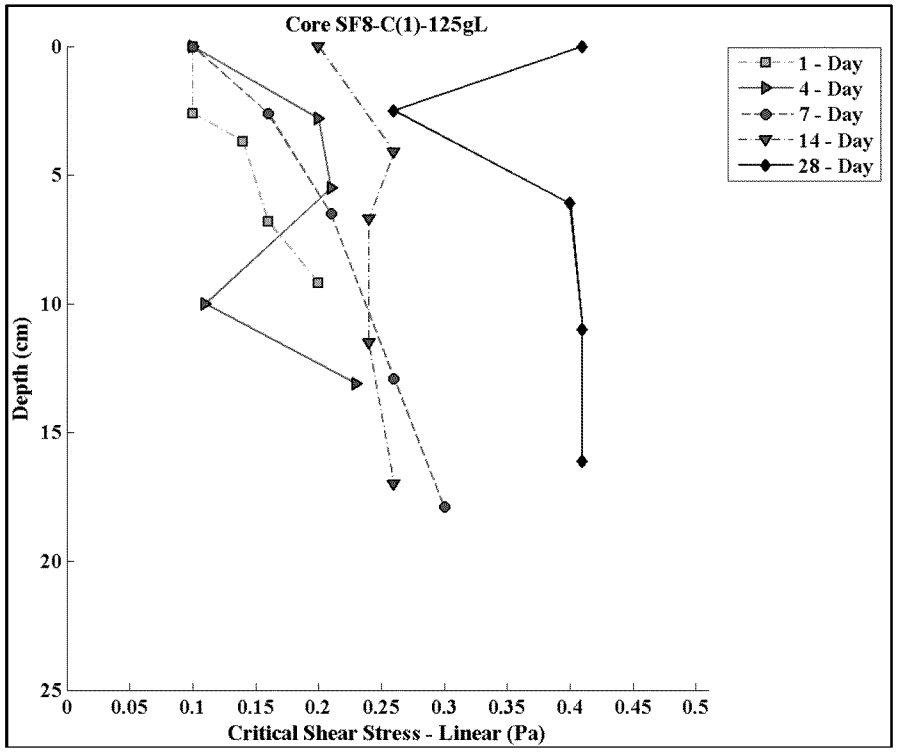

Figure 111. Down core linearly interpolated critical shear stresses for each SF8-C(1) (125 g/L) consolidation core.

3.4.7 SF8-C (2) CONSOLIDATION CORE (100 G/L TARGET CONCENTRATION)

Individual Consolidation Core Results
In general, the SF8-C(2) core descriptions on their respective day of processing were:

- 1 Day: Very low-density, fluidic surface that persisted throughout the core.
- 4 Day: Very low-density, fluidic surface sediment that became slightly denser with depth.
- 7 Day: Very low-density, fluidic surface that became slightly denser with depth.
- 14 Day: Low-density, gelatinous silt surface that became softer and stiffer with depth.
- 28 Day: Low-density, gelatinous silt surface that became softer and stiffer with depth.

Photographs of the SF8-C(2) cores are presented in Figure 112. The erosion rate data for the cores are plotted in Figure 113. Shear stresses ranging between 0.1 to 3.2 Pa were applied to these cores. Erosion rates in all cores generally decreased with depth. An increase in erosion rate was measured in the final depth interval in the 14-day core, but the reason is uncertain.

The intra-core erosion rate ratios of the depth intervals evaluated in each core are shown in Figure 114. Down-core erosion susceptibility was variable for the 1- and 4-day cores. For the 7-, 14- and 28-day cores, the erosion susceptibility generally decreased with depth.

The power law regression fit within each depth interval for the SF8-C(2) consolidation core sets is illustrated in Figure 115. Coefficients and regression statistics from the power law fit analysis, the measured median grain sizes, the computed wet bulk densities and the critical shear stresses for each depth interval, from each core, are presented in Table 115 to Table 124.

Consolidation Core Set Summary
The temporal variation in down-core sediment properties and computed parameters is illustrated in Figure 116 through Figure 118. Figure 116 contains the down-core median grain sizes measured; Figure 117 contains the down-core wet bulk densities computed; and Figure 118 represents the down-core linearly interpolated critical shear stresses.

The down-core structure of the median grain size did not indicate much variability over the consolidation duration aside from larger increases at the deepest depth intervals of the 14- and 28-day cores. Median particle sizes remained in the very fine to fine silt range (6.76 µm to 14.98 µm), and increased to medium to coarse silt (43.71 and 124.9 µm) for the 14- and 28-day cores at the deepest depth.

The down-core wet bulk density profiles illustrated a trend of increasing density both with consolidation duration and depth. Down-core bulk densities increased with depth, punctuated by a large increase in the final samples of the 14- and 28-day cores. Surface

Bulk density for all cores ranged between 1.08 g/cm³ and 1.14 g/cm³; and the bulk densities at the deepest depths of the cores ranged from 1.16 g/cm³ to 1.59 g/cm³.

Though there was some down-core and temporal variation in the linearly interpolated critical shear stresses, the general trend was increasing with depth and time. The core-average linearly inter polated critical shear stresses increased from 0.04 Pa after 1 day to 0.42 Pa after 28 days.

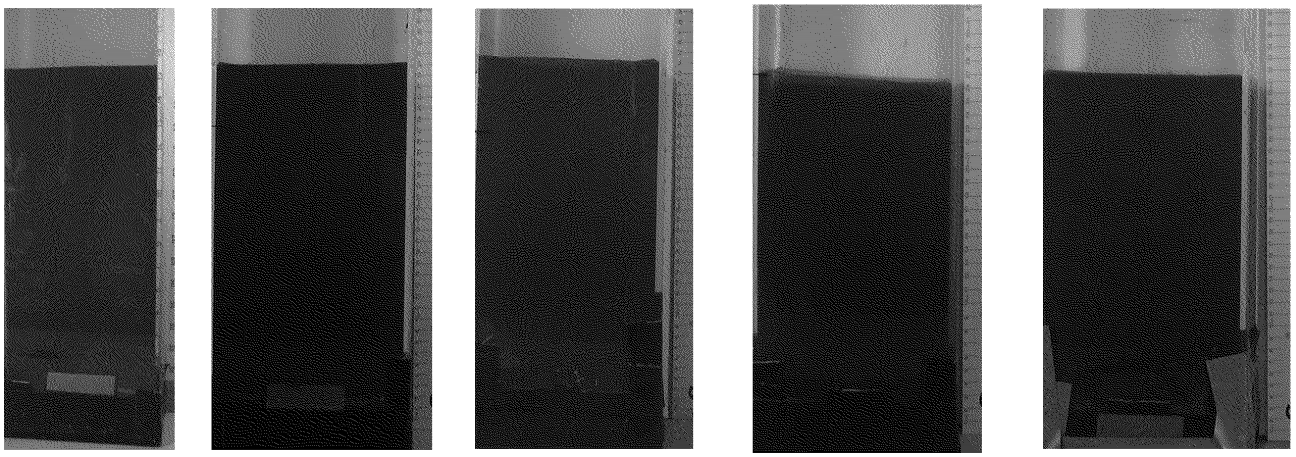

Figure 112. Pre-processing photos for the SF8-C(2) (100 g/L) consolidation core set.

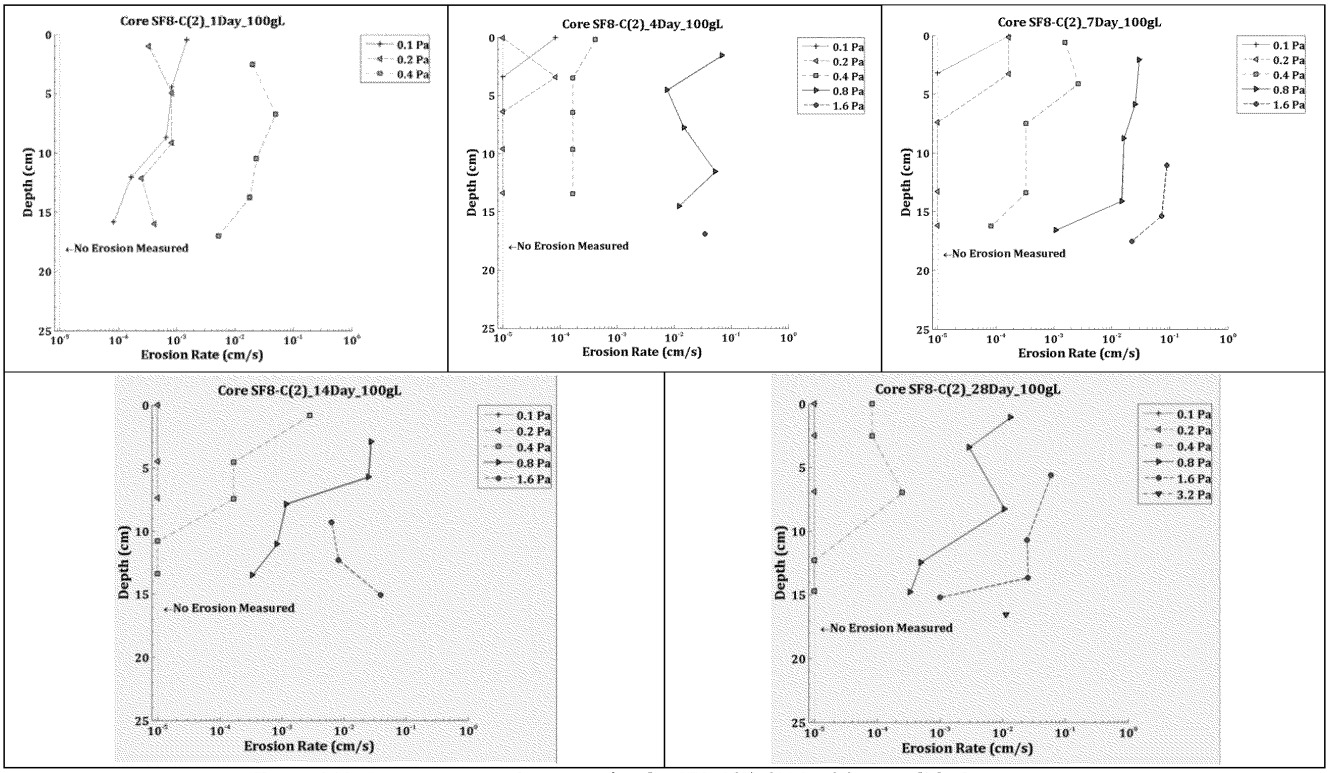

Figure 113. Down-core erosion rates for the SF8-C(2) (100 g/L) consolidation core set.

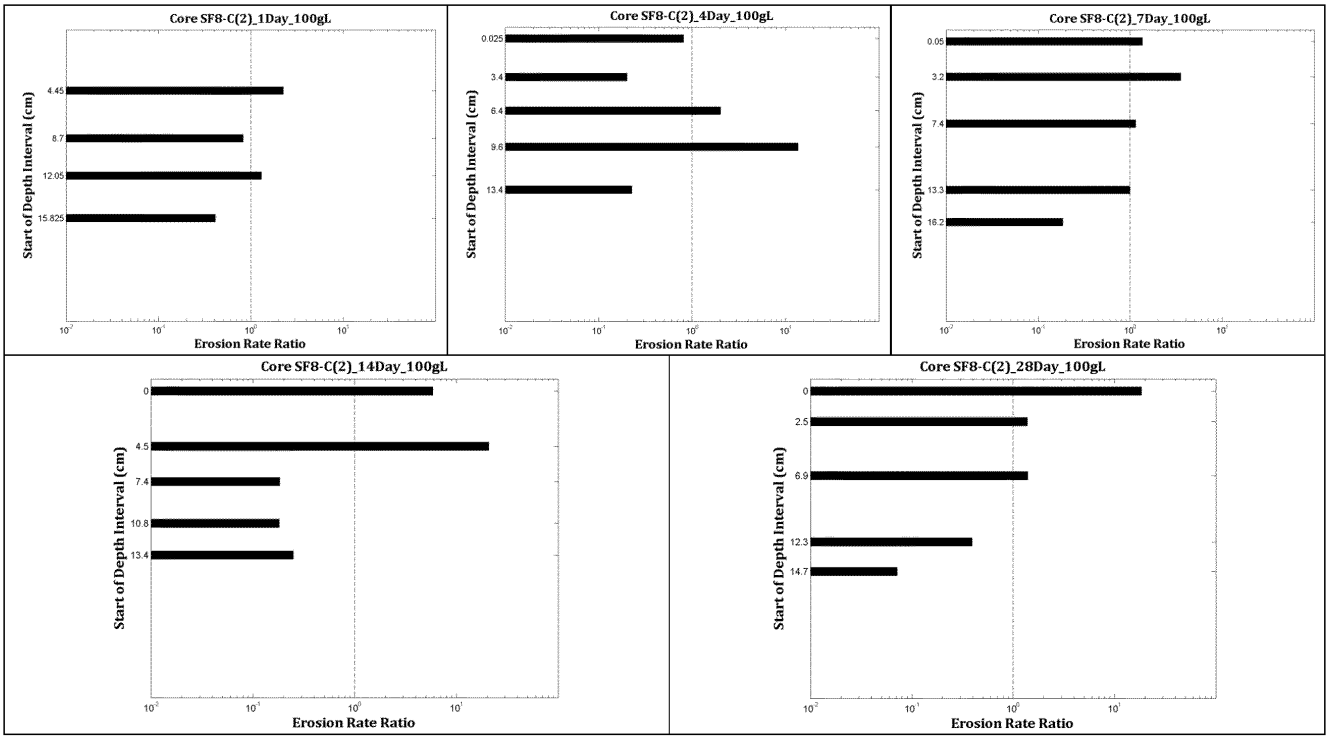

Figure 114. Intra-core erosion rate ratios for the SF8-C(2) (100 g/L) consolidation core set.

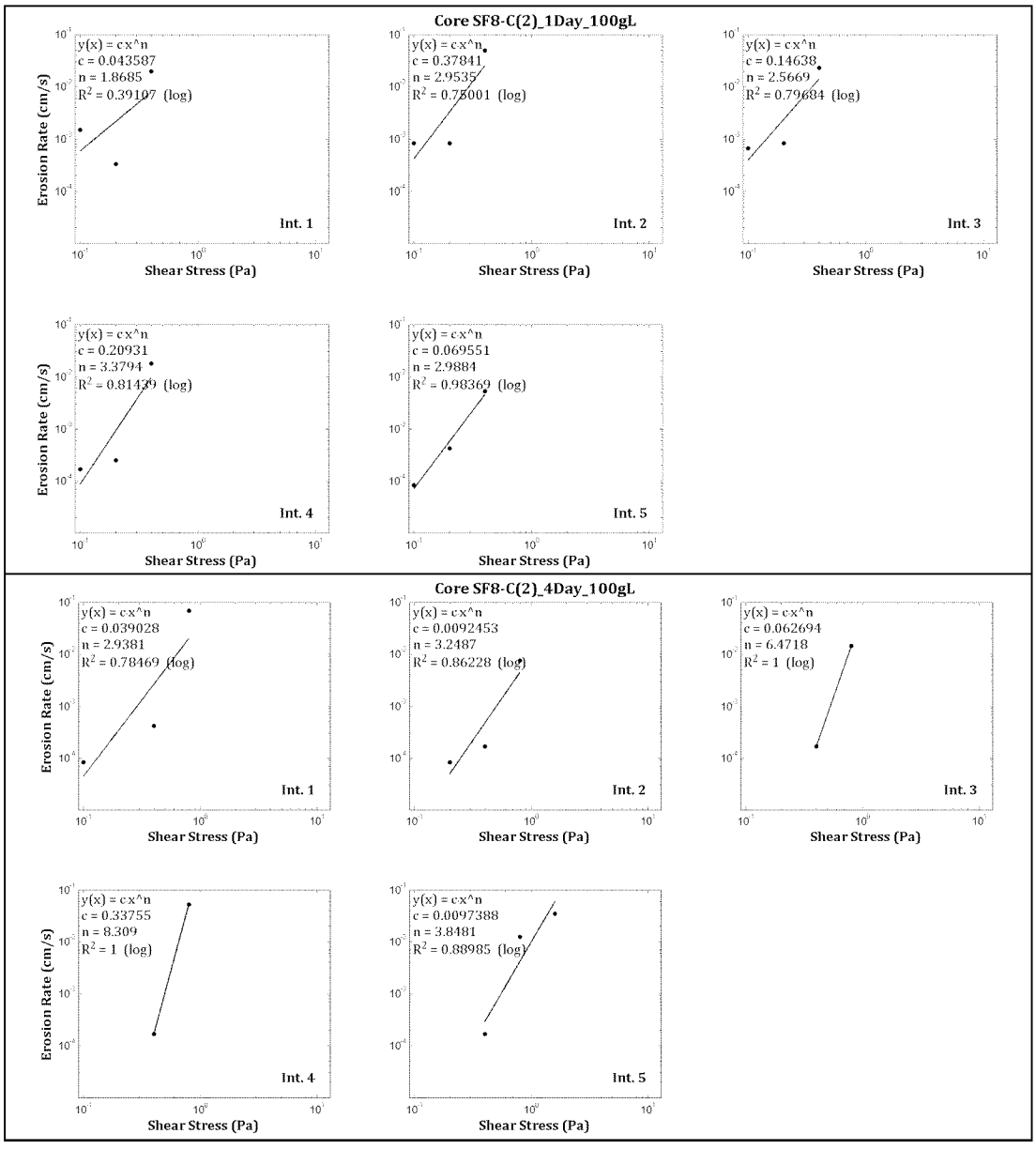

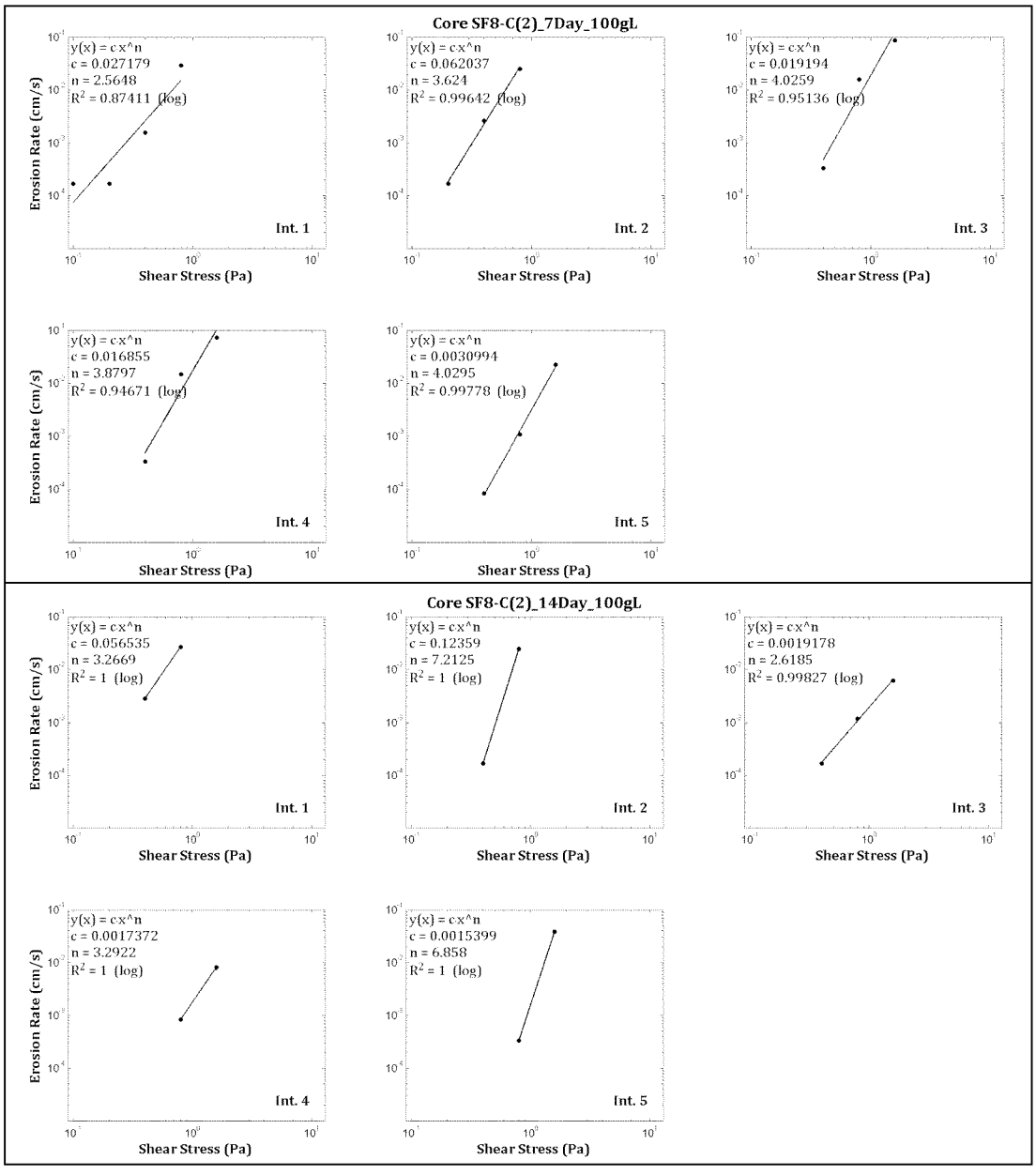

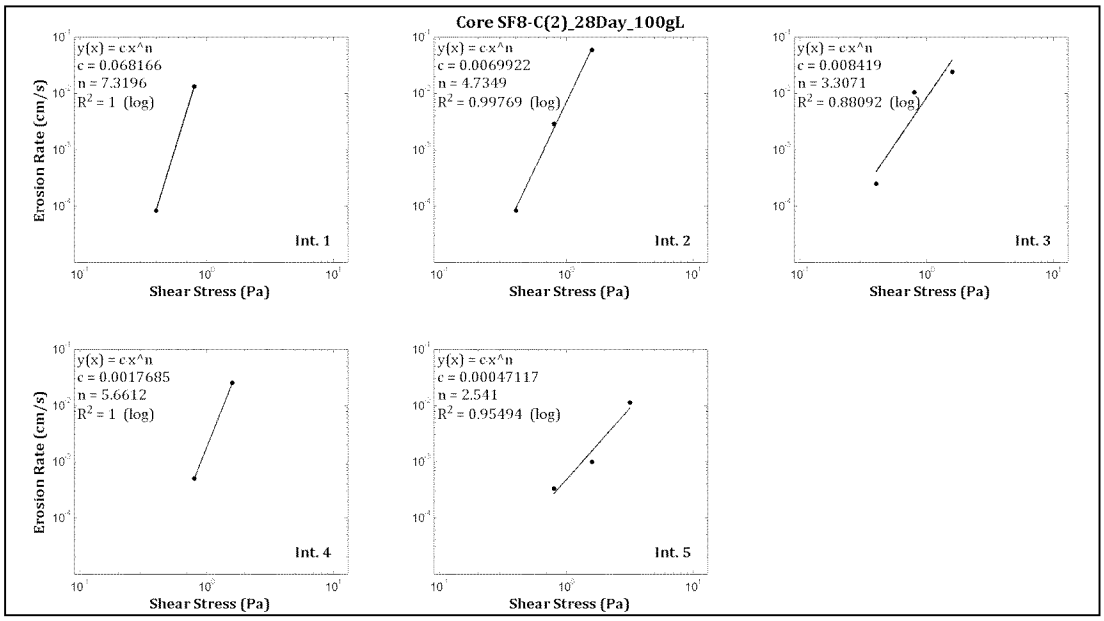

Figure 115. Power law best-fit regression solutions for the SF8-C(2) (100 g/L) consolidation core set (sequential from top to bottom).

Table 115. Power law best-fit variables for specified depth intervals in the SF8-C(2) 1D core.

Depth Interval	Interval Start Depth (cm)	Interval End Depth (cm)	A	n	r^2
1	0.00	4.00	*n/a**	*n/a*	0.39
2	4.20	8.30	0.378409	2.95	0.75
3	8.50	11.60	0.146381	2.57	0.80
4	12.00	15.30	0.209314	3.38	0.81
5	15.80	17.90	0.069551	2.99	0.98

***Insufficient number of erosion rates to calculate via power law regression.**

Table 116. Median grain size, wet bulk density, fraction LOI and critical shear stress for SF8-C(2) 1D.

Sample Depth (cm)	Grain Size (μm)	Wet Bulk Density (g/cm³)	Fraction LOI	τ_0 (Pa)	τ_1 (Pa)	τ_{linear} (Pa)	τ_{power} (Pa)
0.00	6.82	1.08	0.09	0.05	0.10	0.01	*n/a**
4.20	7.10	1.09	0.08	0.05	0.10	0.02	0.06
8.50	7.74	1.11	0.07	0.05	0.10	0.02	0.06
12.00	6.99	1.12	0.07	0.05	0.10	0.05	0.10
15.80	7.77	1.14	0.07	0.05	0.10	0.10	0.11
17.90	9.84	1.16	0.07	*n/a*	*n/a*	*n/a*	*n/a**
Mean	**7.71**	**1.12**	**0.07**	**0.05**	**0.10**	**0.04**	**0.08**

*Insufficient number of erosion rates to calculate via power law regression.
**No erosion rate measurements made at this sample depth; therefore, no critical shear stress determinations are listed.

Table 117. Power law best-fit variables for specified depth intervals in the SF8-C(2) 4D core.

Depth Interval	Interval Start Depth (cm)	Interval End Depth (cm)	A	n	r^2
1	0.00	2.80	0.039028	2.94	0.78
2	3.40	5.50	0.009245	3.25	0.86
3	6.40	9.00	0.062694	6.47	1.00
4	9.60	13.40	0.337548	8.31	1.00
5	13.40	18.30	0.009739	3.85	0.89

Table 118. Median grain size, wet bulk density, fraction LOI and critical shear stress for SF8-C(2) 4D.

Sample Depth (cm)	Grain Size (μm)	Wet Bulk Density (g/cm^3)	Fraction LOI	τ_0 (Pa)	τ_1 (Pa)	τ_{linear} (Pa)	τ_{power} (Pa)
0.00	7.12	1.11	0.11	0.05	0.10	0.10	0.13
3.40	7.47	1.16	0.09	0.10	0.20	0.20	0.25
6.40	7.72	1.17	0.09	0.20	0.40	0.32	0.37
9.60	8.98	1.19	0.08	0.20	0.40	0.32	0.38
13.40	8.63	1.22	0.08	0.20	0.40	0.32	0.30
18.30	8.98	1.29	0.08	*n/a*	*n/a*	*n/a*	*n/a**
Mean	**8.15**	**1.19**	**0.09**	**0.15**	**0.30**	**0.25**	**0.29**

*No erosion rate measurements made at this sample depth; therefore, no critical shear stress determinations are listed.

Table 119. Power law best-fit variables for specified depth intervals in the SF8-C(2) 7D core.

Depth Interval	Interval Start Depth (cm)	Interval End Depth (cm)	A	n	r^2
1	0.00	3.10	0.027179	2.56	0.87
2	3.20	6.80	0.062037	3.62	1.00
3	7.40	12.20	0.019194	4.03	0.95
4	13.30	16.00	0.016855	3.88	0.95
5	16.20	18.10	0.003099	4.03	1.00

Table 120. Median grain size, wet bulk density, fraction LOI and critical shear stress for SF8-C(2) 7D.

Sample Depth (cm)	Grain Size (μm)	Wet Bulk Density (g/cm³)	Fraction LOI	τ_0 (Pa)	τ_1 (Pa)	τ_{linear} (Pa)	τ_{power} (Pa)
0.00	8.21	1.14	0.09	0.05	0.10	0.05	0.11
3.20	8.06	1.18	0.09	0.10	0.20	0.16	0.17
7.40	9.36	1.19	0.08	0.20	0.40	0.26	0.27
13.30	8.87	1.23	0.08	0.20	0.40	0.26	0.27
16.20	9.72	1.28	0.09	0.20	0.40	0.40	0.43
18.10	14.98	1.37	0.08	*n/a*	*n/a*	*n/a*	*n/a**
Mean	**9.87**	**1.23**	**0.08**	**0.15**	**0.30**	**0.23**	**0.25**

*No erosion rate measurements made at this sample depth; therefore, no critical shear stress determinations are listed.

Table 121. Power law best-fit variables for specified depth intervals in the SF8-C(2) 14D core.

Depth Interval	Interval Start Depth (cm)	Interval End Depth (cm)	A	n	r^2
1	0.00	4.10	0.056535	3.27	1.00
2	4.50	6.80	0.123594	7.21	1.00
3	7.40	10.40	0.001918	2.62	1.00
4	10.80	13.30	0.001737	3.29	1.00
5	13.40	16.50	0.001540	6.86	1.00

Table 122. Median grain size, wet bulk density, fraction LOI and critical shear stress for SF8-C(2) 14D.

Sample Depth (cm)	Grain Size (μm)	Wet Bulk Density (g/cm³)	Fraction LOI	τ_0 (Pa)	τ_1 (Pa)	τ_{linear} (Pa)	τ_{power} (Pa)
0.00	7.20	1.14	0.08	0.20	0.40	0.21	0.14
4.50	7.93	1.23	0.08	0.20	0.40	0.32	0.37
7.40	8.32	1.26	0.08	0.20	0.40	0.32	0.32
10.80	8.53	1.30	0.08	0.40	0.80	0.45	0.42
13.40	9.30	1.34	0.07	0.40	0.80	0.52	0.67
16.50	43.71	1.59	0.04	*n/a*	*n/a*	*n/a*	*n/a**
Mean	**14.16**	**1.31**	**0.07**	**0.28**	**0.56**	**0.36**	**0.39**

*No erosion rate measurements made at this sample depth; therefore, no critical shear stress determinations are listed.

Table 123. Power law best-fit variables for specified depth intervals in the SF8-C(2) 28D core.

Depth Interval	Interval Start Depth (cm)	Interval End Depth (cm)	A	n	r^2
1	0.00	2.10	0.068166	7.32	1.00
2	2.50	6.90	0.006992	4.73	1.00
3	6.90	11.90	0.008419	3.31	0.88
4	12.30	14.70	0.001768	5.66	1.00
5	14.70	17.60	0.000471	2.54	0.95

Table 124. Median grain size, wet bulk density, fraction LOI and critical shear stress for SF8-C(2) 28D.

Sample Depth (cm)	Grain Size (μm)	Wet Bulk Density (g/cm³)	Fraction LOI	τ_0 (Pa)	τ_1 (Pa)	τ_{linear} (Pa)	τ_{power} (Pa)
0.00	6.76	1.13	0.09	0.20	0.40	0.40	0.41
2.50	7.28	1.21	0.08	0.20	0.40	0.40	0.41
6.90	8.22	1.25	0.08	0.20	0.40	0.28	0.26
12.30	7.87	1.27	0.08	0.40	0.80	0.48	0.60
14.70	9.37	1.33	0.07	0.40	0.80	0.52	0.54
17.60	24.99	1.54	0.05	*n/a*	*n/a*	*n/a*	*n/a**
Mean	**10.75**	**1.29**	**0.08**	**0.28**	**0.56**	**0.42**	**0.44**

*No erosion rate measurements made at this sample depth; therefore, no critical shear stress determinations are listed.

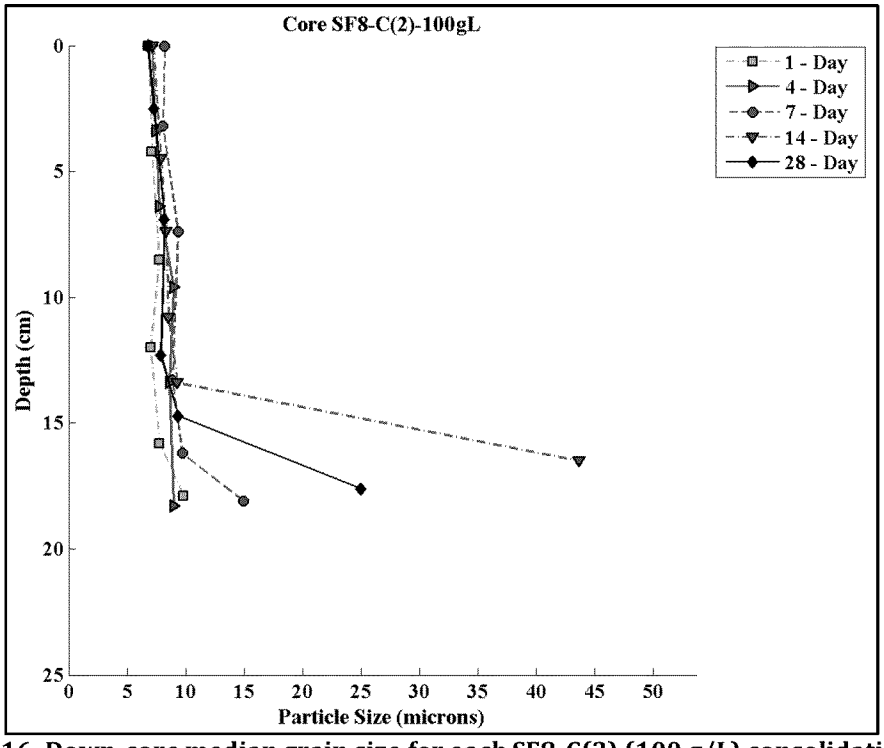

Figure 116. Down-core median grain size for each SF8-C(2) (100 g/L) consolidation core.

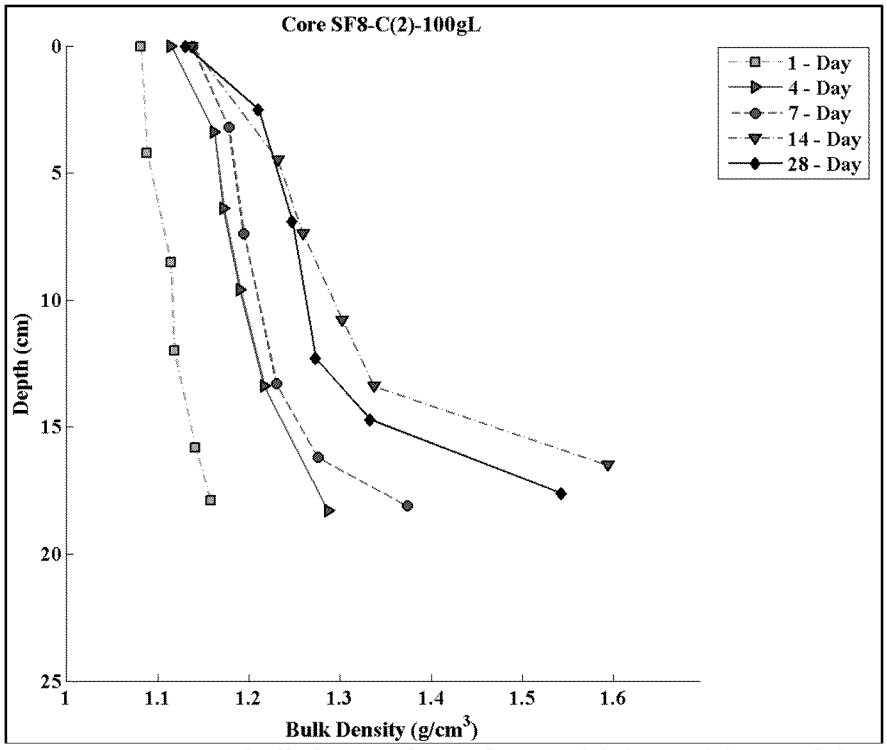

Figure 117. Down-core wet bulk density for each SF8-C(2) (100 g/L) consolidation core.

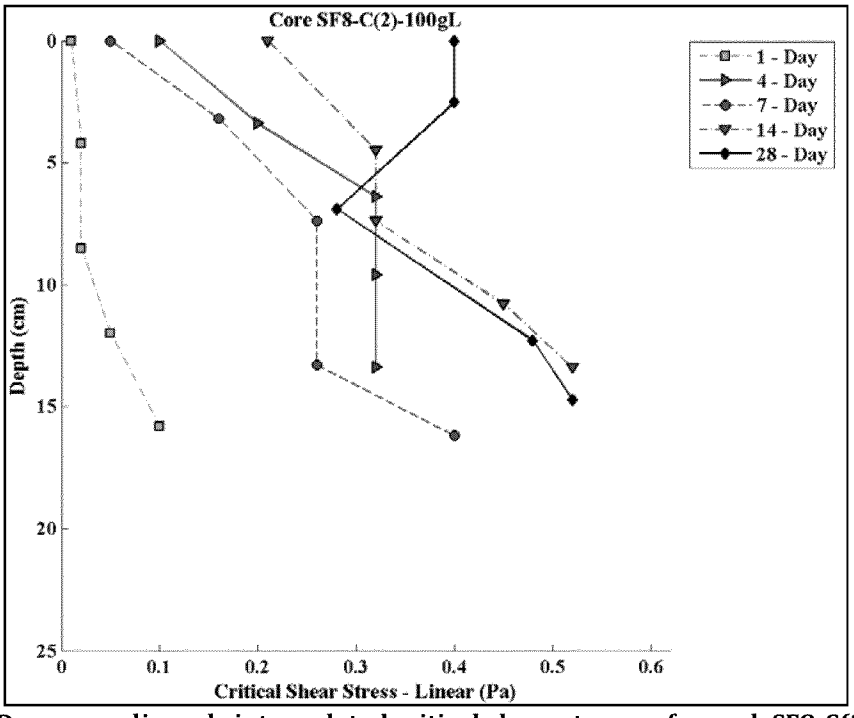

Figure 118. Down core linearly interpolated critical shear stresses for each SF8-C(2) (100 g/L) consolidation core.

3.4.8 SF8-C (3) CONSOLIDATION CORE (350 G/L TARGET CONCENTRATION)

Individual Consolidation Core Results
In general, the SF8-C(3) core descriptions on their respective day of processing were:

- 1 Day: Very low-density, fluidic surface that persisted throughout the core.
- 4 Day: Very low-density, fluidic surface sediment that became slightly denser with depth.
- 7 Day: Very low-density (higher density than previous cores), fluidic surface that became slightly denser with depth.
- 14 Day: Low-density, gelatinous silt surface that became denser with depth.
- 28 Day: Low-density, gelatinous silt surface that became denser with depth.

Photographs of the SF8-C(3) cores are presented in Figure 119. The erosion rate data for the cores are plotted in Figure 120. Shear stresses ranging between 0.1 to 3.2 Pa were applied to these cores. Erosion rates in all cores generally decreased or remained relatively constant with depth.

The intra-core erosion rate ratios of the depth intervals evaluated in each core are shown in Figure 121. Down-core erosion susceptibility decreased as depth increased, becoming more depth-uniform as consolidation duration increased.

The power law regression fit within each depth interval for the SF8-C(3) consolidation core sets is illustrated in Figure 122. Coefficients and regression statistics from the power law fit analysis, the measured median grain sizes, the computed wet bulk densities and the critical shear stresses for each depth interval, from each core, are presented in Table 125 to Table 134.

Consolidation Core Set Summary
The temporal variation in down-core sediment properties and computed parameters is illustrated in Figure 123 through Figure 125. Figure 123 contains the down-core median grain sizes measured; Figure 124 contains the down-core wet bulk densities computed; and Figure 125 represents the down-core linearly interpolated critical shear stresses.

The down-core structure of the median grain size did not indicate much variability over the consolidation duration. The median grain sizes in the cores remained in the very fine to fine silt range, ranging between 8.71 µm and 14.92 µm.

The down-core wet bulk density profiles illustrated a trend of increasing density both with increased consolidation duration and depth. Surface bulk densities ranged between 1.19 g/cm^3 and 1.23 g/cm^3; and the bulk densities at the deepest depths in the cores ranged from 1.22 g/cm^3 to 1.37 g/cm^3.

The linearly interpolated critical shear stresses showed a definitive increasing trend with depth and consolidation time. The core-average linearly interpolated critical shear stresses increased from 0.14 Pa after 1 day to 0.37 Pa after 28 days.

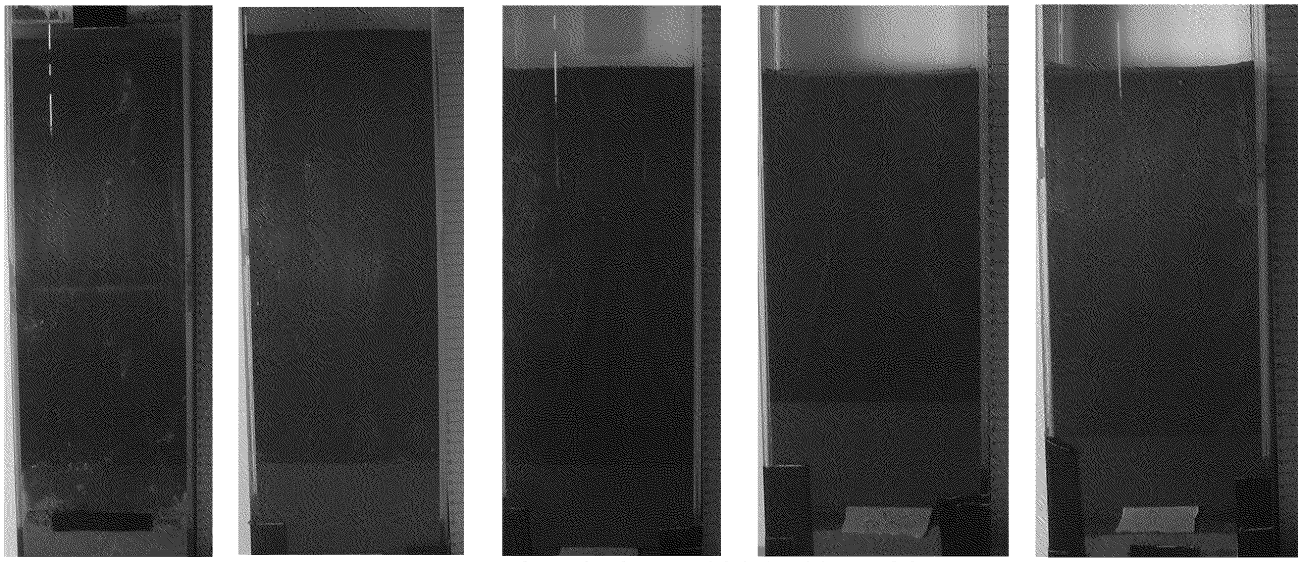

Figure 119. Pre-processing photos for the SF8-C(3) (350 g/L) consolidation core set.

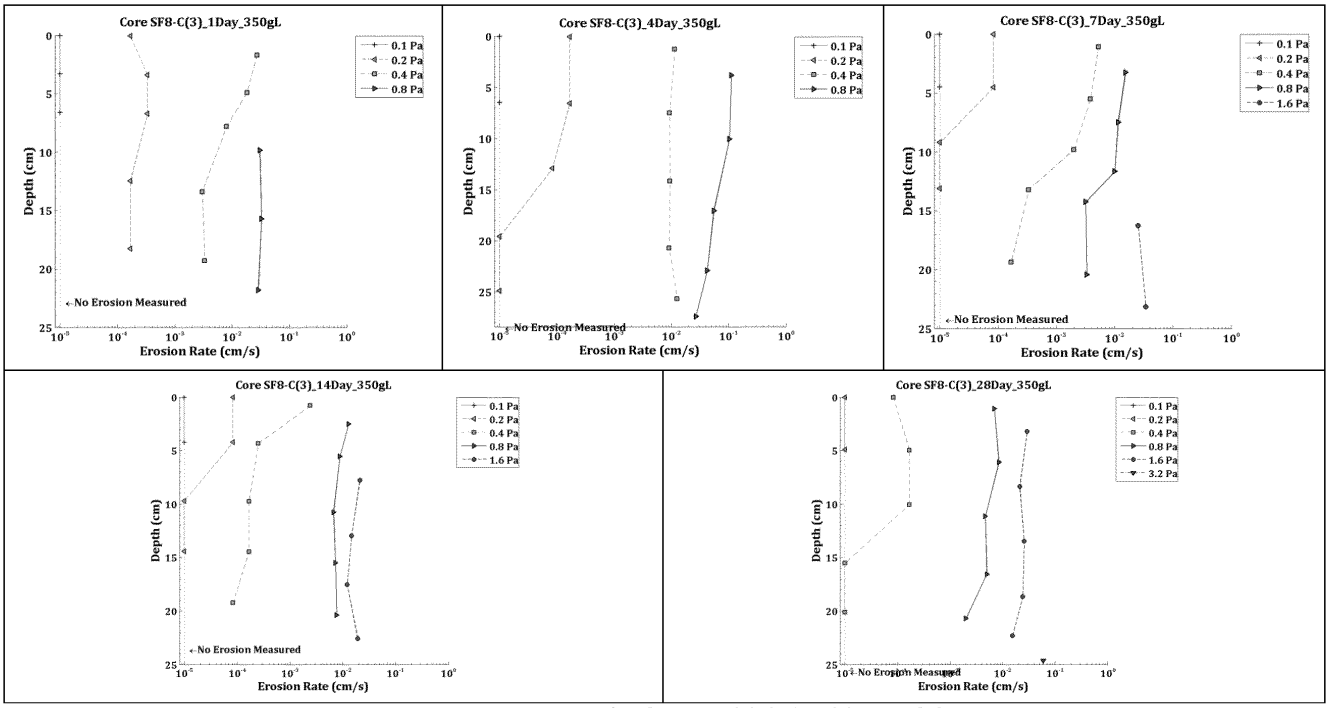

Figure 120. Down-core erosion rates for the SF8-C(3) (350 g/L) consolidation core set.

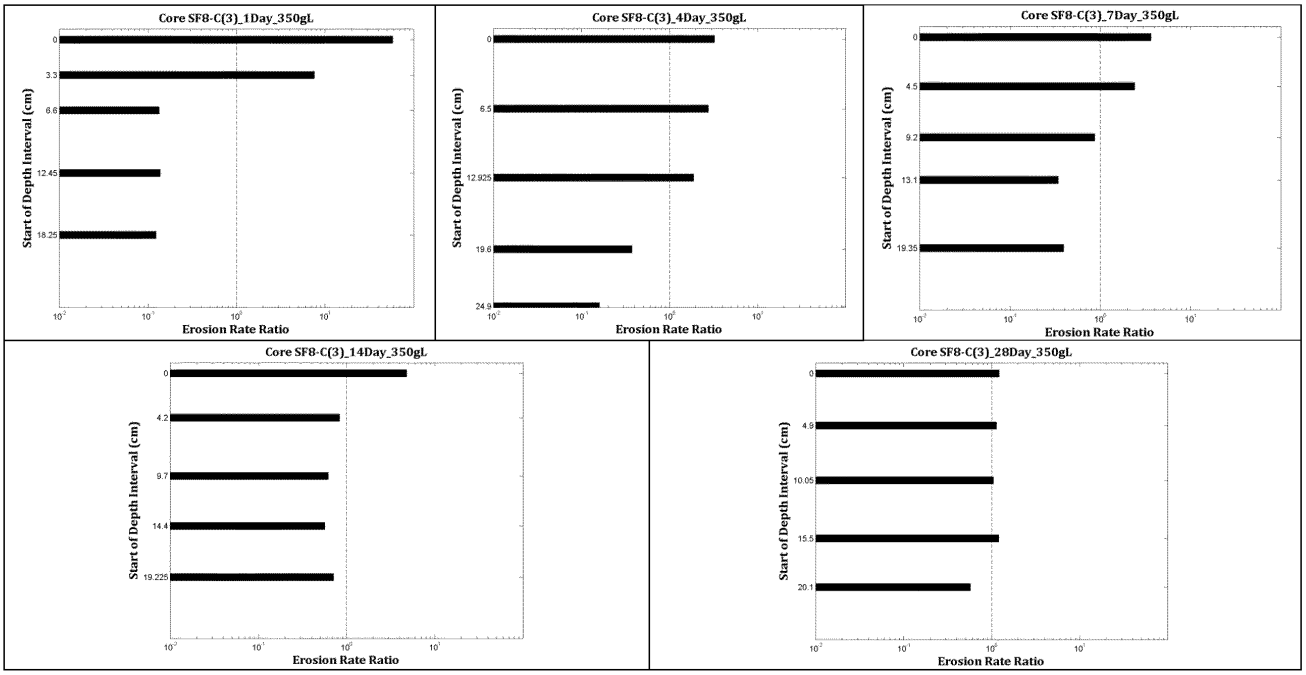

Figure 121. Intra-core erosion rate ratios for the SF8-C(3) (350 g/L) consolidation core set.

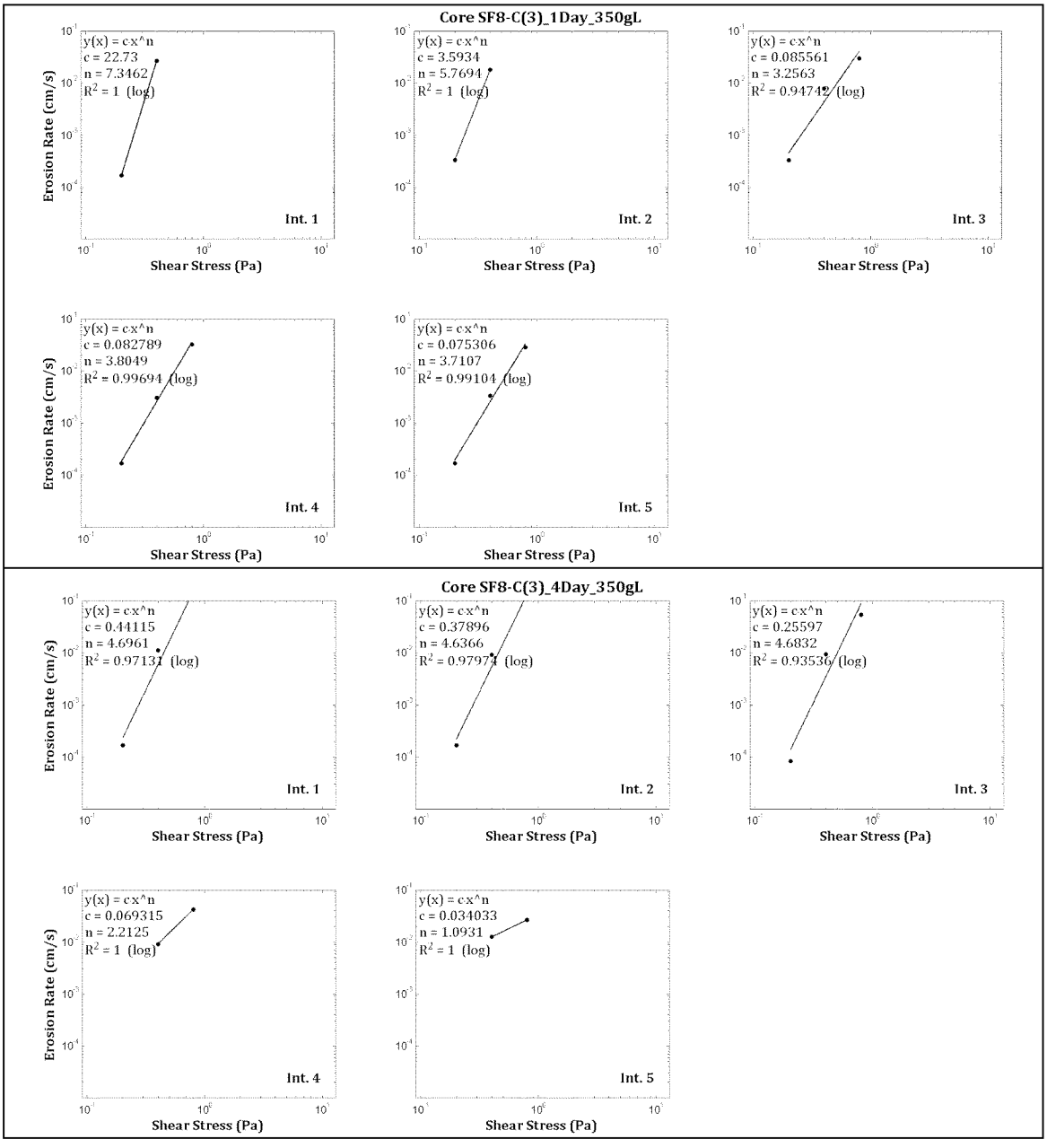

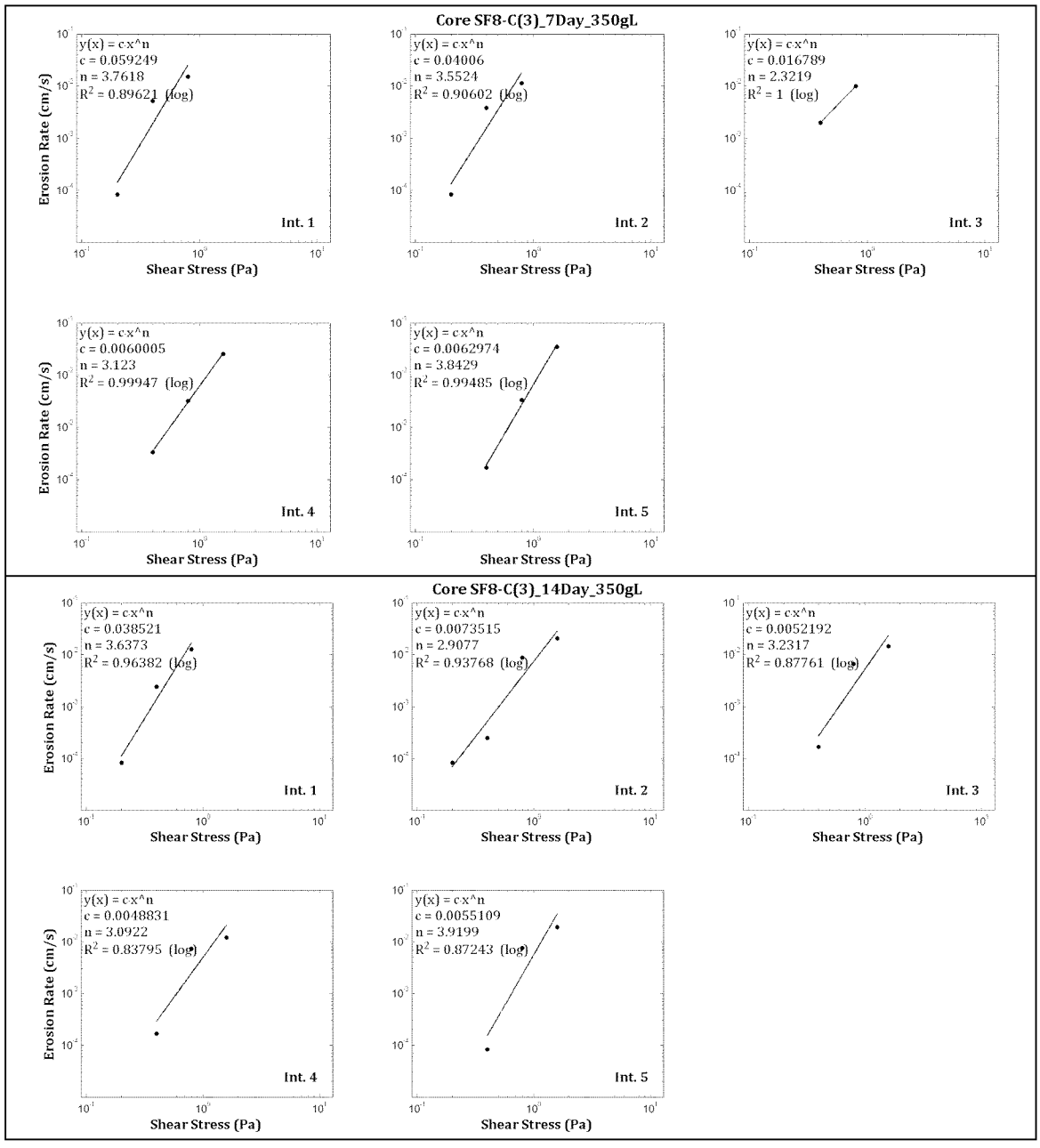

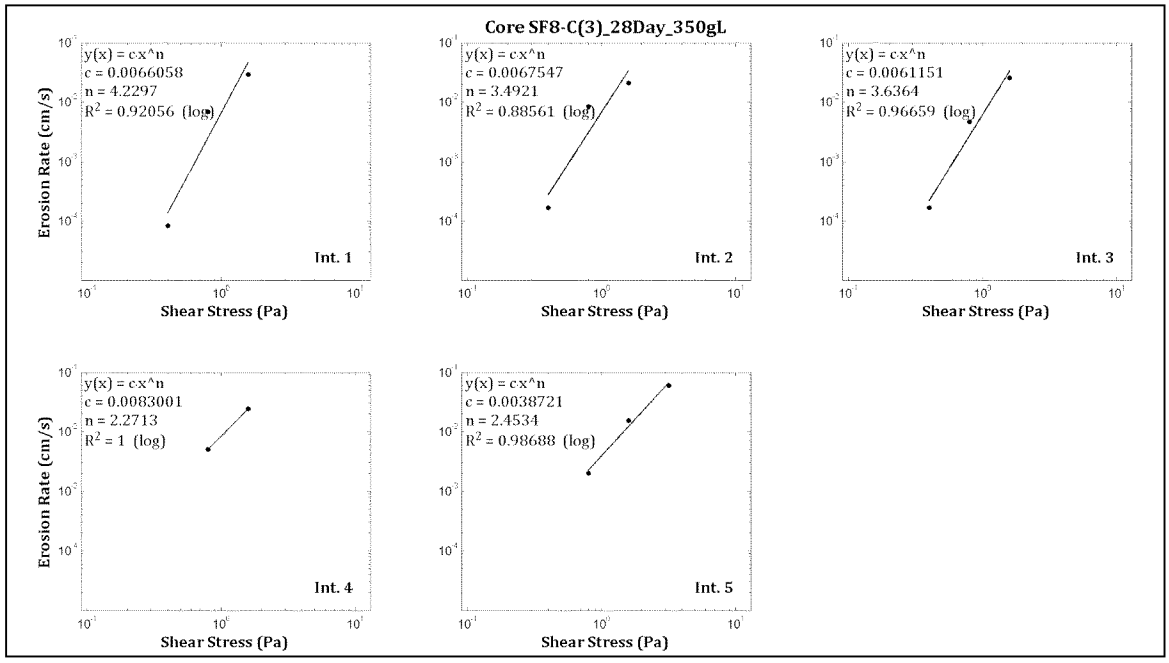

Figure 122. Power law best-fit regression solutions for the SF8-C(3) (350 g/L) consolidation core set (sequential from top to bottom).

Table 125. Power law best-fit variables for specified depth intervals in the SF8-C(3) 1D re-pour core.

Depth Interval	Interval Start Depth (cm)	Interval End Depth (cm)	A	n	r^2
1	0.00	3.30	22.730351	7.35	1.00
2	3.30	6.30	3.593370	5.77	1.00
3	6.60	10.90	0.085561	3.26	0.95
4	12.40	17.10	0.082789	3.80	1.00
5	18.20	23.30	0.075306	3.71	0.99

Table 126. Median grain size, wet bulk density, fraction LOI and critical shear stress for SF8-C(3) 1D re-pour.

Sample Depth (cm)	Grain Size (μm)	Wet Bulk Density (g/cm³)	Fraction LOI	τ_0 (Pa)	τ_1 (Pa)	τ_{linear} (Pa)	τ_{power} (Pa)
0.00	14.92	1.19	0.08	0.10	0.20	0.16	0.19
3.30	8.76	1.20	0.08	0.10	0.20	0.13	0.16
6.60	10.53	1.16	0.10	0.10	0.20	0.13	0.13
12.40	11.47	1.22	0.08	0.10	0.20	0.15	0.17
18.20	10.84	1.22	0.08	0.10	0.20	0.15	0.17
23.30	11.50	1.22	0.08	*n/a*	*n/a*	*n/a*	*n/a**
Mean	**11.34**	**1.20**	**0.08**	**0.10**	**0.20**	**0.14**	**0.16**

*No erosion rate measurements made at this sample depth; therefore, no critical shear stress determinations are listed.

Table 127. Power law best-fit variables for specified depth intervals in the SF8-C(3) 4D core.

Depth Interval	Interval Start Depth (cm)	Interval End Depth (cm)	A	n	r^2
1.00	0.00	5.20	0.441153	4.70	0.97
2.00	6.50	11.70	0.378961	4.64	0.98
3.00	12.90	18.70	0.255971	4.68	0.94
4.00	19.60	24.00	0.069315	2.21	1.00
5.00	24.90	28.40	0.034033	1.09	1.00

Table 128. Median grain size, wet bulk density, fraction LOI and critical shear stress for SF8-C(3) 4D.

Sample Depth (cm)	Grain Size (μm)	Wet Bulk Density (g/cm³)	Fraction LOI	τ_0 (Pa)	τ_1 (Pa)	τ_{linear} (Pa)	τ_{power} (Pa)
0.00	11.24	1.22	0.07	0.10	0.20	0.16	0.17
6.50	14.44	1.22	0.07	0.10	0.20	0.16	0.17
12.90	11.13	1.23	0.07	0.10	0.20	0.20	0.19
19.60	12.75	1.23	0.07	0.20	0.40	0.21	0.05
24.90	11.22	1.24	0.06	0.20	0.40	0.21	0.00
28.40	13.06	1.26	0.07	*n/a*	*n/a*	*n/a*	*n/a**
Mean	**12.31**	**1.23**	**0.07**	**0.14**	**0.28**	**0.19**	**0.12**

*No erosion rate measurements made at this sample depth; therefore, no critical shear stress determinations are listed.

Table 129. Power law best-fit variables for specified depth intervals in the SF8-C(3) 7D core.

Depth Interval	Interval Start Depth (cm)	Interval End Depth (cm)	A	n	r^2
1.00	0.00	4.40	0.059249	3.76	0.90
2.00	4.50	8.45	0.040060	3.55	0.91
3.00	9.20	12.90	0.016789	2.32	1.00
4.00	13.10	17.30	0.006000	3.12	1.00
5.00	19.30	24.90	0.006297	3.84	0.99

Table 130. Median grain size, wet bulk density, fraction LOI and critical shear stress for SF8-C(3) 7D.

Sample Depth (cm)	Grain Size (μm)	Wet Bulk Density (g/cm³)	Fraction LOI	τ_0 (Pa)	τ_1 (Pa)	τ_{linear} (Pa)	τ_{power} (Pa)
0.00	13.46	1.22	0.08	0.10	0.20	0.20	0.18
4.50	10.40	1.24	0.08	0.10	0.20	0.20	0.19
9.20	14.56	1.25	0.10	0.20	0.40	0.21	0.11
13.10	11.76	1.25	0.08	0.20	0.40	0.26	0.27
19.30	12.62	1.26	0.08	0.20	0.40	0.30	0.34
24.90	12.06	1.28	0.07	*n/a*	*n/a*	*n/a*	*n/a**
Mean	**12.48**	**1.25**	**0.08**	**0.16**	**0.32**	**0.23**	**0.22**

*No erosion rate measurements made at this sample depth; therefore, no critical shear stress determinations are listed.

Table 131. Power law best-fit variables for specified depth intervals in the SF8-C(3) 14D core.

Depth Interval	Interval Start Depth (cm)	Interval End Depth (cm)	A	n	r^2
1.00	0.00	3.50	0.038521	3.64	0.96
2.00	4.20	8.80	0.007352	2.91	0.94
3.00	9.70	14.20	0.005219	3.23	0.88
4.00	14.40	18.50	0.004883	3.09	0.84
5.00	19.20	23.60	0.005511	3.92	0.87

Table 132. Median grain size, wet bulk density, fraction LOI and critical shear stress for SF8-C(3) 14D.

Sample Depth (cm)	Grain Size (μm)	Wet Bulk Density (g/cm³)	Fraction LOI	τ_0 (Pa)	τ_1 (Pa)	τ_{linear} (Pa)	τ_{power} (Pa)
0.00	11.10	1.23	0.06	0.10	0.20	0.20	0.19
4.20	9.44	1.27	0.06	0.10	0.20	0.20	0.23
9.70	10.42	1.28	0.06	0.20	0.40	0.32	0.29
14.40	8.71	1.29	0.06	0.20	0.40	0.32	0.28
19.20	10.93	1.30	0.06	0.20	0.40	0.40	0.36
23.60	12.77	1.34	0.06	*n/a*	*n/a*	*n/a*	*n/a**
Mean	**10.56**	**1.29**	**0.06**	**0.16**	**0.32**	**0.29**	**0.27**

*No erosion rate measurements made at this sample depth; therefore, no critical shear stress determinations are listed.

Table 133. Power law best-fit variables for specified depth intervals in the SF8-C(3) 28D core.

Depth Interval	Interval Start Depth (cm)	Interval End Depth (cm)	A	n	r^2
1	0.00	4.30	0.006606	4.23	0.92
2	4.90	9.50	0.006755	3.49	0.89
3	10.00	14.70	0.006115	3.64	0.97
4	15.50	19.70	0.008300	2.27	1.00
5	20.10	26.00	0.003872	2.45	0.99

Table 134. Median grain size, wet bulk density, fraction LOI and critical shear stress for SF8-C(3) 28D.

Sample Depth (cm)	Grain Size (μm)	Wet Bulk Density (g/cm³)	Fraction LOI	τ_0 (Pa)	τ_1 (Pa)	τ_{linear} (Pa)	τ_{power} (Pa)
0.00	9.14	1.23	0.07	0.20	0.40	0.40	0.37
4.90	11.95	1.28	0.07	0.20	0.40	0.32	0.30
10.00	10.51	1.30	0.07	0.20	0.40	0.30	0.32
15.50	11.16	1.30	0.06	0.40	0.80	0.41	0.14
20.10	12.62	1.34	0.07	0.40	0.80	0.42	0.23
26.00	11.59	1.37	0.07	*n/a*	*n/a*	*n/a*	*n/a**
Mean	**11.16**	**1.30**	**0.07**	**0.28**	**0.56**	**0.37**	**0.27**

*No erosion rate measurements made at this sample depth; therefore, no critical shear stress determinations are listed.

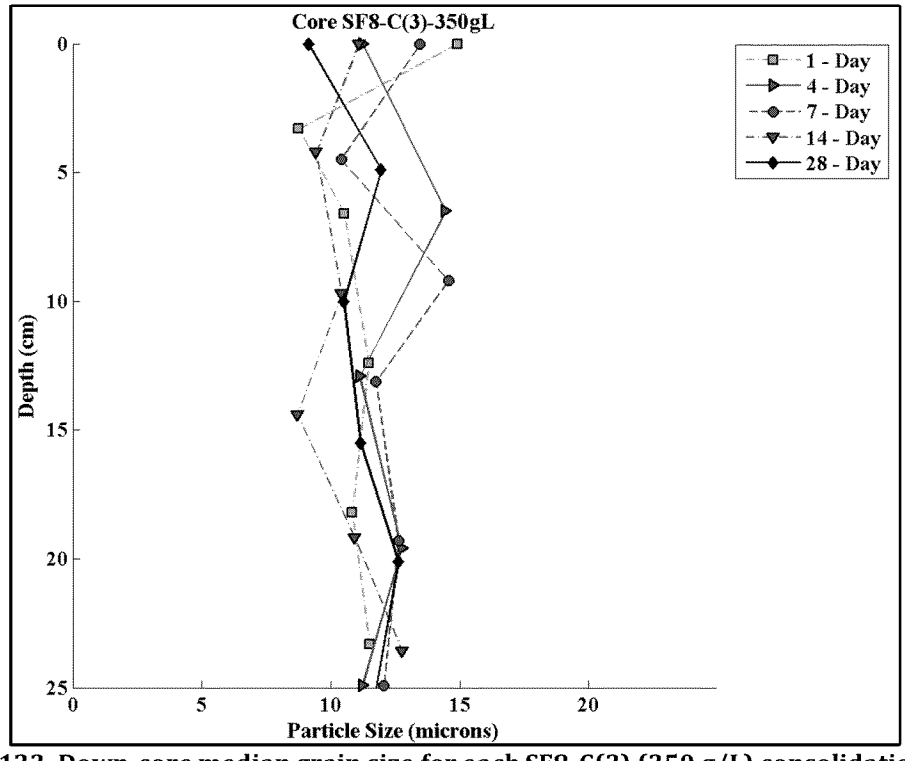

Figure 123. Down-core median grain size for each SF8-C(3) (350 g/L) consolidation core.

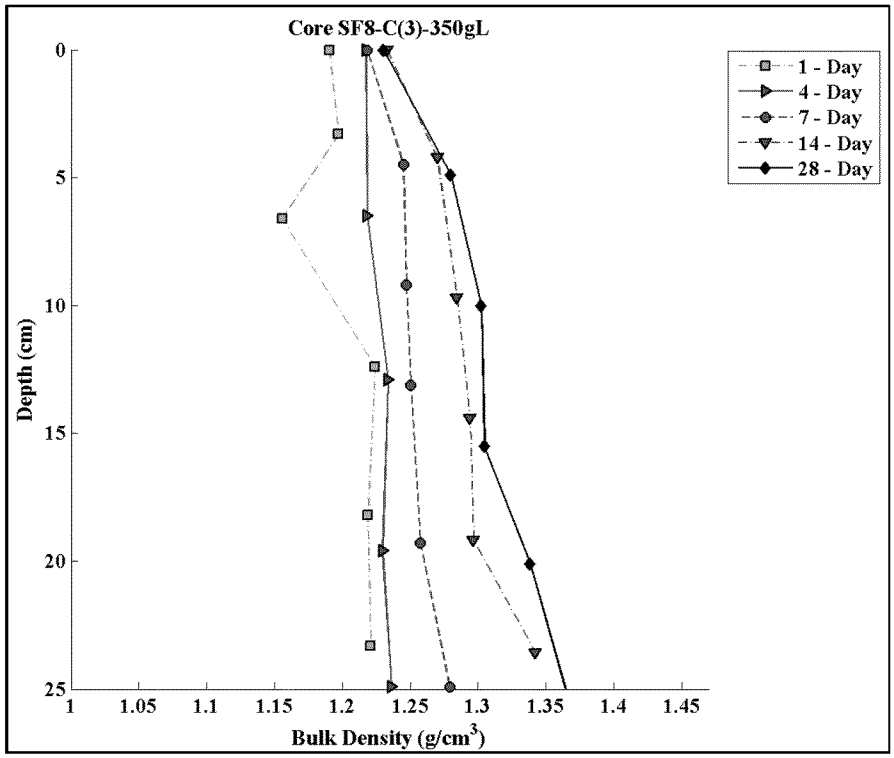

Figure 124. Down-core wet bulk density for each SF8-C(3) (350 g/L) consolidation core.

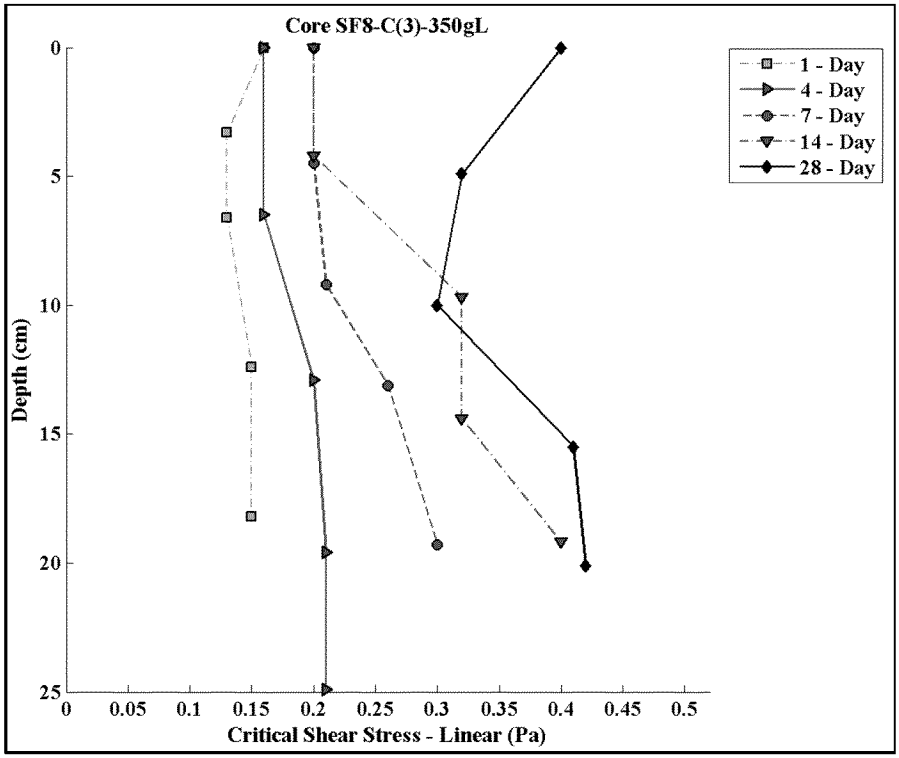

Figure 125. Down core linearly interpolated critical shear stresses for each SF8-C(3) (350 g/L) consolidation core.

SECTION 4 - SUMMARY

4.1 PROJECT SUMMARY

Sea Engineering, Inc. (SEI) presented results from a two-phased SEDFlume analysis: 1) on intact field cores and 2) sediment cores that had been reconstructed from surface sediment obtained from the NBSA. The Phase I Field Effort began October 16, 2012 and was completed November 4, 2012. Twenty-nine field cores were extracted, transported to a proximate facility, and subsequently processed. Processing at a local site prevented potential disturbances to the core structure and sediment stability from long-distance transport.

Bulk surface sediment that was collected during the field effort was shipped to SEI's Santa Cruz, CA, laboratory for the Phase II Laboratory Effort. The laboratory effort began November 11, 2012 and was completed March 15, 2013. Sediment from each NBSA recovery location was slurried to the desired concentration before pouring into five empty core barrels. Each core in a consolidation set was allowed to consolidate for a pre-determined amount of time: 1-day, 4-days, 7-days, 14-days and 28-days. Sediment from 5 locations (SF3-C, SF6-C, SF8-C, SF9-C and SF13-C) was slurried to a target initial concentration of 350 g/L. Two additional consolidation core sets comprising concentrations of 100 g/L and 125 g/L were slurried with the SF8-C sediment to create a total of 35 consolidation cores analyzed (7 sets of 5 cores).

Both the field cores and laboratory cores were eroded to determine erosion rates as a function of shear stress and depth into core. In addition, cores were subsampled during analysis to determine moisture content, loss on ignition fraction and particle size distributions at specific depths within the core. Critical shear stresses were determined for five depth intervals (unless otherwise stated) in each core.

For reference, all ancillary notes and data from this effort are included as appendices to this document:

- Appendix A – Field Core Sampling Sheets
- Appendix B – Field Safety Toolbox Meetings
- Appendix C – Field Core Raw Datasheets
- Appendix D – Field Core Formatted Datasheets
- Appendix E – Field Core Raw LOI Measurements
- Appendix F – Field Core PSD Reports
- Appendix G – Atterberg Limit Data
- Appendix H – Atterberg Limit PSD Reports
- Appendix I – Laboratory Consolidation Core Slurry Raw Measurements
- Appendix J – Laboratory Consolidation Core Raw Datasheets
- Appendix K – Laboratory Consolidation Core Formatted Datasheets
- Appendix L – Laboratory Consolidation Core Raw LOI Measurements
- Appendix M – Laboratory Consolidation Core PSD Reports
- Appendix N – Laboratory Sediment Settling Raw Measurements
- Appendix O – Laboratory Sediment Settling Formatted Measurements

4.1.1 NBSA FIELD AND CONSOLIDATION EROSION TRENDS

In order to visualize the spatial erosion susceptibility of the cores, inter-core erosion rates were computed and plotted. Figure 126 shows the inter-core erosion rates of each field core computed with the *core-averaged* erosion rate and *site-wide-averaged* erosion rate. This plot provides a qualitative overview of the relative core erosion rates compared to all others and can offer some insight into the susceptibility of sediment to erosion based on core location. Based on this figure, the field cores most susceptible to erosion (compared to all the cores collected from the NBSA) were collected from the navigation channel locations: Stations 3, 6, 8 and 13. Further, cores from mudflat stations 4 and 10 were also more susceptible to erosion than other mudflat stations. The remaining core locations were less susceptible to erosion, had slower measured erosion rates and larger computed critical shear stresses.

Figure 127 shows the inter-core erosion rates of each field core computed with the *interval-averaged* erosion rates and *site-wide-averaged* erosion rate. This figure indicates similar erosion susceptibility trends for each core and station location; however it also indicates which depth interval of a core is more or less susceptible to erosion. Most obvious from this figure is that the first depth interval is often the weakest within a core, which makes intuitive sense as that comprises the least consolidated sediment.

Similar inter-core erosion rate ratio plots for the laboratory consolidation cores are illustrated in Figure 128 and Figure 129. Though these data are not directly correlated for a direct correlation to NBSA in-situ spatial trends (because they were reconstructed in a laboratory), they can potentially be useful for qualitative analysis and comparison of the sediment characteristics collected from each site. From Figure 128 it is evident that sediments from SF3-C and SF6-C are least susceptible to erosion; that the sediments from SF8-C become less susceptible to erosion as consolidation time increases (erosion rate ratio decreases over time); and that sediments from SF9-C and SF13-C do not exhibit evidence of temporal variation in erosion susceptibility and susceptibility over the 28 day period.

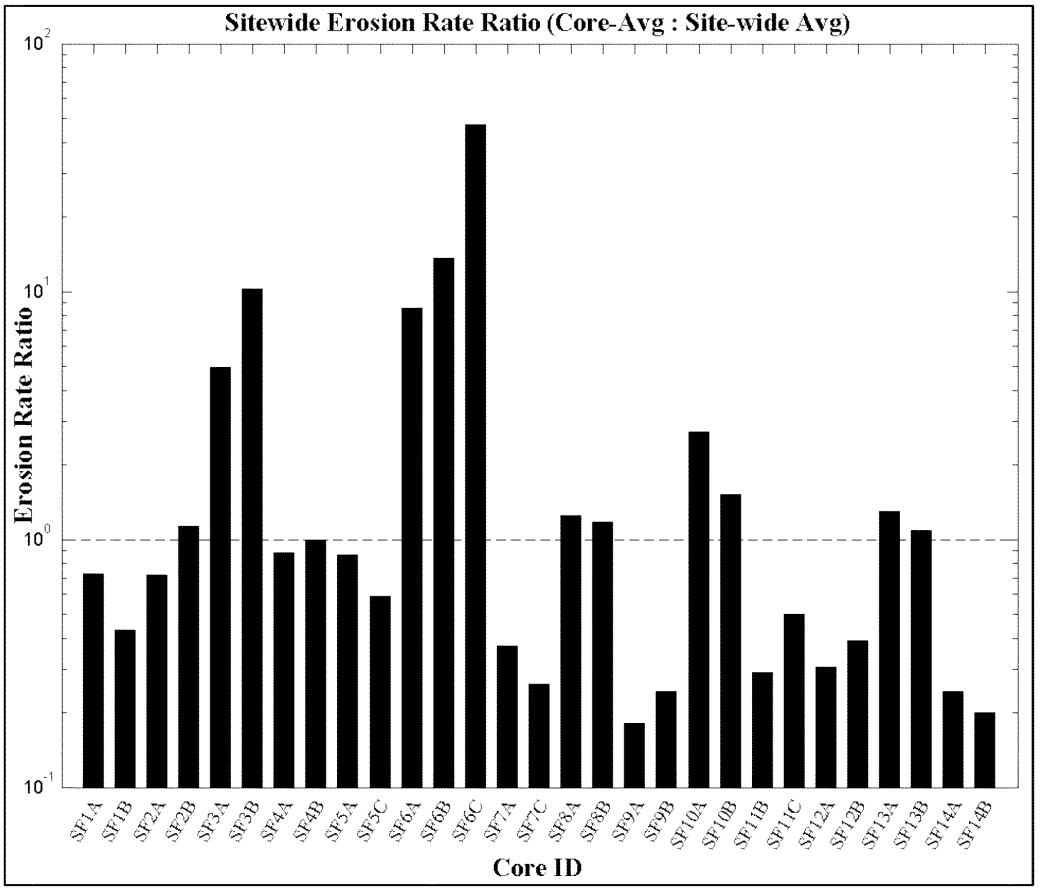

Figure 126. Inter-core erosion rate ratios. Depth-averaged field core erosion rates compared to the site-wide average erosion rate.

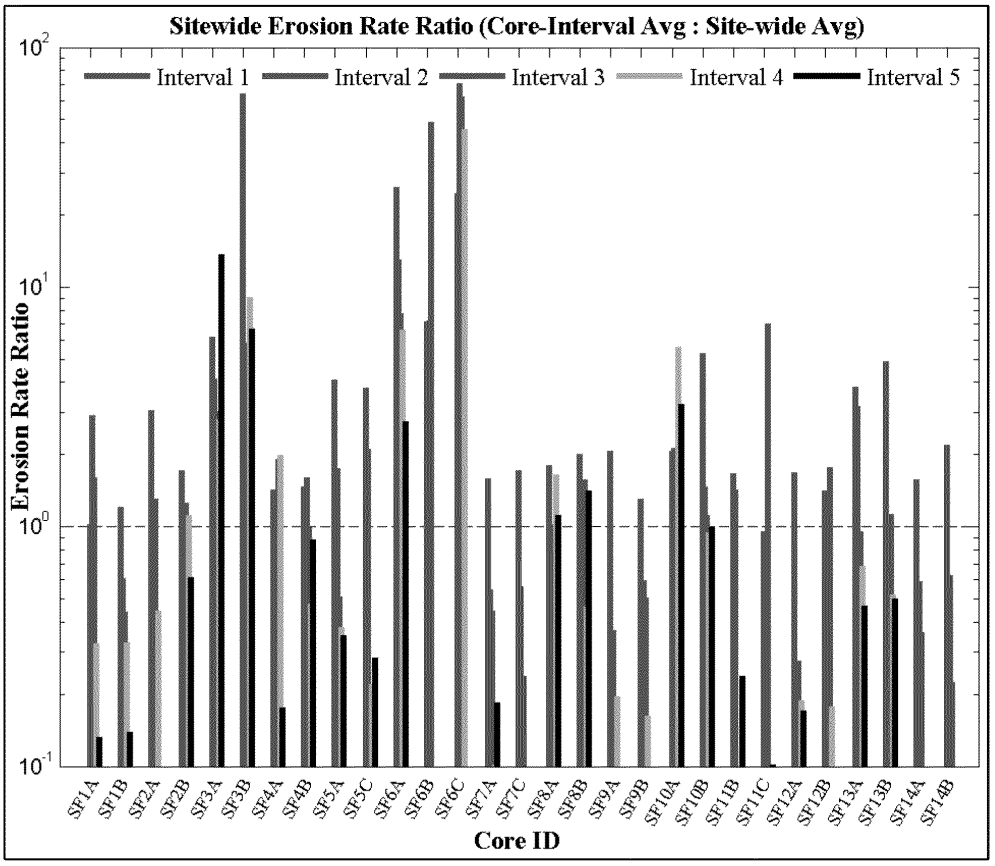

Figure 127. Inter-core erosion rate ratios, by core interval. Field core interval-average erosion rates compared to the site-wide average erosion rate.

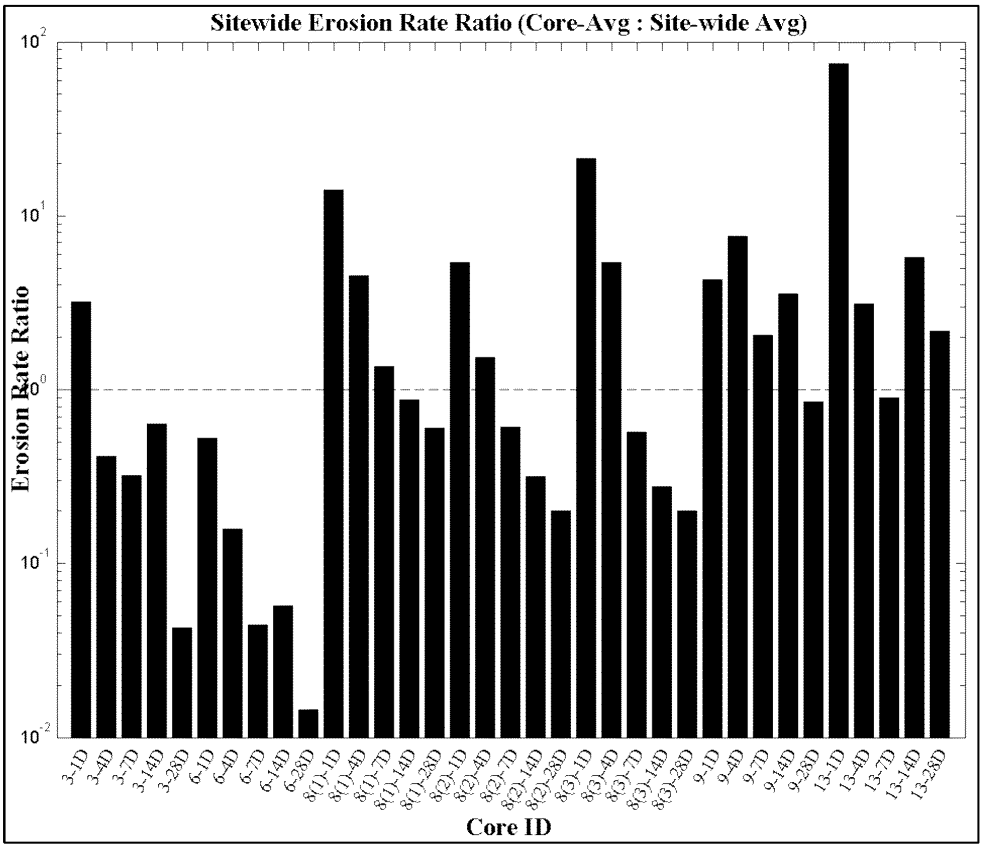

Figure 128. Inter-core erosion rate ratios. Depth-averaged laboratory core erosion rates compared to the consolidation core-wide average erosion rate.

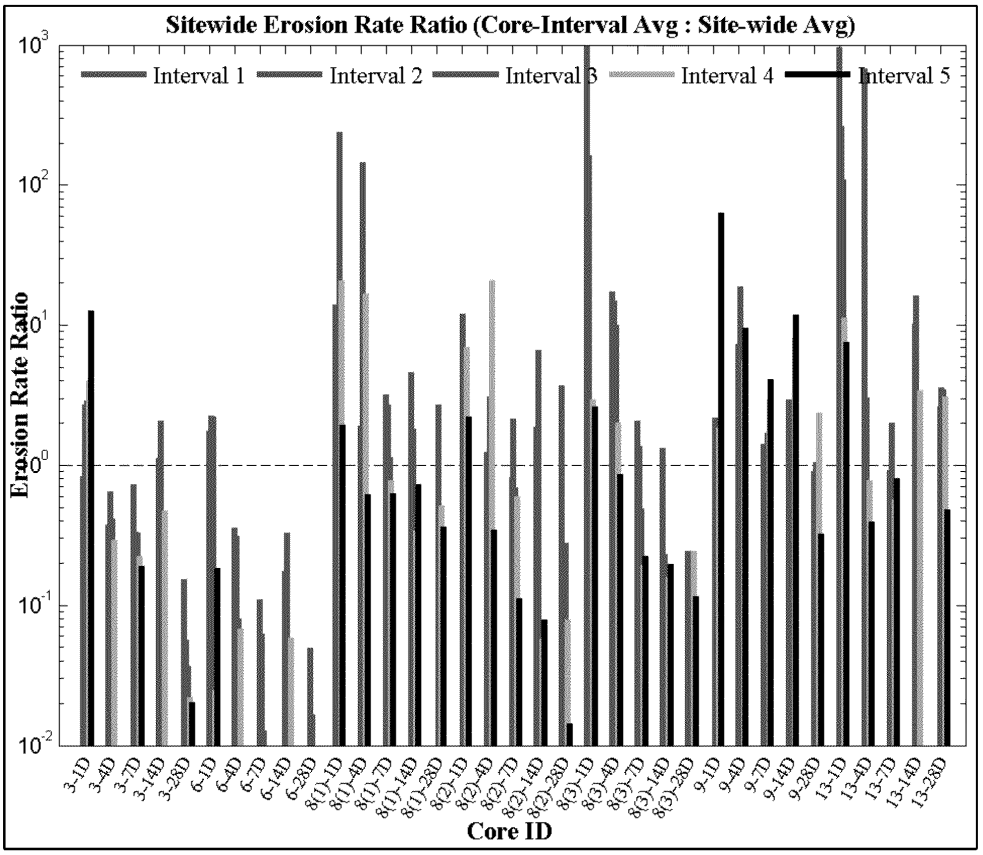

Figure 129. Inter-core erosion rate ratios, by core interval. Laboratory core interval-average erosion rates compared to the consolidation core-wide average erosion rate.

SECTION 5 - REFERENCES

ASTM Standard, 2007, Annual Book of ASTM Standards. ASTM International, West Conshohocken, Pennsylvania, USA. Vol. 04.08 Soil and Rock (I): D 420 - D5611: 314-315.

Hakanson, L., and M. Jansson, 2002, Principles of Lake Sedimentology, Blackburn Press, Caldwell, New Jersey, USA.

Jepsen, R., J. Roberts, and W. Lick, 1997, Effects of bulk density on sediment erosion rates, Water, Air and Soil Pollution, 99:21-31.

McNeil, J., C. Taylor, and W. Lick, 1996, Measurements of erosion of undisturbed bottom sediments with depth, J. Hydr. Engr., 122(6):316-324.

Roberts, J., R. Jepsen, D. Gotthard, and W. Lick, 1998, Effects of particle size and bulk density on erosion of quartz particles, J. Hydr. Engr., 124(12):1261-1267.

SECTION 6 - APPENDICES

APPENDIX A – FIELD CORE SAMPLING SHEETS

APPENDIX B – FIELD SAFETY TOOLBOX MEETINGS

APPENDIX C – FIELD CORE RAW DATASHEETS

APPENDIX D – FIELD CORE FORMATTED DATASHEETS

APPENDIX E – FIELD CORE RAW LOI MEASUREMENTS

APPENDIX F – FIELD CORE PSD REPORTS

APPENDIX G – ATTERBERG LIMIT DATA

APPENDIX H – ATTERBERG LIMIT PSD REPORTS

APPENDIX I – LABORATORY CONSOLIDATION CORE SLURRY RAW MEASUREMENTS

APPENDIX J – LABORATORY CONSOLIDATION CORE RAW DATASHEETS

APPENDIX K – LABORATORY CONSOLIDATION CORE FORMATTED DATASHEETS

APPENDIX L – LABORATORY CONSOLIDATION CORE RAW LOI MEASUREMENTS

APPENDIX M – LABORATORY CONSOLIDATION CORE PSD REPORTS

APPENDIX N – LABORATORY SEDIMENT SETTLING RAW MEASUREMENTS

APPENDIX O – LABORATORY SEDIMENT SETTLING FORMATTED MEASUREMENTS